














 Feng first author 1988-2002 Hu Davies Horbett Carbon STM Fibrinogen Luciferase Albumin

[New](#) [Arrange By](#) [Action](#) [Share](#) [Edit](#) [Tags](#)

name	^	Date Modified	Size	Kind
 Feng 1988 STM tunneling microscopy Albumin hu.pdf		Aug 12, 2006, 7:25 PM	789 KB	PDF D
 Feng 1988 STM Tunneling Microscopy Amino Acids hu.pdf		Aug 12, 2006, 7:19 PM	1.1 MB	PDF D
 Feng 1989 STM tunneling microscopy Proteins hu SEM Conf.pdf		Aug 12, 2006, 7:49 PM	3.6 MB	PDF D
 Feng 1993 Carbon STM tunneling microscopy.pdf		Aug 12, 2006, 5:28 PM	1.9 MB	PDF D
 Feng 1994 Carbon I Protein Adsorption DSC.pdf		Jan 7, 2018, 3:37 PM	845 KB	PDF D
 Feng 1994 Carbon II Protein Adsorption Surface Charge.pdf		Aug 12, 2006, 6:56 PM	2.8 MB	PDF D
 Feng 1994 Carbon III Protein Adsorption Albumin Fibrinogen.pdf		Jan 5, 2018, 10:35 AM	3.5 MB	PDF D
 Feng 1995 Carbon IV Protein Adsorpt...2-D Electrophoresis Corrigendum.pdf		Aug 11, 2006, 9:32 PM	2.9 MB	PDF D
 Feng 1995 Carbon V Protein Adsorpti...Blood Compatibility-compressed.pdf		Nov 10, 2018, 10:36 AM	1.9 MB	PDF D
 Feng 1995 Fibrinogen Adsorption in Horbett bk.pdf		Aug 12, 2006, 11:19 AM	2.5 MB	PDF D
 Feng 1995 Icon Approach Protein Structure Properties unpublished.pdf		Nov 12, 2018, 3:34 PM	4.8 MB	PDF D
 Feng 1996 Fibrinogen Machine Structure Surface Icons unpublished.pdf		Nov 11, 2018, 9:25 PM	5.4 MB	PDF D
 Feng 2002 ISBC Bacterial Luciferase Davies.pdf		Aug 11, 2006, 9:49 PM	802 KB	PDF D

LETTER TO THE EDITOR

Scanning Tunneling Microscopic Images of Adsorbed Serum Albumin on Highly Oriented Pyrolytic Graphite

Human serum albumin molecules, adsorbed on highly oriented pyrolytic graphite (HOPG), have been observed by scanning tunneling microscopy (STM) in air. The images show the details of sub-molecular domains as well as individual molecules with a resolution better than 20 Å. The observed domain arrangement agrees with the expected size and structures of albumin, suggesting that little denaturation has occurred on HOPG. This work further demonstrates that the direct observation of biomolecules by STM is probable. © 1988 Academic Press, Inc.

Scanning tunneling microscopy (STM) has enabled scientists to probe structure and topography at the Angstrom level. STM has been successfully applied to conducting and semiconducting materials (1, 2). Application to biomaterials, however, seems to be a controversial subject. Adsorbed biological substances are normally insulators and are generally mobile. Thus they are difficult to "see" by STM. Although such difficulties can be overcome by surface coating with conducting materials (3, 4), the direct observation of biomaterials is more attractive, as direct observation minimizes artifacts and makes *in situ* measurements possible. A few published papers have given images of bacteriophage (5), DNA (6, 7), lipid bilayers (8), and proteins (9, 10) though the image formation mechanism remains unexplained. Our STM experience suggests that biological substances can be sensed by STM, depending on the type of molecular species, its adsorbed state, its hydration degree, the tip shape, the stability of the STM instrument, etc. In this report we present two STM pictures of protein molecules adsorbed on highly oriented pyrolytic graphite (HOPG). The images reveal the best resolution so far achieved by STM on proteins. The result unambiguously indicates the feasibility of direct observation of biomacromolecules with STM.

Human serum albumin has a concentration of about 42 g/liter in plasma and constitutes 60% of the mass of plasma proteins (11). It is a single polypeptide chain consisting of 584 amino acid residues and having a molecular weight of about 69,000. Albumin has a strong internal structure, held firmly together by 17 disulfide bridges. Figure 1 shows the three-dimensional molecular model. The molecular shape is generally taken as an ellipsoid with dimensions of 40×140 Å. There are three domains within the molecule. The domain structure is believed to be a cylinder formed by six α -helices (11).

The STM images of human albumin are presented in Fig. 2. Figure 2a shows one adsorbed human albumin molecule and some parts of two other molecules on HOPG. They have different orientations. The molecular dimensions are 120 Å in length and 60 Å in width. The slight

deviation in dimensions of the adsorbate from those of the above model may be caused by slight collapse of the native structure in the relatively dry air environment. Three cylindrical, parallel domains can be observed, as expected from the model, suggesting that the surface denaturation is not extensive. In addition to domains, some side loops connecting the domains can also be seen. The fact that domains can be distinguished means that the resolution is about 10 Å. The flat regions around the adsorbed molecules have been identified as bare HOPG. In fact, the tiny ripples along the scanning lines in Fig. 2b are the corrugation of graphitic carbon atoms, commonly observed by STM on HOPG (1). The surface depression to the left of each adsorbed molecule is considered an influence of the adsorbed species. This area should actually be the flat substrate, which can be confirmed by the existence of the atomic corrugations in that region. Similar observations have been reported (12).

Figure 2 gives information on adsorption as well. Certain carbon materials have long been considered to have excellent biocompatibility (13, 14). One of the hypotheses is that there is not much denaturation of proteins adsorbed on a carbon surface. Although HOPG is not quite the same as those carbon materials, its adsorbing behavior may still imply that this hypothesis is reasonable. The albumin molecules essentially kept their native state in the presence of interactions between the adsorbate and the adsorbent. From this respect it is worth studying the adsorption under water in the future.

In summary, we have been able to obtain STM images of albumin and of its domain structure on HOPG. This work confirms that STM can be employed to study some biological substances under certain experimental conditions, such as for protein adsorption on conducting substrates. We have observed several different proteins deposited on HOPG. We consider that the image formation mechanism is related to charge transfer processes in the protein (15). By the aid of scanning tunneling spectroscopy (STS) (16), STM might become a powerful tool to study the electronic properties of proteins.

0021-9797/88 \$3.00

Copyright © 1988 by Academic Press, Inc.
All rights of reproduction in any form reserved.

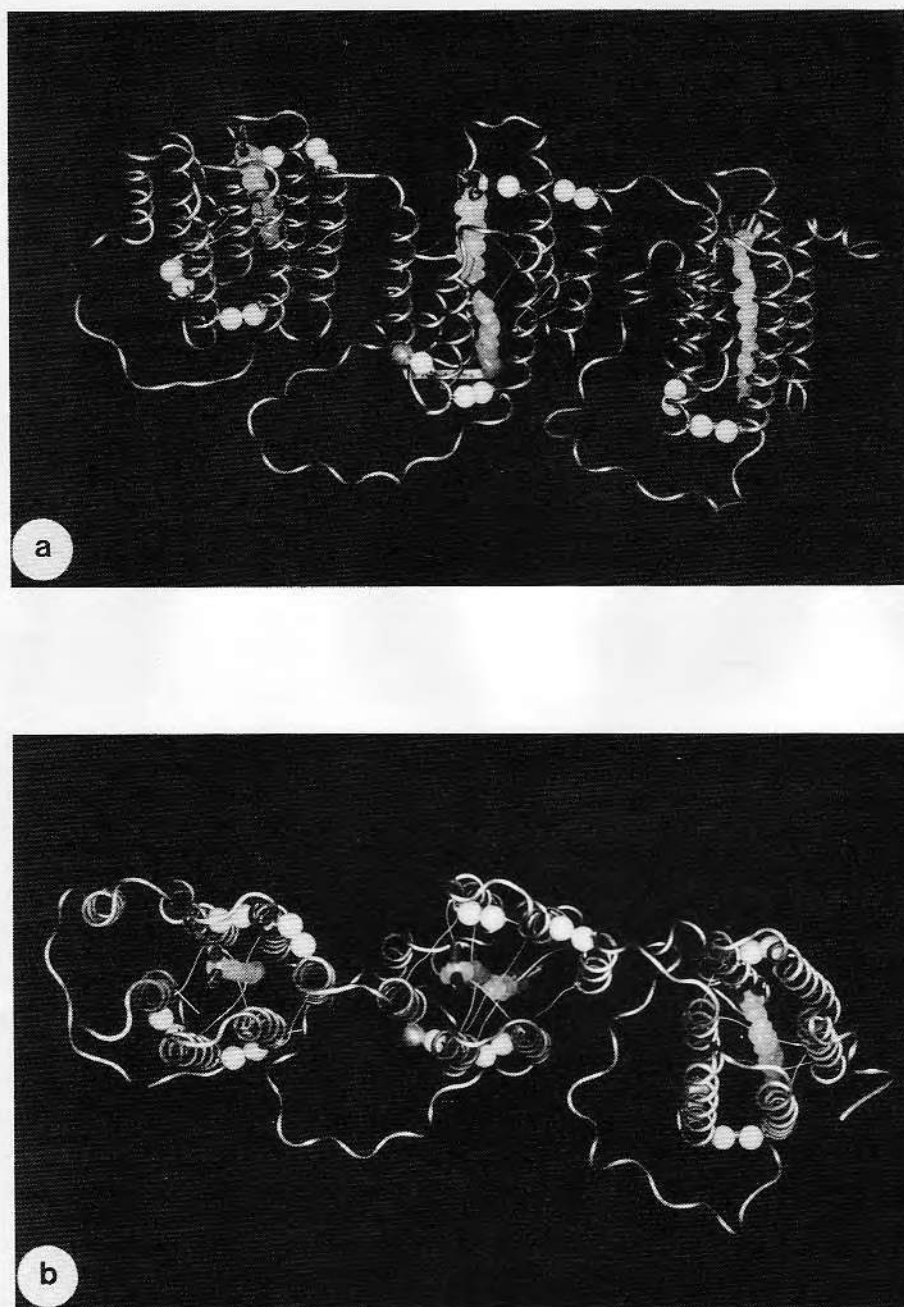


FIG. 1. Backbone three-dimensional model of serum albumin. In this model the wire represents the peptide backbone and the spheres represent disulfide bridges in the long loops. (a) Side view of the model. The three domains are antiparallel to one another. (b) Top view of the same model. The length is 140 Å and the width 40 Å for the entire molecule (from Ref. (11) by permission of the author).

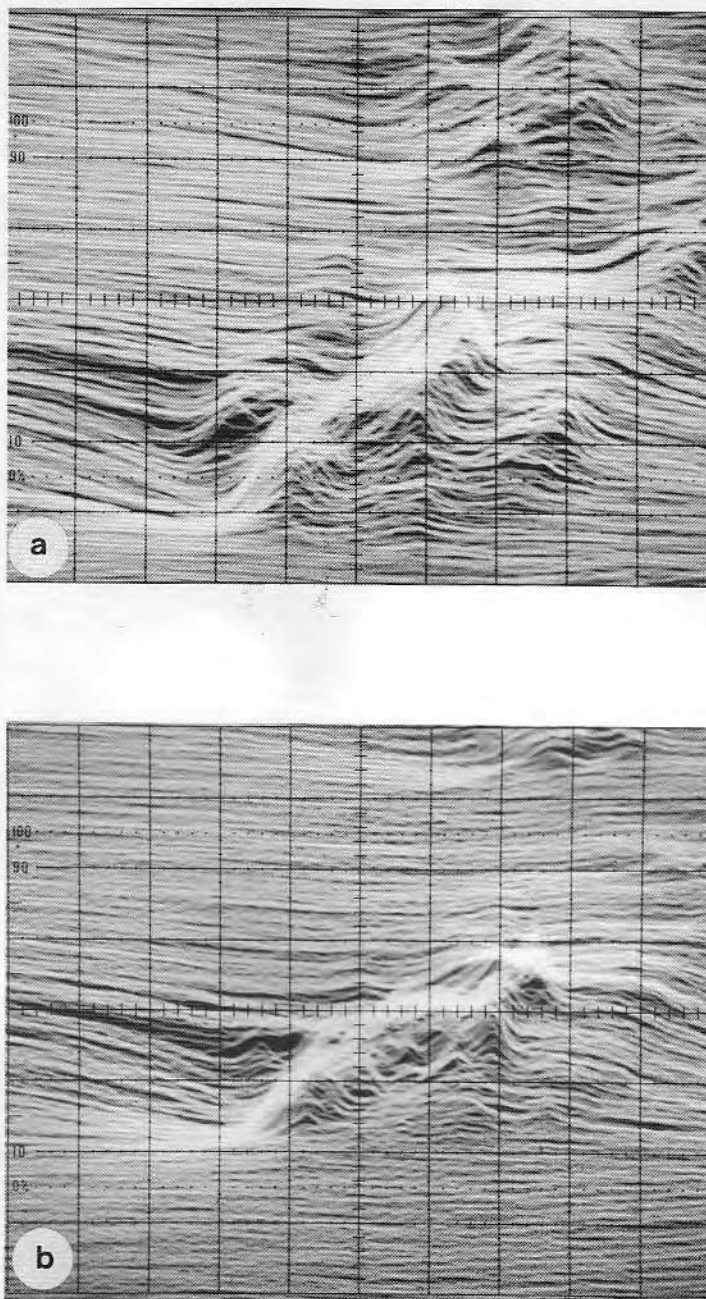


FIG. 2. Images of human albumin on HOPG. The picture dimensions are 200 \AA in the horizontal (x) and 160 \AA in the vertical (y) directions. Since the adsorbate has a very different electronic structure from the substrate, the height (z direction) could not be directly measured. Both (a) and (b) show several different molecules. Three domains can be clearly seen (a). The ripples on the raster lines in (b) are the corrugations of carbon atoms of the HOPG. The sample was prepared by depositing a droplet of albumin (Calbiochem) in phosphate-buffered saline solution (pH 7.4, 10 ppm albumin) onto freshly cleaved HOPG and then the droplet was removed by capillarity with a tissue. The sample was then flushed with water for 10 s and was dried at room temperature for 5 h before observation. The STM was operated in air with a bias voltage of 200 mV, tunneling current of 4 nA, and high feedback gain. The tungsten tip was electrochemically etched in 2 M KOH. Constant height mode was used with the scanning rates 40 Hz in x and 0.05 Hz in y .

ACKNOWLEDGMENTS

We thank Professor C. F. Quate, Stanford University, for stimulating our interest and activity in STM, Dr. Moore of the Union Carbide Corp. for the donation of the highly oriented pyrolytic graphite, and Professor J. R. Brown, University of Texas at Austin, for providing the albumin model pictures. We also thank the Center for Biopolymers at Interfaces, a state of Utah Center of Excellence, for partial support of this work.

REFERENCES

1. Hansma, P. K., and Tersoff, J., *J. Appl. Phys.* **61**, R1 (1987).
2. Hu, C. Z., Feng, L., and Andrade, J. D., *Carbon* **26**, 543 (1988).
3. Amrein, M., Stasiak, A., Gross, H., Stoll, E., and Travaglini, G., *Science* **240**, 514 (1988).
4. Zasadzinski, J. A., Schneir, J., Gurley, J., Elings, V., and Hansma, P. K., *Science* **239**, 1013 (1988).
5. Baro, J. M., Miranda, R., Alaman, J., Garcia, N., Binnig, G., Rohrer, H., Gerber, C., and Carrascosa, J. L., *Nature (London)* **315**, 253 (1985).
6. Travaglini, G., Rohrer, H., Amrein, M., and Gross, H., *Surf. Sci.* **181**, 380 (1987).
7. Lindsay, S. M., and Barris, B., *J. Vac. Technol. A* **6**, 544 (1988).
8. Smith, D. P. E., Bryant, A., Quate, C. F., Rabe, J. P., Gerber, C., and Swalen, J. D., *Proc. Natl. Acad. Sci. USA* **84**, 969 (1987).
9. Dahn, D. C., Watanabe, M. O., Blackford, B. L., Jericho, M. H., and Beveridge, T. J., *J. Vac. Technol. A* **6**, 548 (1988).
10. Horber, J. K. H., Lang, C. A., Hansch, T. W., Heckl, W. M., and Mohwald, H., *Chem. Phys. Lett.* in press.
11. Brown, J. R., and Shockley, P., in "Lipid-Protein Interactions" (P. C. Jost and O. H. Griffith, Eds.), Vol. 1, p. 25. Wiley, New York, 1982.
12. Foster, J. S., Frommer, J. E., and Arnett, P. C., *Nature (London)* **331**, 324 (1988).
13. Haubold, A. D., Shim, H. S., and Bokros, J. C., in "Biocompatibility of Clinical Implant Materials" (D. F. Williams, Ed.), Vol. 2, p. 3. CRC Press, Boca Raton, FL, 1978.
14. Haubold, A. D., *ASAIO J.* **6**, 88 (1983).
15. Kuki, A., and Wolynes, P. G., *Science* **236**, 1647 (1987).
16. Binnig, G., et al., *Phys. Rev. Lett.* **55**, 991 (1985).

L. FENG
C. Z. HU
J. D. ANDRADE¹

Department of Bioengineering and Center
for Biopolymers at Interfaces
University of Utah
Salt Lake City, Utah 84112

Received August 11, 1988; accepted August 16, 1988

¹ To whom correspondence should be addressed.

Scanning tunnelling microscopic images of amino acids

by L. FENG, C. Z. HU and J. D. ANDRADE*, *Department of Bioengineering and Center for Biopolymers at Interfaces, University of Utah, Salt Lake City, Utah 84112, U.S.A.*

KEY WORDS. Amino acids, adsorption, graphite, charge transfer.

SUMMARY

We present images of amino acids adsorbed on highly orientated pyrolytic graphite (HOPG) obtained with the scanning tunnelling microscope (STM) in air. Individual molecules can be observed although the majority of adsorbates appear to form clusters. In the case of leucine, methionine, and tryptophan, two molecules often associate together to form a dimer. Single or dimer glycine molecules were not seen, but a cluster of a number of them was observed. The various adsorbed states may be related to the different interactions between the amino acids and the graphite surface. The mechanism of image formation of the amino acids is probably related to charge transfer mechanisms.

The scanning tunnelling microscope (STM) has been used for studies of a number of organic and biological substances, including copper phthalocyanine Gimzewski *et al.* (1987), sorbic acid, Smith (1987), bacteriophage, Baro *et al.* (1985), DNA, Travaglini *et al.* (1987) and Lindsay & Barris (1988), proteins, Dahn *et al.* (1988), and lipid bilayer, Smith *et al.* (1987) on various substrates. The results have indicated that the STM may be applied in biology owing to its high resolution, ambient and under-liquid working conditions, and easy operation. Here we report the STM observation of four amino acids adsorbed on highly orientated pyrolytic graphite (HOPG).

The STM was provided by the Tunneling Microscope Co. based on the D. Smith design, Smith (1987). The HOPG, from Union Carbide, was readily peeled with a tape. Tryptophan (trp) was from Calbiochem-Behring Co. and glycine (gly), leucine (leu), and methionine (met) were from Sigma Chemical Co. Their chemical structures and planar dimensions based on the CPK[®] atomic models (Ealing Corp.) are shown in Fig. 1. Their aqueous solutions were prepared by dissolving amino acids in pure water (10 M Ω /cm). The concentrations were all 0.1 mg/ml for the STM measurement. A drop of the solution was placed on a freshly cleaved HOPG surface for 5 min before the surface was flushed with ultra-pure water for a very short time. The adsorbed specimens were dried at room temperature and normal pressure for at least overnight before the image was taken. The STM study was performed in air. Constant height mode was used as it gave better resolution and less distorted images than the constant current mode, Smith (1987). In this mode the gap distance is held invariant, and the tunnelling current

*To whom correspondence should be addressed.

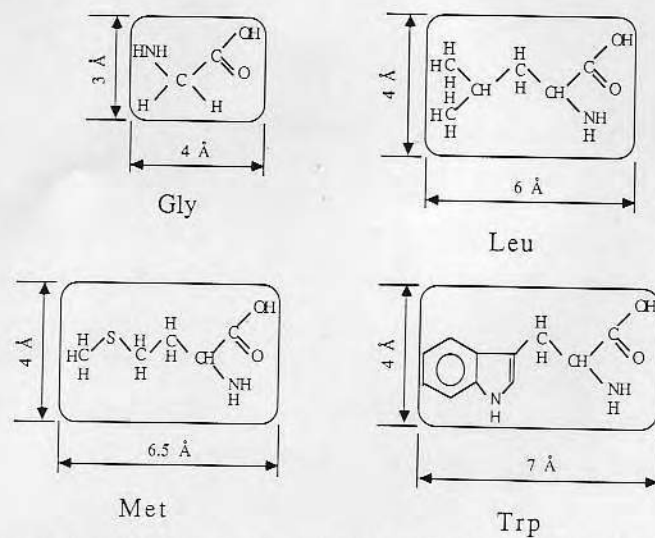


Fig. 1. Chemical structures and molecular sizes, estimated from the CPK[®] atomic models, for the four amino acids.

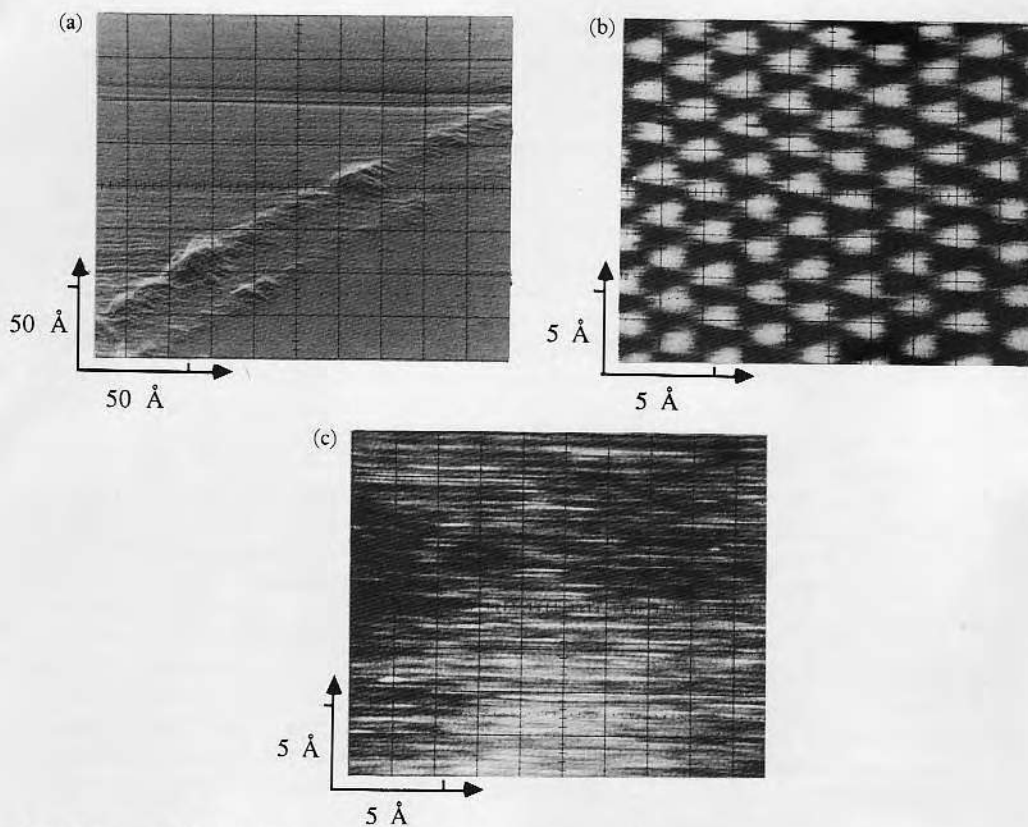


Fig. 2. Images of deposited trp. (a) Low magnification image. (b) High magnification graphitic image of the upper left part of (a). (c) High magnification trp image of the lower right part of (a).

changes according to the surface contour and composition during x-y scanning of the tip. It is this change that provides information on the adsorbed species. The tungsten tip was electrochemically etched in a 2 M KOH aqueous solution (Smith, 1987). Operating parameters included 1–2 nA tunnelling current, 0.2–0.8 V bias voltage, and 1 kHz scan rate in X direction and 1 Hz in Y direction. The images were displayed by a grey-scale oscilloscope and the pictures were taken by a CRT camera.

In order to assure that amino acid molecules could be observed under the STM, a relative large amount of trp was deposited on HOPG without flushing. Figure 2(a) shows that there are two rows dividing the picture into two parts. When the magnification was increased to ten times, the image of the upper left part, Fig. 2(b) is that characteristic of a typical HOPG surface. The lower right part, Fig. 2(c) shows no graphitic character, however, and the surface was much rougher. Here the current variation reached 5 nA during scanning. Since these two pictures were taken under identical conditions and almost simultaneously, it is thought that they represent two different surface states. The latter, Fig. 2(c) image, should be of the adsorbate layer and the rows in Fig. 2(a) are presumably its edge. Therefore, amino acids can change the tunnelling current and can be detected by the STM. The principle of the STM has been described in detail, Hansma & Tersoff (1987). Amino acids and proteins have long been thought to be semiconductors since charge transfer can occur between their functional groups with the aid of impurities, such as metal ions or water (Gutmann & Lyons, 1967; Jortner & Bixon, 1987); particularly, sorbed water may play a very important role (Panitz, 1987). Water could 'raise the dielectric constant and therefore stabilize the electron-hole pair, thus increasing the number of charge carriers', (Eley & Leslie, 1963), which would enhance the tunnelling current via charge transfer mechanisms.

The majority of the images showed segregated clusters. The non-uniform distribution was a routine observation in these studies. Despite their rare occurrence some individual molecules were observed and they are clearly shown in Figs. 3–6 for each of the four amino acids. We suggest that the bright humps represent the amino acid molecules because: (a) the dimensions of the four species, estimated with reference to the graphitic crystal lattice, agree with those from the molecular models (see the insertions in each figure); (b) the 'bright humps' were frequently observed for the adsorbed samples but similar images were not seen on clean HOPG

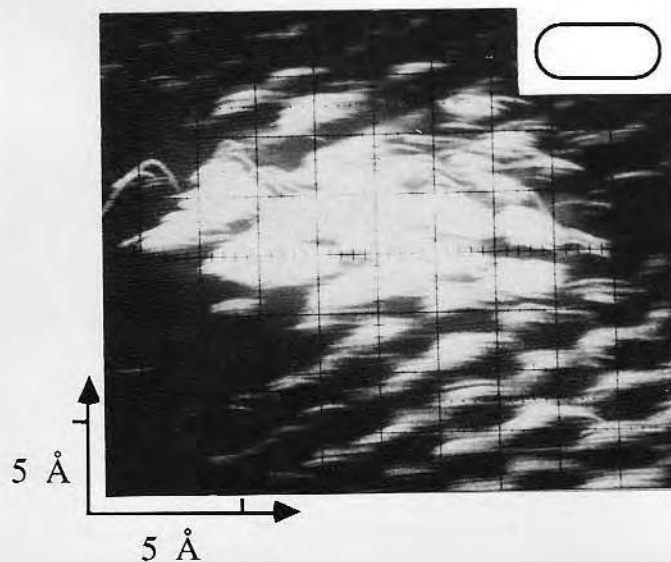


Fig. 3. Gly image. The insertion is the molecular size, based on CPK models, of the same magnification as the image. A number of gly molecules apparently pack together. The distance in between is about 3 Å.

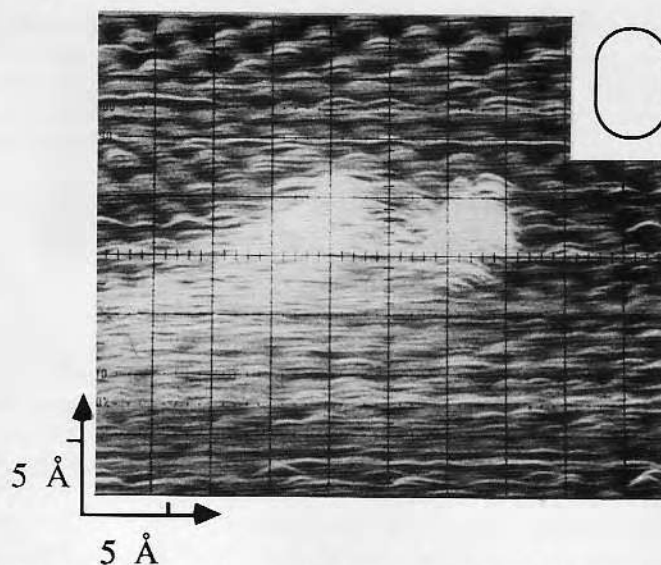


Fig. 4. Trp image. The insertion is the molecular size, based on CPK models, of the same magnification as the image. A dimer of two parallel packed molecules can be seen. The distance in between is about 9 Å.

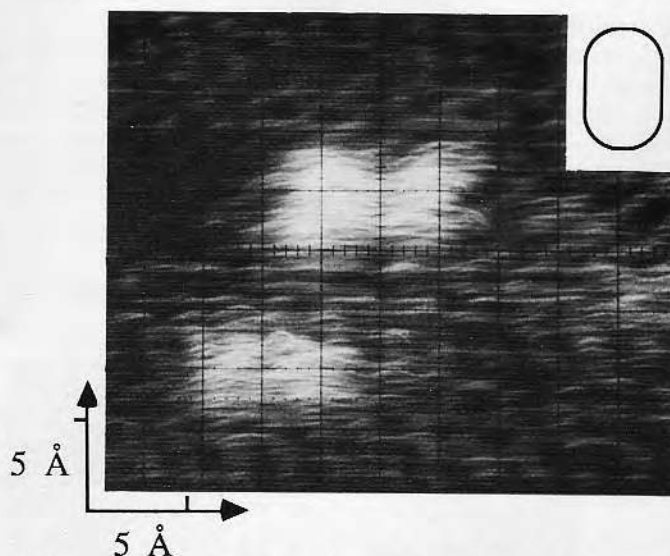


Fig. 5. Leu image. The insertion is the molecular size, based on CPK models, of the same magnification as the image. Three leu molecules can be seen, two of which are associated to form a dimer. The distance between the two is about 5 Å.

surfaces or on a control sample which had undergone identical sample preparation procedures except for no amino acids; (c) taking pictures of the bright humps proved to be difficult since they tended to escape very easily due to their weak interactions with the substrate; (d) adsorption from the atmosphere was not given strong consideration because graphite surface images were routinely obtained on 'clean' HOPG, even samples used several days after cleavage; (e) hydrocarbon impurities, if any, are not normally seen by STM, (Schneir &

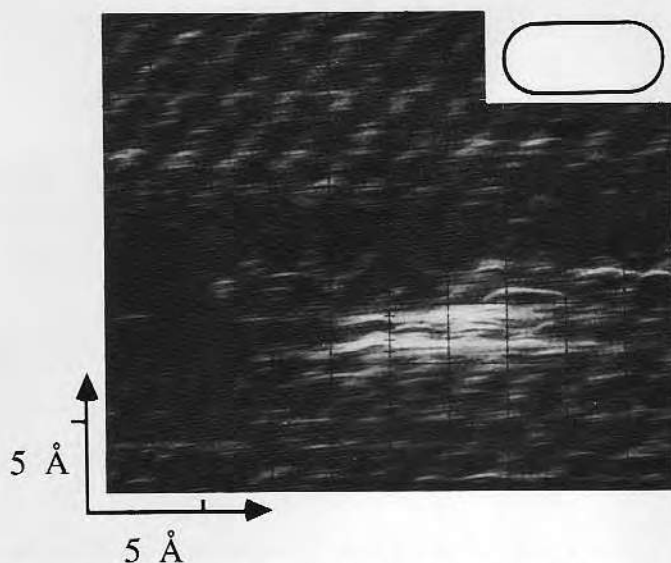


Fig. 6. Met image. The insertion is the molecular size, based on CPK models, of the same magnification as the image. One met molecule is lying horizontally on HOPG. Dimers were often observed but the pictures are poor in quality.

Hansma, 1987); and (f) all the pictures in this paper are representative of many observation events.

It is interesting to look at the molecular packing of the different adsorbates. The simplest amino acid, gly, formed arrays, each of which contains a number of gly molecules (Fig. 3). Another characteristic is the dimer aggregation for both trp and leu (Figs. 4 and 5). Dimers were also observed with met. The dimer or trimer phenomenon was not uncommon except for gly. In fact it was very difficult to spot a single separated molecule, such as met in Fig. 6. A dimer was not a double tip artefact because not everything on the image was doubled. It is thought there are two reasons for the dimer or multimer formation. Amino acids can form pairwise 'side-on' associations in their aqueous solutions, (Lilley, 1985). The dimer association may remain intact during the adsorption process. On the other hand, a single amino acid molecule does not have a strong interaction with the HOPG surface. Without the association, it would be quite volatile due to its low molecular weight. This explains its observed mobility under the STM observation. That is why we often located one single molecule but it soon disappeared before we could take a picture. Those that were imaged may have adhered to some sort of surface defect, which could increase adsorbent-adsorbate interactions. The smaller amino acids require more intermolecular interactions in order to form a stable adsorbed state. It is why we only saw gly clusters rather than dimers.

At this time the possibility of selective adsorption of impurities cannot be completely ruled out and further work is necessary, such as scanning tunnelling spectroscopy, (Smith, 1987). Although we have much more to observe and to learn about electron tunnelling and STM analysis of amino acids and larger biomolecules, it is clear that STM offers considerable potential for surface studies of biomolecules.

ACKNOWLEDGMENTS

We thank Professor C. F. Quate for stimulating our interest and activity on STM and Dr D. Smith for assistance with the STM. We also thank Dr Moore of the Union Carbide Corp. for the donation of the highly orientated pyrolytic graphite. This work was funded by the Center for Biopolymers at Interfaces, University of Utah.

REFERENCES

- Baro, J.M., Miranda, R., Alaman, J., Garcia, N., Binnig, G., Rohrer, H., Gerber, C. & Carrascosa, J.L. (1985) Determination of surface topography of biological specimens at high resolution by scanning tunneling microscopy. *Nature*, **315**, 253-254.
- Dahn, D.C., Watanabe, M.O., Blackford, B.L., Jericho, M.H. & Beveridge, T.J. (1988) STM imaging of biological structures. *J. Vac. Sci. Technol. A*, **6**, 548-552.
- Eley, D.D. & Leslie, R.B. (1963) Electrical conduction in solid protein. In: *Electronic Aspects of Biochemistry; proceedings* (ed. by B. Pullman), pp. 105-117. Academic Press, New York.
- Gimzewski, J.K., Stoll, E. & Schlittler, R.R. (1987) Scanning tunneling microscopy of individual molecules of copper phthalocyanine adsorbed on polycrystalline silver surfaces. *Surface Sci.* **181**, 267-271.
- Gutmann, F. & Lyons, L.E. (1967) *Organic Semiconductors*, pp. 421-447. Wiley & Son, New York.
- Hansma, P.K. & Tersoff, J. (1987) Scanning tunneling microscopy. *J. Appl. Phys.* **61**, R1-R23.
- Jortner, J. & Bixon, M. (1987) Charge exchange between localized sites. In: *Protein Structure* (ed. by R. Austin), pp. 277-308. Springer-Verlag, New York.
- Lilley, T.H. (1985) *Chemistry and Biochemistry of Amino Acids* (ed. by G. C. Barrett), pp. 591-624. Chapman & Hall, London.
- Lindsay, S.M. & Barris B. (1988) Imaging DNA molecules on a metal surface under water by STM. *J. Vac. Technol. A*, **6**, 544-547.
- Panitz, J.A. (1987) Electron tunneling used as a probe of protein adsorption at interfaces. In: *Proteins at interfaces* (ed. by J. Brash and T. Horbett), pp. 422-434. Amer. Chem. Soc. Symp. Series 343, Washington, DC.
- Schneir, J. & Hansma, P.K. (1987) Scanning tunneling microscopy and lithography of solid surfaces covered with nonpolar liquids. *Langmuir*, **3**, 1025-1027.
- Smith, D.P.E. (1987) *New applications of scanning tunnelling microscopy*. Ph.D. thesis, Stanford University, Stanford, CA.
- Smith, D.P.E., Bryant, A., Quate, C.F., Rabe, J.P., Gerber, C. & Swalen, J.D. (1987) Images of a lipid bilayer at molecular resolution by scanning tunneling microscopy. *Proc. natl. Acad. Sci. USA*, **84**, 969-972.
- Travaglini, G., Rohrer, H., Amrein, M. & Gross, H. (1987) Scanning tunneling microscopy on biological matter. *Surface Sci.* **181**, 380-390.

SCANNING TUNNELING MICROSCOPY OF PROTEINS ON GRAPHITE SURFACES

L. Feng, J.D. Andrade*, and C.Z. Hu

Department of Bioengineering & Center for Biopolymers at Interfaces
 College of Engineering
 University of Utah
 Salt Lake City, Utah 84112
 U. S. A.

(Received for publication April 09, 1989, and in revised form July 29, 1989)

Abstract

We applied scanning tunneling microscopy (STM) to the observation of amino acids and proteins deposited and/or adsorbed on highly oriented pyrolytic graphite (HOPG).

Although many questions remain, it is demonstrated that relatively high resolution images of uncoated proteins can often be obtained in air. We present images of five amino acids (glycine, leucine, lysine, methionine and tryptophan) and three proteins (lysozyme, albumin and fibrinogen) under various conditions of deposition and adsorption. We discuss the role of affinity of the amino acids and proteins to the substrate, their adsorbed states and distribution, and STM tip-induced deformation and/or destruction.

STM studies of adsorbed proteins are expected to provide useful and even unique information on the conformation and packing of the proteins.

Introduction

Scanning tunneling microscopy (STM) is a new and fast growing surface analysis and imaging technique. In the seven or so years since its invention by Binnig and Rohrer (Binnig et al., 1982), STM has been gradually increasing in popularity in the imaging of conducting and semi-conducting surfaces (Binnig and Rohrer, 1985, Quate, 1986, and Hansma and Tersoff, 1987). Such rapid progress is due to the unparalleled capabilities of STM compared with other forms of microscopy: (1) ultra-high resolution down to atomic dimensions, (2) three-dimensional images, especially with a very high sensitivity in the vertical direction, (3) a variety of operating conditions, including vacuum, air and even liquids, (4) observation range from 10^{-6} to 10^{-10} m, (5) the ability to do tunneling spectroscopy, and (6) relatively inexpensive equipment.

The operating principle of STM is surprisingly simple. When a metal needle-like probe (tip) is brought close enough to a conducting surface (1-10 Angstroms), electrons tunnel through the gap between the tip and the surface under an appropriate bias voltage, producing a tunneling current. The tunneling current is a function of the bias voltage and the shape of the barrier (related to work function) and is extremely sensitive to the gap distance. The tunneling current is changed by a factor of 10 when the distance changes just 1 Angstrom for a local work function of 4 eV. It is this strong distance dependence that is the reason for STM's high vertical resolution. When the tip is rastered across the surface using a piezoscanner, a feedback network adjusts the height of the tip above the substrate surface to keep the tunneling current constant; this is called the constant current mode. Alternately, the change in the tunneling current can be recorded at a constant tip height: the constant height mode. In

KEY WORDS: Scanning tunneling microscopy, Biological applications, Highly oriented pyrolytic graphite, Proteins, Amino acids, Lysozyme, Albumin, Fibrinogen.

*Address for correspondence:
 Department of Bioengineering
 College of Engineering, University of Utah
 Salt Lake City, UT 84112
 U.S.A. Phone No. (801) 581-4379

both modes a surface topographical map is obtained (Hansma and Tersoff, 1987), as in Figure 1, if the substrate has a chemically homogeneous surface. Suppose there is an adsorbed molecule on a conducting surface; it may perturb the magnitude of the local tunneling current due to a change in local work function. The molecule is "imaged" through the change of the local current. This is the probable mechanism by which an adsorbate is detected by STM (Panitz, 1987 and Spong et al. 1989). Since the adsorbate usually does not have the identical chemical composition and structure as the substrate, the tunneling current map does not necessarily represent the same surface topography.

Since our group has a strong involvement in the study of proteins at interfaces (Andrade, 1985), we have a particular interest in applying STM to this area. Our rationale is as follows: conventional TEM or SEM generally needs a high vacuum system, which often distorts the protein native state. Often a coating is necessary to minimize sample charging and to enhance the contrast; such coating can easily introduce artifacts and thereby decrease the useful resolution. Labeling adsorbed proteins with heavy metals, such as gold, does not give a sufficiently high resolution in the SEM, and it depends on labeling efficiency and other factors. However, with an in-air-operated STM it is possible to observe proteins in their hydrated state in a humid environment. It is even possible to see proteins in solution with an appropriately designed and constructed STM. Proteins are considered semiconductive in their usual hydrated state (Jortner and Bixon, 1987).

The resolution of STM for protein molecules should be higher than in SEM or TEM. So long as the substrate conducts electricity, STM may be employed.

A brief review of STM applications in biology

Listed here are the major obstacles in applying STM to the study of proteins. (1) They are, in general, poor conductors of electricity so that they may not significantly alter the tunneling current; (2) they are relatively soft and flexible so that they tend to "smear out" the image and lower the resolution because of their motion and relaxation in the presence of the tip and the applied electric field; (3) their molecular structure is often not well characterized so that image interpretation is difficult; and (4) they may have weak interactions with the conducting substrate to which they are attached so that they are often perturbed or moved by the moving tip. Nevertheless, many biological as well as organic substances in different forms have been observed by STM. A few review papers are now available (Hansma et al., 1988 and Zasadzinski, 1989).

The very first paper of STM images of a biological substance, DNA, appeared in 1983 (Binnig and Rohrer, 1983), unveiling the possible application of STM in biology. Baro et al. (1985, 1986) reported the surface topography of bacteriophage f29 on graphite. There have been a number of papers on imaging Langmuir-Blodgett films on different substrates by STM, with arachidate on graphite (Smith et al., 1987), dimyristoylphosphatic acid on both

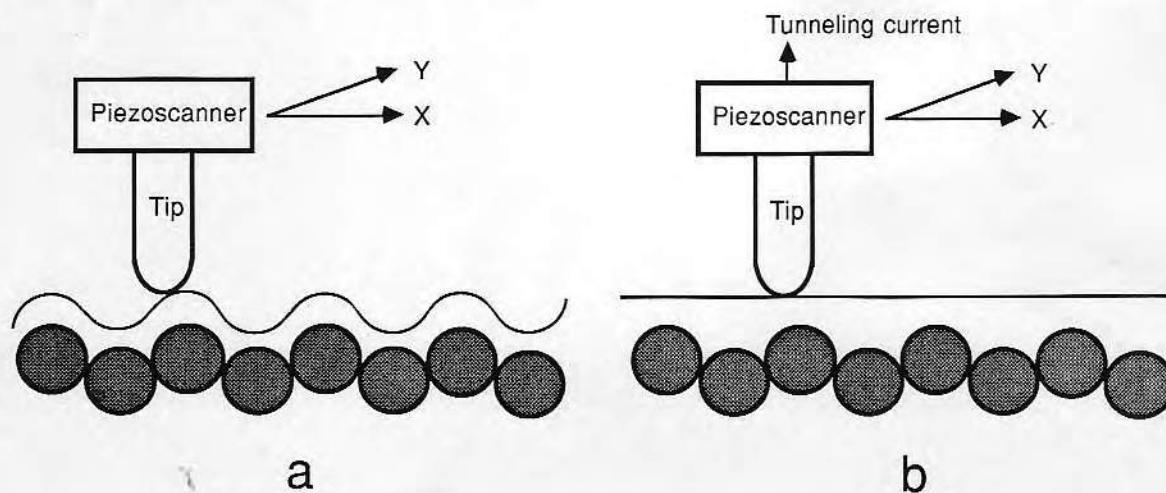


Figure 1. Schematic expression of operating principles of scanning tunneling microscopy in either the constant current mode and constant height mode.

graphite and gold (Horber et al., 1988), o-tricosenoic and 12,8-diynoic acids (Cd salts) on silicon wafer and graphite (Braun et al., 1988). It seems that with such regularly packed structures, the molecules are much easier to image and distinguish and the resolution is higher compared to individual or randomly packed molecules. The same is true when imaging liquid crystals (Foster and Frommer, 1988 and Spong et al., 1989) and TTF-TCNQ crystals (Sleator and Tycko, 1988). Stemmer et al. (1987) have managed to image biological membranes (porin membrane). Membranes prepared by freeze-fracture replica methods show much more detail (Joseph et al., 1988). Studies of single stranded DNA have produced impressive results. Travaglini et al. (1987) started the study of bare DNA molecules. Later the same group obtained images of DNA by means of conducting film coatings (Amrein et al., 1988). Beebe et al. (1989) achieved a similar resolution on uncoated double-stranded DNA using STM. DNA images under water were obtained by Barris et al. (1988) and Lindsay et al. (1989).

Few papers have dealt with the subject of STM observation of proteins. One of the earliest papers on protein STM images was by Dahn et al. (1988). While their work was mainly on bacterial sheaths, a globular protein, ovalbumin, was imaged. The molecules had become flattened and elongated presumably due to the dehydration. Horber et al. (1988) studied Concanavalin A embedded in a lipid film. They claimed that the four subunits of Con A might be seen. Simic'-Krstic' et al. (1989) recently observed microtubules on graphite fixed in 0.1% glutaraldehyde in both freeze dried and hydrated states. Microtubules frequently appeared buckled, semiflattened and/or twisted. Collagen strands of 15 Angstroms in diameter on graphite were imaged by Voelker et al. (1988). They suggested that the periodic spikes from the strand represented pyrrolidine rings of the proline and hydroxyproline amino acid residues. In contrast to the DNA images, proteins on a conducting substrate generally show a less defined structure and poorer resolution.

Since protein adsorption properties play an important role in the applications of biomaterials, we believe that it is worthwhile to utilize STM to explore the details in conformation and packing of adsorbed proteins. STM may also provide information on the electronic structure of proteins which will certainly benefit molecular electronics studies. In the rest of the paper, we will introduce our published and unpublished STM work on five amino acids and three proteins (Feng et al., 1988 and 1989).

Experiments

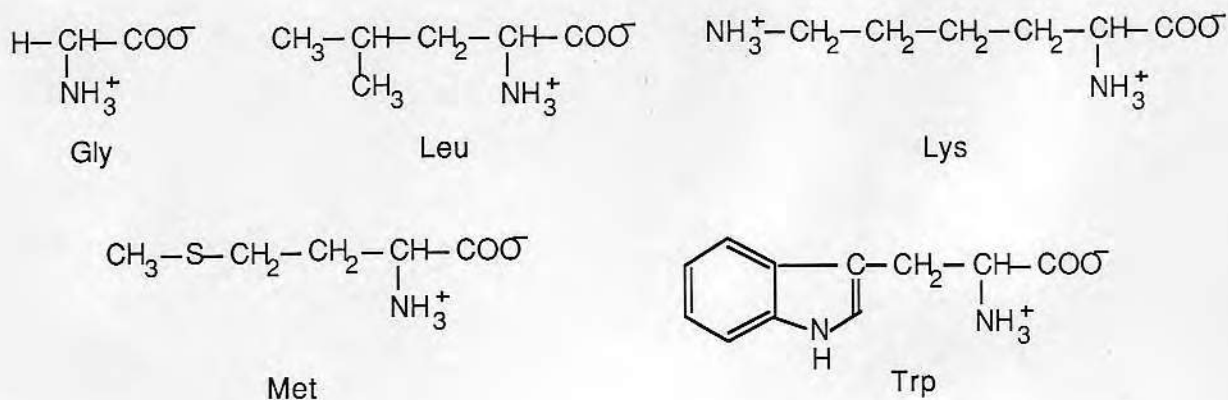
The substrate was highly oriented pyrolytic graphite (HOPG) from Union Carbide. As a routine substrate for STM, HOPG is a semimetal and relatively inert material. Cleaved by an adhesive tape, HOPG readily provides a large (1 mm x 1 mm) clean area with an atomically flat plane. Tryptophan (trp) was from Calbiochem and glycine (gly), leucine (leu), lysine (lys), and methionine (met) were from Sigma. Hen lysozyme was from Calbiochem, human serum albumin from Calbiochem and human fibrinogen from Calbiochem and Sigma. The amino acids and proteins were dissolved either in ultra-pure water (10 MΩ/cm) or in pH 7.4 phosphate buffered saline (PBS); amino acid concentrations were 0.1 mg/ml and protein concentrations were from 0.001 mg/ml (1 ppm) to 0.1 mg/ml (100 ppm). A droplet of the solution was pipetted onto a newly cleaved HOPG surface, which was either promptly removed by capillarity (for a deposited sample) or allowed to rest for 5 min before being flushed with ultra-pure water (for an adsorbed sample). All samples were dried at room temperature and ambient atmosphere (22°C and 20-50% R.H.).

Our STM was provided by the Tunneling Microscope Co. (Smith, 1987). STM tips were prepared by electrochemical etching a tungsten wire, 0.5 mm in diameter, in a 2 M KOH solution under a 20-30 V a. c. potential. The tips had diameters from 0.1-1 mm at the end as measured by TEM. STM was operated in air; both constant height and constant current modes were used. Parameters for a typical constant height mode were 200-800 mV bias voltage (Vb), tips being negative with respect to samples, 1-2 nA tunneling current (It), 1 KHz scan rate in x direction and 1 Hz in y direction. Parameters for a typical constant current mode were 50-400 mV bias voltage, tips being negative with respect to samples, 1-4 nA tunneling current, 30 Hz scan rate in x direction and 0.05 Hz in y direction. The magnification was calibrated by the lattice parameters of HOPG substrate. Real-time images were processed by a band pass filter to minimize high frequency noise, and displayed by an oscilloscope. The pictures were recorded from the oscilloscope by a CRT camera.

Results and discussion

Amino acids (Feng et al., 1988)

We first studied the amino acids since they are the simpler building blocks of complex proteins. All five amino acids adsorbed on HOPG were easily seen as aggregates (Figure 2). Adsorbates occupied roughly 5-10% of



a

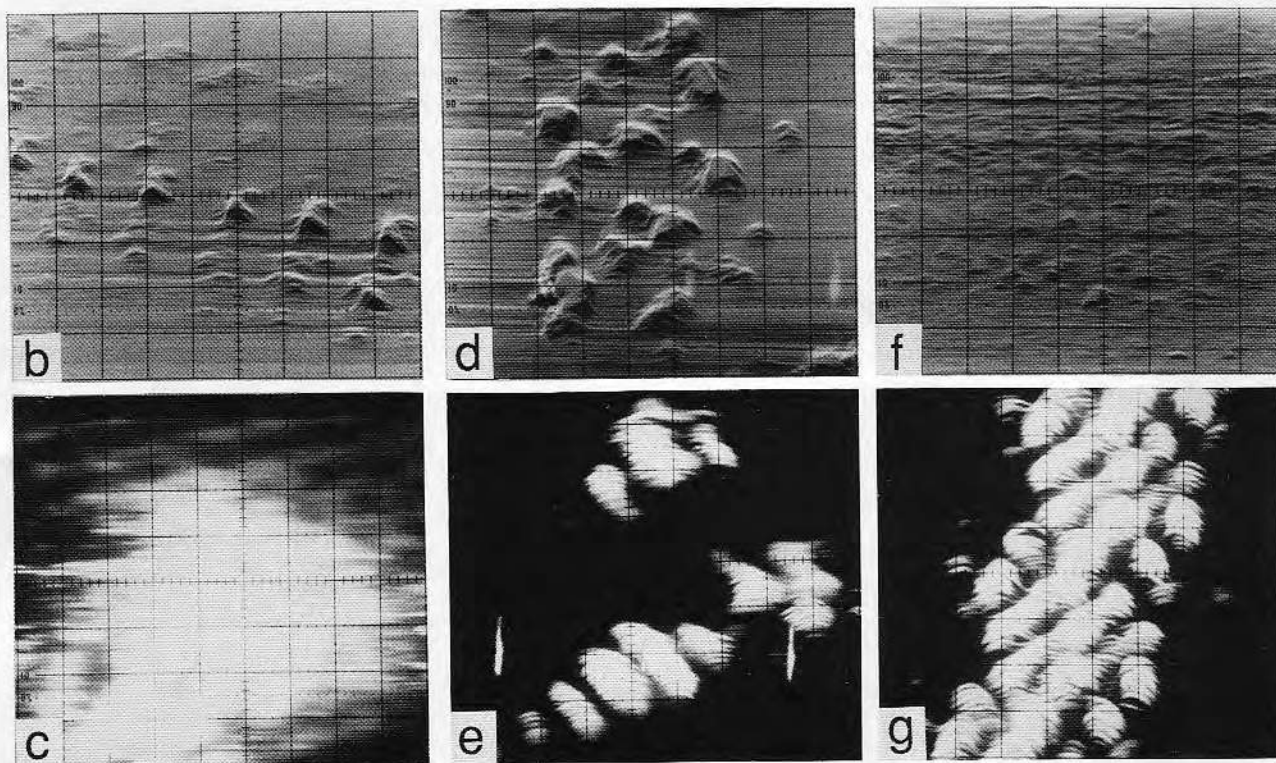


Figure 2. (a) Molecular formulas of the five amino acids. (b) - (g) Amino acids adsorbed from 0.1 mg/ml aqueous solutions on HOPG as aggregates: (b) Gly (Vb = 500 mV, It = 1 nA, 25 Angstroms/div): (c) One of the humps in (b), 2.5 Angstroms/div; (d) Lys (Vb = 300 mV, It = 1 nA, 25 Angstroms/div); the white vertical lines are photo defects; (e) Higher magnification of (d), 2.5 Angstroms/div; the white vertical lines are photo defects; (f) Met (Vb = 800 mV, It = 1 nA, 25 Angstroms/div); (g) Higher magnification of met (Vb = 300 mV, It = 1.8 nA, 2.5 Angstroms/div). In (c), (e) and (g), individual molecules can be barely seen. Constant height mode was used.

total surface, according to a statistical estimate with many regions. This value is much less than that expected from our radioisotope measurements, which gave about 80% coverage if monolayer adsorption was assumed. The discrepancy may be due to: (1) the presence of multilayer adsorbates which had been truncated by the STM tip because the gap distance was of the order of 1 Angstrom, (2) loss of adsorbates from the substrate when they were impounded by the rigid tip, and/or (3) incapability of imaging some adsorbates since they did not modify the tunneling current. From Figures 2 (c), (e) and (g) one could distinguish a few single molecules in those clusters. The apparent difference in their sizes is thought due to their different distances to the tip since they were randomly packed. More often than not, separate individual amino acid molecules were hard to find, presumably due to weak interactions between them and the substrate. Sometimes a molecule was spotted but it quickly disappeared from the image before a picture could be taken.

Occasionally, a few amino acid molecules were caught and imaged with better resolution, as in Figure 3. We suggest that the bright humps represent amino acid molecules because: (1) the dimensions of the three species, estimated with reference to the graphite crystal lattice, agree with those expected from the molecular models (see the insertions in each figure); (2) "bright humps" were frequently observed for the adsorbed samples but similar images were not seen on clean HOPG surfaces or on a control sample which had undergone identical sample preparation procedures except for no amino acids; (3) taking pictures of the bright humps turned out to be difficult since they tended to escape very easily due to their weak interactions with the substrate; (4) adsorption from the atmosphere was not given strong consideration because graphite surface images were routinely obtained on "clean" HOPG, even samples used several days after cleavage; (5) hydrocarbon impurities, if any, are not normally seen by STM, Schneir and Hansma(1987); and (6) all the pictures in this paper are representatives of many observation events. Dimers or trimers are relatively more stable than monomers in terms of interactions with the substrate so that they were immobile for a sufficient time for producing a photograph. No dimers or even trimers could be seen on gly samples because of gly's much smaller molecular weight and size.

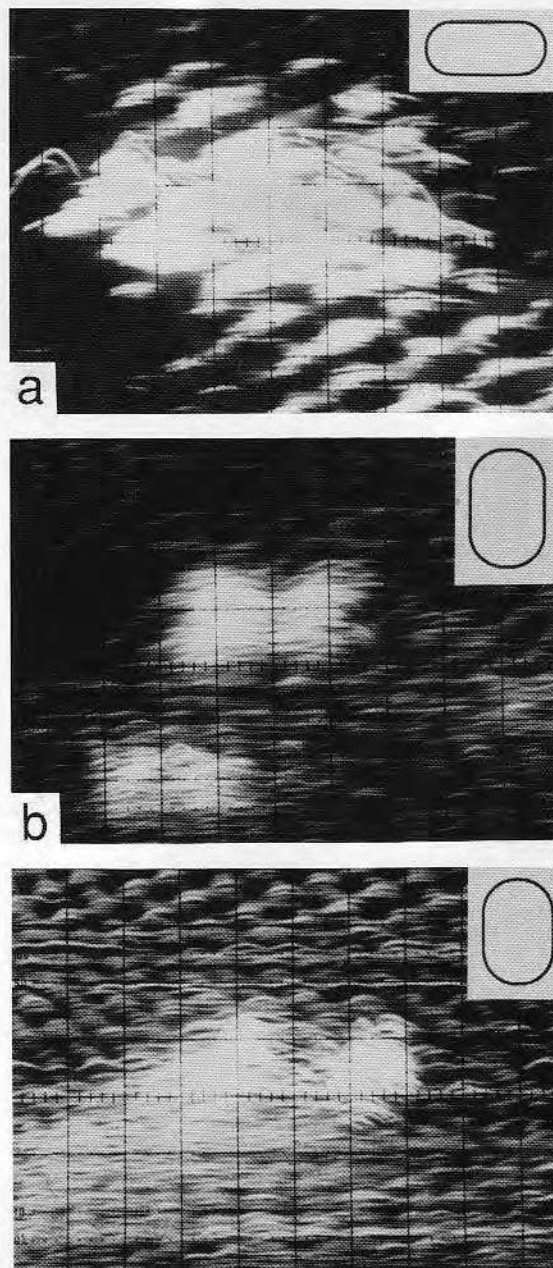


Figure 3. Images of individual amino acid molecules with constant height mode. The graphite substrate can be seen underneath. The insertions are the molecular sizes based on CPK models of the same magnification as the images. (a) Gly image (1.9 Angstroms/div in x and 3.2 Angstroms/div in y), a number of gly molecules apparently pack together; (b) Leu image (2.8 Angstroms/div in x and 3.2 Angstroms/div in y), three leu molecules being seen, two of which are associated to form a dimer; (c) Trp image (3.3 Angstroms/div in x and 3.8 Angstroms/div in y), a dimer of two parallel packed molecules being seen.

Hen egg-white lysozyme

Hen egg-white lysozyme is a small compact protein with molecular weight of 14,600, made up of a single polypeptide chain of 129 amino acids. Four disulfide bonds cross-link the molecule and provide high stability. Lysozyme has an ellipsoidal shape, with dimension of $45 \times 30 \times 30$ Angstroms (Stryer, 1988). ESCA measurement, Figure 4, shows that lysozyme has a large affinity for HOPG. The adsorbed monolayer (the plateau of the adsorption isotherm) was formed within 5 min even when the solution concentration was as low as 0.01 mg/ml, and virtually no desorption was detected.

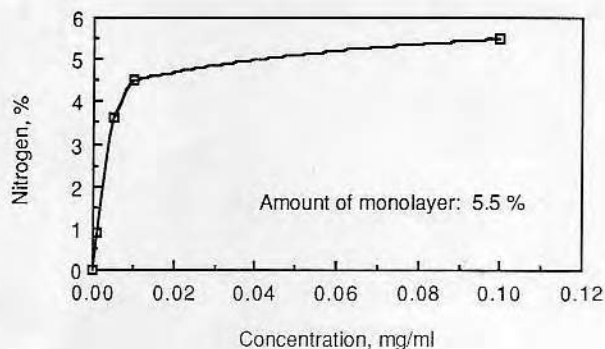


Figure 4. Lysozyme adsorption isotherm detected by ESCA (HP 5958C); adsorption time 5 min at 22°C, and water rinse 1 min.

In Figure 5(a), adsorbed lysozyme is observed by the constant height mode. The molecules apparently collapsed and merged into a rough film. The adsorbate film was apparently thin enough to have avoided being cut through by the STM tip. A very small number of molecules remained roughly of globular shape (Figure 5(b)). But this time their top portions were apparently truncated by the tip. In order to image the whole molecule, the constant current mode should be a better method for molecules with dimensions of more than several Angstroms.

Figure 6 is the image using the constant current mode. Again no individual molecules are recognizable even with higher magnification. Compared with Figure 5(a), this picture shows much rough adsorbates with many "hills" and "valleys". One of the reasons might be that the constant current mode tolerated much larger sized objects since the tip tried to go over them. Another possible reason is that the tip tended to mechanically push the molecules and piled them up if they did not enhance the

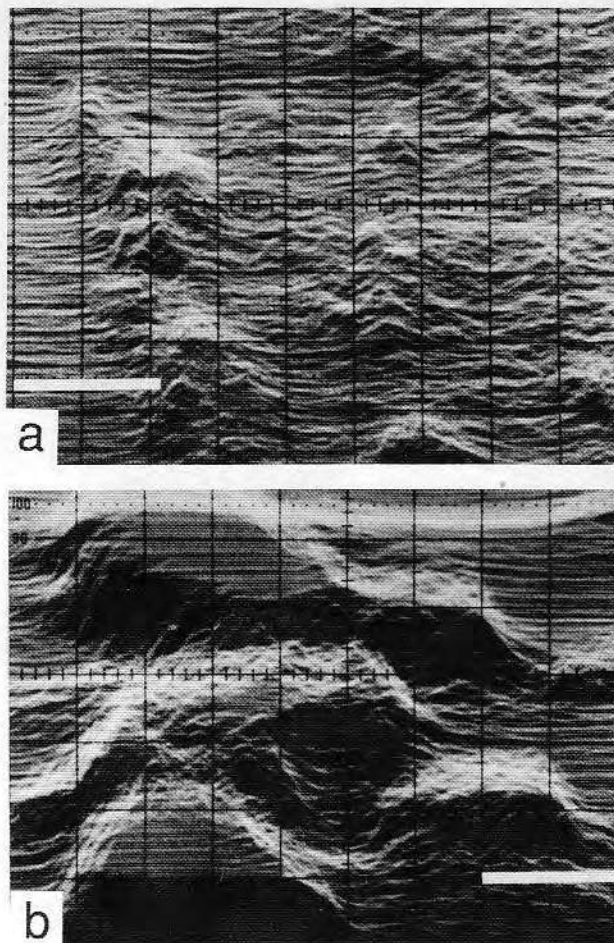


Figure 5. STM images of adsorbed lysozyme on HOPG, adsorption conditions: 0.1 mg/ml concentration, adsorption time 5 min at 22°C, and water rinse 1 min; STM conditions: constant height mode, $V_b = 800$ mV, $I_t = 2$ nA. (a) Most lysozyme molecules merged into a rough adsorbed layer, bar = 40 Angstroms. (b) In very few cases globular molecules remained but their top portions were apparently truncated by the tip, bar = 40 Angstroms.

tunneling current sufficiently to provide response in the gap distance adjustment. The latter perhaps dominated since lysozyme molecules had high resistivity and therefore were hardly "seen" by the tip.

Human serum albumin (Feng et al., 1988)

Human serum albumin consists of a single polypeptide chain of 584 amino acids with a molecular weight of about 69,000. Albumin has a strong internal structure, held firmly together by seventeen disulfide bridges. Figure 7

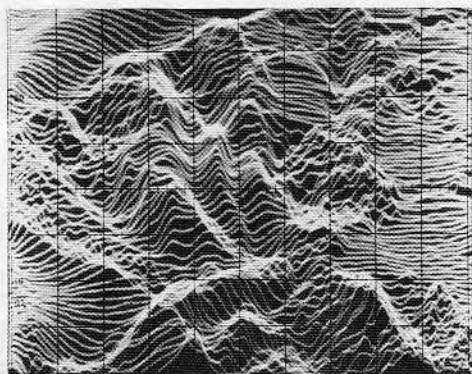


Figure 6. STM images (100 Angstroms/div) of adsorbed lysozyme on HOPG, adsorption conditions: 0.1 mg/ml concentration, adsorption time 5 min at 22°C, and water rinse 1 min; STM conditions: constant current mode, $V_b = 300$ mV, $I_t = 1.8$ nA.

shows the three-dimensional molecular model (Brown and Shockley, 1982). The molecular shape is generally taken as an ellipsoid with dimensions of 40 x 140 Angstroms. There are three domains within the molecule. The domain structure is believed to be a cylinder formed by six α -helices. This structure has now been partially confirmed by the recent x-ray crystal structure analysis (Carter et al., 1989).

The STM images of human albumin are presented in Figure 8 although they have been difficult to repeat. Figure 8(a) shows one adsorbed human albumin molecule and some parts of two other molecules on HOPG. They have different orientations. The molecular dimensions are 120 Angstroms in length and 60 Angstroms in width. The slight deviation in

dimensions of the adsorbate from those of the above model may be caused by slight collapse of the native structure in the relatively dry air environment. Three cylindrical, parallel domains can be observed, as expected from the model, suggesting that the surface denaturation may not be extensive. In addition to domains, some side loops connecting the domains can also be seen. The fact that domains can be distinguished means that the resolution is about 10 Angstroms. The flat regions around the adsorbed molecules have been identified as bare HOPG. In fact, the tiny ripples along the scanning lines in Figure 8(b) are the corrugation of graphitic carbon atoms, commonly observed by STM on HOPG. The surface depression to the left of each adsorbed molecule is due to the delayed time response of the tip, which was scanning from right to left. Figure 8 gives information on adsorption as well. The albumin molecules essentially maintained a nearly native state in the presence of interactions between the adsorbate and the adsorbent. There has been little apparent denaturation.

Human fibrinogen

The importance of fibrinogen adsorption to the understanding of the blood-compatibility of materials and the molecule's unique three-nodular structure lured us to observe it with STM. Fibrinogen is a big protein with molecular weight of 341,000. From the molecular model in Figure 9(a), we see that its dimensions are approximately 450 Angstroms in length and 65 Angstroms in diameter (Williams, 1981). Although we never succeeded in imaging an intact fibrinogen molecule, it turned out that we have ended up with much more information about STM itself.

Figure 9(b) displays a typical fibrinogen molecule, which looks like a "slab". Referring to Figure 9(a), one realizes that the macromolecule observed

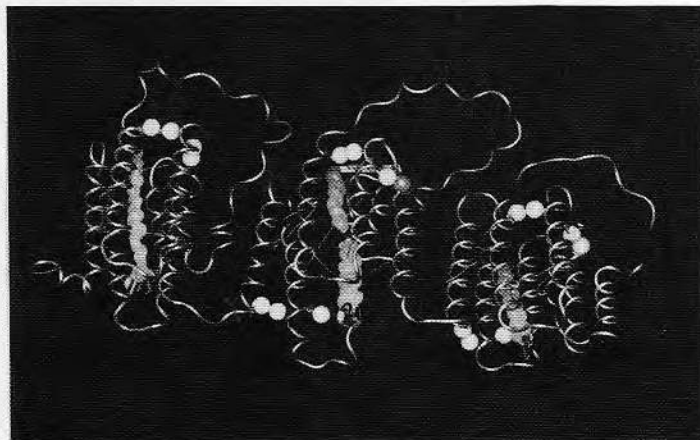


Figure 7. Backbone 3 dimensional model of serum albumin. In this model the wire represents the peptide backbone and the spheres represent disulfide bridges in the long loops. The three domains are antiparallel to one another. The length is 140 Angstroms and the width 40 Angstroms for the entire molecule (from Brown and Shockley, 1982 by permission of the author). See reference.

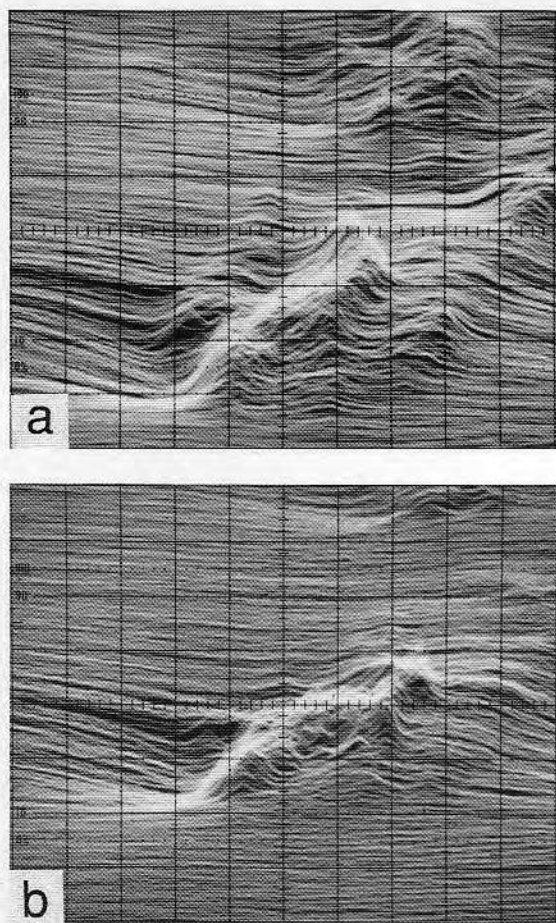
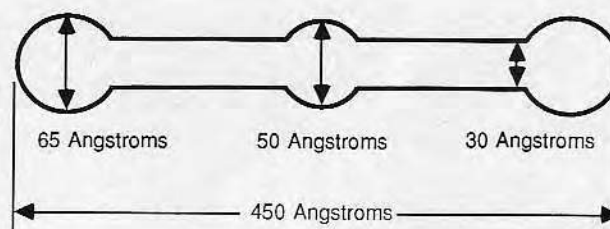


Figure 8. Images of human albumin on HOPG. The picture dimensions are 200 Angstroms in the horizontal (x) and 160 Angstroms in the vertical (y) directions. Since the adsorbate has a very different electronic structure from the substrate, the height (z direction) could not be directly measured. Both (a) and (b) show several different molecules. Three domains can be clearly seen (a). The ripples on the raster lines in (b) are the corrugations of carbon atoms of the HOPG. The sample was prepared by depositing a droplet of albumin PBS solution (10 ppm albumin) onto freshly cleaved HOPG and then the droplet was removed by capillarity with a tissue. The sample was then flushed with water for 10 sec and was dried at room temperature for 5 h before observation. The STM was operated at a bias voltage of 200 mV, tunneling current of 4 nA and high feedback gain. The constant current mode was used.



a

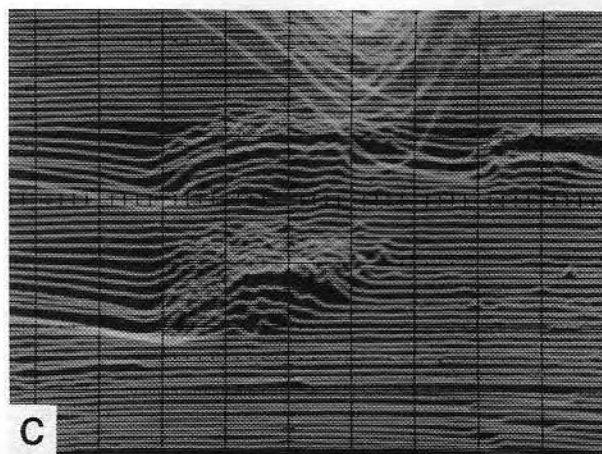
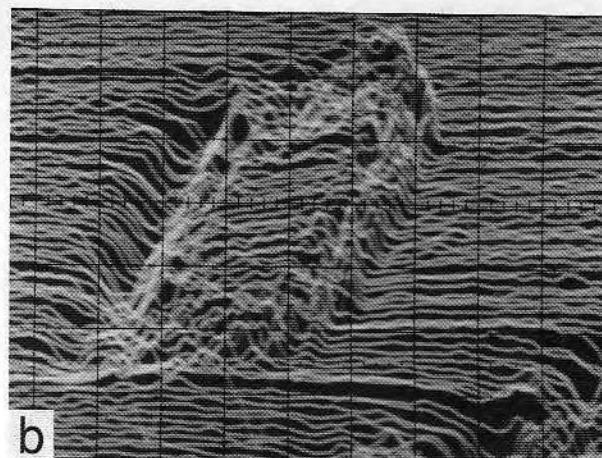


Figure 9. (a) A fibrinogen molecular model from Williams (1981); the globular domains at both ends may be elongated (90 x 40 Angstroms). (b) A typical fibrinogen molecule observed by STM on HOPG (deposited from a 20 ppm aqueous solution), constant current, $V_b = 200$ mV, $I_t = 1$ nA, 100 Angstroms/div. (c) An image of 3 separated domains of a fibrinogen molecule which originally was a similar slab as the one in (a), constant current, $V_b = 200$ mV, $I_t = 1.5$ nA, 100 Angstroms/div. The picture was taken when the trace of water on the sample just disappeared.

in Figure 9(b) had been so severely deformed that it had lost its key characteristics. While its length remained relatively unchanged its width expanded to 400 from 65 Angstroms and its height was reduced to about 15 from 65 Angstroms. The more miserable thing is that it did not show the three domain structure. From the deviation of the molecular dimensions, it is reasonable to suppose that the tip had heavily squeezed, depressed, and thus distorted the fibrinogen molecule. Although fibrinogen has a large molecular size, it appears to not sufficiently increase the tunneling current. Thus, the tip could not discern this huge molecule because it judged the surface morphology by sensing the local tunneling current rather than atomic or molecular topography. Note Figure 9(c): the picture started with a "slab" at the center. A moment later the "slab" suddenly burst into three "caps", probably representing the three deformed node-like domains. This could occur because this sample was just barely dried so the molecule was softer and less adhered and/or denatured. The linking chains between the domains had apparently

been fractured such that the domains were no longer in an axis but rather randomly scattered.

The "slabs" certainly were not part of the substrate, as might be suggested, since they were quite mobile on the substrate. The whole process is illustrated in Figure 10. A single molecule did not have sufficient interaction with the substrate HOPG to immobilize itself. As we mentioned before, owing to some degree of mechanical contact, the tip was driving fibrinogen molecules around and they kept moving until many of them packed together, which increased their mutual interaction. This sort of dynamic process was observed with several different samples.

Although a few individual molecules were imaged, the majority of the STM images showed aggregates of fibrinogen molecules, as in Figure 11, in which the lower left hand flat region was the HOPG substrate. In spite of our attempt to create the conditions favoring the formation of separate molecules, their distribution seems to have nothing to do with the methods of preparation of

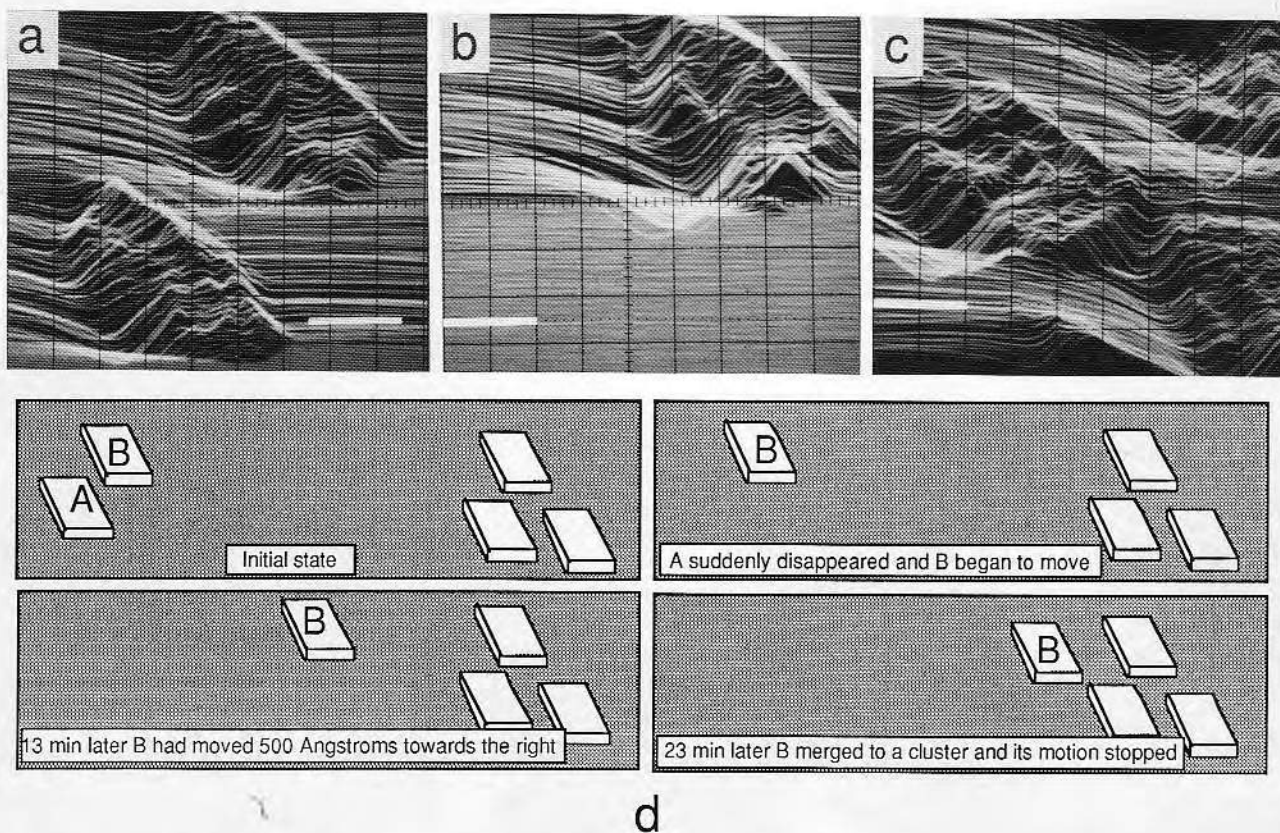


Figure 10. A dynamic process of fibrinogen molecules on HOPG, constant current, $V_b = 200$ mV, $I_t = 3$ nA, 100 Angstroms/div. (a)-(c) recorded the motion and (d) illustrates the entire process.

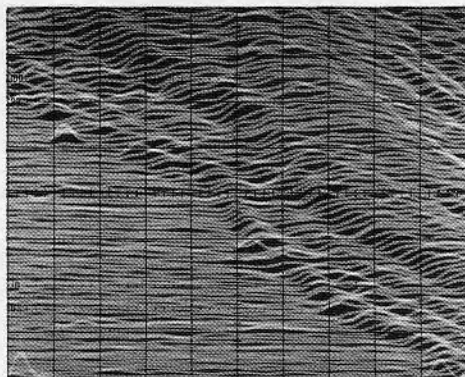


Figure 11. An edge of adsorbed fibrinogen aggregate, whose area was larger than 1 x 1 mm. The lower left handed flat region was the HOPG substrate (Deposited from a 5 ppm PBS solution, constant current, $V_b = 800$ mV, $I_t = 2$ nA, 100 Angstroms/div).

samples, be it deposit or adsorption, whether or not water flushed, and high or low concentrations of the solutions. Just as in the lysozyme case, it is suspected that the tip had driven and piled up segregated molecules into clusters. But this time we have more confidence in this suggestion, since we have evidence of such a dynamic process.

Remarks

Although there is no doubt that protein molecules can be observed on a conducting substrate by STM, depending on various circumstances, the difficulty is how to observe them without altering their initial adsorbed state, how to reproducibly obtain similar images, and under what conditions an adsorbed protein molecule can be unambiguously observed. A number of important questions have to be answered: What is the mechanism of image formation of such poorly conductive substances? What role do the tip geometry and surface chemistry play? What is the major interaction between the tip and a protein molecule: mechanical or electronic? What effects does the conducting substrate impose, such as its deformation, electron density, etc? What is the role of sample hydration or water sorption? We are continuing to address these questions.

Conclusions

Our STM work on proteins adsorbed on HOPG can be summarized as follows:

(1) Both amino acids and proteins can be seen by STM under certain conditions despite some difficulties.

(2) Amino acids are adsorbed both as aggregates and as individual molecules. Single molecules are apt to escape under the STM tip since their interactions with the substrate are weak.

(3) Hen egg-white lysozyme undergoes a conformational change upon adsorption and/or STM visualization.

(4) The high resolution images of human albumin show great promise for STM applications to protein adsorption.

(5) The STM tip may deform human fibrinogen due to mechanical contact, because of its large molecular size and poor conductivity.

(6) Fibrinogen molecules can move over the substrate, driven by the tip, causing them to pile up into clusters.

Acknowledgements

We thank Dr. A. Moore, the Union Carbide Corp., for a gift of HOPG. We especially thank Dr. C. Quate, Stanford U., for stimulating our interest and aiding our STM work on proteins. The images of lysozyme obtained in Quate's Lab in February, 1987 (unpublished) encouraged us to apply STM to the study of adsorbed proteins.

The Center for Biopolymers at Interfaces, a state of Utah Center of Excellence, supported the work. Partial support was also provided by the Office of Naval Research (ONR) contract N00014-88-0415 (W. Bascom, P. I.).

References

- Amrein M, Stasiak A, Gross H, Stoll E, Travaglini G (1988) Scanning tunneling microscopy of recA-DNA complexes coated with a conducting film *Science* **240**, 514-516.
- Andrade JD (1985) Principles of protein adsorption. In: *Surface and Interfacial Aspects of Biomedical Polymers*. Vol. 2, Plenum, New York, pp. 1-80.
- Baro AM, Miranda R, Alaman J, Garcia N, Binnig G, Rohrer H, Gerber Ch, Carrascosa JL (1985) Determination of surface topography of biological specimens at high resolution by scanning tunneling microscopy *Nature* **315**, 253-254.
- Baro AM, Miranda R, Carrascosa JL (1986) Application to biology and technology of the scanning tunneling microscope operated in air at ambient pressure *IBM J. Res. Development* **30**, 380-386.
- Barris B, Knipping U, Lindsay SM, Nagahara L, Thundat T (1988) Images of DNA fragments in an aqueous environment by scanning tunneling microscopy *Biopolymers* **27**, 1691-1696.
- Beebe TP, Wilson TE, Ogletree DF,

- Katz JE, Balhorn RB, Salmeron MB, Siekhaus WJ (1989) Direct observation of native DNA structures with the scanning tunneling microscope *Science* **243**, 370-372.
- Binnig G, Rohrer H (1983) Scanning tunneling microscopy. In: *Trends in Physics*. Janta J and Panatoflicek (eds.), European Physical Society, Petit-Lancy, Switzerland, pp.38-46.
- Binnig G, Rohrer H (1985) The scanning tunneling microscope *Scientific American* **253**, 50-56.
- Binnig G, Rohrer H, Gerber Ch, Weibel E (1982) Surface studies by scanning tunneling microscopy *Phys. Rev. Lett.* **49**, 57-61.
- Braun HG, Fuchs H, Schrepp W (1988) Surface structure investigation of Langmuir-Blodgett films *Thin Solid Films* **159**, 301-314.
- Brown JR, Shockley P (1982) Serum albumin: structure and characterization of its ligand binding sites. In: *Lipid-protein interactions*. Jost PC, Griffith OH (eds.), Vol. 1, Wiley, New York, pp. 25-68.
- Carter DC, He XM, Munson SH, Twigg PD, Gernert KM, Broom MB, Miller TY (1989) Three-dimensional structure of human serum albumin *Science*, **244**, 1195-1198.
- Dahn DC, Watanabe MO, Blackford BL, Jericho MH, Beveridge TH (1988) STM imaging of biological structures *J. Vac. Sci. Technol. A* **6**, 548-552.
- Feng L, Hu CZ, Andrade JD (1989) Scanning tunneling microscopic images of amino acids *J. Microscopy* **152**, 811-816.
- Feng L, Hu CZ, Andrade JD (1988) Scanning tunneling microscopic images of adsorbed serum albumin on highly oriented pyrolytic graphite *J. Colloid Interface Sci.* **126**, 650-653.
- Foster JS, Frommer JE (1988) Imaging of liquid crystals using a tunneling microscope *Nature* **333**, 542-545.
- Hansma PK, Tersoff J (1987) Scanning tunneling microscopy *J. Appl. Phys.* **61**, R1-R23.
- Hansma PK, Elings VB, Marti O, Bracker CE (1988) Scanning tunneling microscopy and atomic force microscopy: application to biology and technology *Science* **242**, 209-216.
- Horber JKH, Lang CA, Hansch TW, Heckl WM, Mohwald H (1988) Scanning tunneling microscopy of lipid films and embedded biomolecules *Chem. Phys. Lett.* **145**, 151-158.
- Jortner J, Bixon M (1987) Charge exchange between localized sites. In: *Protein Structure*. Austin R (ed.), Springer-Verlag, New York, pp. 277-308.
- Joseph AN, Zasadzinski J, Schneir J, Gurley J, Elings V, Hansma PK (1988) Scanning tunneling microscopy of freeze-fracture replicas of biomembranes *Science* **239**, 1013-1015.
- Lindsay SM, Thundat T, Lagahara L, Knipping U, Rill RL (1989) Images of the DNA double helix in water *Science* **244**, 1063-1064.
- Panitz JA (1987) Electron tunneling used as a probe of protein adsorption at interfaces. In: *Proteins at interfaces*. Brash J and Horbett T (eds.), Amer. Chem. Soc., Washington, DC, pp. 423-433.
- Quate CF (1986) Vacuum tunneling: a new technique for microscopy *Phys. Today* Aug., 26-33.
- Schneir J, Hansma PK (1987) Scanning tunneling microscopy and lithography of solid surfaces covered with nonpolar liquids *Langmuir* **3**, 1025-1027.
- Simic'-Krstic' Y, Kelley M, Schneiker C, Krasovich M, McCuskey R, Koruga D, Hameroff S (1989) Scanning tunneling microscopy (STM) of microtubules *FASEB Journal*, in press.
- Sleator T, Tycko R (1988) Observation of individual organic molecules at a crystal surface with use of a scanning tunneling microscope *Phys Rev. Lett.* **60**, 1418-1421.
- Smith DPE, Bryant A, Quate CF, Rabe JP, Gerber Ch, Swalen JD (1987) Images of a lipid bilayer at molecular resolution by scanning tunneling microscopy *Proc. Natl. Acad. Sci. USA* **84**, 969-972.
- Smith DPE (1987) New applications of scanning tunneling microscopy Ph D dissertation, Stanford University, Stanford, CA.
- Spong JK, Mizes HA, LaComb LJ, Dovek MM, Frommer JE, Foster JS (1989) Contrast mechanism for resolving organic molecules with tunneling microscopy *Nature* **338**, 137-139.
- Stemmer A, Rechelt R, Engel A, Rosenbusch JR, Ringger M, Hidber HR, Guntherodt HJ (1987) Scanning tunneling and scanning transmission electron microscopy of biological membranes *Surface Sci.* **181**, 394-402.
- Stryer L (1988) In: *Biochemistry*. 3rd edition, Freeman, New York, p. 203.
- Travaglini G, Rohrer H, Amrein M, Gross H (1987) Scanning tunneling microscopy on biological matter *Surface Sci.* **181**, 380-390.
- Voelker MA, Hameroff SR, He JD, Dereniak EL, McCuskey RS, Schneiker CW, Chvapil TA, Bell TS, Weiss LB (1988) STM imaging of molecular collagen and phospholipid membranes *J. Microscopy* **152**, 557-566.
- Williams RC (1981) Morphology of bovine fibrinogen monomers and fibrin oligomers *J. Mol. Biol.* **150**, 399.
- Zasadzinski JAN (1989) Scanning

tunneling microscopy with applications to biological surfaces. *BioTechniques* 7, 174-187.

Discussion with Reviewers

A Aviram: Can you give a possible explanation of the conduction mechanism of the studied proteins?

Authors: At the present time, there is no general theory which can explain the conduction mechanism of STM images of poorly- or even non-conductive adsorbates. Several hypotheses have been suggested, however, for some particular cases. For example: a) sorbed water may play a role in enhancing the tunneling current; b) near the Fermi level there are some empty states which can relay electrons; c) adsorbates may change the work function of the substrate underneath so that the local environment is different, etc. We did notice the effect of humidity upon the imaging of amino acids and proteins as more of these molecules could be observed in a relatively humid environment than a dry one.

Surface atomic and domain structures of biomedical carbons observed by scanning tunneling microscopy (STM)

L. Feng and J.D. Andrade*

Department of Materials Science and Engineering and Department of Bioengineering, 2480 MEB, University of Utah, Salt Lake City, Utah 84112

STM has been used to study the surface domain and atomic structures of three biomedical carbons: glassy carbon (GC), low-temperature isotropic carbon (LTI), and ultra-low-temperature isotropic carbon (ULTI). The images show atomic lattices on both GC and LTI, but not on ULTI. The lattices contain many defects; lattices in GC are more ordered than those in LTI. The images also show patchlike carbon crystallites with sizes of

3–15 nm for GC, 2–8 nm for LTI, and 1–3 nm for ULTI. The crystallites form surface domains that may differ in surface properties due to different orientations of the crystallites. Mechanical polishing makes the LTI surface more amorphous and more homogeneous. Based on the STM observations, we evaluate several hypotheses on the blood compatibility of biomedical carbons. © 1993 John Wiley & Sons, Inc.

INTRODUCTION

Biomedical carbons have a reputation for good biocompatibility.^{1–3} A number of hypotheses have been proposed as to how their surfaces interact with plasma proteins (Fig. 1). One hypothesis^{4,5} states that the carbon surface is chemically inert and thus does not have strong interactions with proteins. The adsorbed proteins preserve their native conformations at the interface because of the lack of driving forces for their conformational changes upon adsorption [Fig. 1(A)]. Another hypothesis⁶ proposes a “domain match” mechanism that is concerned with protein surface heterogeneity.⁷ If the surface of a biomaterial is heterogeneous because microdomains have different surface properties, the adsorbed protein will experience “balanced forces” at the interface by matching their surface patches with those of the carbon surfaces. The matching may include hydrophobic interactions, electrostatic forces, hydrogen bonding, etc. [Fig. 1(B)]. Still another hypothesis^{2,8,9} suggests that the carbon surface becomes blood compatible by becoming coated and passivated by the adsorbed layer of plasma proteins [Fig. 1(C)]. To test these hypotheses one needs to understand the surface structure of the carbon.

Scanning tunneling microscopy (STM) provides the information on surface electronic structure and morphology of a sample. It has been widely applied to conductors and semiconductors because of its high resolution, high surface sensitivity, and other capabilities.¹⁰ The conductive nature of biomedical carbons enables them to be observed under STM. Although a lot of STM work has been done on graphite, especially on highly oriented pyrolytic graphite (HOPG), little has been done on other forms of carbon. Marchon et al.¹¹ observed small graphite-like domains on pyrolytic carbon and found that the domain size is larger for carbon samples pyrolyzed at higher temperatures. The domain resolution in the study was limited to 10 nm because of the nature of their STM tip. In separate work¹² they also imaged atomic structures on surfaces of amorphous hard carbon films, prepared by DC magnetron sputtering, observing small graphitic domains and some five-membered carbon rings in many disordered areas. Elings and Wudl¹³ examined a number of carbons, including GC. Although some ordered regions 1–3 nm in size and rows of atoms were observed, no individual atoms were distinguishable except on the graphite samples. Kakagiri and Kaizuka¹⁴ imaged carbon deposited on graphite with a resolution of less than 1 nm, seeing hillocks and finding a connection between roughness and the film thickness. Hoffman et al.¹⁵ documented STM observation of surfaces

*To whom correspondence should be addressed.

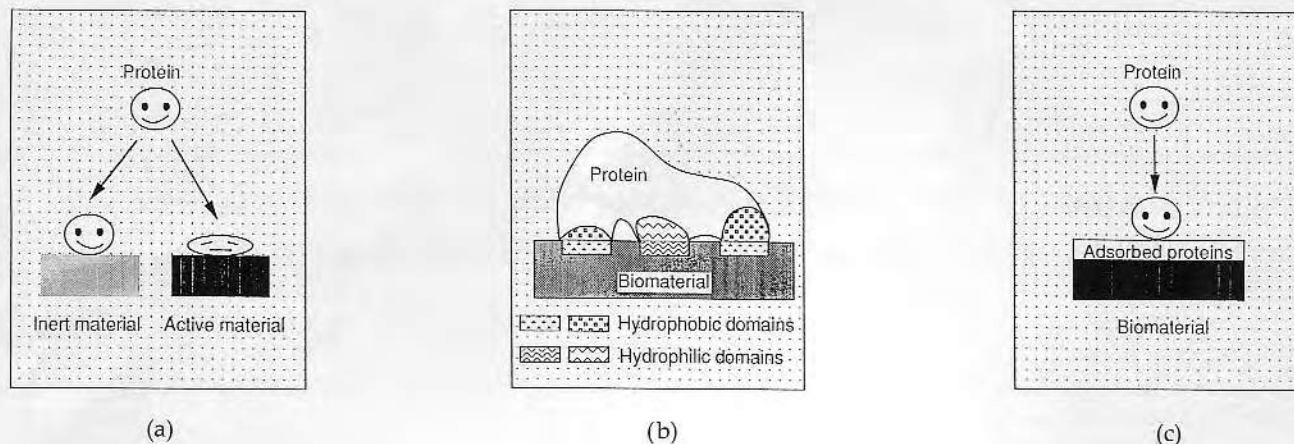


Figure 1. Schematic representations of three hypotheses on the blood compatibility of biomedical carbons (see text for details): (a) the inertness hypothesis; (b) the domain matching hypothesis, using hydrophobicity-matching as an example; and (c) the passivation hypothesis.

of P-55 pitch based carbon fibers before and after surface treatments. On as-received fibers they saw some small graphitic regions as large as 20 nm and many disordered structures at the atomic scale.

We observed the surfaces of three biomedical carbons, in as-received and polished forms, by using STM. We obtained information on the surface morphology, atomic packing, nanocrystallite domains, and effects of mechanical polishing, at an atomic level. We discuss three hypotheses (Fig. 1) in terms of STM observations.

EXPERIMENTS

Glassy carbon (GC) was purchased from Atomergic Chemetals Corp. (Cat. #: V25-44). Both low-temperature isotropic (LTI) carbon (silicon-alloyed) and ultra-low-temperature isotropic carbon (ULTI) (deposited on polyethylene terephthalate substrate) were gifts from Sorin Biomedica (Saluggia (VC), Italy). All the samples were cut to about 5 mm \times 3 mm pieces by a diamond blade to facilitate mounting in the STM.

As-received samples were cleaned sequentially in Milli-Q water (resistance: 15 M Ω), acetone (GR, EM Science), and dichloromethane (AR, Mallinckrodt), each for 5 min, in a low-power ultrasonic cleaner (Model 250, E/MC, RIA Research). They were air-dried after cleaning. The GC and LTI were further polished by hand. The final polishing was carried out with a 0.05- μ m alumina slurry (Buehler) to obtain a mirrorlike surface. For comparison, a different power size, 0.3- μ m alumina slurry (Buehler), and a different type of powder, 600-grit emery paper, were also used during the final polishing. ESCA measurements showed that all samples had comparable oxygen

content: O/(C + O) signal ratio was 11% for the as-received, 11% for the emery paper polished, 10% for the 0.3- μ m alumina polished, and 11% for the 0.05- μ m alumina polished. The cleaning steps were identical to those used for the as-received samples. Electron transfer reactions showed that the polished surface could be further cleaned with the organic solvents. For example, the heterogeneous rate constants, k° , of ferro-/ferri-cyanide (0.2 mmol/L) reaction on polished LTI electrodes were 1.5×10^{-2} cm/s and 5.3×10^{-2} cm/s, before and after they were sonicated in CH₂Cl₂ for 2 min. The higher k° suggested the cleaner surface.

A NanoScope II (Digital Inst.) with STM Head-A was utilized for the measurement. The observation was performed in air with constant height mode. All the samples were imaged with mechanically sharpened Ir/Pt tips at a bias voltage of 0.1 V and a tunneling current of 1.0 nA. There was a chance that the sample surface could be modified by the tip-sample interaction. The factors involved include tunneling current, bias potential, and properties of the sample itself (electron density, strength, and hardness). For instance, due to the difference of their structures, a layer of graphite is easily removed by a tip, but a turbostratic carbon is much more difficult to damage. To assure that our carbon samples were unmodified during STM scanning, many other combinations of voltage (0.02–0.4 V) and current (0.2–3 nA) were also tested, all resulting in similar images. Whether an image has been filtered is indicated in its figure caption.

RESULTS

Among the three as-received samples the GC shows the most ordered structure, with many "quasi-

crystalline" turbostratic patches (domains) of 3–15-nm size [Fig. 2(a)]. The sandy-grain-like structures on many domains are, in fact, individual carbon atoms. These crystallites are thought to orient such that their basal planes are nearly parallel to the sample plane because only on the basal plane can ordered atomic packing be observed. The apparently noisy regions are considered to be crystallites which expose their edge planes on the surface. STM cannot probe these surfaces well because they are rough and full of defects. Figures 2(b) and 2(c) show small regions on two of the domains. The misplaced atom, shown by the arrow in Figure 2(b), and line dislocations, shown by the arrows in Figure 2(c), highlight the lack of long-range ordering within a single crystallite. The distance between two visible adjacent atoms measured from Figures 2(b) and 2(c) is 0.28 ± 0.03 nm, while that of the graphite lattice (picture not included) is measured as 0.25 ± 0.02 nm.

As-received LTI has a rough surface, containing many large and small granules. Figure 3(a) shows three large granules with diameters of about 200 nm and peak-to-valley vertical distances of about 50 nm. The individual large granules are made up of many small granules about 40 nm in size. The large granules are readily seen by SEM,^{1,2} but the small granules have not previously been reported. Although not as frequently and noticeably as in the case of the GC, quasi-crystalline patches (domains) are also observed, shown in Figure 3(b). Compared with their GC counterparts, for LTI the atoms are less orderly packed, the range of ordering is shorter, and the domain sizes, 2–8 nm, are smaller. It is difficult for STM to image individual atoms on a disordered surface. If the *c*-plane of a carbon crystallite is not oriented parallel to the sample plane, STM will not show the ordered atomic packing due to the effects of irregular shape edges and defects. Meanwhile, the as-received LTI has a very rough surface, as shown in Figure 3(a). The roughness, together with small ordered regions, and random crystallite orientation, made it more difficult to obtain a good image at the atomic scale. Nevertheless, recognizable domains with ordered atomic arrays were often seen and the images were reproducible. For example, Figure 3(b) shows at least five such domains. Figure 3(c) represents one of the LTI images that display relatively clear atomic structures. The picture is composed of several domains, possibly with different orientations. The upper left area appears to have little order with loose carbon flakes (white streaks). We think it could consist of either very poorly formed basal planes or nonhorizontally oriented basal planes. The one at the lower right corner is similar. The one at the lower right corner is similar. The area at the upper right, toward the middle, shows a relatively well organized atomic pattern. However, its basal planes are wavy rather than flat, and appear to be closely parallel to the sample surface. On the

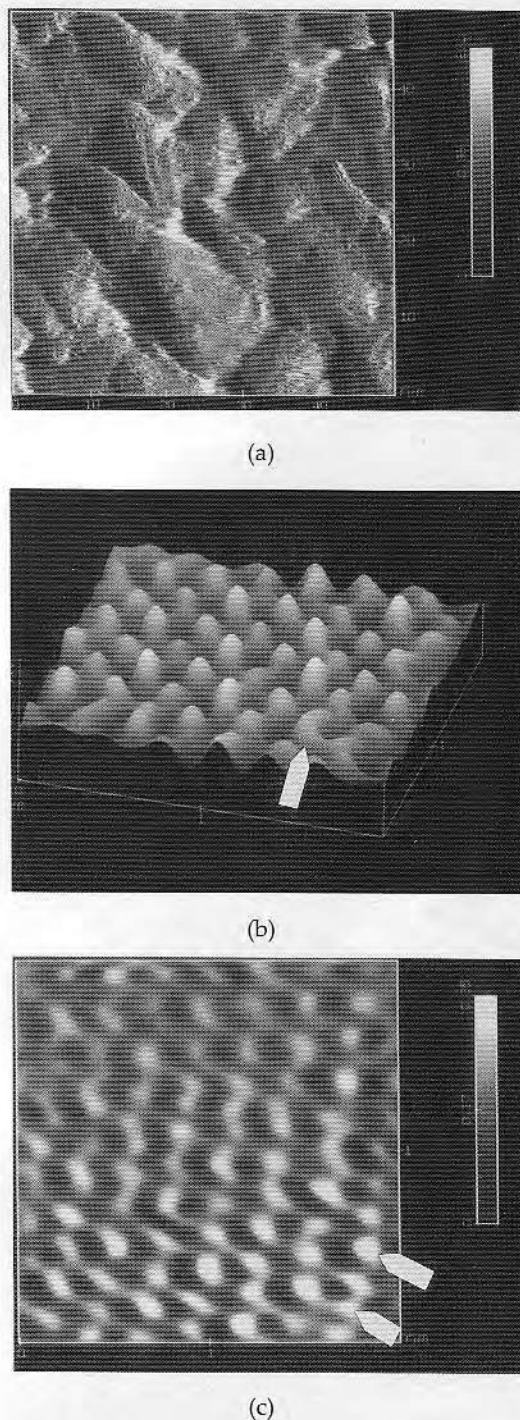
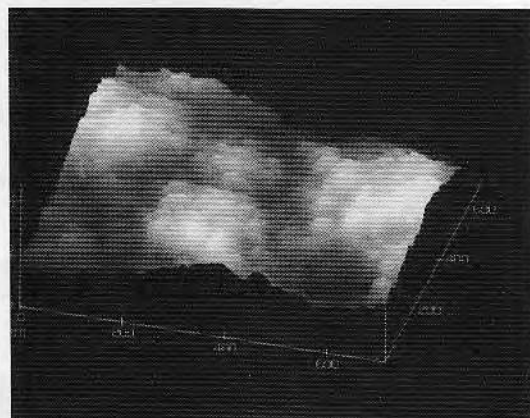


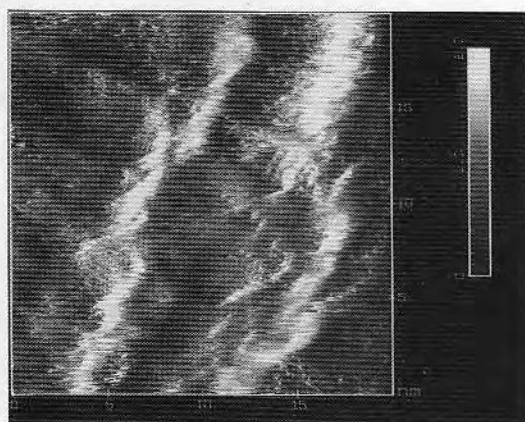
Figure 2. STM images of as-received glassy carbon (GC): (a) mosaics of patches (domains) with the size of 3–15 nm; (b) a filtered image showing atomic arrays and a misplaced atom (*arrow*), where the interatomic distance is 0.28–0.31 nm; and (c) another filtered image showing atomic arrays and a few line dislocations (*arrows*), where the interatomic distance is 0.22–0.26 nm.

other hand, the edge plane of the lower left area may be on the sample surface, since the distances between two adjacent rows are about 0.35 nm, which is close to the interlayer distance of graphite.

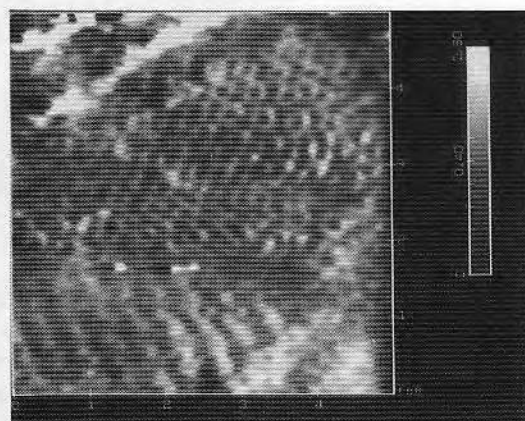
Surfaces of ULTI appear to be the roughest of all three. As shown in Figure 4(a), the peak-valley distance is more than 100 nm. They also have the smallest domain areas, only 1–3 nm, and the low-



(a)



(b)



(c)

Figure 3. STM images of as-received low-temperature isotropic carbon (LTI): (a) surface morphology and granular structure, where the large granules have the diameter of about 200 nm and peak-to-valley distances of about 50 nm, and the small granules have the size of about 40 nm; (b) mosaics of patches (domains) with the size of 2–8 nm; (c) a filtered image showing atomic arrays and several different domain areas (see discussion in text).

est ordering in atomic packing. Figure 4(b) typifies the STM images of the ULTI: Atomic arrays are not observed.

From the surface atomic structure point of view, alumina polishing does not change the GC surface very much, while it significantly modifies the LTI surface. After polishing, the atomic order of the GC surface is preserved to some extent. Figure 5(a) represents such a case, where ordering can still be seen on the upper part of the picture. Some images with lower magnification show scratch-like features that may be due to the polishing. For polished LTI, although the surface becomes much smoother, ordered atomic structures are gone [see Fig. 5(b)]. Comparing Figure 5(b) (polished LTI) with Figure 3(c) (unpolished LTI), we realize that the polished surface has been apparently modified to a more random and amorphous structure. It also becomes more homogeneous because the difference among domains [Fig. 3(c)] disappears.

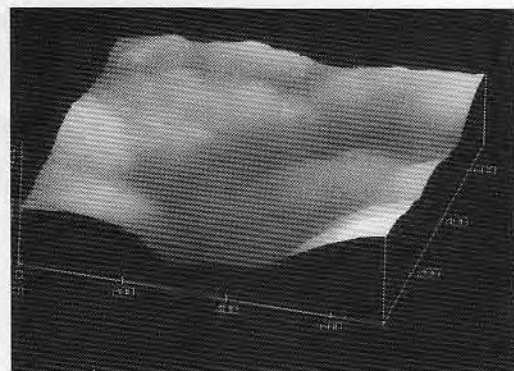
DISCUSSION

This preliminary study suggests that the ordering of atomic packing in the three carbons is, in descending order, GC > LTI > ULTI. The STM observations suggest that unpolished surfaces of LTI [Fig. 3(c)] are heterogeneous from domain to domain, realized by different atomic organizations and crystallite orientations. The edge plane or the basal plane with many defects tends to be more energetic and chemically active than the defect-free basal plane in graphite crystallites.^{16–17} Therefore, one can suggest that the different domains in Figure 3, for example, may have different surface adsorption properties. It should be pointed out that carbon surfaces in air are prone to chemically adsorbing oxygen atoms, mainly in the region of defects and crystallite edges. This makes these regions more dissimilar to a perfect basal plane.

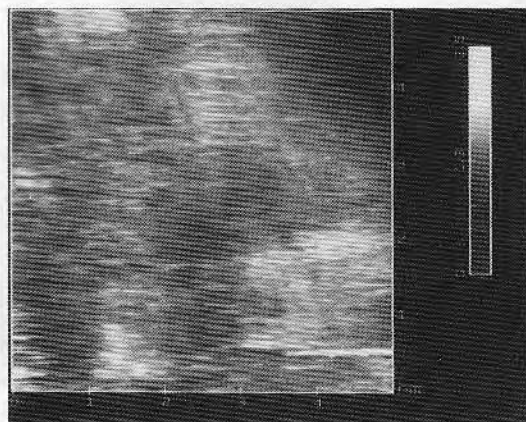
Since LTI used in artificial heart valves is polished, we also studied polished LTI. The improvement of blood biocompatibility by polishing presumably occurs because a smooth surface traps fewer proteins and cells and they are replenished faster by flowing blood.^{1,2} But in fact polishing does more than just smoothing. As shown in Figure 5(b), the surface of the polished LTI tends to be more amorphous. Such a change could play a role in its surface energetics and chemical reactivity. The polishing of LTI actually changes the surface by modifying the original crystalline structure through creating more edges and defects. Figure 6 schematically represents this suggested modification process. This modification seems to be a general outcome of polishing, since similar modified surfaces have been observed when polished with different polishing powders. So far, two

important deductions can be formulated: Polishing makes the surface more homogeneous as well as amorphous, and the surface should become more energetic and chemically active. It is important to note that although certain polishing procedures may vary for different sources of LTI valves, our conclusion should be true, because we have used different sizes of polishing powders (0.05 and 0.3 μm) and different polishing methods (emery paper and alumina).

Another inference is that inertness and domain matching [Figs. 1(a) and (b)] may not be the principal origins of the biocompatibility of LTI. Carbon valves may have largely lost those two characteristics due to the polishing process, and yet they are considered blood compatible. The other hypothesis [Fig. 1(c)] may merit further consideration, because a surface with higher energy may adsorb proteins more tenaciously, so that the protecting protein layer would be more stable. Such a surface could be more blood compatible.

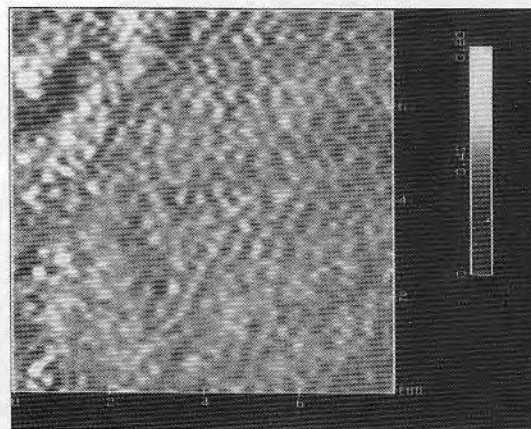


(a)

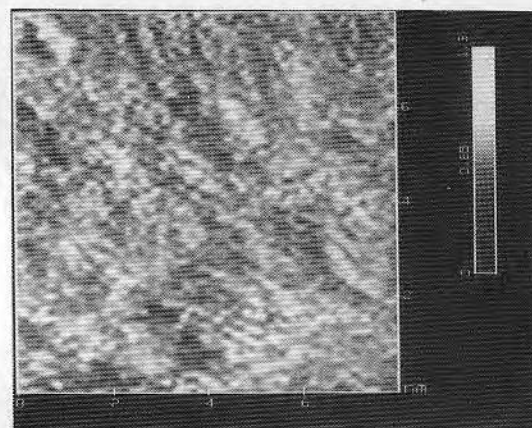


(b)

Figure 4. STM images of as-received ultra-low-temperature isotropic carbon (ULTI): (a) surface morphology where the granules have the diameter of about 400 nm and peak-to-valley distances of about 100 nm; and (b) mosaics of patches (domains) with barely recognizable ordering, a number of rows roughly slanting from the upper left to the lower right.



(a)



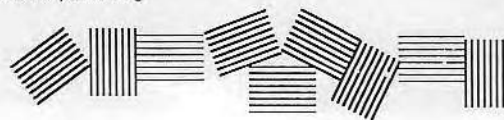
(b)

Figure 5. STM images (filtered) of polished glassy carbon (a), where ordered atomic packing is still seen in the upper region, and polished low-temperature isotropic carbon, (b), where no ordering can be seen.

CONCLUSIONS

- (1) Scanning tunneling microscopy is able to reveal the surface morphologies of biomedical carbons, down to an atomic level.
- (2) Although all three carbons have turbostratic structures, the STM images suggest that the ordering

Before polishing



After polishing



Figure 6. Schematic representation of effects of polishing on the surface morphology of low-temperature isotropic carbon (see discussion in text).

of atomic packing can be arranged in descending order: GC > LTI > ULTI.

(3) Domain sizes are also in descending order: GC > LTI > ULTI.

(4) Polishing appears to make the LTI surface more homogeneous and more amorphous than the unpolished LTI.

The authors thank Sorin Biomedica for the carbon samples. This work was supported by the Center for Biopolymers at Interfaces, University of Utah.

References

1. J. C. Bokros, L. D. LaGrange, and F. J. Schoen, "Control of structure of carbon for use in bioengineering," in *Chemistry and Physics of Carbon*, Vol. 9, P. L. Walker (ed.), Dekker, New York, 1972, pp. 103-171.
2. J. C. Bokros, "Carbon biomedical devices," *Carbon*, **15**, 355-371 (1977).
3. A. D. Haubold, H. S. Shim, and J. C. Bokros, "Carbon in biomedical devices," in *Biocompatibility of Clinical Implant Materials*, Vol. 2, D. F. Williams (ed.), CRC Press, Boca Raton, 1979, pp. 3-24.
4. T.-H. Chiu, E. Nyilas, and L. R. Turcotte, "Microcalorimetric and electrophoretic studies of proteins from plasma," *Trans. ASAI*, **24**, 389-402 (1978).
5. V. L. Gott and A. Furuse, "The current status of in vivo screening of synthetic implant materials for blood compatibility," *Med. Instr.*, **7**, 121-124 (1973).
6. J. D. Andrade, S. Nagaoka, S. Cooper, T. Okano, and S. W. Kim, "Surfaces and blood compatibility," *ASAI*, **10**, 75-84 (1987).
7. J. D. Andrade, V. Hlady, A.-P. Wei, and C.-G. Golaner, "A domain approach to the adsorption of complex proteins: preliminary analysis and application to albumin," *Croatica Chem. Acta*, **63**, 527-538 (1990).
8. R. E. Baier, "Key events in blood interactions at non-physiologic interfaces—a personal primer," *Artif. Organs*, **2**, 422-426 (1978).
9. C. P. Sharma, "LTI carbons: blood compatibility," *J. Colloid Interface Sci.*, **97**, 585-586 (1984).
10. For example, see P. K. Hansma and J. Tersoff, "Scanning tunneling microscopy," *J. Appl. Phys.*, **61**, R1-R23 (1987).
11. B. Marchon, S. Ferrer, D. S. Kaufman, and M. Saleron, "The surface topography of pyrolytic carbons and of gold thin films by scanning tunneling microscopy: grain boundaries and surface defects," *Thin Solid Films*, **154**, 65-73 (1987).
12. B. Marchon, W. Siekhaus, and M. Salmeron, "Observation of graphitic, amorphous and diamond-like structures on the surface of hard carbon films by scanning tunneling microscopy," *Phys. Rev. B*, **39**, 12907-12910 (1989).
13. V. Elings and F. Wudl, "Tunneling microscopy on various carbon materials," *J. Vac. Sci. Technol.*, **A6**, 412-414 (1988).
14. N. Kakagiri and H. Kaizuka, "Scanning tunneling microscopy measurements of carbon deposited on to graphite," *J. Microsc.*, **156**(3), 267-272 (1989).
15. W. P. Hoffman, W. C. Hurley, T. W. Owens, and H. T. Phan, "Advantage of the scanning tunneling microscope in documenting changes in carbon fibre surface morphology brought about by various surface treatments," *J. Mater. Sci.*, **26**, 4543-4553 (1991).
16. J. Abrahamson, "The surface energies of graphite," *Carbon*, **11**, 337 (1973).
17. R. M. Wightman, P. M. Kovach, W. G. Kuhr, and K. J. Stuffs, "Methods to improve electrochemical reversibility at carbon electrodes," *J. Electrochem. Soc.*, **131**, 1578-1583 (1984).

Received June 10, 1991

Accepted May 18, 1992

Protein adsorption on low-temperature isotropic carbon:

I. Protein conformational change probed by differential scanning calorimetry

L. Feng and J. D. Andrade*

Departments of Bioengineering and Materials Science and Engineering, 2480 MEB, University of Utah, Salt Lake City, UT 84112

This is the first of a set of articles on protein adsorption on low-temperature isotropic carbon (LTIC), a reputed blood compatible material. Surface-induced conformational changes of albumin, fibrinogen, and some small proteins were measured by differential scanning calorimetry (DSC) on LTIC powders and colloidal silica. The LTIC surface significantly alters the DSC response (denaturation?) in proteins studied in different buffer solutions. We use the term "denaturation" to refer to altered protein behavior in the adsorbed state. Hydrophobic interactions between LTIC and the proteins are thought to be the major driving force.

The presence of air at the water-carbon interface seems to prevent the surface denaturation of fibrinogen. The silica surface greatly denatures albumin but only slightly denatures fibrinogen. Because LTIC is considered to be a nonthrombogenic material, but silica is considered to be a thrombogenic one, whether a surface denatures adsorbed proteins cannot be the sole criterion for its blood compatibility. The latter largely depends on what protein the surface denatures, and in what sequences. © 1994 John Wiley & Sons, Inc.

INTRODUCTION

Low-temperature isotropic carbon (LTIC) is reported to be a blood compatible material.^{1,2} Despite its wide applications in cardiovascular devices, it is still unclear and even controversial as to how LTIC achieves acceptance in a blood environment. Because of the important role played by adsorbed proteins in blood compatibility,³ we chose to study protein adsorption on LTIC and other model surfaces to obtain insight into the mode of interaction between LTIC and proteins.⁴ By integrating all the information from several experimental techniques,⁵⁻⁷ and from the literature, we present a relatively complete picture of LTIC and protein adsorption.⁸

This article uses differential scanning calorimetry (DSC) to measure the calorimetric enthalpy of thermal denaturation of a protein both in solution and on a surface. From the difference on the transition heat, we deduced conformational changes of adsorbed proteins on LTIC and silica powders; we call this effect surface-induced "denaturation." The conformational status of adsorbed proteins is thought to be important to the blood compatibility of prosthetic cardiovascular implants, although the specifics are largely unknown and controversial. Nyilas,^{9,10} Baier,¹¹ and Bokros¹

considered LTIC to be an inert material inducing little conformational change in adsorbed proteins. On the other hand, Sevastianov,¹² Kaelble,¹³ and Sharma¹⁴ suggested that the LTIC surface is coated with a thick film of bland plasma proteins, held so tenaciously that they can not be easily removed. Riccitelli observed conformational change of proteins adsorbed on carbon.¹⁵ It was difficult for us to accept that the LTIC surface would not denature adsorbed proteins, because of the similarity of the surface structure and hydrophobicity of carbon to many organic polymers as most hydrophobic surfaces do denature proteins.^{16,17} We postulated that LTIC may also denature proteins, but that such denaturation is generally undetected.

Methods for measuring the conformation of adsorbed proteins include FTIR,¹⁸ FTIR-ATR,¹⁹ CD,²⁰ hydrodynamic thickness,²¹ TIRF,²² enzyme activities,²³ and immunoassay.²⁴ Using DSC to investigate protein thermal denaturation has become a well-established procedure for studying the domain structure and thermal stability of proteins and of their domains.²⁵ DSC was used to study the domain structures of fibrinogen structure^{26,27} and complement C1s,²⁸ conformational transitions of meromyosin,²⁹ solution properties of albumin,^{30,40} and thermal stability of model proteins.³¹ Pioneering work by de

*To whom correspondence should be addressed.

Baillou et al. detected the conformational change of fibrinogen adsorbed on glass beads.²¹

The notion of using DSC to study adsorption induced denaturation is straightforward. We assume that the structure of a protein or of a major domain exists in "two pseudo states": either native (folded) or denatured (unfolded). The denatured state may have different structures depending on different denaturation routes. Nevertheless, as far as the thermodynamic transition is concerned, different denatured structures are indistinguishable. Thermal denaturation is not observed if the protein has been denatured upon adsorption. In other words, the adsorbed conformation is considered denatured if the protein does not undergo the expected "melting" transition. Although the issue of non-native or different adsorbed states is debatable,³² the consideration of different "states" of denatured proteins will not affect the conclusion from this work, as long as such non-native states do not significantly participate in the thermal transition.

The "two pseudo state" assumption is applicable to individual domains within a single protein molecule. A specific domain will not show thermal denaturation if it has already been denatured by a surface. However, this does not mean that the other domains of the same molecule will not be thermally responsive; they will if their conformations have not been significantly changed. In other words, individual domains or even parts of them can be denatured independently. The work by Privalov is a good example.²⁶ The key assumption used here is that any native structure in any part of the molecule can only be denatured once, either by surfaces or by heat. It should be pointed out that because of sensitivity and noise level, our data on conformational changes only have macroscopic significance. Very small changes in protein conformations may not be detected, such as those that can be probed by immunoassays.³³

EXPERIMENTAL

Materials

Low-temperature isotropic carbon powders were ground by ball milling silicon-alloyed LTIC frag-

ments, a gift from Sorin Biomedica (Italy), in a ceramic jar for 5 h. Their average diameters were 0.2 μm , with very broad distributions. The BET surface area was 54.4 m^2/g , but not all this area can be available to proteins. We have estimated that the accessible surface of LTIC is 18 m^2/g .⁴ Colloidal silica 40% water suspension (from 0.02 μm and about 100 m^2/g) was purchased from Johnson Mattley (Ward Hill, MA). No stabilizer was added in the suspension.

Two plasma proteins and four small model proteins were studied (Table 1). The three chemical reagents used in phosphate-buffered saline (PBS) were all super-pure grades: sodium dibasephosphate (Ultrapur) was from J. T. Baker Chemical (Phillipsburg, NJ). Sodium hydroxide (Suprapur) and sodium chloride (Suprapur) were from EM Science (Gibbstown, NJ). Sodium acetate and acetic acid for the acidic buffer were analytical reagents from Mallinckrodt (Parks, KY). Glycine for the basic buffer was electrophoretically pure from Hoefer Scientific Instruments (San Francisco, CA). Water for the buffers was double-distilled from predeionized water.

Buffer solutions

The buffer should prevent the protein of interest from precipitating or aggregating upon denaturation at elevated temperature. Otherwise, the native to denatured transition would be buried in a much greater exothermic transition of aggregation. Another preference for a buffer is that its pH should be in the vicinity of pH 7.4 so that protein behavior from DSC measurements could be correlated to its properties measured in other experiments.⁵⁻⁷ The first prerequisite could usually be met by using a buffer with a pH away from the isoelectric point of the protein.²⁶ Hence, the buffers for most of the proteins studied were either acidic or basic compared with pH 7.4. Table II lists the buffer used for each proteins and their denaturation data from the literature. The reason why human fibrinogen (either from Calbiochem or Kabi) was not used was that no buffer was found that could prevent the protein from aggregating during the DSC run. Even with BFG, the only applicable

TABLE I
Proteins Used in DSC Experiments

Protein	Albumin	Fibrinogen	Lysozyme	Cytochrome c	Myoglobin	Ribonuclease A
Abbreviation	HSA	BFG	LSZ	CYT	MGB	RNAse
Source	Human serum	Bovine plasma	Hen eggwhite	Tuna heart	Horse heart	Bovine pancreas
Mw, daltons	65,000	340,000	14,300	12,170	18,800	13,700
pI	4.7	5.8	10.7	10	7.8	9.6
Domains	Multiple	Multiple	Single	Single	Single	Single
Supplier	ICN Biomedical (Irvine, CA)	Sigma (St. Louis, MO)	Sigma	Sigma	Sigma	Sigma

buffer was glycine at pH 8.5, among the buffers tested. In fact, HSA was the only protein studied that did not precipitate in PBS after being thermally denatured. Despite the variation of buffer, we still believe that the unique information content of DSC is instructive.

Prewetting of powders

Air trapped in the pores of LTIC can complicate the water-solid interface in at least two ways: by reducing the effective interfacial area for protein adsorption and by creating a triple air-water-solid interface and an air-solid interface,³⁴ proteins at these interfaces may take different conformations and have different adsorption properties. To minimize such effects, the powders were evacuated using molecular sieve adsorption pump (VacSorb Pump, Varian), which produces very low contamination. LTIC powders in a test tube were degassed until the vacuum reached 50×10^{-3} mm Hg or lower. A slightly degassed buffer solution was later introduced into the tube to soak and wet the powders that had been under vacuum (vacuum prewetting). For comparison LTIC powders were also prewetted by simply pouring buffer solutions onto them at atmospheric pressure (air prewetting). Because the colloidal silica had already been wetted by water, its prewetting was simply by dilution with the buffers.

Adsorption procedure

Protein adsorption took place in DSC ampoules made from stainless steel. For studies using vacuum-

prewetted LTIC and colloidal silica, a given amount of the prepared powder-buffer suspension was pipetted into a 1 ml ampoule. Concentrated protein solution was added (2.0 mg for HSA and 1.0 mg for other proteins). Pure buffer was added until the ampoule attained the required weight (deviation less than 0.5 mg). The total mass of a sample (suspension or solution) was about 600 mg, which differed slightly for individual ampoules. For the air-prewetted LTIC, the powders were directly weighed inside an ampoule. About 0.2 ml buffer was added to wet the adsorbent, with prewetting taking 30 min. Everything thereafter was identical to the vacuum-prewetted LTIC. The precisely weighed ampoules were tightly sealed. Adsorption took about 1 h at room temperature while the ampoules were slightly rocked to provide mixing.

DSC instrument and operation

The calorimeter (Hart Scientific, Pleasant Grove, UT) was designed for biologic applications with a sensitivity 100 times higher than a traditional DSC, recording from 100 to 1 mW with a baseline stability of 0.15 mW. For the measurement of protein denaturation, the temperature scan was programmed as: 1) scanning down from 20°C to 15°C; 2) staying at 15°C for 10 min; 3) scanning up from 15°C to 95°C for HSA and MGB, and to 105°C for BFG and other small proteins; and 4) scanning down from 95°C or 105°C to 20°C. The rate of temperature up scanning was 1.0°C/min, and that of down-scanning was 1.5°C/min. The scan rate chosen for an experiment is a compromise between a desired sensitivity and separation of overlapping transitions. The background calibration curve for each sample was obtained with the same am-

TABLE II
Buffer Solutions for Six Proteins and Their Thermal Denaturation Parameters

Protein	Buffer	Concentration (mM)	pH	NaCl (mM)	T _m (°C)*	ΔH (kJ/mole)†
HSA	PBS‡	10	7.4	150	60, 68, 80§	976
BFG	Glycine	50	8.5	0	56, 95**	2259, 2134**
MGB	Glycine	50	11.1	0	70††	115††
LSZ	Acetate	10	4.1	50	77‡‡	135‡‡
CYT	Acetate	10	4.1	50	63§§	77§§
RNase	Acetate	10	4.1	50	55, 64	102, 116

*Thermal denaturation temperature.

†Molar calorimetric enthalpy (equaling transition heat per molar protein).²⁶

‡Phosphate-buffered saline (NaH₂PO₄ + NaOH + NaCl).

§Three transitions at pH 7.0 (10 mM phosphate + 30 mM NaCl).⁴⁰

||Total heat of the three transitions.⁴⁰

**Two transitions at pH 8.5 (50 mM glycine buffer).²⁶

††At pH 11.1 (40 mM glycine buffer).³¹

‡‡At pH 4.5 (40 mM glycine buffer).³¹

§§At pH 4.6 (40 mM glycine buffer).³¹

|||At pH 3.7 and 5.4, respectively (40 mM glycine buffer).³¹

poule, same weight, and similar solid content. The only variant was protein. The background for HSA was the second run of the same sample. During the second run HSA had no transition, as it had been denatured during the first run and was not renatured when the temperature was cooled down. The background curves for other proteins were obtained by running DSC on solid-buffer suspensions without the proteins. All the thermograms shown in this article are background subtracted. The enthalpy change (ΔH) of a transition is obtained from the peak area. Except for albumin, DSC for other proteins under a specific condition was run twice; thus no error bars are given in the figures, but the ΔH differences between the duplicates were around 10%.

RESULTS

Typical DSC thermograms

The curves in Figure 1 represent typical DSC thermograms of HSA in PBS at pH 7.4 and BFG in 50 mM glycine buffer at pH 8.5. Similar thermograms have been observed for HSA³⁰ and for BFG.^{26,27} HSA has three transitions with peak temperatures at 62, 67, 78°C and a total transition heat of 976 kJ/mole. They may represent the denaturation of the three major domains of HSA.²⁶ At pH 8.5, BFG has two transitions with peak temperatures at 55 and 96°C, and transition heats of 1,770 and 1,670 kJ/mole, respectively. The data are comparable to those in Table II. According to Privalov, the lower temperature transition peak of BFG is due to denaturation of its end domains (D), and the one at higher temperature is due to the middle domain (E).²⁶

We have assumed that if an adsorbed protein is denatured, it cannot undergo further thermal transition. Thus, the ΔH of the transition becomes smaller in the presence of adsorbents, or even zero if the surface adsorbs and denatures all the protein mole-

cules. The decrease in enthalpy change thus depends on the ratio of the amount of protein and on the available surface area. A higher surface area should adsorb and denature more proteins, resulting in a smaller ΔH . Figure 2 illustrates that, indeed, the more adsorbent, the smaller the transition peak. There is also a disproportionality of nondenatured HSA and the amount of powder at low LTIC doses (10 and 20 mg). This relation does not exist at high doses of LTIC, probably because excess powders reduce the effective surface area for protein adsorption due to aggregation. This phenomenon is discussed in detail elsewhere.⁷ While the heat of transition is reduced, the transition is also shifted toward higher temperature. The phenomenon was also noticed by Uedaira et al.³⁵

One of the complications of running DSC with LTIC suspensions is the interference of the powders. We often found that endothermic peaks appeared on thermograms of suspension samples, mostly after the protein became thermally denatured. For example, a broad peak appears between 51 and 63°C on the curve of 50 mg LTIC in Figure 2. Sometimes the peaks could be several times larger than those of the protein transitions. We think that these irregular transitions come from dispersion of previously aggregated powders. Such a process is likely aided by elevated temperatures and by proteins that act as surfactants or stabilizers at the solid-water interface. Using less powder was an effective way of reducing those unwanted peaks. The compromise was to use the minimum amount of powder protein that would give the required sensitivity.

Enthalpy of thermal denaturation of proteins on LTIC

The fraction of thermally denatured protein (FTDP) is defined as: $FTDP = \Delta H(\text{ads})/\Delta H(\text{soln})$, where

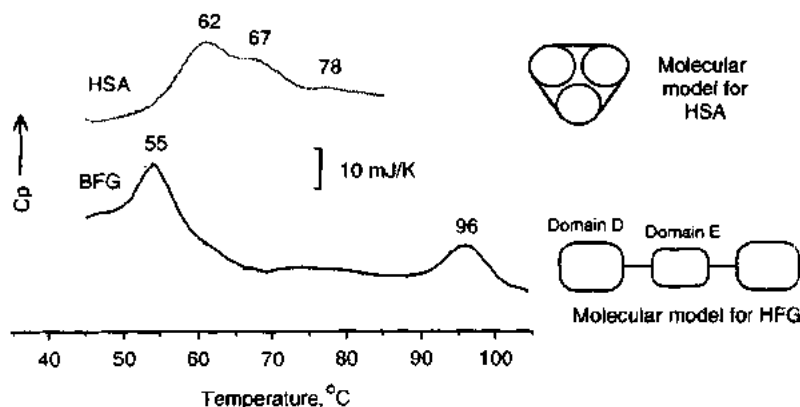


Figure 1. Typical DSC thermograms for HSA at pH 7.4 (10 mM phosphate + 50 mM NaCl) and BFG at pH 8.5 (50 mM glycine). Domain D of BFG denatures at 55°C and E at 96°C.

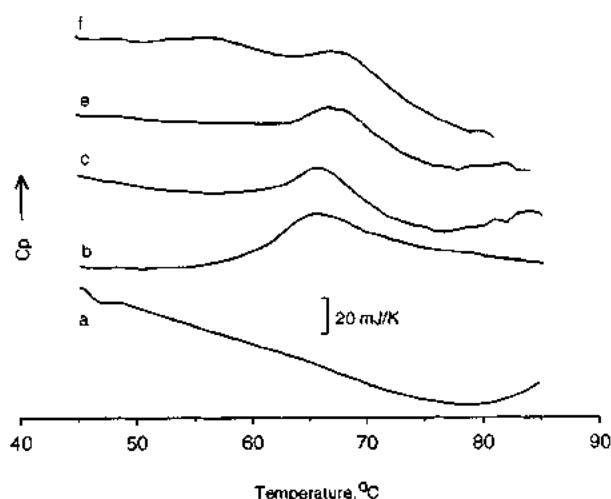


Figure 2. DSC thermograms of denaturation of HSA in the presence of different amounts of LTIC powders. Curve a: PBS + 30 mg LTIC powders, no protein; Curves b–f: PBS + 2.0 mg HSA + 0, 10, 20, and 50 mg LTIC powders, respectively.

$\Delta H(\text{ads})$ (kJ/mole) is the enthalpy change of a transition in the presence of adsorbent and $\Delta H(\text{soln})$ is that for the same amount of protein in the absence of adsorbents. The absolute value of ΔH is not important if only the nondenatured fraction is desired. Figure 3 is the FTDP of HSA as a function of amounts of LTIC powders. Decreases in the transition peaks is obviously a result of the presence of the adsorbent. Because LTIC has a high tendency to adsorb proteins, the surface should be largely covered by proteins after 1 h incubation. Our radioisotope experiments show that the surface concentration of HSA from PBS is 2.5–4.5 mg/m² when the solution concentration is 0.1–2 mg/ml. The concentration of 1.0 ml PBS-

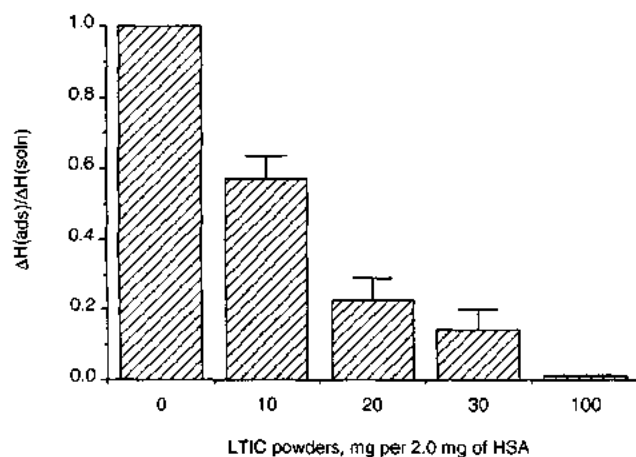


Figure 3. Fraction of thermally denatured HSA in the presence of LTIC powders. The error bars show standard deviations calculated from five samples for each column. The estimated accessible surface area of LTIC is 0.18 m²/10 mg.

buffered HSA can be depleted from 1.6 to 0.5 mg/ml by 30 mg/ml, that of BFG from 1.1 to 0.2 mg/ml, detected by ultraviolet spectroscopy. The surface concentration is estimated at 1.7 and 2.0 mg/m², respectively.⁴ The protein surface concentration may not be the same for samples with different amounts of adsorbent, as they deplete the soluble protein to different extents. We think this variable-coverage adsorption is acceptable because we are only interested in finding out whether the surface can denature proteins.

Both the vacuum- and air-pretreated powders reduce FTDP HSA, suggesting that HSA can be denatured at both the carbon–water interface and the carbon–air–water interface. However, the presence of trapped air may reverse the course of BFG surface denaturation. Figure 4 shows the FTDP of BFG after it was incubated with LTIC powders pretreated either by air (A) or by vacuum (B). The results suggest that the carbon–water interface can denature BFG, but the air–water interface cannot. This was not expected, because most studies show that the air–water interface favors the formation of a monolayer of denatured plasma proteins.³⁶ This phenomenon deserves a fur-

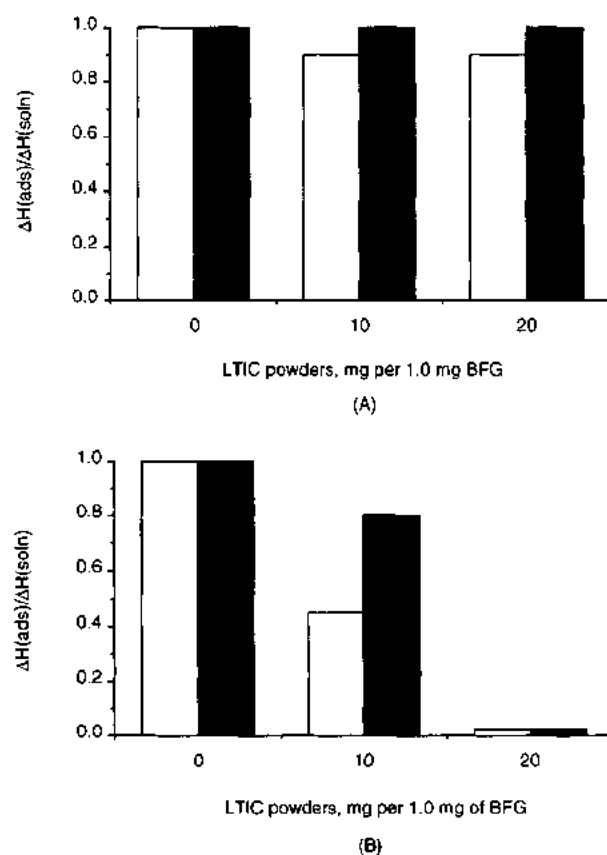


Figure 4. Fractions of thermally denatured BFG in the presence of LTIC powder: (A) Nondegassed and (B) degassed LTIC before buffer pretreatment; white: 1st transition and black: 2nd transition.

ther look. Figure 4 also suggests that domain D may be more susceptible to surface induced denaturation because the first transition peak is smaller than the second one. The vacuum-pretreated LTIC surface may also denature all the small proteins tested (Fig. 5); among them, MGB appears to be the most susceptible to surface denaturation. Again there is no proportionality between the amount of FTDP and the amount of LTIC.

Denaturation of HSA and BFG on silica

From the change of FTDP, we suggest that the silica surface substantially denatures HSA but only moderately denatures BFG (Fig. 6). For adsorbed albumin (human or bovine) on silica, both the denatured case³⁷ and nondenatured case³⁸ have been encountered. With a surface area of about 100 m²/g and its nonporous and hydrophilic nature, silica definitely provides much more accessible surface for adsorption of BFG. Therefore, it is fair to say that the silica surface little changes the conformation of BFG. This observation was also made by Macmillan from CD experiments.²⁰

DISCUSSION

Significance of the fraction of thermally denatured protein (FTDP)

Besides our suggestion of destabilization of the surface adsorbed protein, the decrease of the FTDP might be a result of another process—surface stabil-

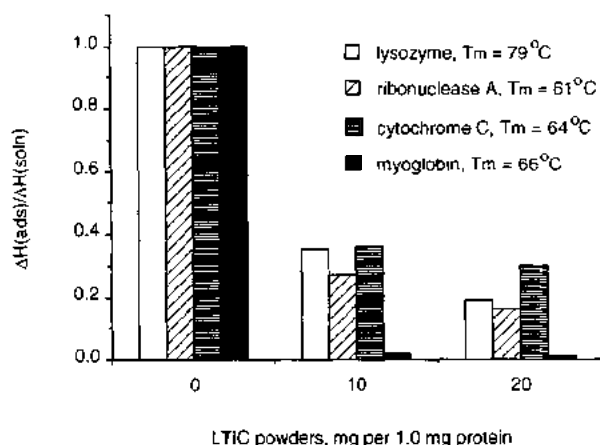


Figure 5. Fractions of thermally denatured model proteins: myoglobin in glycine buffer (pH 11.1) and others in acetate buffer (pH 4.1). The thermal denaturation temperatures are very close to those corresponding values in the literature (Table II).

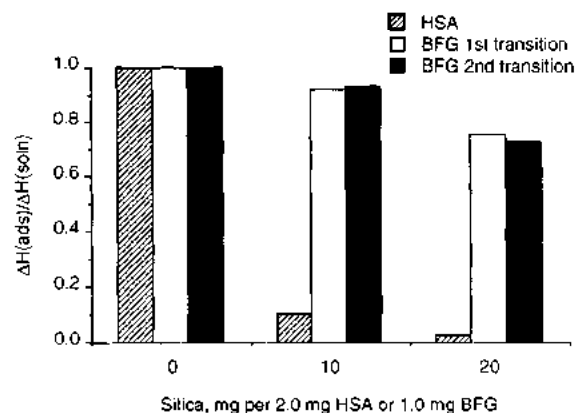


Figure 6. Fractions of thermally denatured HSA and BFG in the presence of colloidal silica; hatched: HSA, white: 1st transition of BFG, and black: 2nd transition of BFG.

ization of the adsorbed protein so that it does not thermally denature in the temperature range. Thus, there is no surface-induced denaturation. However, we can probably rule out this possibility by the following argument.

The structure of surface immobilized (physically adsorbed or chemically bonded) proteins can be stabilized or destabilized by the surface. Thermal stability of proteins may be increased when they are immobilized on a surface, probably as a result of restriction and blocking of unfolding pathways by the surface.⁴¹ However, hydrophobic surfaces denature (destabilize) proteins and are not appropriate for covalent immobilization.⁴² Most solid substrates used for immobilizing proteins are hydrophilic surfaces.^{42,43} Even on a hydrophilic surface, stability of protein can be decreased. Steadman et al.⁴⁴ studied thermal denaturation of seven proteins adsorbed on silica using DSC and other techniques. The major observed effect of surface adsorption on protein stability is destabilization.

If one argues that diminishment or disappearance of a normal denaturation transition implies surface stabilization, it would mean a large enhancement in the structural stability of the adsorbed protein. It is unlikely that a surface could completely prevent an immobilized protein from thermal denaturation in the temperature range of 20–105°C, unless there is substantial conformational change. Therefore, in either the destabilization or the stabilization case, the conformation of the adsorbed protein has been altered by the surface, i.e., denaturation.

The LTIC surface denatures proteins

It is not unexpected that carbon surfaces denature all the proteins used in this work. Hydrophobic sur-

faces are generally more likely to change the conformation of adsorbed proteins than hydrophilic ones, as denatured proteins can maximize their interactions with the surfaces through hydrophobic interactions.^{16,19} The LTIC surface is relatively hydrophobic^{1,2,4} there is a fairly high interfacial energy with water, manifested by lack of water wettability and by the tenacious binding of proteins.⁴ The LTIC surface can also adsorb proteins via a charge-transfer interaction (forming π - σ or π - π complexes with aromatic amino acid residues of adsorbed proteins.^{8,45} This type of interaction may enhance the denaturation tendency of LTIC, as those residues are often buried inside the protein. By the same token, it is understandable why hydrophilic surfaces such as silica do not denature proteins as readily as their hydrophobic counterparts.

It is a misconception to think that an "inert" surface does not exert a strong interaction with proteins. When adsorption is driven mainly by hydrophobic interactions, the major gain of negative free energy change is not directly from the surface-protein interaction, but rather from the entropy increase due to dehydration from the hydrophobic surface.¹⁷ Even though the surface-protein interaction may be weak, the adsorption driving force can be strong because of the large gain of entropy upon freeing surface-perturbed water. Actually, the hydrophobic interaction is commonly characterized by a large entropy increase and a relatively small enthalpy effect.³⁹ LTIC has been considered to be an inactive material because of its low heat of protein adsorption (ΔH).^{5,9} However, low ΔH does not necessarily mean low ΔG . In fact, ΔH in many protein adsorption systems is positive.³⁹ In these cases, adsorption is driven by more negative $T\Delta S$. The ΔG is predominantly governed by the $T\Delta S$ term for the interaction between a protein and hydrophobic surfaces such as LTIC.³⁸ In conclusion, despite its low adsorption enthalpy, LTIC does strongly adsorb proteins, primarily by hydrophobic interactions.

Disparity of silica toward HSA and BFG denaturation

It is somewhat surprising to get opposite denaturation results for HSA and BFG on the silica surface. Because of its high surface activity and low solution stability,³⁸ fibrinogen probably needs no conformational change to bring down the interfacial energy. The degree of unfolding depends on the balance between the cohesive energy of the proteins and protein-surface interactions.³⁹ The folding energy of a protein is just one of the factors that determine whether the adsorbed protein will be denatured.

Other important factors include the protein surface activity and the nature of interfacial interactions.³⁷

CONCLUSIONS

DSC experiments on adsorbed proteins show that the LTIC surface denatures all proteins studied in a number of buffers with different pHs: HSA in PBS of pH 7.4; BFG in glycine buffer of pH 8.5; LSZ, RNase, and CYT in acetate buffer of pH 4.1; and MGB in glycine buffer of pH 11.1. From this general trend, we suggest that LTIC surfaces tend to denature most plasma proteins. We believe that the major driving force for protein denaturation is hydrophobic interactions. The DSC data also show that the colloidal silica surface significantly denatures HSA in PBS of pH 7.4, but only slightly denatures BFG in glycine buffer of pH 8.5. The denaturation ability of silica is apparently smaller than that of LTIC, possibly because of the lack of hydrophobic interactions. However, hydrophobic interactions are not the only driving force for protein denaturation, as indicated in the silica case. It is worthwhile doing further research on this nonhydrophobic denaturation process. Whether a surface denatures adsorbed proteins cannot be the sole criterion for its blood compatibility, which also depends on what proteins are denatured and in what sequence. For example, LTIC may first adsorb and denature albumin in blood. The adsorbed albumin (a bland protein) layer passivates the substrate and prevents the activation of blood coagulation proteins.⁸

The authors thank Sorin Biomedica for providing the LTIC sample. This work was supported by the Center for Biopolymers at Interfaces, University of Utah.

References

1. J. C. Bokros, L. D. LaGrange, and J. Schoen, "Control of structure of carbon for use in bioengineering," in *Chemistry and Physics of Carbon*, Vol. 9, Walker (ed.), Dekker, New York, 1972, pp. 103-171.
2. A. D. Haubold, H. S. Shim, and J. C. Bokros, "Carbon biomedical devices," in *Biocompatibility of Clinical Implant Materials*, Vol. 2, D. F. Williams (ed.), CRC Press, Boca Raton, 1981, pp 3-42.
3. A. S. Hoffman, "Modification of material surfaces to affect how they interact with blood," *Ann. N.Y. Acad. Sci.*, **516**, 96-101 (1987).
4. L. Feng, "Biomedical carbon surfaces and their interactions with plasma proteins," PhD dissertation, University of Utah, 1993.
5. L. Feng and J. D. Andrade, "Protein adsorption on low temperature isotropic carbon: II. Effects of surface charge of solids," *J. Colloid Interface Sci.*, in press.
6. L. Feng and J. D. Andrade, "Protein adsorption on low temperature isotropic carbon: III. Isotherms, com-

- petitivity, desorption, and exchange of adsorption of human albumin and fibrinogen," *Biomaterials*, in press.
7. L. Feng and J. D. Andrade, "Protein adsorption on low temperature isotropic carbon: IV. Competitive adsorption studied by two-dimensional electrophoresis," *Colloids and Surfaces* in press.
8. L. Feng and J. D. Andrade, "Protein adsorption on low temperature isotropic carbon: V. What makes it blood compatible via protein adsorption?" Submitted.
9. T.-H. Chiu, E. Nyilas, and L. R. Turuse, "Microcalorimetric and electrophoretic studies of proteins from plasma," *Trans. Amer. Soc. Artif. Int. Organs*, **24**, 389-402 (1978).
10. T.-H. Chiu, E. Nyilas, and D. M. Lederman, "Thermodynamics of native protein/foreign surface interactions. IV. calorimetric and microelectrophoretic study of human fibrinogen sorption onto glass and LTI-carbon," *Trans. Amer. Soc. Artif. Int. Organs*, **22**, 498-512 (1976).
11. R. E. Baier, V. L. Gott, and A. Feruse, "Surface chemical evaluation of thromboresistant materials before and after venous implantation," *Trans. Amer. Soc. Artif. Int. Organs*, **16**, 50-57 (1970).
12. V. I. Sevastianov, "Role of protein adsorption in blood compatibility of polymers," *CRC Crit. Rev. in Biocompatibility*, **4**, 109-154 (1988).
13. D. H. Kaelble and J. Moacanin, "A surface energy analysis of bioadhesion," *Polymer*, **18**, 475-482 (1977).
14. C. P. Sharma, "LTI carbons: Blood compatibility," *J. Colloid Interface Sci.*, **97**, 615-616 (1984).
15. S. D. Riccitelli, F. H. Bilge, and R. C. Eberhart, "Adsorbed protein visualization on LTI carbon," *Trans. Am. Soc. Artif. Intern. Organs*, **30**, 420-426 (1984).
16. A. L. Iordanski, A. JA. Polischuk, and G. E. Zaikov, "Structural and kinetic aspects of blood plasma protein adsorption on the surface of hydrophobic polymers," *Rev. Macromol. Chem. Phys.* **C23**, 33-59 (1983).
17. W. Norde, "Adsorption of proteins from solution at the solid-liquid interface," *Adv. Colloid Interface Sci.*, **25**, 267-340 (1986).
18. Y. Ito, M. Sisido, and Y. Imanishi, "Adsorption of plasma proteins and adhesion of platelets onto novel polyetherurethaneureas—relation between denaturation of adsorbed proteins and platelet adhesion," *J. Biomed. Mater. Res.* **24**, 227-242 (1990).
19. D. R. Lu and K. Park, "Effect of surface hydrophobicity on the conformational changes of adsorbed fibrinogen," *J. Colloid Interface Sci.*, **144**, 271-281 (1986).
20. C. R. McMillian and A. G. Walton, "A circular dichroism technique for the study of adsorbed protein structure," *J. Colloid Interface Sci.*, **48**, 345-349 (1974).
21. N. de Baillou, P. Dejardin, A. Schmitt, and J. L. Brash, "Fibrinogen dimensions at an interface: Variations with bulk concentration, temperature, and pH," *J. Colloid Interface Sci.*, **100**, 167-174 (1984).
22. J. D. Andrade, V. L. Hlady, and R. A. van Wageningen, "Effects of plasma protein adsorption on protein conformation and activity," *Pure Appl. Chem.*, **56**, 1345-1350 (1984).
23. R. A. Edwards and R. E. Huber, "Surface denaturation of proteins: The thermal inactivation of β -galactosidase (*Escherichia coli*) on wall-liquid surfaces," *Biochem. Cell Biol.*, **70**, 63-68 (1992).
24. J. Soria et al., "Conformational change in fibrinogen induced by adsorption to a surface," *J. Colloid Interface Sci.*, **107**, 204-208 (1985).
25. P. L. Privalov, "Scanning microcalorimeters for studying macromolecules," *Pure Appl. Chem.*, **52**, 479-497 (1980).
26. P. L. Privalov, "Domains in the fibrinogen molecule," *J. Mol. Biol.*, **159**, 665-683 (1982).
27. J. W. Donovan and E. Mihalyi, "Conformation of fibrinogen: Calorimetric evidence for a three-nodular structure," *Proc. Nat. Acad. Sci. USA*, **71**, 4125-4128 (1974).
28. L. V. Medved, T. F. Busby, and K. C. Ingham, "Calorimetric investigation of the domain structure of human complement C1s: Reversible unfolding of the short consensus repeat units," *Biochemistry*, **28**, 5408-5414 (1989).
29. J. W. Shriver, "Differential scanning calorimetry of a conformation in heavy meromyosin," *Arch. Biochem. Biophys.*, **283**, 472-474 (1990).
30. M. Yamasaki and H. Yano, "Differential scanning calorimetric studies on bovine serum albumin: I. Effects of pH and ionic strength," *Int. J. Biol. Macromol.*, **12**, 263-268 (1990).
31. P. L. Privalov and N. N. Khechinashvili, "A thermodynamic approach to the problem of stabilization of globular protein structure: a calorimetric study," *J. Mol. Biol.*, **86**, 665-684 (1974).
32. T. A. Horbett and J. L. Brash, "Proteins at interfaces: Current issues and future prospects," in *Proteins at Interfaces*, J. L. Brash and T. A. Horbett (eds.), ACS Symp. **343**, Washington, DC, 1987, pp. 1-33.
33. C. Zamarron, M. H. Ginsberg, and E. F. Plow, "Monoclonal antibodies specific for a conformationally altered state of fibrinogen," *Thromb. Haemostats*, **64**, 41 (1990).
34. A. L. Iordanski, A. JA. Polischuk, and G. E. Zaikov, "Structural and kinetic aspects of blood plasma protein adsorption on the surface of hydrophobic polymers," *Rev. Macromol. Chem. Phys.* **C23**, 33-59 (1983).
35. H. Uedaira, A. Yamauchi, J. Nagasawa, H. Ichijo, T. Suehiro, and K. Ichimura, "The effect of immobilization in photocrosslinked polymer on the thermal stability of invertase," *Seni Gakkaishi*, **41**, T317 (1985).
36. T. A. Horbett, "Protein adsorption on biomaterials," in *Biomaterials: Interfacial Phenomena and Applications*, *Adv. Chem. Ser. Vol. 199*, S. L. Cooper and N. A. Peppas (eds.), ACS, Washington, DC, 1982, pp. 233-244.
37. A. Kondo, S. Oku and K. Higashitani, "Structural changes in protein molecules adsorbed on ultrafine silica particles," *J. Colloid Interface Sci.*, **143**, 214-221 (1991).
38. B. W. Morrissey, "The adsorption and conformation of plasma proteins: A physical approach," *Ann. N.Y. Acad. Sci.*, **283**, 50-64 (1977).
39. E. Dickinson and S. R. Euston, "Simulation of adsorption of deformable particles modelled as cyclic lattice chains: A simple statistical model of protein adsorption," *J. Chem. Soc. Faraday Trans.*, **86**, 805-809 (1990).
40. E. I. Tiktopulo, P. L. Privalov, S. N. Borisenko, and G. V. Troitskii, "Microcalorimetric study of domain organization of serum albumin," *Mol. Biol.*, **19**, 884-889 (1985).
41. R. Ulbrich-Hofmann, R. Golbik, and W. Damerau, "Fixation of the unfolding region—a hypothesis of enzyme stabilization," in *Stability and Stabilization of Enzymes*, W. J. J. van den Tweel, A. Harder, and R. M. Buitelaar (eds.), Elsevier, Amsterdam, 1992, 497-504.
42. J. M. S. Cabral and J. F. Kennedy, "Covalent and coordination immobilization of proteins," in *Protein Im-*

- mobilization: Fundamentals and Applications*, R. F. Taylor (ed.), Marcel Dekker, New York, 1991, pp. 73-138.
43. M. P. J. Kierstan and M. P. Coughlan, "Immobilization of proteins by noncovalent procedure: Principles and Applications," in *Protein Immobilization: Fundamentals and Applications*, R. F. Taylor (ed.), Marcel Dekker, New York, 1991, pp. 13-71.
 44. B. L. Steadman, C. C. Thompson, C. R. Middaugh, K. Matsuno, S. Vrona, E. Q. Lawson, and R. V. Lewis, "The effects of surface adsorption on the thermal stability of proteins," *Biotech. Bioeng.*, **40**, 8-15 (1992).
 45. J. Porath, "Explorations into the field of charge-transfer adsorption," *J. Chromatogr.*, **159**, 13-24 (1978).

Received August 3, 1993

Accepted January 26, 1994

Protein Adsorption on Low-Temperature Isotropic Carbon

II. Effects of Surface Charge of Solids

L. FENG AND J. D. ANDRADE¹

Department of Bioengineering and Department of Materials Science and Engineering, 2480 MEB, University of Utah, Salt Lake City, Utah 84112

Received June 15, 1993; accepted March 8, 1994

Protein adsorption on low-temperature isotropic carbon (LTIC) and on gold electrodes was studied via changes in their double-layer capacitance. The surface charge of the electrodes was controlled by a DC potential. The more negatively charged LTIC always adsorbed more proteins from near neutral or acidic solutions, regardless of the charge on the proteins. Adsorption patterns did not change when the solution ionic strength was varied. At pH 7.4 the more negatively charged gold adsorbed the more positively charged proteins. Kinetic data indicate that higher adsorbed amounts were accompanied by higher initial adsorption rates. The electrostatic interaction did not appear to play a significant role in the interactions between the proteins and LTIC. Our hypothesis suggests hydrophobic and interfacial water properties are involved in protein adsorption on LTIC.

© 1994 Academic Press, Inc.

INTRODUCTION

The role of the surface charge of blood-contacting implants on their blood compatibility is still controversial. Although most solids with positive zeta potential are thrombogenic (1), the negative surface potential is not a guarantee of non-thrombogenicity (2, 3). While some highly nonthrombogenic surfaces are negatively charged, such as endothelium (4) and heparin (2), some potent thrombogenic surfaces are also negatively charged, like glass (3).

We have systematically studied protein adsorption onto low-temperature isotropic carbon (LTIC). Our objective was to examine how such a reputed blood compatible material interacts with proteins. Our studies are based on the belief that the nature of the adsorbed protein film eventually determines how the surface interacts with blood (6).

The effect of surface charge of polymers (7-13) and metals (1, 13-15) on protein adsorption has been studied. The data cannot be satisfactorily explained by considering only the overall electrostatic interaction. There are cases where a surface adsorbs more proteins that possess the same type of charge, or a surface adsorbs less protein that has the opposite

type of charge, or the interaction between them shows no apparent dependence on charge. Such examples are fibrinogen and albumin on glassy carbon and platinum (16), albumin and ribonuclease on polystyrene (8), albumin on silver iodide and α -Fe₂O₃ (8), fibrinogen on polydimethylsiloxane and polyelectrolyte complex (10), fibrinogen on germanium (12), fibrinogen on mercury and platinum (14), and cytochrome c and lysozyme on polystyrene (13). A general conclusion from these studies is that in solution of normal ionic strength, electrostatic interactions do not play a major role in protein adsorption (2, 17, 18).

Impedance measurements are a classical way of studying adsorption of organics on metal electrodes (19) and have been applied to protein adsorption on metal and carbon electrodes (1, 16, 20-27). The technique can readily record variations of double-layer capacitance, from which one can acquire information on protein adsorption kinetics, surface coverage, and isotherms. The principle of the measurement is shown in Fig. 1. The solid-liquid interface is represented as an equivalent electric circuit composed of solution resistance (R_s), in series with double-layer (also called differential or charging) capacitance (C_d) in parallel with faradaic (redox) impedance (Z_f) (21). The protein solutions used in this work contained no added electroactive species that could undergo redox reactions in the applied potential range. The contribution to the impedance from adventitious trace redox processes, such as the quinone-like oxides on LTIC or oxygen in solution, were suppressed by applying a high-frequency AC signal (20). Therefore, Z_f is treated as infinity and the measured impedance is approximately equal to the sum of the real term R_s and the imaginary term C_d . C_d is determined by the nature of the electrode surface and the electrolyte solution, including adsorption on the electrode. Adsorbed protein molecules displace ions and water molecules from the surface, inducing redistribution of the charge and causing changes in capacitance, usually (but not always) reducing C_d (1, 24, 26). It is difficult, however, to pinpoint all the factors that affect C_d , mainly due to our limited knowledge of the double-layer structure (28). According to Lundstrom, capacitance yields information on the number of contact

¹ To whom correspondence should be addressed.

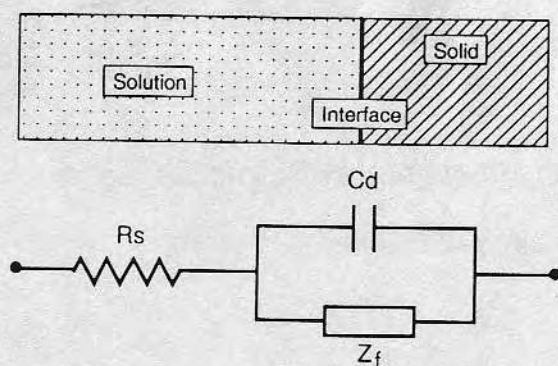


FIG. 1. Principles of impedance measurements. Equivalent circuit for the impedance at a solid-water interface: R_s , solution resistance; C_d , double-layer capacitance; and Z_f , Faradaic impedance.

points or contact area of protein and surface (29). In principle, the surface coverage (θ) can be estimated from the change in C_d , provided that the potential of zero charge of the electrode and the surface tension at this potential are known (19). When the two parameters are not available, an empirical equation can be substituted as a first approximation (19),

$$C_d = C_{d\theta=0} \cdot (1 - \theta) + C_{d\theta=1} \cdot \theta + (q_{\theta=1} - q_{\theta=0}) \frac{d\theta}{dV}, \quad [1]$$

where $C_{d\theta=0}$, $C_{d\theta=1}$, $q_{\theta=0}$, and $q_{\theta=1}$ represent the capacitance and the surface charges when $\theta = 0$ and $\theta = 1$, respectively. Since $d\theta/dV$ is not usually known, and $C_{d\theta=1}$ is also difficult to define, a "normalized capacitance change" (NCC) was used,

$$\begin{aligned} \text{NCC} &= \frac{C_{d\theta=0} - C_d}{C_{d\theta=0}} = \frac{C_d(t=0) - C_d(t)}{C_d(t=0)} \\ &= \frac{C_d(0) - C_d}{C_d(0)} = \frac{\Delta C}{C_d(0)}, \end{aligned} \quad [2]$$

where t is the adsorption time. NCC is dimensionless and can be considered as a measure of the adsorbed amount (24, 30), although it is neither θ nor any absolute value for surface concentration (Γ).

EXPERIMENTAL

Materials

Silicon-alloyed LTIC, manufactured for artificial heart valves, was a gift from Sorin Biomedica (Italy). Relevant data for the four proteins studied are listed in Table 1. HSA and HFG are plasma proteins which play important roles in blood compatibility. SOD and LSZ are simple single domain proteins whose structures are well known. Note the isoelectric points (pI) for these four proteins. At pH 7.4, the first three are overall negatively charged, while LSZ has a net positive charge. All the proteins were used without further purification. The chemicals used for phosphate buffered saline (PBS) were all super pure grades: sodium dibasephosphate (Ultrapur) from J. T. Baker Chemical (Phillipsburg, NJ), sodium hydroxide (Suprapur) and sodium chloride (Suprapur) from EM Science (Gibbstown, NJ), sodium acetate and acetic acid (analytical reagents) from Mallinckrodt (Parks, KY), and glycine (electrophoretically pure) from Hoefer Scientific Instruments (San Francisco, CA). Water for the buffers was double distilled in a quartz distiller (Heraeus, Quarzschmelze, Germany) from predeionized water. Unless specifically indicated, all the buffer solutions contained 10 mM buffer substances (phosphate, acetate, or glycine) and 100 mM NaCl.

Electrodes and the Cell

LTIC working electrodes were assembled by forcing LTIC disks of 3 mm (diameter) \times 2 mm (thickness) into hot Kel-F (the 3M trade name for polychlorotrifluoroethylene) tubes. After cooling, the shrunk tubes held the disks firmly. The possible voids between the carbon side wall and the Kel-F inner wall were filled with wax for insulation. A copper wire was electrically connected to the LTIC disk by carbon paste.

TABLE 1
Four Proteins Studied in this Work

Protein	Albumin	Fibrinogen	Superoxide dismutase	Lysozyme
Abbreviation	HSA	HFG	SOD	LSZ
Source	Human serum	Human plasma	Bovine liver	Hen egg white
Preparation	Crystallized	Lyophilized	—	Lyophilized
Purity, %	98	95 ^a	—	95
Mol wt., kDa	65	340	15.5	14.3
Isoelectric point	4.7	5.8	4.6	10.7
Domains	Multiple	Multiple	Single	Single
Supplier	ICN Biomedicals, Irvine, CA	Calbiochem, La Jolla, CA	DDI Pharm., Mountain View, CA	Calbiochem., La Jolla, CA

^a Clottable percentage.

A gold working electrode 3 mm in diameter was purchased from Bioanalytical Systems (West Lafayette, IN).

Two electrodes were used, which was considered acceptable because the current involved was too small to affect the interfacial state of the reference electrode (21). Another LTIC disk served as the reference electrode with a surface area 15 times larger than that of the working LTIC electrode. Such a high area ratio helps minimize the uncertainty of the capacitance change at the reference electrode (30). Conventional reference electrodes, standard calomel electrode (SCE) or Ag/AgCl electrode, were intentionally avoided due to the difficulty of cleaning. Convective flow was provided by magnetic stirring at 200 rpm. Before each adsorption experiment, the interior of the cell, together with the reference electrode, was cleaned by soaking in 96% pure sulfuric acid (Mallinckrodt) for 15 min, thoroughly washing with Milli-Q water (Millipore, Bedford, MA), and finally rinsing with double-distilled water.

Instrument and Operation

Both the working and the reference electrodes were connected to the measuring leads of a multifrequency LCR meter (HP 4274A). The meter imposed an AC voltage with frequency of 1.0 kHz and amplitude of 10 mV across the two electrodes, measured the amplitude and phase angle of the ensuing current, and computed the corresponding capacitance and resistance according to the series model. Data were collected by a computer at preset time intervals (2 s to 1 min). An attached DC offset imposed a DC bias voltage across the two electrodes.

Prior to each adsorption measurement the working electrode was polished by hand with 0.3 μm alumina slurries for about 2 min, rinsed with a stream of Milli-Q water, sonicated in two portions of Milli-Q water (each for 5 min), rinsed with acetone (EM), and dried in air. Caution was taken in every cleaning step to avoid potential contamination. The clean and dry electrode was immersed in 1.80 ml of pure buffer in the cell. In most cases the recorded capacitance of bare electrodes had some initial decrease and became nearly constant after 10–20 min. Then 0.20 ml of a concentrated protein solution was pipetted into the buffer, which was being stirred. The change in capacitance vs time was recorded on line.

XPS Verification

X-ray photoelectron spectroscopy (XPS), 5950B ESCA Spectrometer (Hewlett-Packard), was used as an independent method for detection of adsorbed proteins on LTIC plates. Protein adsorption was carried out in a way similar to the impedance experiment. At the end of adsorption the LTIC plates were rinsed with pure buffer, dried in air, and directly mounted in the slots of the XPS sample holder and covered by gold-plated masks. Analysis conditions were X-

ray power 400 W, flood gun off, aperture closed, and 20 cycles of narrow scans (20 eV width). The elemental ratio was computed from the narrow scan C-1s and N-1s spectra (31). PBS residues did not interfere with the measurement.

RESULTS

Capacitance Curves

Capacitance vs time is plotted in Fig. 2. $C_d(0)$ is the steady-state Cd value before addition of protein. Upon addition of protein solution, Cd starts decreasing, initially very fast but then gradually slowing down, and finally nearly levels off. Some curves reached steady state in a short time while others required longer than 40 min. For most measurements the normalized incremental change, $(C_d(k+1) - C_d(k))/C_d(0)$, with k being minutes, was very small, less than 0.05% per minute after 15–20 min of adsorption. Thus 20 min was chosen as the cutoff time, where the Cd was taken as the steady or plateau value ($C_d(P)$). So was NCC(P), or simply NCC. Adsorption rates will be described by the initial rate of NCC, i.e., $(d(\text{NCC})/dt)_{t=0}$.

Isotherms

Isotherms for capacitance change can be constructed by plotting NCC(P) values against their corresponding protein concentrations. Figure 3 shows such an isotherm for HSA obtained at 0 mV DC voltage. It clearly shows that NCC gradually increases with protein concentration until reaching the plateau, suggesting that the change in Cd represents the change in surface coverage or surface concentration. The isotherm does not reach plateau until high HSA concentrations. The radioactive probe method (32) yields a similar isotherm. This type of isotherm is often observed on hydrophobic surfaces (30, 33).

Correlation of Charge Density vs DC Voltage

When imposing a DC voltage on a conductive electrode, one alters the charge density on the surface. Charge density

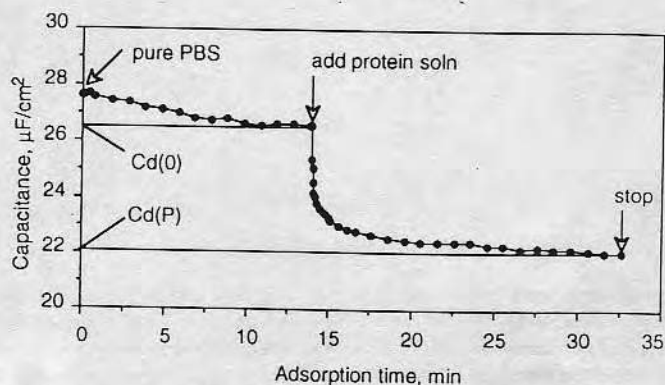


FIG. 2. Procedures for protein adsorption and change in capacitance of an LTIC electrode with adsorption time.

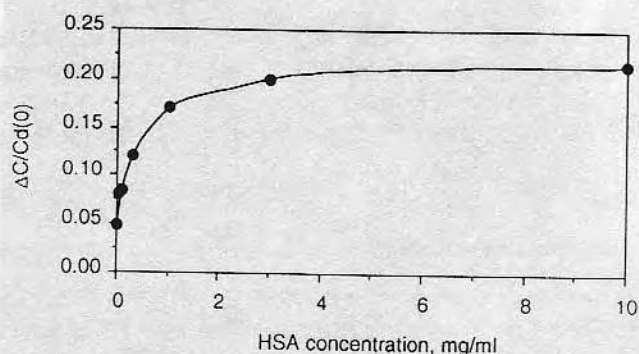


FIG. 3. Capacitance isotherms due to HSA adsorption on LTIC electrodes.

(q) of a bare surface as a function of the voltage (U) can be precisely calculated from Eq. [3] if one knows the capacitance $Cd_{q=0}$ and the potential U of zero charge ($U_{q=0}$), assuming that Cd varies linearly with U (16):

$$q(U) = \frac{(U - U_{q=0}) \cdot (Cd + Cd_{q=0})}{2} \quad [3]$$

In this work only the increment of q (Δq) as a function of U can be estimated as $U_{q=0}$ was not known. Δq is roughly $2\text{--}2.5 \text{ mC/cm}^2$ for every 100 mV . The variation of charge density is within the range frequently used with particle substrates (9). For the purpose of considering charge effects, it is sufficient to know that higher U produces higher q , and the variation of q is roughly proportional to that of U . As for a reference, $U_{q=0}$ for a glassy carbon is $+50 \text{ mV}$ vs that of SCE, i.e., $+300 \text{ mV}$ vs that of normal hydrogen electrode in 100 mM PBS (16).

Charge Effects on Protein Adsorption on LTIC

Figures 4 and 5 are the plots of NCCs vs electrode potentials in PBS, pH 7.4, at different NaCl concentrations. The

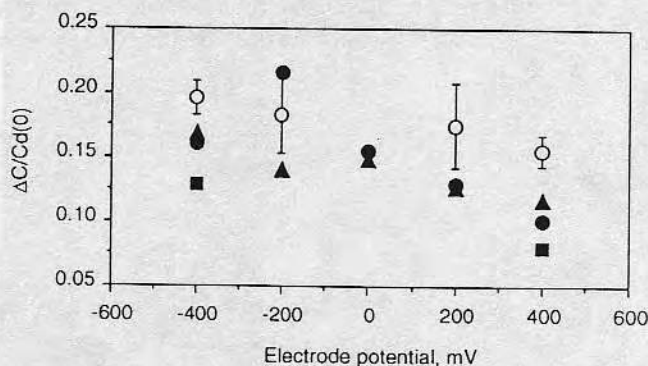


FIG. 4. Normalized capacitance change due to adsorption of 0.50 mg/ml HSA (solid) and 0.05 mg/ml HFG (open) on an LTIC electrode from PBS (pH 7.3) as functions of its potentials. Note that both proteins are negatively charged. HSA adsorption at different ionic strengths with 10 mM phosphate and 100 mM NaCl (triangles), 10 mM phosphate and 100 mM NaCl (circles), and 4 mM phosphate only (squares).

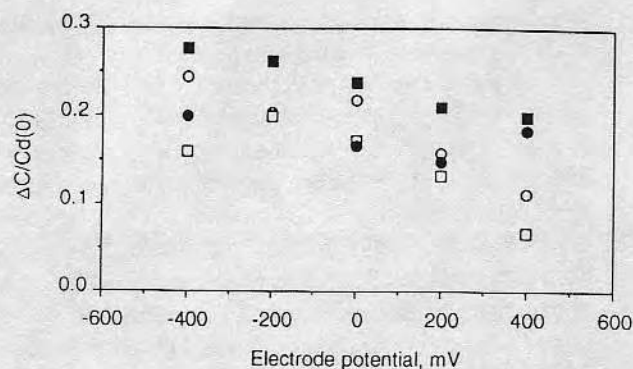


FIG. 5. Normalized capacitance change due to adsorption of 0.10 mg/ml LSZ (solid) and 0.10 mg/ml SOD (open) on an LTIC electrode as functions of its potentials from PBS (pH 7.2) with 10 mM phosphate and 100 mM NaCl (circles) and 10 mM NaCl (squares). Note that LSZ is positively charged and SOD is negatively charged.

data indicate that more negatively charged electrodes adsorb more proteins, regardless of the net charge or size of the protein, or of the ionic strength. For example, at pH 7.4 HSA, HFG, and SOD all bear negative charges while LSZ has a positive charge. SOD and LSZ are very small proteins compared with HSA and HFG. Yet they all behave similarly when the potential is varied. Such a relationship holds with solutions of high (100 mM NaCl), intermediate (10 mM NaCl) (Figs. 4 and 5), and low (4 mM NaCl) ionic strength (Fig. 4). The pattern of protein adsorption on LTIC defies what a simple electrostatic argument would suggest, even at low ionic strength which enhances electrostatic interactions.

Figure 6 shows the change in NCCs vs electrode potentials in both acidic (pH 4.0) and basic (pH 10.5) solutions. HSA has a net positive charge at pH 4.0; yet its NCC- U relationship is very similar to that when it is charged negatively at pH 7.4. At pH 10.5, where HSA becomes negative but LSZ

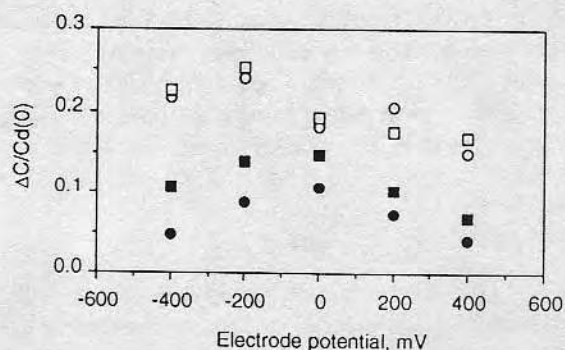


FIG. 6. Normalized capacitance change due to adsorption of 0.50 mg/ml HSA (circles) and 0.10 mg/ml LSZ (squares) from acidic (pH 4.0, acetate, open) and basic (pH 10.6, glycine, solid) solutions (100 mM NaCl) as functions of electrode potentials. Note that HSA is positively charged at pH 4.0 but negatively charged at pH 10.6 while LSZ is positively charged at pH 4.0 but almost without the net charge at pH 10.6.

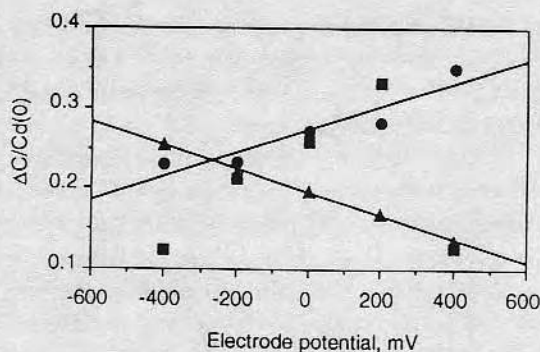


FIG. 7. Normalized capacitance change due to adsorption of 0.50 mg/ml HSA (circles), 0.05 mg/ml HFG (squares), and 0.10 mg/ml LSZ (triangles) from PBS (10 mM phosphate and 100 mM NaCl, pH 7.4) on a gold electrode as functions of electrode potentials. Note that HSA and HFG are negatively charged but LSZ is positively charged.

is probably without a net charge, the maxima of their NCCs appear at $U = 0$ mV. Increasing either voltage reduced the NCCs. This adsorption pattern bears a close resemblance to the adsorption of uncharged organics on metals as a function of electrode potential and will be discussed later.

Charge Effects on Protein Adsorption on Gold

Gold is a good comparison or reference for carbon as it is thrombogenic (1, 34), has high surface energy (35), and is hydrophilic (if not contaminated) (36). As Fig. 7 demonstrates, the interactions between the gold surface and the proteins follow that expected from electrostatic interactions, i.e., more positively charged surface adsorbs more negatively charged proteins, such as HSA and HFG, or vice versa, such as LSZ. For all three proteins the change in NCC on gold is larger than that on LTIC for identical protein concentrations and buffer conditions. The ratio of NCC on gold vs NCC on LTIC is 1.3 for HFG and 1.7 for HSA, possibly indicating a higher surface concentration on gold. This is consistent with the result by Williams and Williams (36): HSA surface concentration is 3.9 mg/m^2 on gold after 1-h incubation compared to 2.0 mg/m^2 on LTIC after 3-h incubation (32).

Charge Effects on Rates of Protein Adsorption

Figure 8 shows the initial rate of NCC, $(d(\text{NCC})/dt)_{t=0}$, as a function of the potentials on both LTIC and gold electrodes. Although the points are somewhat scattered, the general trend for the change in $(d(\text{NCC})/dt)_{t=0}$ vs U is consistent with that in NCC vs U ; i.e., on LTIC the more negatively charged surface adsorbs proteins faster initially but on gold the more negatively charged surface adsorbs positive proteins faster or vice versa. It suggests that a high adsorption rate (including both transport and reaction processes) usually results in high surface concentration. It may be also true that a high surface concentration is usually accompanied by a high adsorption rate.

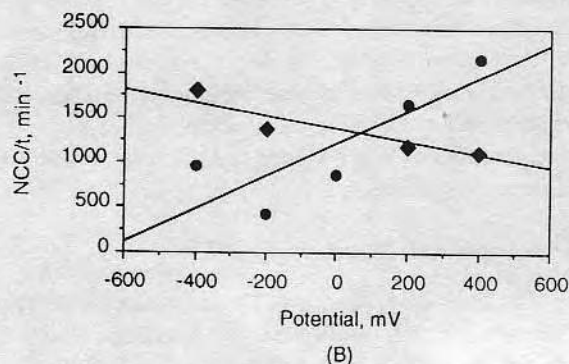
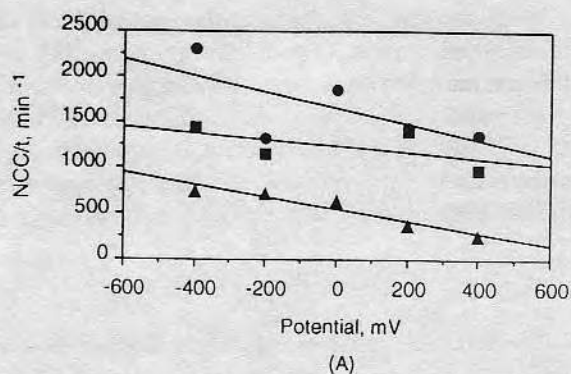


FIG. 8. Initial rates of normalized capacitance change due to protein adsorption from PBS (10 mM phosphate and 100 mM NaCl, pH 7.4) as functions of electrode potentials on LTIC (A) and gold (B). Protein concentrations (mg/ml): HSA, 0.50 (circles); HFG, 0.05 (squares); SOD, 0.50 (triangles); and LSZ, 0.10 (diamonds).

XPS as an Independent Test

XPS provided another measure of Γ as a function of the charge density of the solids. Two LTIC plates were connected to the DC offset. Proteins were allowed to adsorb onto the plates at potentials identical in amplitudes but opposite in polarities. The Γ of HSA adsorbed on these plates measured by XPS is displayed in Fig. 9. Since clean LTIC and PBS

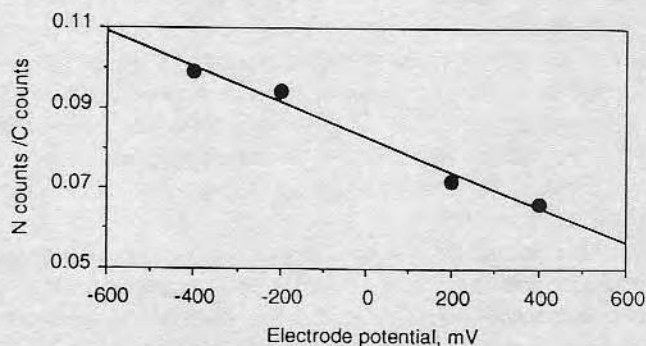


FIG. 9. XPS measurements of the nitrogen signal from 0.50 mg/ml HSA adsorbed from PBS (10 mM phosphate and 100 mM NaCl, pH 7.4) on LTIC surfaces with different potentials.

have no detectable nitrogen, nitrogen signals are attributed to adsorbed protein. Indeed the XPS data confirm that the LTIC surface, with more negative charge, adsorbs more HSA. Adsorption of HFG shows the same trend but the potentials of LTIC (± 400 mV) have virtually no effects on LSZ adsorption, which is comparable to the corresponding points in Fig. 5 (data for HFG and LSZ not shown) (5).

DISCUSSION

The foregoing results clearly show that under neutral and acidic conditions the more negatively charged LTIC adsorbs more protein, regardless of the nature of the proteins. Similar results were obtained with glassy carbon and platinum as the electrodes by Bernabeu and Caprani (16). They speculated that cations bridged the negatively charged surface and proteins. We examine several processes that may be responsible for the insignificant role of electrostatic interactions in protein adsorption on LTIC.

Five Possible Mechanisms

- (1) The dominant interaction is between the surface and a patch or domain on the protein of opposite charge (2, 11).
- (2) Counterions bridge or screen (2, 16, 17).
- (3) Negative phosphate or other anions may be specifically adsorbed, compensating the positive charge on LTIC.
- (4) Adsorption of oppositely charged proteins reverses the sign of the surface charge (37).
- (5) Hydrophobic interactions are so dominant that electrostatic interactions are insignificant (13, 38).

Examination of the Validity of the Five Hypotheses

(1) Charged patches are not responsible because overall electrostatic interactions are operative for protein adsorption on the gold electrode. Electrostatic interactions seem to be solid-dependent rather than protein-dependent. Besides, if a surface tends to adsorb proteins whenever they have oppositely charged regions, then the positive LTIC surface should adsorb more LSZ and HSA through interactions with their negative patches even though the global proteins are positively charged (39).

(2) Cation bridging can be discounted because the only dominant cations are sodium cations, which have very low screening activity (40). Chloride anions would have higher screening ability. The effect of cation bridging, were it present, would have been reduced in a solution with much lower ionic strength (8, 13).

(3) The specific anion adsorption argument is inappropriate because similar adsorption patterns are seen while using nonphosphate solutions (data not shown) (5). Compared with water molecules, contact-adsorbed ions occupy only a small portion of a solid surface even under extremely high potentials (41).

(4) The charge reversal process cannot explain the initial adsorption rate which does not indicate that negative proteins were adsorbed faster on a more positive LTIC surface before the charge reversal happened.

(5) The hydrophobic nature of LTIC surfaces (43), the tendency of adsorbed proteins to denature (44), and irreversible adsorption (32) suggest that the hydrophobic interaction is the dominant force for protein adsorption on LTIC. Specifically, the phenomenon of suppressed electrostatic interaction is frequently seen when proteins are adsorbed on hydrophobic surfaces (13, 16, 38, 45), where hydrophobic interactions tend to override electrostatic interactions (46). Yet this simple overriding mechanism cannot explain why the negative LTIC surface adsorbs more proteins than the positive carbon surface.

Our Hypothesis

We formulate a tentative hypothesis that is essentially a modification of the hydrophobic dominance theory, with addition of the influence of interfacial water: *the imposed charge on LTIC alters the structure of water near the interface, with a more negative charge making the solvation water easier to displace by proteins*. This means that the water on a more negatively charged LTIC is less organized so there is less entropic gain when it is displaced, or that negative LTIC creates a small gap between the water and the surface so proteins are easier to attach to the surface. In order to be adsorbed, proteins have to compete with the interfacial water for surface adsorption sites (28, 47). The structure of the interfacial water thus greatly affects adsorption of either ionic or nonionic species (47). Although the higher surface charge density makes the water-surface interaction stronger, other factors of the water solvent, such as reorientation, clusters, local ordering, and hydrogen bonding, also modify the interaction (28, 47). Urry believes that there exists a competition between apolar and polar species for water of hydration. Existence of charge on a hydrophobic surface can destructure nearby water molecules involved in hydrophobic hydration. Subsequently an increase in surface charge decreases hydrophobic interactions (48). That is why the potential for a maximal surface concentration (U_m) of organic adsorption is near $U_{q=0}$ (41, 47). The Cd- U plot looks like Fig. 6 for protein adsorption at pH 10.6. However, U_m is not usually equal to $U_{q=0}$ because other interactions are also involved, such as those due to water structuring at charged surfaces. Thus U_m is not necessarily equal to $U_{q=0}$. On many metal electrodes U_m appears at more negative potentials than $U_{q=0}$ (41). For LTIC, the Γ - U relation may look like the one in Fig. 10. An inference can be used to explain Fig. 6. When pH is 10.6, U_m probably happens to be at the zero potential (U_0) of the x axis. It is equivalent to shifting the curve in Fig. 10 toward the right until the U_m overlaps $U_{q=0}$.

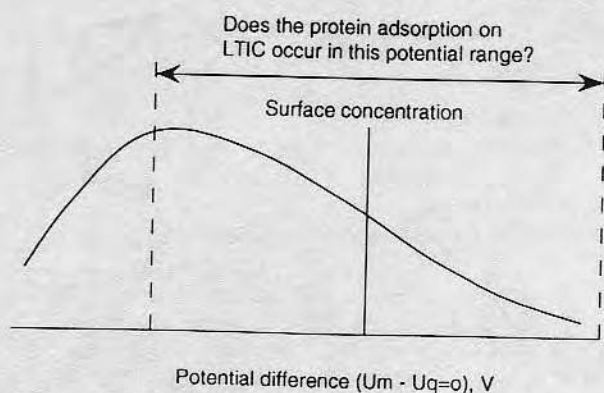


FIG. 10. Hypothesis on the carbon-water interface and protein adsorption. The hypothetical Γ - U relationship: the monotonical decrease in Γ with U may fall in the range of the LTIC potential variation.

About the Initial Adsorption Rates

The electrostatic interaction, being a long-range force, should reverse the C_d - U dependence of the initial adsorption rate (Fig. 9), a diffusion-controlled process. However, hydrophobic interactions are also long range (51). The interaction force between two mica surfaces coated with proteins shows that the hydrophobic interaction is in the range of 60 nm while the electrostatic interaction appears at 75 nm (52). Tilton *et al.* showed that the hydrophobic force is operative as far as 25–80 nm (53).

CONCLUSIONS

Impedance measurements probe protein adsorption by detecting changes in double-layer capacitance. Surface charge effects of LTIC and gold on protein adsorption are studied by imposing a DC offset. At pH 7 and 4, the more negatively charged LTIC adsorbs more proteins of either positive or negative charge. Variation of ionic strength has no significant effect on this trend. At pH 7 the charged gold surface adsorbs more proteins that bear opposite charge to the gold. The initial adsorption rate has a similar relation with the surface charge as does the surface concentration. The electrostatic interaction is not of major significance in the interactions between the LTIC surface and the proteins studied. We hypothesize that the hydrophobic interaction is stronger than the electrostatic interaction. The hydrophobic interaction can be altered through changing the structure of interfacial water by the imposition of charge on the LTIC surface. The capacitance change due to protein adsorption as a function of the surface potential shows the importance of considering the process as a competition between proteins and water for the solid surface. The state of interfacial water and its interactions with the surface play an integral role in protein adsorption. The effect of surface charge on protein adsorption, especially on hydrophobic surfaces, is a complex process,

which cannot be directly explained by the simple electrostatic interaction. That is probably why surface charge cannot be the sole factor in determining the thrombogenicity of a blood-contacting material.

ACKNOWLEDGMENTS

We thank Sorin Biomedica for providing the LTIC sample. We acknowledge helpful discussions with Drs. Vladimir Hlady and James McIntyre of the University of Utah. This work was supported by the Center for Biopolymers at Interfaces, University of Utah.

REFERENCES

1. Ivarsson, B., and Ljunstrom, L., *CRC Crit. Rev. Biocompat.* **2**, 1 (1986).
2. Andrade, J. D., and Hlady, V., *Adv. Polym. Sci.* **79**, 3 (1986).
3. Chuang, H. Y. K., in "Blood Compatibility, Vol. 1" (D. F. Williams, Ed.), p. 88. CRC Press, Boca Raton, 1987.
4. Hench, L. L., and Ethridge, E. C., "Biomaterials: An Interfacial Approach." Academic Press, New York, 1982.
5. Feng, L., Ph.D. Dissertation. University of Utah, 1993.
6. Hoffman, A. S., *Ann. N.Y. Acad. Sci.* **516**, 96 (1987).
7. Norde, W., and Lyklema, J., in "Ions in Macromolecular and Biological Systems" (D. H. Everett and B. Vincent, Eds.), p. 11. Scientifica, Bristol, 1977.
8. Koutsoukos, P. G., Mumme-Young, C. A., Norde, W., and Lyklema, J., *Colloids Surf.* **5**, 93 (1982).
9. Elgersma, A. V., Zsom, R. L. J., Norde, W., and Lyklema, J., *J. Colloid Interface Sci.* **138**, 145 (1991).
10. Schmitt, A., Varoqui, R., Uniyal, S., Brash, J. L., and Pusiner, C., *J. Colloid Interface Sci.* **92**, 145 (1983).
11. Lesins, V., and Ruchenstein, E., *Colloid Polym. Sci.* **266**, 1187 (1988).
12. Mattson, J. S., *Science* **181**, 1055 (1973).
13. Kondo, A., and Higashitani, K., *J. Colloid Interface Sci.* **150**, 344 (1992).
14. Ramasamy, N., Lucas, T. R., Stanczewski, B., and Sawyer, P. N., in "Topics in Bioelectrochemistry and Bioenergetics, Vol. 3" (G. Milazzo, Ed.), p. 243. Wiley, Chichester, 1980.
15. Morrissey, B. W., Smith, L. E., Stromberg, R. R., and Fenstermaker, C. A., *J. Colloid Interface Sci.* **56**, 557 (1976).
16. Bernabeu, P., and Caprani, A., *Biomaterials* **11**, 258 (1990).
17. Brash, J. L., in "Blood Compatible Materials and Devices" (C. P. Sharma *et al.*, Eds.), p. 3. Technomic, Lancaster, 1991.
18. Koutsoukos, P. G., Mumme-Young, C. A., Norde, W., and Lyklema, J., *Colloids Surf.* **5**, 93 (1982).
19. Frumkin, A. N., in "Modern Aspects of Electrochemistry, Vol. 3" (Bockris and Conway, Eds.), p. 149. Butterworths, Washington, DC, 1964.
20. Bernabeu, P., Tamisier, L., de Cesare, A., and Caprani, A., *Electrochim. Acta* **33**, 1129 (1988).
21. Bard, A. J., and Faulkner, L. R., "Electrochemical methods," pp. 316, 551. Wiley, New York, 1980.
22. Stone, G., and Srinivasan, S., *J. Phys. Chem.* **74**, 1088 (1970).
23. Lecomte, M. F., Clavilier, J., Dode, C., Elion, J., and Miller, I. R., *J. Electroanal. Chem.* **163**, 345 (1984).
24. Ivarsson, B. A., Hegg, P.-O., Lundstrom, K. I., and Jonsson, U., *Colloids Surf.* **13**, 169 (1985).
25. Nakata, S., Yoshikawa, K., and Matsuda, T., *Biophys. Chem.* **42**, 213 (1992).
26. Caprani, A., and Lacour, F., *Bioelectrochem. Bioenerg.* **26**, 241 (1991).
27. Dryhurst, G., Kadish, K. M., Scheller, F., and Rennerberg, R., "Biological Electrochemistry, Vol. 1," p. 419. Academic Press, New York, 1982.
28. Bockris, J. O'M., and Gonzalez-Martin, A., in "Spectroscopic and Diffraction Techniques in Interfacial Electrochemistry," NATO ASI Series

- 320 (C. Gutierrez and C. Melendres, Eds.), p. 1. Kluwer Academic, Dordrecht, 1990.
29. Lundstrom, I., *Prog. Colloid Polym. Sci.* **70**, 76 (1985).
30. Lundstrom, I., Ivarsson, B., Jonsson, U., and Elwing, H., in "Polymer Surfaces and Interfaces" (W. J. Feast and H. S. Munro, Eds.), p. 201. Wiley, 1987.
31. Andrade, J. D., in "Surface and Interfacial Aspects of Biomedical Polymers, Vol. 1" (J. D. Andrade, Ed.), p. 105. Plenum Press, New York, 1985.
32. Feng, L., and Andrade, J. D., submitted for publication.
33. Watanabe, N., Shirakawa, T., Iwahashi, M., and Seimiya, T., *Colloids Polym. Sci.* **264**, 903 (1981).
34. Ramasamy, N., Lucas, T. R., Stanczewski, B., and Sawyer, P. N., in "Topics in Bioelectrochemistry and Bioenergetics, Vol. 3" (G. Milazzo, Ed.), p. 243. Wiley, Chichester, 1980.
35. Bever, M. B., "Encyclopedia of Materials Science and Engineering, Vol. 3," p. 2033. MIT Press, Cambridge, 1986.
36. Williams, R. L., and Williams, D. F., *Biomaterials* **9**, 206 (1988).
37. Morrissey, B. W., *Ann. N.Y. Acad. Sci.* **283**, 50 (1977).
38. Shirahama, H., Lyklema, J., and Norde, W., *J. Colloid Interface Sci.* **139**, 177 (1990).
39. Horsley, D., Herron, J., Hlady, V., and Andrade, J. D., in "Proteins at Interfaces" (J. L. Brash and T. A. Horbett, Eds.), p. 290. ACS Symposium 343, Washington, DC, 1987.
40. Roe, S., in "Protein Purification Methods" (E. L. V. Harris and S. Angal, Eds.), p. 175. Irl Press, Oxford, 1989.
41. Bockris, J. O'M., and Reddy, A. K. N., "Modern Electrochemistry," Vol. 2, Chap. 7, p. 623. Plenum, New York, 1970.
42. Giacver, I., and Keese, C. R., in "Proteins at Interfaces" (J. L. Brash and T. A. Horbett, Eds.), p. 582. ACS Symposium 343, Washington, DC, 1987.
43. Feng, L., and Andrade, J. D., submitted for publication.
44. Feng, L., and Andrade, J. D., *J. Biomed. Mater. Res.* (1994), in press.
45. Schmitt, A., Varoqui, R., Uniyal, S., Brash, J. L., and Pusiner, C., *J. Colloid Interface Sci.* **92**, 145 (1983).
46. Mattson, J. S., *Science* **181**, 1055 (1973).
47. Guidelli, R., and Aloisi, G., in "Electrified Interfaces in Physics, Chemistry and Biology," NOTA ASI Series 335 (R. Guidelli, Ed.), p. 337. Kluwer Academic, Dordrecht, 1992.
48. Urry, D. W., *Prog. Biophys. Mol. Biol.* **57**, 23 (1992).
49. Vernov, A., and Steele, W. A., *Langmuir* **8**, 155 (1992).
50. Suzuki, S., *et al.*, *Science* **257**, 942 (1992).
51. Isrealachvili, J. N., "Intermolecular and Surface Forces," pp. 102, 207. Academic Press, London, 1985.
52. Luckham, P. F., and Ansarif, M. A., *Br. Polym. J.* **22**, 233 (1990).
53. Tilton, R. D., Robertson, C. R., and Gast, A. P., *Langmuir* **7**, 2710 (1991).

Protein adsorption on low temperature isotropic carbon

III. Isotherms, competitiveness, desorption and exchange of human albumin and fibrinogen

L. Feng and J.D. Andrade

Department of Bioengineering and Department of Materials Science and Engineering, 2480 MEB, University of Utah, Salt Lake City, UT 84112, USA

In this paper we consider the adsorption of albumin and fibrinogen on low temperature isotropic carbon (LTIC). A subsequent paper considers the adsorption of other plasma proteins [Feng L, Andrade JD, *Colloids and Surfaces* (in press)]. Carbon fragments and silica plates were used as adsorbents. Adsorption was carried out by incubating the adsorbents in solutions of ^{125}I -labelled and unlabelled proteins (single component system), or with buffer-diluted human plasma (multicomponent system). Adsorbed proteins then underwent displacement by buffer, by single protein solutions or by dilute plasma. Results show that the LTIC substrate adsorbs a large amount of proteins before saturation, which may be due to multilayer adsorption. LTIC also irreversibly holds adsorbed proteins against the exchange agents used; little adsorbed proteins can be displaced, even after a very short adsorption time. There is no preferential adsorption for either albumin or fibrinogen on LTIC from their binary solutions, suggesting that both proteins have high affinities for the surface. Such strong interactions between LTIC and proteins are not attributed to electrostatic interactions. On the other hand, protein adsorption on the silica surface is selective and reversible, with a much higher affinity for fibrinogen than albumin and an even higher affinity for some other plasma proteins. The electrostatic interaction is thought to be the major force responsible for silica protein binding. The paper also discusses the effect of sequential protein addition to a solution on the surface concentration and suppression of adsorption of both proteins in the presence of other plasma proteins. A very important conclusion is that the LTIC surface is very active towards protein adsorption.

Keywords: Protein adsorption, blood compatibility, carbon, silica, radioisotopes

Received 28 June 1993; accepted 23 August 1993

Low temperature isotropic carbon (LTIC), a reputed blood compatible material, is mainly used as prosthetic heart valves. It is supposed to strongly interact with adsorbed proteins since its surface is basically hydrophobic and of relatively high energy¹⁻⁴. On the other hand, some studies indicated that the LTIC surface is inert and has weak interactions with proteins. For example, it has been reported that the adsorbed proteins were not conformationally changed⁵, had short residence time and were easily desorbed³. Does LTIC achieve its blood compatibility via strong or weak interactions with plasma proteins? If the former is true, the surface is probably passivated by tenaciously adsorbed protein layers. If the latter holds the surface should be intrinsically weak or passive to plasma proteins. We have taken a comprehensive look at this controversial issue in our series of studies^{4, 6-9}.

Our working hypothesis was that due to its surface characteristics (conductive, relatively non-polar, relatively high surface energy and especially relatively hydrophobic⁹), LTIC is bound to have a strong tendency to adsorb proteins, resulting in a strongly adsorbed and denatured protein layer. In a previous report we showed that the LTIC surface largely alters the conformation of adsorbed proteins⁷. In this paper we examine other attributes of LTIC on the adsorption of human serum albumin (HSA) and human fibrinogen (HFG), two important plasma proteins in the context of blood compatibility. Some of the issues addressed are adsorption isotherms from singular and multicomponent solutions, competitive adsorption from HSA/HFG binary systems and dilute plasma, desorption in buffer solutions, exchange by proteins, or exchange by surfactants. To accomplish these tasks we utilized the radioisotope labelling method for detection of adsorbed protein, competitive adsorption and protein exchange¹⁰⁻¹². We also used silica as a comparison

Correspondence to Dr J.D. Andrade.

substrate, since it has a very different surface from LTIC: it is very polar, hydrophilic, non-porous, non-conductive and of high charge density.

EXPERIMENTAL

Materials

LTIC fragments of 0.2–1.0 mm and LTIC plates of 10 × 12 mm were from Sorin Biomedica (Saluggia, Italy). Before adsorption, LTIC plates were polished and rinsed in accordance with the procedure published elsewhere⁹. LTIC fragments were used as received without further treatment. Due to the limited supply of plates, most results were obtained on the fragment samples. Plate samples were used mainly for calibration purposes. Because of the similarities of the structures and the compositions for the unpolished and the polished carbons, it is assumed that adsorption results are comparable between LTIC fragments and plates⁹. Fused silica microscope plates, 2.7 × 7.5 × 0.1 cm, from ESCO Product Co. were cut into 1.2 × 1.0 cm pieces. They were soaked in a chromic acid bath at 80°C for 30 min and thoroughly rinsed with Milli-Q water (Millipore, Bedford, MA) and then with double distilled water prepared with a quartz distiller (Heraeus, Quarzschmelze, Germany). After use, the silica plates were precleaned in chromic acid until the gamma counts returned to background level. The recycled plates then underwent an identical cleaning procedure to the new ones. Pyrex glass culture tubes, in which the experiment took place, were cleaned in the same way.

Two plasma proteins were used without further purification: HSA (crystallized, purity 98%) from ICN Biomedicals (Irvine, CA) and HFG (crystallized, 95% clottable) from Calbiochem (La Jolla, CA). Citrated human plasma, centrifuged at 4000g for 5 min and pooled from 10 individuals, was purchased from the Blood Bank of University Hospital, University of Utah. Radioisotope ¹²⁵I was purchased from Amersham (Arlington Heights, IL) in the form of sodium iodide in dilute NaOH solution with a specific activity of 17 mCi/mg or 100 mCi/ml. Auxiliary chemicals for labelling were Chloramine T from Eastman Kodak (Rochester, NY) and sodium thiosulphate from Fisher Scientific (Fair Lawn, NJ). The chemicals used for phosphate-buffered saline (PBS) were all super pure grades: sodium dibasephosphate (Ulrix) was from J.T. Baker Chemical (Phillipsburg, NJ). Sodium hydroxide (Suprapur) and sodium chloride (Suprapur) were from EM Science (Gibbstown, NJ). Unless indicated, the buffer applied was PBS with 10 mM phosphate and 150 mM NaCl dissolved in double distilled water. The buffer capacity was high enough that the pH of a 10 mg/ml HSA solution was slightly decreased to 7.2 from 7.4 of the pure PBS.

Labelling procedure

Labelling of ¹²⁵I on HSA and HFG followed the modified procedure of Tollefsen *et al.*¹³. Briefly, 1.5 mg HSA or 1.0 mg HFG were dissolved in 1.0 ml PBS. So were 10.0 mg Chloramine T and 12.0 mg

sodium thiosulphate in 2.5 ml PBS in two separate tubes. Five microlitres of Na¹²⁵I solution were pipetted into the protein solution. Once 50 µl Chloramine T solution were added, the labelling took place right away. After 60 s 50 µl sodium thiosulphate solution was added to terminate the reaction. The resultant solution was purified by passing it through a Sephadex G-25 column (Pharmacia, Piscataway, NJ). About 15 ml PBS were added to wash the column. Three 0.5 ml portions of the highest concentrations of the labelled protein were collected. They were mixed together as the hot protein solution. Its concentration was checked with a UV spectrometer, around 1.0 mg/ml for HSA and 0.20 mg/ml for HFG. The activity was measured with a Beckman radioisotope detector (Model 170M). The calibration coefficient (CC), c.p.m./mg protein, was calculated by Equation 1:

$$CC \text{ (counts/mg)} = \frac{\text{c.p.m. (counts)}}{\text{Vol (ml)} \cdot \text{Cb (mg/ml)}} \quad (1)$$

where Vol is the volume of solution for counting, usually 3.0 µl, and Cb is the bulk concentration of the protein. The typical specific activities are 2.0 × 10⁷ c.p.m./mg (10 mCi/mg) for HSA and 1.0 × 10⁸ c.p.m./mg (50 mCi/mg) for HFG, i.e. about one ¹²⁵I residue for every 3000 HSA or 100 HFG molecules. The solution of the labelled protein was stored in a refrigerator at 2–8°C for further use within 2 wk.

Adsorption and elution

Protein solutions were prepared by first dissolving the cold protein in PBS and then adding the hot one. Slight heating was needed to accelerate dissolution of HFG but the temperature was kept under 40°C. The ratio of the labelled to the unlabelled (hot/cold) for either single protein solutions or spiked dilute plasma was in the range of 1:20 to 1:40 for fragments, and 1:4 to 1:10 for plates, as the former has a higher surface area than the latter. The bulk protein concentration was either measured by UV spectroscopy or simply calculated from the mass of dry pure proteins and the solution volume. The activity of a newly prepared solution was measured each time and its CC was calculated by Equation 1. This way the counts to mass relation did not change with radioisotope decay.

Fifty milligrams of LTIC fragments were weighed in a polypropylene scintillation tube, or an LTIC or silica plate was put in a Pyrex culture tube. They were prewetted by 1.0 ml PBS for at least 2 h before being mixed with the concentrated protein solutions. The tubes where adsorption was taking place were incubated at room temperature while being lightly shaken. At the end of adsorption, each plate was taken out and flushed with a stream of PBS for 10 s. The activity was counted with the plate on the detector's platform. For the fragment sample, the protein solution was removed with a pipette, PBS poured in, the solid and liquid mixed on a mixer (Vortex Genie Mixer, Scientific Product, Evanston, IL), and the washing PBS removed again. Similar steps of washing and discharging were repeated three to five times. Further rinsing would bring down the counts no more than 1%. The

solid sample in the tube were counted. The surface concentration (mg/m^2) was calculated by Equation 2. Usually samples in a batch were measured in duplicate or triplicate.

$$\Gamma = \frac{\text{c.p.m. (counts)}}{\text{CC (counts/mg)} \cdot \text{Surface area (m}^2\text{)}} \quad (2)$$

After the initial counting, the solid substrates were dispersed and immersed in 1.0–1.5 ml eluting solutions for elution or exchange. Some studies avoid exposing the protein-coated fragment surface to air before elution, because the air–protein or air–water interface could accidentally modify the state of the adsorbed protein. It turned out that this was not necessary since there was no difference in protein displacement whether or not the fragments had been exposed to air before elution.

RESULTS

Adsorption isotherms

Two concerns in experiments using labelled proteins are if the labelled protein can be successfully separated from the labelling agent, e.g. ^{125}I , and if the label modifies the genuine adsorption properties of the protein¹⁰. One only measures the properties of the labelled protein but discusses the unlabelled protein in general; such generalization should be justified¹⁰. Even though the labelling method we use has been well established, we performed a simple test to check the adsorption preference¹⁵. Hot and cold proteins were mixed in different ratios while the total protein concentration was kept constant. Conceptually, if the surface preferentially adsorbs the labelled protein, the higher ratio of hot to cold will result in a higher surface concentration, or vice versa. The results⁹ (not shown) show that there is no significant difference in surface concentrations for the three ratios. Therefore, it is probably safe to say that there is no preferential adsorption of the labelled or unlabelled HSA and HFG onto the LTIC surface under these conditions.

Figure 1 shows adsorption isotherms of HSA and HFG on LTIC fragments from PBS solutions after 3 h incubation. The isotherm of HSA on polished LTIC plates is similar to that in Figure 1⁹. It should be emphasized that the precise surface area of the fragments was not known. An estimate was obtained by dividing the surface concentration of HSA on the fragments (mg/g) by that on the plates (mg/m^2) to get the area (m^2/g) of the fragments, assuming that the adsorbed amounts on both LTIC substrates are the same. For example, when using 0.10 mg/ml HSA solution, the surface concentration on fragments was 0.055 mg/g and that on plates was 2.5 mg/m². The ratio of 0.055:2.5 is 0.0220 m²/g, which is the approximate surface area for the fragments. We noted that the surface area of fragments was slightly dependent on the prewetting time: a longer wetting time shows a marginally higher surface area. For instance, the adsorbed amount of HSA on the fragments prewetted for 16 h is about 10% higher than that on the fragments

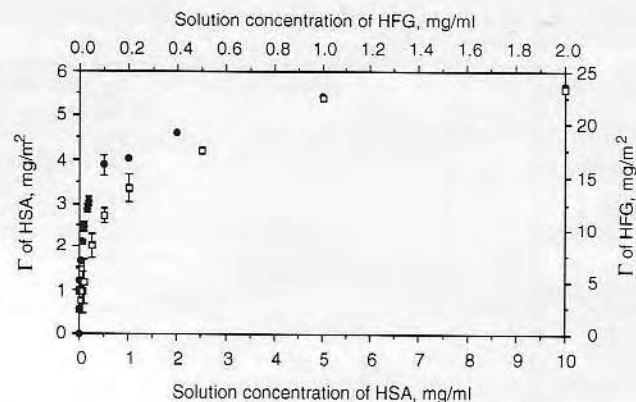


Figure 1 Adsorption isotherms of HSA, ●, and HFG, □, on LTIC fragments after 3 h incubation.

of 2 h prewetting, probably due to slow penetration of water into the pores. Because of this uncertainty and that from the surface area estimation, the calculated surface concentration on LTIC fragments can be treated only as semi-quantitative values.

Observations from the isotherms are:

1. The isotherms for both proteins do not reach plateau until high bulk concentrations are used: about 5.0 mg/ml for HSA and 1.0 mg/ml for HFG. The result for HSA is in concert with that from the impedance measurement⁸, where LTIC plates were used.
2. The surface concentrations are high at the plateaus for both proteins: 5.8 mg/m² for HSA and 23 mg/m² for HFG.
3. The surface concentration of HFG is about two to five times higher than that of HSA for the same bulk concentration solutions. The ratio of surface concentration of HSA to HFG is 0.18 at 1.0 mg/ml, comparable to the ratio of 0.24 at 1.0 mg/ml on ultra-low temperature isotropic carbon¹⁶, which has a very similar surface structure to LTIC¹⁰.

Table 1 lists HSA adsorption results from undiluted plasma and from concentrated HSA solution. With a concentration of 40 mg/ml, approximately the concentration of HSA in plasma¹⁷, the surface concentration is 23 mg/m². At such a high protein concentration, the solution pH has become 6.1 instead of 7.4. HSA can adsorb more when the solution pH is closer to its pI (pH 4.7)¹⁸. Nevertheless, the result indicates that on LTIC the surface concentration can be very high (see later discussion). The surface concentration of HSA is still around 7 mg/m² from undiluted plasma (pH 7.4). This is a very high surface concentration, because now the adsorption of HSA is competed by other plasma proteins, some of which have very high surface activities, such as HFG. The topics of competitive adsorption and protein exchange will be discussed later.

Multistep adsorption

We designed this set of experiments to examine inhibition effects of earlier adsorbed proteins (preadsorption) on later adsorbed ones (postadsorption). The adsorbents were first incubated in a solution of unlabelled

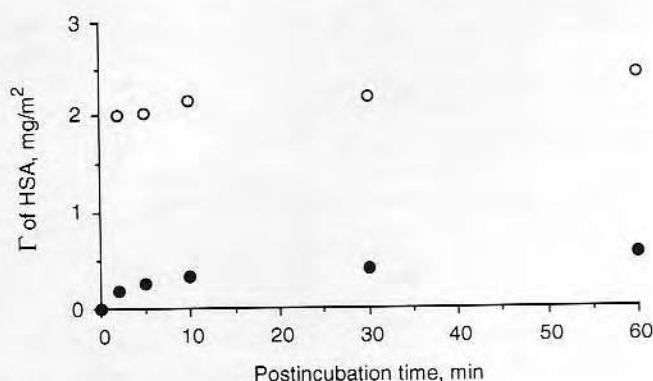
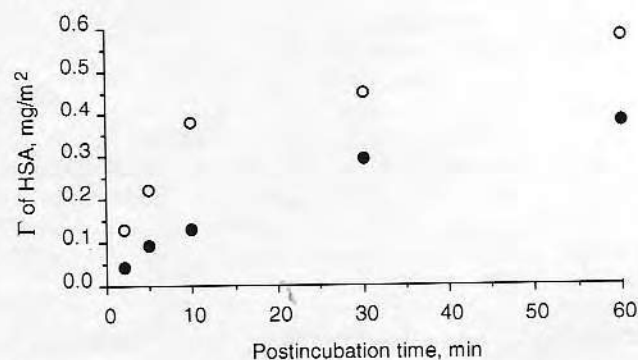
Table 1 Surface concentration of human serum albumin (HSA) on low temperature isotropic carbon fragments from undiluted plasma and concentrated HSA solution

Protein solution	Adsorption time (h)	Before exchange (mg/m ²)	After exchange* (mg/m ²)	Unexchanged (%)
Plasma	3	6.5 ± 0.1	5.3 ± 0.0	81.5
	13	7.9 ± 0.8	5.9 ± 0.1	75.2
HSA [†]	3	23.4 ± 0.0	17.0 ± 0.7	72.7
	18	23.3 ± 0.1	17.8 ± 0.7	76.6

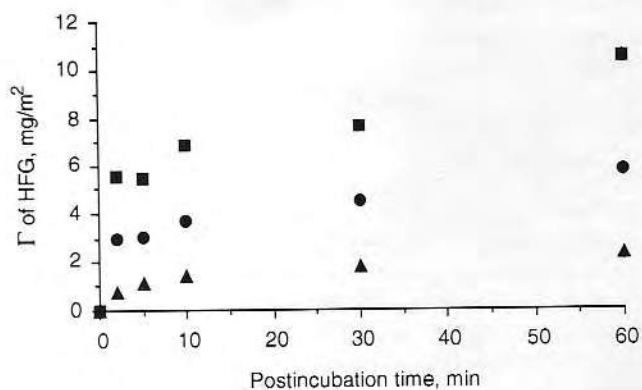
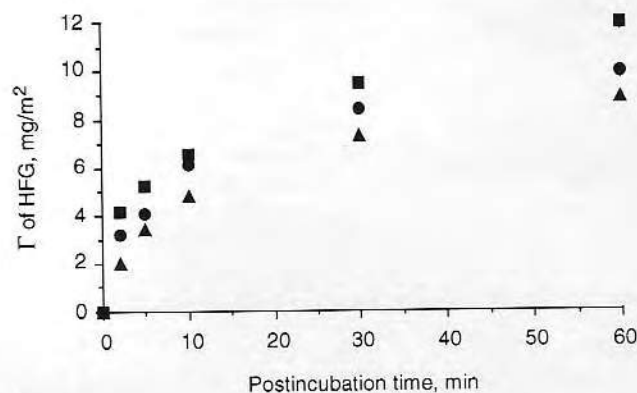
*Exchanging solution: 0.1 mg/ml HSA in PBS for 18 h.

[†]Concentration: 40 mg/ml; pH 6.1.

proteins for a certain amount of time and then a solution of labelled proteins was added for postadsorption. Surface concentrations were measured at different time intervals. Figures 2 and 3 show suppression of HSA and HFG adsorption, respectively, by preadsorption of HSA. Figure 4 illustrates these results and presents tentative explanations. In Figure 2a the unlabelled HSA was first adsorbed on LTIC fragments. After 2 h, the labelled HSA was added. Obviously, postadsorption was greatly suppressed by the previously adsorbed HSA on LTIC as the surface concentration for 60 min postadsorption is reduced by about 77%. The percentage reduction is even higher when the postincubation time is shorter. Note that the HSA concentration for preadsorption was just 0.10 mg/ml, a rather dilute one. The above observation indicates that the postadsorbed HSA cannot replace the preadsorbed HSA, so it only fills some voids or stays on top of the preadsorbed protein (Figure 4a). On silica (Figure 2b),

**a****b****Figure 2** Surface concentrations of postadsorbed HSA (0.10 mg/ml) on LTIC fragments, **a**, and on silica, **b**, with, ●, and without, ○, 2 h preadsorption of 0.10 mg/ml HSA.

although the preadsorption still reduces the postadsorption, its effect is much lower than that on LTIC, only a 23% decrease at a concentration of 0.10 mg/ml, indicating possible incomplete coverage of the preadsorption or protein exchange (Figure 4b). In Figure 3, the postadsorbed protein was HFG but the preadsorbed one was still HSA. In this case, 0.10 mg/ml HSA preadsorption can only reduce postadsorbed HFG by 46% on LTIC. Preadsorption of a higher concentration of HSA, 1.0 mg/ml, can bring the surface HFG level down by 80%. This suggests that much of the HFG can stay on top of the preadsorbed HSA (Figure 4c). At the higher concentration, preadsorbed HSA probably results in fewer voids and may be HSA multilayer adsorption, and thus has a higher suppression capability (Figure 4d). On silica, the influence of

**a****b****Figure 3** Surface concentrations of postadsorbed HFG (0.10 mg/ml) on LTIC fragments, **a**, and silica plates, **b**, with and without 2 h preadsorption of HSA. ■, No preadsorption; ●, 0.10 mg/ml HSA preadsorption; ▲, 1.0 mg/ml HSA preadsorption.

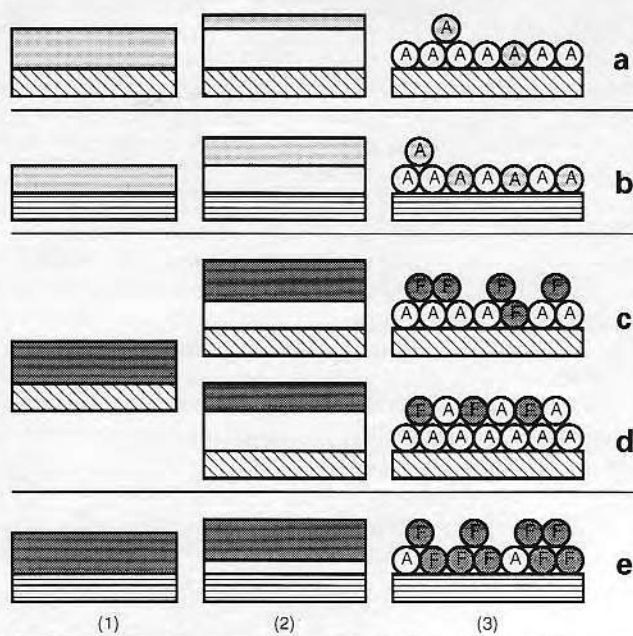


Figure 4 Schematic representations of Figures 2 and 3. The thickness of adsorbed proteins shows only the relative amount with no implication of structure of protein layers. Column: 1, without preadsorption; 2, with preadsorption; 3, cartoon graphics of 2. **a** for Figure 2a, **b** for Figure 2b, **c** for Figure 3a with 0.10 mg/ml HSA preadsorption, **d** for Figure 3a with 1.0 mg/ml HSA preadsorption and **e** for Figure 3b. ▨, carbon substrate; ▩, silica substrate; □, unlabelled HSA; ▤, labelled HSA; ▥, labelled HFG.

preadsorption is very small; even 1.0 mg/ml HSA preadsorption merely reduces subsequent adsorbed HFG by 27%. Notice that HFG results in much higher surface concentration on silica than HSA (Figure 4e), implying very different affinities of these two proteins for the substrate. Significant protein exchange is expected due to weak adsorption of HSA on silica.

Figure 5 shows the results of HSA adsorption on LTIC fragments from single-step and multistep protein addition. In the former case, LTIC was incubated in HSA solutions of 0.02, 0.07 and 0.20 mg/ml, respectively, for 60 min and the surface concentrations were measured. In the later cases, the adsorption first took place in the solution of 0.02 mg/ml for 5 or 60 min. For the two-step adsorption, the adsorbent was incubated in the solution of 0.07 mg/ml for another 60 min. For the three-step adsorption, the LTIC fragments underwent a third incubation in 0.20 mg/ml HSA. As indicated in Figure 5, the surface concentrations are very similar for all cases, regardless of how many steps of adsorption were used, so long as the solution concentration for the last adsorption is the same.

Competitive adsorption of HSA and HFG

Figures 6 and 7 show that the presence of other plasma proteins suppresses the adsorption of HSA and HFG to different extents on either LTIC or silica substrates. In both single protein and diluted plasma solutions, the proteins of interest were adjusted to certain concentrations, as indicated along the x-axes, and the plasma was diluted accordingly. For instance, since the approximate concentration of HSA in plasma is 40 mg/

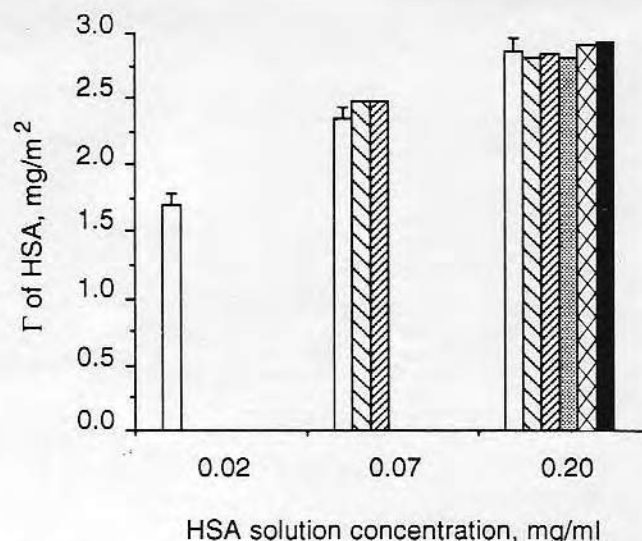


Figure 5 Single-step versus multistep adsorption of HSA on LTIC fragments. □, One step (adsorption time 60 min); ▨, two steps (5 and 60 min); ▩, two steps (60 and 60 min); ▤, three steps (5, 5 and 60 min); ▥, three steps (5, 60 and 60 min); ▦, three steps (60, 60 and 60 min).

ml, plasma was diluted by PBS to 1:400 to get 0.10 mg/ml of HSA. By the same token, plasma was diluted to 1:30 for HFG to achieve the same concentration,

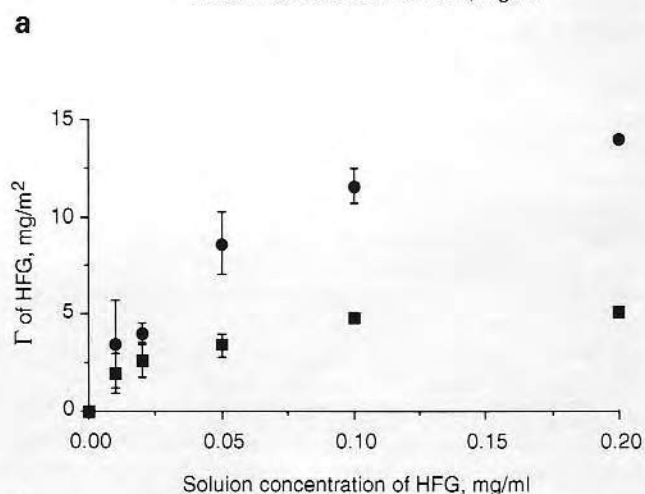
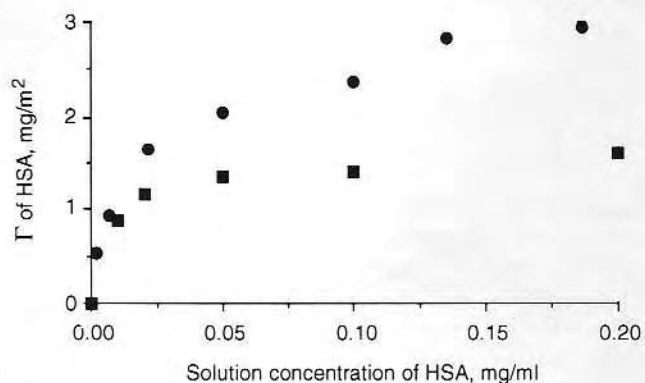


Figure 6 Adsorption isotherms of HSA, **a**, and HFG, **b**, on LTIC fragments from single protein solutions, ●, and from diluted plasma, ■.

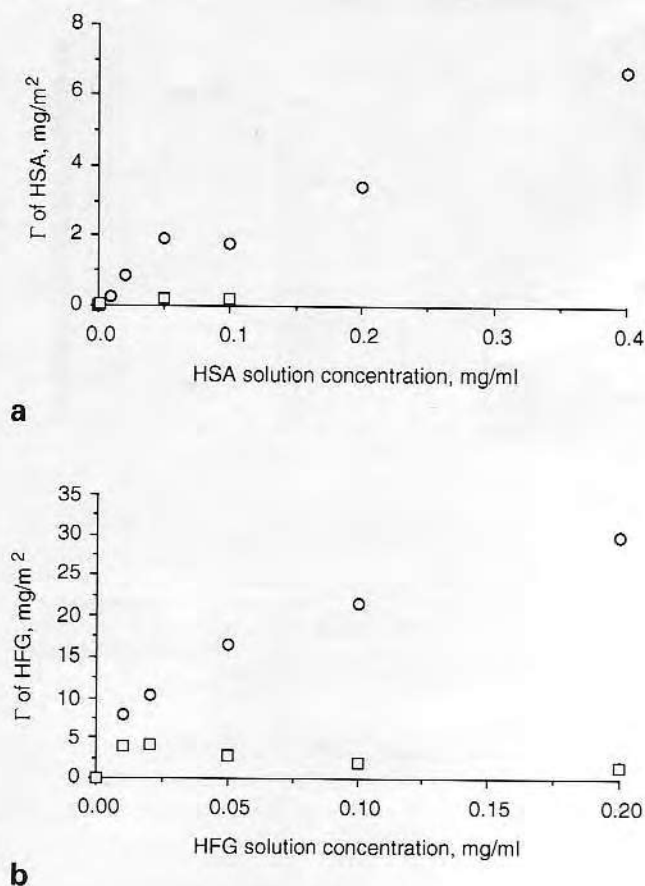


Figure 7 Adsorption isotherms of HSA, **a**, and HFG, **b**, on silica plates from single solutions, ○, and from diluted plasma, □.

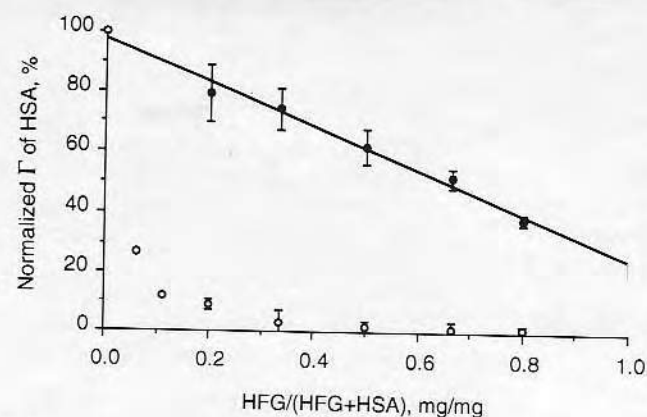
assuming that HFG in plasma is about 3 mg/ml¹⁵. From Figure 6, at the HSA concentration of 0.20 mg/ml in both the diluted plasma and single HSA solution, the surface concentration of HSA is 1.6 mg/m² from the diluted plasma, while it is 3.0 mg/m² from the single HSA solution. So, in the presence of other plasma proteins, the adsorbed HSA is 55% of that in the absence of them. HFG is 35% for the same comparison. The mass of HSA is a little more than 50% of the total mass of plasma proteins, while HFG is no more than 4%. It is very interesting to note that 55% of the normalized surface concentration for HSA is almost the same as the 50% ratio of HSA *versus* total plasma proteins. This implies that the LTIC surface adsorbs proteins from a mixture according to their compositions, and also suggests that multilayer adsorption of HSA from dilute plasma is negligible. Therefore, at least for the first layer of adsorbed proteins on LTIC, there is no preferential adsorption. This phenomenon will be further discussed later. It is also informative to compare 35% of the normalized surface concentration for HFG and 3% of HFG in total plasma proteins. The surface concentration of HFG is still very high, even though a total protein concentration 25 times greater is competing for the adsorption. Since HFG cannot successfully compete with HSA for direct surface sites on LTIC (shown later), we suggest that the disproportional surface concentration of HFG is because HFG adsorbs in multilayers, presumably on surfaces of

already adsorbed proteins. Our results from two-dimensional gel electrophoresis further showed these different adsorptivities of HSA and HFG⁶.

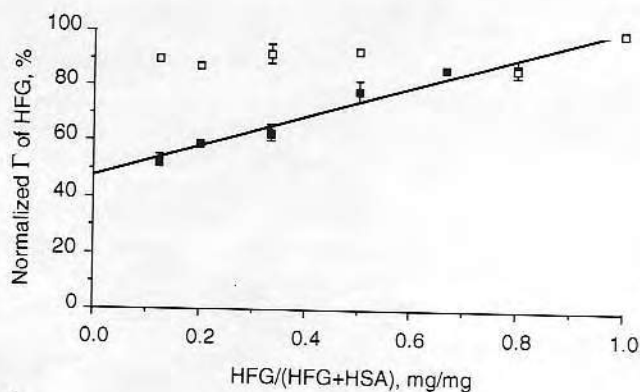
The suppressed adsorption of HSA and HFG is much more significant on silica. The surface concentrations for both proteins become very low in the presence of other plasma proteins. Neither HSA nor HFG can compete and adsorb on silica. Notice that at lower total protein concentration, the suppression of HFG is not so great as that at the higher concentration, even though the protein ratio is not changed. Nearly identical curves were reported by Wojciechowski *et al.* on glass after 5 min of adsorption¹⁹; they attributed this to the Vroman effect, in which up to a certain protein concentration little lateral interaction takes place, but beyond the threshold concentration, surface 'crowding' begins to take effect so that HFG is rapidly displaced from the surface. There are two alternative explanations: at low concentration the amount of proteins that can displace adsorbed HFG, e.g. high molecular weight kininogen (HMWK, <100 µg/ml plasma) and high density lipoproteins (HDL)^{11,18}, is not sufficient to displace all adsorbed HFG; and at low concentration many surface sites are available for all proteins, so increasing concentration increases HFG occupancy, but high concentration promotes competitiveness²⁰.

To make the interpretation simpler, a binary system was prepared by mixing unlabelled HFG with labelled HSA at different ratios for one set of solutions, and unlabelled HSA with labelled HFG for another. Adsorption was measured on LTIC and silica substrates. The results are shown in Figure 8. Both (a) and (b) use the weight composition of HFG in the protein mixtures as the abscissa. In Figure 8a, the HSA concentration was kept at 0.10 mg/ml and the amount of HFG was varied to achieve the ratio values, e.g. HFG is 0.005 mg/ml when HFG/(HFG + HSA) is 0.05 and 0.40 mg/ml when the ratio is 0.80. In Figure 8b, the constant is HFG concentration (0.10 mg/ml) and the variant is HSA concentration, e.g. HSA is 0.70 mg/ml when HFG/(HFG + HSA) is 0.125 and is 0.025 mg/ml when the ratio is 0.80. Therefore, the total protein concentrations of HFG + HSA vary along the x-axes. They are not usually equal for a given composition in Figure 8a and Figure 8b. For the ordinates the normalized HSA surface concentration is used in Figure 8a and the normalized HFG surface concentration is used in Figure 8b. The normalized surface concentration is defined as the ratio of the adsorbed amount from the binary mixture to that from the single protein solution. For example, on LTIC the surface concentration is 2.4 mg/m² for the single component solution of 0.10 mg/ml HSA and is 1.4 mg/m² for the binary solution of HFG/(HFG + HSA) = 0.50, with the HSA solution concentration still being 0.10 mg/ml. The normalized surface concentration is thus 58.3%. From the practical point of view, Figure 8a and b complement each other, both revealing the following facts:

1. On LTIC the surface concentrations for both proteins are proportional to their compositions in the mixtures, but not on a one-on-one basis, suggesting the absence of preferential adsorption on LTIC, as discussed before.



a



b

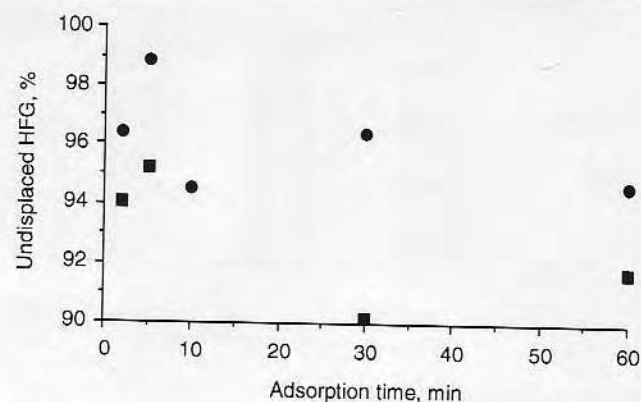
Figure 8 Ratios of surface concentrations of HSA, **a**, and HFG, **b**, from HSA/HFG binary systems versus those from their singular systems on LTIC fragments, ●, ■, and silica plates, ○, □, after 3 h incubation. **a**, 0.10 mg/ml HSA; **b**, 0.10 mg/ml HFG.

- Silica is overwhelmingly occupied by HFG unless its composition is below 10%. This result is similar to Fenstermaker's²¹. This clearly shows the preference of HFG over HSA on silica.

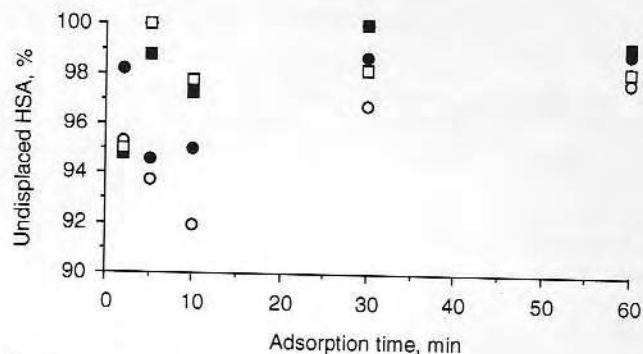
Reversibility of adsorption

Reversibility of adsorption is described here by three terms: elutability, exchangeability and displaceability. The first term is defined as how much protein can be washed off or displaced from a surface by PBS in the absence of added proteins. The second is how much adsorbed protein can be displaced or exchanged by proteins in solution, which can be HSA, HFG or plasma solutions. The third stands for the percentage of proteins that are displaced from a surface after elution or exchange. A variety of solutions were used to study reversibility and they fall into three categories: dilution of solution, changes in ionic strength and exchange against displacers (proteins or surfactants)²¹.

As Figure 9 shows, very little displacement of both proteins takes place on LTIC after 2 or 18 h incubation in pure PBS, HSA, HFG or diluted plasma; both elutability and exchangeability are less than 10%. Less than 2 min of adsorption is long enough to sufficiently stabilize the adsorbed protein. This phenomenon has



a



b

Figure 9 Undisplaced HFG, **a**, and HSA, **b**, from LTIC fragments as functions of their adsorption time; adsorption solutions: 0.10 mg/ml of HSA or HFG; and exchange solutions: **a**, 0.20 mg/ml HFG, ■, and 0.6% plasma, ●, for 2 h; **b**, pure PBS, ■, □, and 0.20 mg/ml HSA, ●, ○, for 2 h, ■, ●, and 18 h, □, ○.

also been indicated in Table 1, where elutability of adsorbed HSA from 3 or 18 h incubation is similar. Postadsorbed proteins, however, need more time to strengthen the adsorption. As shown in Figure 10, when postadsorption was shorter than 10 min, displacement of HSA is relatively significant, in contrast to the preadsorbed value. For instance, after 2 h exchange, the undisplaced HSA is 61 and 72% when postadsorption time is 2 and 5 min, respectively. After

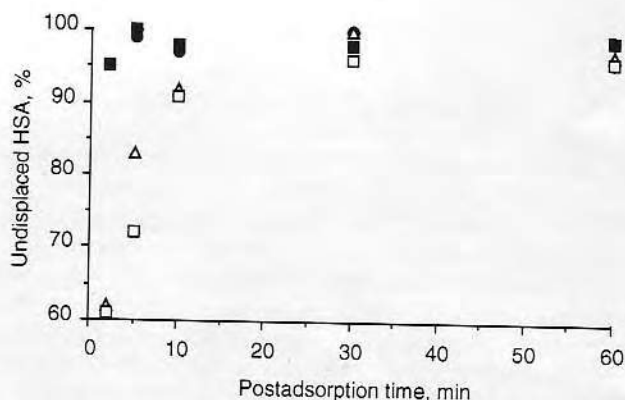


Figure 10 Undisplaced preadsorbed, ■, ●, and postadsorbed, □, △, HSA (0.10 mg/ml) from LTIC with 0.20 mg/ml HSA solution. Exchange time: ●, △, 2 h; ■, □, 16 h.

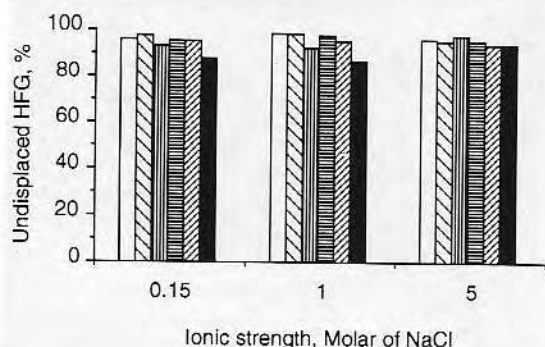


Figure 11 Effects of ionic strength on elution of HSA, **a**, and HFG, **b**, from LTIC fragments after 3 h adsorption. □, 0.02 mg/ml protein concentration, 2 h elution time; ▨, 0.10 mg/ml, 2 h; ▩, 1.00 mg/ml, 2 h; ▤, 0.02 mg/ml, 17 h; ▥, 0.10 mg/ml, 17 h; ■, 1.00 mg/ml, 17 h.

10 min the undisplaceability is higher than 90%. This shows that the stabilization of HSA on top or in voids of a proteinated surface takes longer than on a bare carbon surface.

One way of increasing the buffer elutability is to increase its ionic strength to minimize the electrostatic interaction between adsorbed proteins and the surface¹. Figure 11 shows the elutability of HSA and HFG from LTIC at three ionic strengths. Higher ionic strength apparently has no effect, even when the incubation time is as long as 17 h. This result further eliminates any major role played by electrostatic interactions between the LTIC surface and the adsorbed proteins¹. Proteins on LTIC are so difficult to remove that even 2% sodium dodecyl sulphate only elutes 18% of adsorbed HSA after 16 h incubation. A significant portion of adsorbed HSA can be exchanged if the surface is incubated in a fairly concentrated protein solution for prolonged times²². The displaced HSA is as high as 30% when the exchanging solution is 1:10 diluted plasma (about 8 mg/ml total proteins) over an incubation time of 100 h⁹. Although this may not seem very high, 30% is the highest amount ever achieved on LTIC in this work. However, we must be aware that in addition to protein exchange, another possible consequence of long-term incubation is proteolytic degradation of adsorbed proteins that prolonged incubation may have brought about²³. So, the adsorbed protein could be stripped from the surface by chemical rather than solely physical mechanisms.

In contrast to the case of LTIC substrates, proteins are readily eluted or exchanged from silica surfaces. Usually, about 50% of adsorbed protein can be displaced either by pure PBS or protein solutions in a matter of a few hours. Figure 9a demonstrates that either dilute plasma or solution HFG can effectively displace adsorbed HFG from silica in only 2 h. Actually, pure PBS is equally effective as an eluent. The elutability depends on adsorption time, as expected; less time results in higher elution. Figure 12 shows that the HFG adsorbed after HSA pre-coating is more difficult to elute. This plot looks like a mirror of Figure 4b, suggesting that the HFG that has displaced HSA may be harder to elute. Figure 13 shows the exchange of adsorbed HSA with solution HSA as the exchanging agent. Two facts are worth noticing: unlike

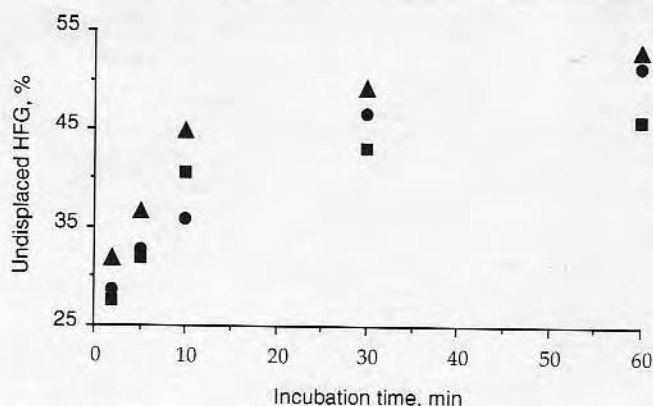


Figure 12 Displacement of HFG from silica plates after 2 h elution with PBS as functions of adsorption time and 2 h preadsorption of HSA. ■, No preadsorption; ●, 0.10 mg/ml HSA preadsorption; ▲, 1.00 mg/ml HSA preadsorption.

HFG, postadsorbed HSA is easier to elute, and the percentage of exchanged HSA is comparable to that of HFG, although HSA's absolute surface concentration is much lower than that of HFG. It was also observed that moderate increases in ionic strength of eluent PBS enhanced protein elutability to some extent (Figure

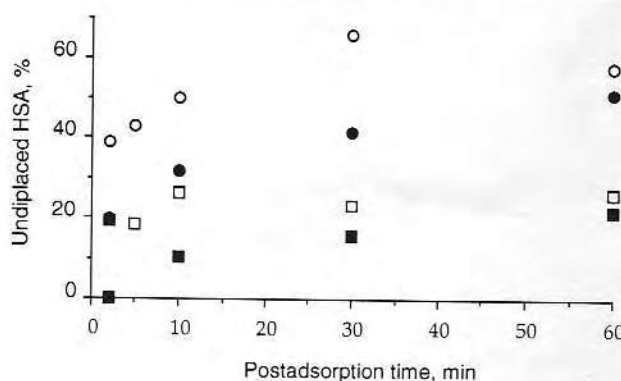


Figure 13 Displacement of postadsorbed HSA from silica plates (incubation 2 h, ●, ○, and 16 h, ■, □, by 0.20 mg/ml HSA as a function of adsorption time with, ●, ■, and without, ○, □, preadsorption of 0.10 mg/ml HSA.

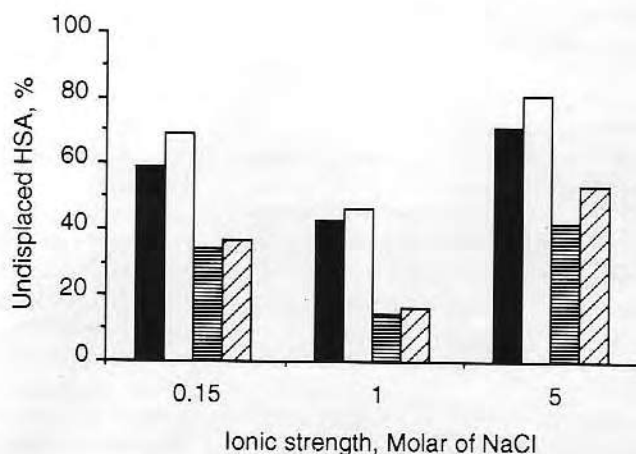


Figure 14 Effects of ionic strength on HSA displaceability from silica plates. ■, 0.10 mg/ml adsorption concentration, 2 h elution time; □, 1.00 mg/ml, 2 h; ▨, 0.10 mg/ml, 17 h; ▩, 1.00 mg/ml, 17 h.

14). This effect suggests that electrostatic interactions play a significant role in protein adsorption on silica¹. A very high NaCl concentration lowers the elutability, a consequence of salting out, i.e. too high a salt concentration results in precipitation of proteins in solution.

DISCUSSION

Monolayer or multilayer adsorption

Although proteins often adsorb as monolayers²⁴, multilayer adsorption is not uncommon, especially when the solution concentration is high²⁵. The surface concentration corresponding to a monolayer varies and is dependent on the protein, its molecular orientation and conformational state, and the type of substrate. The theoretical monolayer coverage for HSA is 2.5 mg/m² for side-on orientation and 8.2 mg/m² for end-on orientation²². The values for HFG are 2.0 and 18 mg/m², respectively¹. Thus, if judged only by the isotherms, almost all the detected surface concentrations in Figure 1 will fall into the monolayer range. Nevertheless, multilayer adsorption cannot be ruled out based on the following facts:

1. A monolayer is usually achieved with a solution of 0.05–0.15 mg/ml proteins²⁶, with a surface concentration around 2.0 mg/m². For instance, for HSA it is 1.7 on polyethylene, silicone rubber, polyvinyl chloride and polyether urethane^{22,25}, 2.1 on polyvinyl chloride¹¹, and 0.8 mg/m² on polystyrene²⁷. Incidentally, there is an inflection between the concentrations of 0.5 and 1.0 mg/ml at the surface concentration around 2.5 mg/m², in agreement with most monolayer values. The monolayer amount for bovine fibrinogen is 14 on polyether urethane-nylon, 12 on polyvinyl alcohol²⁸, 4.2 on polyethylene and polyvinyl chloride²⁵, and 3.0 on polymethyl methacrylate-based polymers²⁹.
2. The large amount of adsorption, 23 mg/m², from the solution of 40 mg/ml HSA is surely beyond the monolayer range.
3. Saturation (plateau) values do not necessarily indicate monolayer coverage; it could be a factor of 2 or more above or below³⁰.
4. With a powerful eluent, the elution of adsorbed HSA from higher concentration solutions is larger than that from the lower ones (data not shown)⁹. One explanation is that the adsorbed proteins in the outer layers are easier to remove.

In multicomponent systems, more than one layer adsorption seems to be more prominent, especially for HFG. The supporting facts are:

1. Even though LTIC has been likely entirely covered by HSA from its 1.0 mg/ml solution, the postadsorption of HFG from its 0.10 mg/ml solution is still impressive, 2.3 mg/m² after 60 min postadsorption (Figure 3a). Since displacement of adsorbed HSA can be neglected, most adsorbed HFG has to be on top of the HSA layer.
2. When its concentration is 0.10 mg/ml in the diluted plasma, the surface concentration of HFG reaches 4.7 mg/m², not much lower than that of the single

HFG solution, 12.0 mg/m² (Figure 6b). Recall that HFG constitutes less than 4% of the total mass of all plasma proteins. It is likely that most adsorbed HFG actually resides on adsorbed proteins with larger abundance, for instance HSA.

No preferential adsorption on LTIC

Figure 8 contains rich information on protein adsorption, in addition to confirming the overwhelming surface activity of HFG on silica. It suggests that the LTIC surface has no selectivity in adsorbing either HFG or HSA, as there is no noticeable preference of adsorption for either protein. There is a nearly linear relationship of surface concentration of both proteins to their respective composition in the solution. The percentages on the y-axis *versus* the composition on most parts of the x-axis are straight lines, but are not diagonal. For example, when its composition is 50%, HFG reaches more than 70% of its surface concentration of the single HFG solution. At the same composition where HSA is also 50%, the HSA surface concentration is still 60%. This is controversial: the presence of HFG has a smaller influence on HSA adsorption than is expected from its composition (Figure 8a), but the presence of HSA also has a smaller influence on HFG adsorption based on the same argument (Figure 8b). So, which protein is more active in this case? The answer is: neither of them, unlike the postulation that LTIC was selective to HSA. This phenomenon is very close to the hypothesis of Sharma: LTIC has the same tendency to adsorb both HSA and HFG based on the analysis of surface energetics³¹. Their surface compositions are primarily determined by their ability to arrive at the surface, i.e. their relative abundance in solution and their diffusion coefficients. Teflon and polyurethanes may have similar properties³². Finally, the slight off-diagonal relationship may be due to three possibilities: different packing patterns for the adsorption from a binary system, synergetic adsorption and multilayer adsorption.

Reversibility of adsorption

The present work clearly demonstrates a very important phenomenon: the LTIC surface irreversibly adsorbs proteins but silica does not. Adsorption of proteins to carbon is so tenacious that even layers other than the first one may not be displaced (Table 1). No effective static method has been found to elute adsorbed proteins from LTIC. This agrees with the general observation that protein adsorption is irreversible on hydrophobic surfaces^{1,21}. Such strong adsorption very likely emanates from the hydrophobic interaction, attributed to being the principal force for protein conformational stability³³. Moreover, this study finds that, on LTIC, adsorption irreversibly can be achieved in a short time, less than 2 min. On the other hand, adsorption on silica is quite reversible, in agreement with most studies on silica or on other hydrophilic surfaces^{1,21}. Adsorbed protein layers can probably be renewed all the time. The weak binding of silica to proteins could be the consequence of the

relative indifference of the silica surface towards both proteins and water, mainly due to its hydrophilicity²².

A dilemma in protein adsorption

On LTIC as well as on other hydrophobic materials, protein adsorption is generally characterized by the following phenomena:

1. kinetic saturation—initial fast adsorption rates which then quickly slow down and finally level off;
2. isotherms—surface concentration *versus* solution concentration shows an S-shaped curve;
3. irreversibility—adsorbed proteins cannot be removed by ordinary solution.

These characteristics turn the whole adsorption process into a mystery. If protein adsorption is a one-way process (irreversibility), why should the surface concentration stop increasing while the coverage is way below the complete monolayer when adsorption is from solutions with low protein concentration? Proteins would eventually cover the whole surface, although a lower concentration solution may take longer. Therefore, why is there an isotherm in the first place? Every curve would finally become a straight and flat line if the surface is like a protein sink.

Lundstrom *et al.*³⁴ have reported that on hydrophobic (dichlorodimethylsilane-treated) silica surfaces, the surface concentration of human fibronectin is significantly less after successive (multistep) addition of the protein than that after direct (single-step) addition, although the same final concentration is reached. Adsorption on hydrophilic silica exhibits much smaller differences for different additions. Soderquist made a similar observation with HSA on a lysine-phenylalanine co-polymer surface³⁵. The different behaviour is thought to be due to the fact that larger structural changes take place on hydrophobic surfaces³⁶. The adsorbed proteins on a hydrophobic surface are severely flattened due to conformational change, so that they occupy more of the available surface and leave later-arriving proteins fewer sites to adsorb. At the higher bulk concentration, the collision rate of proteins on a solid surface is higher, such that many of them have arrived at the surface before the adsorbed protein can fully stretch out (denature). Thus, the surface concentration is higher. On the other hand, at a lower bulk concentration adsorbed proteins have enough time to spread out because fewer neighbours are around due to the low rate of collision. Such a surface will not adsorb much more protein, even in a more concentrated solution, because not much solid surface is available. The assumption is that there is no multilayer adsorption. Obviously, LTIC is different from those hydrophobic surfaces. It adsorbs proteins without being influenced by the protein feeding history (Figure 5). Some possible mechanisms are: slight flattening of adsorbed proteins (even though they are denatured), fast denaturation rate and an existing monolayer at a bulk concentration of only 0.02 mg/ml. Other possible reasons are: lateral diffusion that could be a reason for blocking the collision of other incoming proteins³⁷, mutual repulsion of adsorbed proteins with the same charge³⁰

and different adsorption centres with a spectrum of activated free energies of adsorption³⁸.

CONCLUSIONS

This work demonstrated that LTIC can adsorb large amounts of HSA and HFG before saturation (plateau) is reached. Higher surface concentrations may reflect multilayer adsorption. The final surface concentration of HSA on LTIC does not change with the manner of protein addition (direct or successive) as long as the protein concentrations are the same for the last added solution. Despite the competition of other proteins, adsorption of HSA and HFG onto LTIC from diluted plasma solutions is only moderately suppressed. The suppression of their adsorption on silica is much more pronounced. Preadsorption of LTIC by HSA inhibits the subsequent adsorption of HSA significantly, and that of HFG moderately. This implies that some postadsorption takes place on the preadsorbed HSA. Preadsorption of silica by HSA has much less effect, suggesting a less effective preadsorption or/and an exchange process. There is no preferential adsorption of either HSA or HFG on LTIC from an HSA/HFG binary system, but silica preferentially adsorbs HFG. All these phenomena are connected to the fact that unlike those on silica, adsorbed proteins on LTIC can hardly be displaced either by buffer or by protein solutions. This conclusion is further confirmed by the directly designed experiments of protein displacement. In dilute protein solution, the displaceability of adsorbed HSA and HFG is less than 10% on LTIC but more than 50% on silica. The electrostatic interaction is shown not to be the driving force for the adsorption of HSA or HFG on LTIC, but it is probably for their adsorption on silica. All these factors strongly suggest that LTIC has a large tendency to adsorb proteins and keep them irreversibly. The reality is that the LTIC surface is very active in protein adsorption in spite of its chemical inertness.

ACKNOWLEDGEMENTS

We thank Sorin Biomedica for providing the LTIC sample. This work was supported by the Center for Biopolymers at Interfaces, University of Utah.

REFERENCES

- 1 Brash JL. Role of plasma protein adsorption in the response of blood to foreign surfaces. In: Sharma CP *et al.*, eds. *Blood Compatible Materials and Devices*. Lancaster: Technomic, 1991: 3–24.
- 2 Bokros JC, LaGrange LD, Schoen J. Control of structure of carbon for use in bioengineering. In: Walker, ed. *Chemistry and Physics of Carbon*, Vol. 9. New York: Dekker, 1972: 103–171.
- 3 Baier RE, Gott VL, Feruse A. Surface chemical evaluation of thromboresistant materials before and after venous implantation. *Trans Am Soc Artif Int Organs* 1970; **16**: 50–57.

- 4 Feng L, Andrade JD. Protein adsorption on low temperature isotropic carbon: What makes it blood compatible via protein adsorption? (submitted).
- 5 Chiu T-H, Nyilas E, Turuse LR. Microcalorimetric and electrophoretic studies of proteins from plasma. *Trans Am Soc Artif Int Organs* 1978; **24**: 389-402.
- 6 Feng L, Andrade JD. Protein adsorption on low temperature isotropic carbon: IV. Competitive adsorption studied by two-dimensional electrophoresis. *Colloids and Surfaces* (in press).
- 7 Feng L, Andrade JD. Protein adsorption on low temperature isotropic carbon: I. Protein conformational change probed by differential scanning calorimetry. *J Biomed Mater Res* (in press).
- 8 Feng L, Andrade JD. Protein adsorption on low temperature isotropic carbon: II. Effects of surface charge of solids. *J Colloid Interface Sci* (in press).
- 9 Feng L. Biomedical carbon surfaces and their interactions with plasma proteins. *PhD Dissertation*, University of Utah, 1993.
- 10 Andrade JD. Principles of protein adsorption. In Andrade JD, ed. *Surface and Interfacial Aspects of Biomedical Polymers*, Vol. 2. New York: Plenum, 1985: 1-80.
- 11 Chuang HYK. Interaction of plasma proteins with artificial surfaces. In: Williams DF, ed. *Blood Compatibility*, Vol. 1. Boca Raton, FL: CRC Press, 1987: 88-104.
- 12 Brash J. The fate of fibrinogen following adsorption at the blood-biomaterial interface. *Ann NY Acad Sci* 1987; **516**: 206-222.
- 13 Tollefson DM, Feagler JR, Majerus PW. The binding of thrombin to the surface of human platelets. *J Biol Chem* 1974; **249**: 2646-2651.
- 14 Osterman LA. *Methods of Protein and Nucleic Acid Research 2: Immunoelectrophoresis and Application of Radioisotopes*. Berlin: Springer, 1984: 65-143.
- 15 Aptel J, Voegel JC, Schmitt A. Adsorption kinetics of proteins onto solid surfaces in the limit of the interfacial interaction control. *Colloids and Surfaces* 1988; **29**: 359-371.
- 16 Borovetz HS, Molek GE, Levine G, Hardesty RL, Haubold A D. Protein adsorption *in vitro* onto biomaterial surfaces covered with ULTI carbon. *Biomater Med Dev Artif Organs* 1982; **10**: 187-203.
- 17 Andrade JD, Hlady V. Plasma protein adsorption: the big twelve. *Ann NY Acad Sci* 1987; **516**: 158-172.
- 18 Norde W. Adsorption of proteins from solution at the solid-liquid interface. *Adv Colloid Interface Sci* 1986; **25**: 267-340.
- 19 Wojciechowski P, Hove PT, Brash JL. Phenomenology and mechanism of the transient adsorption of fibrinogen from plasma (Vroman effect). *J Colloid Interface Sci* 1986; **111**: 455-465.
- 20 Horbett TA. Mass action effects on competitive adsorption of fibrinogen from hemoglobin solutions and from plasma. *Thromb Haemostas* 1984; **51**: 174-181.
- 21 Morrissey, BW. The adsorption and-conformation of plasma proteins: a physical approach. *Ann NY Acad Sci* 1977; **283**: 50-64.
- 22 Brash JL, Uniyal S, Samak Q. Exchange of albumin adsorbed on polymer surfaces. *Trans Am Soc Artif Int Organs* 1974; **20**: 69-76.
- 23 Keogh JR, Velander FF, Eaton JW. Albumin-binding surfaces for implantable devices. *J Biomed Mater Res* 1992; **26**: 456-471.
- 24 Schmitt A, Varoqui R, Uniyal S, Brash JL, Pusiner C. Interaction of fibrinogen with solid surfaces of varying charge and hydrophobic-hydrophilic balance: 1. Adsorption isotherms. *J Colloid Interface Sci* 1983; **92**: 145-156.
- 25 Young BR, Pitt WG, Cooper SL. Protein adsorption on polymeric biomaterials: I. Adsorption isotherms. *J Colloid Interface Sci* 1988; **124**: 28-43.
- 26 Elgersma AV, Zsom RLJ, Norde W, Lyklema J. The adsorption of bovine serum albumin on positively and negatively charged polystyrene latices. *J Colloid Interface Sci* 1990; **138**: 145-156.
- 27 Lundstrom I. Models of protein adsorption on solid surfaces. *Prog Colloid Polym Sci* 1985; **70**: 76-82.
- 28 Sato H, Tomiyama T, Morimoto H, Nakajima A. Structure and activity changes of proteins caused by adsorption on material surfaces. In: Brash JL, Horbett TA, eds. *Proteins at Interfaces*, ACS Symp. 343, Washington, DC, 1987: 77-87.
- 29 Lindon JN *et al.* Platelet activation by polyalkyl acrylates and methacrylates: the role of surface-bound fibrinogen. In: Brash JL, Horbett TA, eds. *Proteins at Interfaces*, ACS Symp. 343, Washington, DC, 1987: 507-526.
- 30 Horbett TA, Brash JL. Proteins at interfaces: current issues and future prospects. In: Brash JL, Horbett TA, eds. *Proteins at Interfaces*, ACS Symp. 343, Washington, DC, 1987: 1-33.
- 31 Sharma CP. LTI carbons: blood compatibility. *J Colloid Interface Sci* 1984; **97**: 615-616.
- 32 Horbett TA. Protein adsorption on biomaterials. In: Cooper SL, Peppas NA, eds. *Biomaterials: Interfacial Phenomena and Applications, Advances in Chemistry Series*, Vol. 199. Washington, DC: ACS, 1982: 233-244.
- 33 Dill KA. Dominant forces in protein folding. *Biochemistry* 1990; **29**: 7133-7155.
- 34 Lundstrom I, Ivarsson B, Jonsson U, Elwing H. Protein adsorption and interaction at solid surfaces. In: Feast WJ, Munro HS, eds. *Polymer Surfaces and Interfaces*. Chichester: John Wiley, 1987: 201-230.
- 35 Soderquist ME, Walton AG. Structural changes in proteins adsorbed on polymer surfaces. *J Colloid Interface Sci* 1980; **75**: 386-392.
- 36 Ivarsson B, Ljunstrom I. Physical characterization of protein adsorption on metal and metaloxide surfaces. *CRC Crit Rev Biocompat* 1986; **2**: 1-96.
- 37 Tilton RD, Robertson CR, Gast AP. Lateral diffusion of bovine serum albumin adsorbed at the solid-liquid interface. *J Colloid Interface Sci* 1990; **137**: 192-203.
- 38 Sevastianov VI, Kulik EA, Kalinin ID. The model of continuous heterogeneity of protein-surface interactions for human serum albumin and human immunoglobulin G adsorption onto quartz. *J Colloid Interface Sci* 1991; **145**: 191-206.

see Corrigendum
last page

Protein adsorption on to low-temperature isotropic carbon

4. Competitive adsorption on carbon and silica studied by two-dimensional electrophoresis

L. Feng, J. D. Andrade *

Department of Bioengineering and Department of Materials Science and Engineering, 2480 MEB, University of Utah, Salt Lake City, UT84112, USA

Received 6 August 1993; accepted 13 January 1995

Abstract

Two-dimensional polyacrylamide gel electrophoresis (2D PAGE) was applied to the study of competitive protein adsorption from diluted human plasma. We obtained the depletion (adsorption) of some 25 plasma proteins in the presence of low-temperature isotropic carbon (LTIC) or silica powders. The depletion data are used as a measure of protein adsorptivity. Generally, proteins of lowest abundance have the highest tendency to associate with the two solid surfaces studied. The adsorptivity of a protein is largely determined by its solubility. Most proteins detected exhibit similar depletion behavior on both adsorbents, suggesting a multilayer adsorption process. Three proteins, hemopexin, apolipoprotein A I, and apolipoprotein A II, are depleted differently in the presence of LTIC and silica powders.

Keywords: Carbon; Silica; Plasma proteins; Protein adsorption; Two-dimensional electrophoresis

1. Introduction

One of the drawbacks of *in vitro* studies of protein adsorption is that the solution conditions are different from the *in vivo* environment. Body fluids are complex systems, containing a variety of dissolved or suspended species [1]. There are at least 200 different plasma proteins in blood, constituting about 7–8% of plasma [2]. However, *in vitro* protein adsorption is usually carried out in a single-component solution with a purified protein. Even in a competitive adsorption study, rarely more than three different purified proteins are used [3–5]. It is therefore difficult to correlate the protein adsorption propensity of a solid surface

derived from such highly ideal *in vitro* experiments to its behavior in a real bioenvironment. Although dilute plasma is sometimes used for *in vitro* protein adsorption, usually only one kind of protein is measured at a time [5,6], which makes tedious work of investigations into adsorption properties of even a few proteins from the mixture. Besides, the targeted protein has to be labeled so that it can be detected. Labeling may unintentionally modify the protein itself and thus its adsorptivity. Elution of adsorbed protein followed by one-dimensional electrophoresis [7,8] and “iodograms” [9] have been used to identify multiple proteins. The sensitivity of these methods is subject to limitations in the removal of proteins from the surface and possible deleterious effects of the surfactants used [7]. Using radio immunoassay, up

* Corresponding author.

to 10 proteins from plasma can be detected on a surface for a single adsorption process [10]. However, appropriate antibodies are required for detecting the adsorbed proteins of interest. There are also concerns about the generality of antibody binding to epitopes on adsorbed proteins.

Two-dimensional polyacrylamide gel electrophoresis (2D PAGE) can detect many proteins in a mixture [11–16]. For the study of competitive protein adsorption from a multicomponent solution, this technique demonstrates the following advantages:

(1) detection of individual proteins from a multicomponent system simultaneously, quickly, and conveniently;

(2) no protein labeling, thus eliminating the risk of modifying protein structure and properties;

(3) no need to purify proteins;

(4) high sensitivity (limitation below 0.02 ng mm^{-2}) and large dynamic range for quantification (from 0.02 to 2 ng mm^{-2} on PAGE gels of 1 mm thickness) [16].

In this paper, we present the results of competitive protein adsorption onto carbon and silica powders from diluted human plasma.

2. Experimental

2.1. Materials

Low-temperature isotropic carbon (LTIC) powders were obtained by ball milling silicon alloyed LTIC fragments (a gift from Sorin Biomedica, Italy) in a ceramic jar for 5 h. Their average diameters were $0.2 \mu\text{m}$ with very broad distributions. The BET surface area was $54.4 \text{ m}^2 \text{ g}^{-1}$, but the protein accessible area was much smaller, estimated at around $18 \text{ m}^2 \text{ g}^{-1}$ [17]. The surface to volume ratio was about $3.6 \times 10^5 \text{ cm}^{-1}$, assuming that the density of LTIC was 2.0 g cm^{-3} [18]. Silica powders were from Sigma (St. Louis, MO) with sizes of $0.5\text{--}10 \mu\text{m}$ and a surface area of $1.5 \text{ m}^2 \text{ g}^{-1}$. Citrated plasma, purchased from the Blood Bank, University of Utah Hospital, was pooled from 10 individuals and stored in aliquots below -20°C . Phosphate buffered saline (PBS; phosphate 10 mM + NaCl 150 mM , pH 7.4) was prepared

with sodium dibasephosphate (Ultrix) from J.T. Baker, and sodium hydroxide (Suprapur) and sodium chloride (Suprapur) from EM Science. The extensive list of chemicals with their specifications and sources used in 2D PAGE has been published elsewhere [12].

2.2. Depletion of PBS diluted plasma

LTIC powders were vacuum degassed before being prewetted with PBS. The procedure has been described in detail elsewhere [19]. The pooled plasma (100%) was thawed at room temperature just before the experiment. It was prediluted to 10% with PBS and then pipetted into a polypropylene centrifuge tube containing a certain amount of prewetted LTIC powder. PBS was added to fill the tube to 1.7 ml . The suspension of the powders, plasma proteins and PBS was well mixed, and the final plasma concentration was $1/30$ of the normal concentration (i.e. 3.3%). The tube was incubated at room temperature (22°C) while being rotated for continuous mixing. At a preset time interval, the tube was centrifuged for 1.0 min ; $50 \mu\text{l}$ of the supernatant was transferred to another tube for use as the 2D PAGE sample. The procedure for silica powders was similar except that a vacuum was not needed before prewetting. Control samples were treated identically, although no vacuum degassing was used as there were no adsorbents in the solutions.

Two experimental parameters were varied: the amount of adsorbent (LTIC 0.025 , 0.05 , 0.10 g ; silica 0.10 , 0.33 , 1.00 , 2.00 g) and the incubation time (5 min , 1 h , 12 h). The goal for the former was to find out which protein was most or least likely to be depleted. When a small amount of adsorbent is present, the most surface active proteins should be depleted owing to the limited surface area. Depletion of less surface active proteins can be detected when a higher surface area is available. Since protein concentration also influences the degree of depletion, this latter quantity will be presented as a normalized value. Different incubation times provide information on adsorption kinetics and protein exchange.

2.3. Operation of 2D PAGE

The 2D PAGE apparatus was the ISO-DALT system (Hoefer Scientific Instruments, San Francisco, CA) [14,15], which can run 20 gels at a time. The operation is briefly introduced here; see Refs. [13] and [15] for details.

(1) Isoelectric focusing (IEF) gels were prepared in small glass tubing (1.5 mm interior diameter) by polymerizing acrylamide with cross-linker *N,N'*-methylenebisacrylamide. Ampholytes (3–10) were used to create a pH gradient along the gels after prefocusing. Diluted plasma samples were loaded on top of the gels. IEF was run at 1100 V for 20 h. After the run, the IEF gel was hydrodynamically pushed out of the glass tubing ready for the second-dimension run.

(2) The IEF gel was carefully positioned on top of a slab gel that had been sandwiched between two glass plates and polymerized with a gradient in cross-link density. The IEF gel was fixed in place with agarose glue. Electrophoresis was carried out in a glycine buffer with sodium dodecyl sulfate (SDS) at 50 mA per gel for 8–10 h.

2.4. Staining and quantification

Protein chains in the slab gel were detected by highly sensitive silver staining [16]. The slab gels were thus separated from the glass plates and were fixed in a solution of 50% ethanol and 10% acetic acid overnight, stabilized in a 2% glutaraldehyde solution of pH 9.5 for 60 min, stained in a solution of 0.7% silver nitrate for 75 min, developed in a solution of formaldehyde and citric acid, stopped in an acetic solution, and finally immersed in a 20% ethanol solution overnight. The wet gel was enclosed in a polyethylene zip-lock bag for storage and was analyzed within 3 days.

A charge-coupled-device (CCD) camera (14 bits, Photometrics LTD, Tucson, AZ) interfaced with a Macintosh II computer was used to obtain transmission digitized images. The optical density was calibrated using specific protein standards. To quantify a particular protein chain, the location

and size of the spot were first specified, and then the area was measured, the local background subtracted, and the integrated optical density (IOD) computed.

2.5. Important facts

The following two important facts must be kept in mind before analyzing the results.

(1) The definition of surface concentration or adsorbed amount (Γ) measured in this experiment (depletion) is not equivalent to those involving a thorough rinse with buffer before taking measurements. In the latter case, the sample surface only contains proteins that cannot be washed off. However, the adsorption assessed by the depletion method includes superficially bound proteins, which can be eluted by buffer rinse. In other words, the Γ measured in this case should be higher.

(2) 2D PAGE is a semi-quantitative technique. Many factors contribute to deviations in comparing the IOD of a spot at the same position among different gels, such as loading errors, variations among individual gels (size, thickness, pH gradient, and cross-linking density), protein losses in solution treatments after electrophoresis, contamination at each stage of operation, time variation in development, and uncertainties in the digitization with the CCD camera. To minimize these adverse effects, a protein standard, soybean trypsin inhibitor (STI), was incorporated into every loading sample before running IEF. All other IODs of protein chains were normalized by the IOD of the external standard STI. However, owing to different staining efficiencies for different protein chains and heterogeneity within a gel (e.g. different thicknesses in different regions), this external calibration did not solve all the problems. Thus, even for the same batch (i.e. the same sample loaded on different gels that were cast, run, fixed stained and stored at the same time), 20–30% deviations in IODs were common among different gels for bigger and darker spots, reaching as much as 50% or even higher than 100% for smaller and lighter spots. Hence, the value to be given is the median IOD from three gels for each sample; no standard deviation was calculated.

3. Results

3.1. Quantitation of proteins

Fig. 1 displays two typical 2D PAGE gel images. Fig. 1(A) is the map of a non-depleted plasma (control) sample, in which many protein chains have been identified according to the patterns of known proteins as well as standard plasma protein maps [12,14,20]. Fig. 1(B) is the map of a depleted sample, in which the corresponding spots become lighter or have disappeared compared to those in Fig. 1(A). One cannot compare absolute quantities of different proteins in terms of their IODs, as silver has different staining efficiencies for different proteins. Nevertheless, it is justifiable to compare amounts of the same proteins before and after they are depleted. The percentage of the depleted amount (DA) of a particular protein chain can be calculated by Eq. (1):

$$DA\% = \left(1 - \frac{\text{IOD of the chain after depletion}}{\text{IOD of the chain before depletion}} \right) \times 100 \quad (1)$$

The abundance of a detectable protein was estimated by its “normalized amount” (NA), defined by the ratio of the IOD of the protein to that of albumin. Notice that the NA of a protein is not usually equal to the ratio of its concentration to that of albumin, because different proteins have different efficiencies of silver staining and not all protein chains can be detected by 2D PAGE.

3.2. Percentile depletion of plasma proteins

The values for protein depletion (adsorption) in Tables 1 and 2 are based on the percentiles, i.e. DA in Eq. (1). The total depletion (next to last rows) of all detectable proteins was calculated by Eq. (2):

$$\text{Total depletion \%} = \frac{\sum DA_i \cdot NA_i}{\sum NA_i} \times 100 \quad (2)$$

where the depleted amount of protein i (DA_i) is weighted by its normalized amount, NA_i . The last row is the depletion of all detectable proteins

excluding albumin. Again, these are rough estimates as the DA values are not very accurate, and not all the plasma proteins are detectable.

A thorough survey of Tables 1 and 2 produces some general observations (note that in the discussion below, depletion or adsorption are on a percentile basis).

(1) Depletion is not identical for all plasma proteins on both adsorbents. In other words, adsorption is competitive on these surfaces; some proteins disappear from the solution very quickly and completely, while some mostly remain in solution, e.g. fibrinogen vs. albumin.

(2) With some exceptions, on both surfaces the proteins with high abundances of plasma are depleted slowly and slightly, such as albumin, immunoglobulin, α_1 antitrypsin, transferrin, and haptoglobin, but proteins of low concentration in plasma tend to adsorb rapidly and completely, such as apo C III', C4, and G4 glycoprotein (Fig. 2).

(3) The exceptions on LTIC adsorbents are apo A II, prealbumin, and α_1 acid glycoprotein, whose concentrations are not very low but whose depletion is among the lowest. The opposites are fibrinogen, α_2 HS glycoprotein, α_2 macroglobulin, hemopexin, and plasminogen, whose concentrations range from medium to high, yet whose depletion is high.

(4) The exceptions on silica for both categories are (A) hemopexin, α B glycoprotein, prealbumin, and α_1 acid glycoprotein, and (B) fibrinogen, apo A I, apo A II, and α_2 macroglobulin.

(5) No perceptible protein exchange occurs on LTIC, i.e. statistically, there are only forward transitions from lower depletion to higher depletion but no backward ones (Fig. 3). A similar situation showing lack of displacement was observed with the silica surface [17].

(6) The next to last rows in Tables 1 and 2 indicate that the total depleted amount is not proportional to the adsorbate amount. As shown in Fig. 4, the higher the concentration of adsorbent, the less adsorption per unit mass.

(7) Albumin has a relatively low depletion percentage as indicated by comparison of its DA to the total depletion, or even more clearly to the total depletion excluding albumin itself. The last

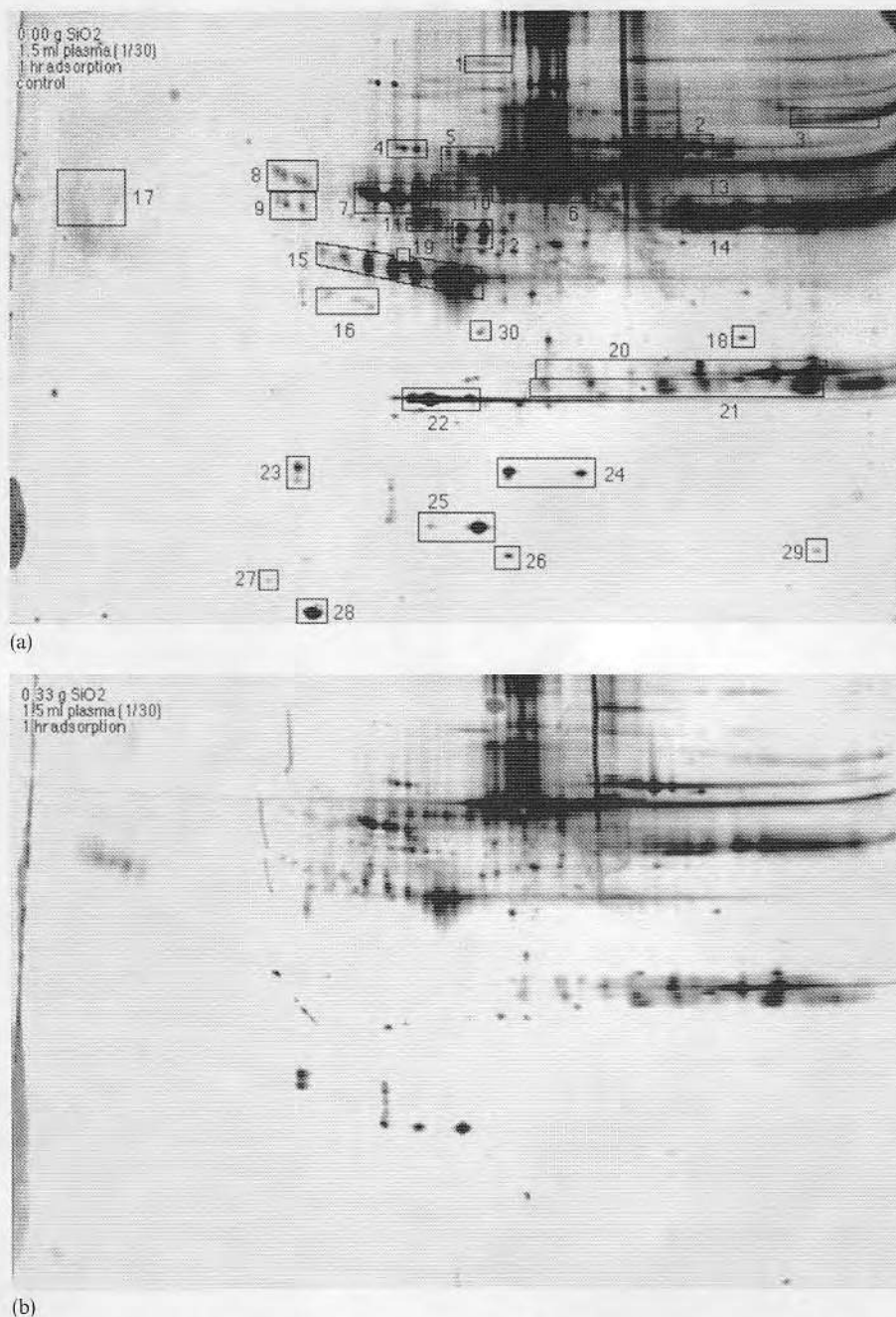


Fig. 1. Plasma proteins on 2D PAGE gels from a non-depleted (control) sample (A) and a depleted sample (B). Some identified proteins and protein chains are as follows: (1) α_2 macroglobulin; (2) transferrin; (3) plasminogen; (4) α_1 B glycoprotein; (5) hemopexin; (6) albumin; (7) α_1 antitrypsin; (8) α_1 antichymotrypsin; (9) α_2 HS glycoprotein; (10) Ig A chains; (11) Gc globulin; (12) fibrinogen γ chain; (13) fibrinogen β chain; (14) Ig γ chains; (15) haptoglobin β chain; (16) G4 glycoprotein; (17) α_1 acid glycoprotein; (18) C4 γ chain; (19) apolipoprotein A IV; (20) Ig λ chains; (21) Ig κ chains; (22) apolipoprotein A I; (23) soybean trypsin inhibitor; (24) haptoglobin α_2 chain; (25) prealbumin; (26) haptoglobin α_1 chain; (27) apolipoprotein C III; (28) apolipoprotein A II; (29) hemoglobin; (30) apolipoprotein E.

Table 1
Depletion (adsorption) of plasma proteins on LTIC powders^a (%)

Plasma protein ^b	Normalized amount ^c	Amount of LTIC in mg (total surface area in m ²) ^d								
		25 (0.45)			50 (0.90)			100 (1.8)		
		5 min	1 h	12 h	5 min	1 h	12 h	5 min	1 h	12 h
Albumin	100	13	17	15	8	13	23	36	33	50
α_1 acid glycoprotein	6	10	44	53	5	18	47	26	51	71
α_1 antichymotrypsin	8	37	45	19	75	86	98	100	100	100
Antithrombin III	9	28	11	29	58	54	78	81	91	100
α_1 antitrypsin	34	15	30	40	29	28	50	63	64	68
Apolipoprotein A I	21	9	27	29	27	27	42	38	48	76
Apolipoprotein A II	4	40	47	50	29	59	68	62	83	82
Apolipoprotein A IV	2	25	57	48	58	93	100	100	100	100
Apolipoprotein C III-1	1	65	100	100	100	100	100	100	100	100
Apolipoprotein C III-2	1	59	100	100	100	100	100	100	100	100
Apolipoprotein E	3	58	73	100	100	100	100	100	100	100
C4	1	53	71	81	90	86	100	100	100	100
Fibrinogen	12	96	98	99	100	100	100	99	100	100
Gc globulin	5	34	61	56	74	83	100	100	100	100
α B glycoprotein	3	32	41	43	54	67	83	16	81	92
G4 glycoprotein	3	57	—	64	100	100	100	100	100	100
α_2 HS glycoprotein	8	90	100	100	100	100	100	100	100	100
Haptoglobin	64	15	40	36	29	24	55	43	55	70
Hemoglobin	1	21	30	30	22	64	83	59	69	96
Hemopexin	22	29	53	59	100	100	100	100	100	100
Immunoglobulin	44	54	44	46	65	58	66	76	95	97
α_2 macroglobulin	4	80	90	97	98	95	—	100	100	100
Plasminogen	6	67	45	85	81	79	97	100	100	100
Prealbumin	8	17	25	40	41	36	61	61	67	91
Transferrin	37	25	13	27	31	30	37	41	63	71
Total depletion		28	35	38	40	41	55	58	65	75
Total DA excluding albumin		32	41	48	51	50	65	65	75	85

^a Volume for all solutions, 1.7 ml.

^b Estimated amounts of total plasma protein: 4.5 mg, assuming 8 mg plasma proteins per ml of plasma. Concentration, 2.6 mg ml⁻¹.

^c Normalized IOD for each protein divided by the IOD of albumin for the control samples.

^d Assuming 18 m² g⁻¹ accessible surface area.

columns (the highest solid surface area and longest adsorption time) can be taken as an example. The comparison of the DA of albumin with the last two rows gives 50% vs. 75% and 85% in the presence of LTIC, and 42% vs. 66% and 74% in the presence of silica.

(8) Fibrinogen has a very high depletion percentage, both kinetically and thermodynamically, on both LTIC and silica. In only 5 min its depletion reached 96% on LTIC and 85% on silica, even when the lowest amount of adsorbent was used.

(9) The depletion patterns of proteins on LTIC

and silica are strikingly similar. With only a few differences ((3) and (4) (in Fig. 1), about 21 out of 25 plasma proteins follow similar depletion pattern on both surfaces.

4. Discussion

4.1. Effective surface area for protein adsorption

We can estimate the protein surface concentration on both surfaces from the total depletion

Table 2

Depletion (adsorption) of plasma proteins on silica powders after 12 h incubation^a (%)

Plasma protein ^b	Relative amount ^c	Amount of silica in g (total surface area in m ²) ^d			
		0.10 (0.15)	0.33 (5.0)	1.00 (1.5)	2.00 (3.0)
Albumin	100	6	21	44	42
α_1 acid glycoprotein	6	8	31	15	37
α_1 antichymotrypsin	8	6	46	77	89
Antithrombin III	9	0	31	77	100
α_1 antitrypsin	34	0	6	26	70
Apolipoprotein A I	21	26	91	91	90
Apolipoprotein A II	4	37	98	99	100
Apolipoprotein A IV	2	15	100	100	100
Apolipoprotein C III-1	1	58	100	100	100
Apolipoprotein C III-2	1	100	100	100	100
Apolipoprotein E	3	85	98	90	100
C4	1	51	100	100	100
Fibrinogen	12	87	90	90	84
Gc globulin	5	0	34	63	87
α B glycoprotein	3	16	31	65	67
G4 glycoprotein	3	23	100	100	100
α_2 HS glycoprotein	8	2	92	95	97
Haptoglobin	64	0	29	68	76
Hemopexin	22	12	18	60	71
Immunoglobulin	44	9	30	63	64
α_2 macroglobulin	4	100	100	100	100
Plasminogen	6	13	23	70	100
Prealbumin	8	0	11	42	35
Transferrin	37	17	25	53	53
Total depletion		12	34	59	66
Total DA excluding albumin		14	38	64	74

^a Volume for all solutions, 1.7 ml.^b Estimated amounts of total plasma protein: 4.5 mg, assuming 8 mg plasma proteins per ml of plasma. Concentration, 2.6 mg ml⁻¹.^c Normalized IOD for each protein divided by the IOD of albumin for the control samples.^d Assuming 1.5 m² g⁻¹ surface area.

of identified proteins, the surface area and the amount of adsorbent (Tables 1 and 2). Fig. 4 shows that the larger amount of adsorbent adsorbs fewer proteins per unit mass. A similar result is reported in Ref. [17], where the amount of denatured proteins was not proportional to the amount of LTIC powder. Such a relationship could be the results of two processes:

(1) smaller amounts of adsorbent adsorb less protein so that the solution concentration is higher, producing a higher surface concentration;

(2) more adsorbent causes more aggregation of adsorbent particles so that the surface area per unit mass becomes smaller.

The former can be expected from the adsorption

isotherms and from possible multilayer adsorption [17]. The latter may be due to a slightly smaller ratio of the volume of protein solution to the volume of adsorbent. To allow for this effect, we extrapolated Γ to zero adsorbent mass, which is shown in Fig. 4 as bold curves. We thereby estimated that the surface concentrations of the identified proteins are 6.0 mg m⁻² on LTIC and 4.0 mg m⁻² on silica.

4.2. Similar depletion on both adsorbents

Similar percentage depletion of plasma proteins by LTIC and silica adsorbents is not expected. We anticipated that the two surfaces should have

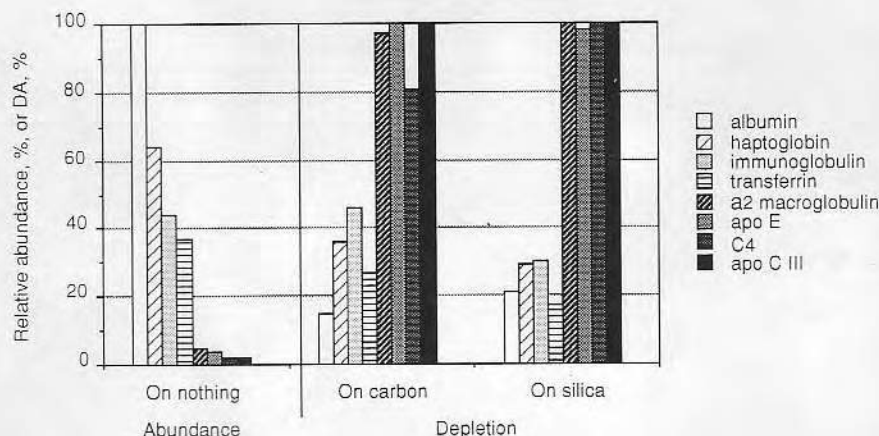


Fig. 2. Inverse relationship between abundance of proteins in plasma and their depleted amounts.

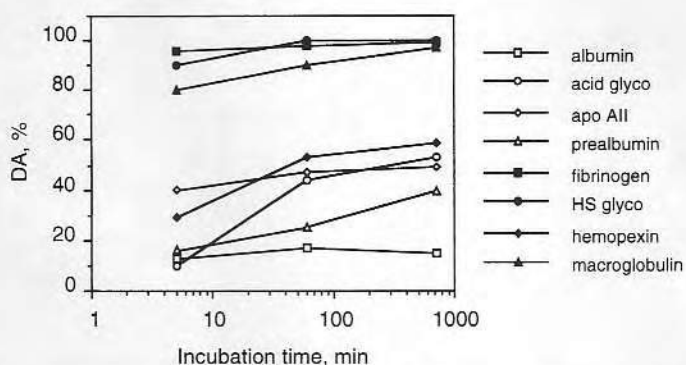


Fig. 3. Depletion kinetics from 2D PAGE experiments with 1.7 ml (1/30) diluted plasma and LTIC powder (25 mg).

different protein compositions, especially when smaller amounts of adsorbent are used, where adsorption is more competitive. There are several possible mechanisms causing such results:

- (1) the two substrates adsorb similar proteins;
- (2) the present technique cannot discriminate between different adsorbents;
- (3) the surface is not completely covered by protein so that there is little competition in adsorption;
- (4) there is a multilayer adsorption, making the depletion apparently similar on the two surfaces [17,21].

We believe the last process to be the most reasonable. The total amount of protein in the dilute plasma is relatively high: 2.6 mg ml^{-1} before

any depletion and about 0.7 mg ml^{-1} after the highest depletion. As no rinse was used, loosely bound proteins are considered to be adsorbed.

4.3. Adsorptivity and abundance

All proteins are surface active, but their adsorptivity is different. These experiments show that for most proteins there exists a rough inverse relationship between adsorptivity and abundance, despite the suggestion that there is little connection between protein abundance and adsorption tendency [22]. The propensities of plasma proteins for depletion may well depend on their biological functions. The phenomenon that abundant plasma proteins have a lower tendency to be depleted than

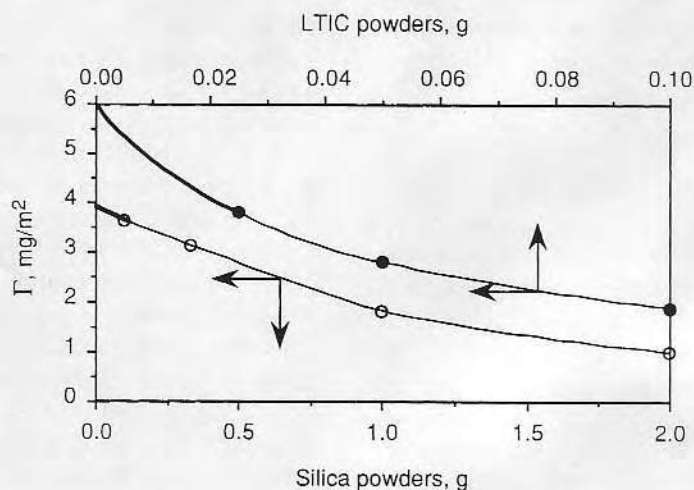


Fig. 4. Normalized surface concentration of plasma proteins by solid surface area on LTIC and silica as a function of amounts of the substrates. Volume of the 1/30 diluted plasma: 1.7 ml. Assuming a plasma protein concentration of 80 mg ml^{-1} , and surface area of $18 \text{ m}^2 \text{ g}^{-1}$ for LTIC and $1.5 \text{ m}^2 \text{ g}^{-1}$ for silica.

less common ones has already been observed [22,23], i.e. abundant proteins with low binding affinity adsorb first, but are gradually displaced by trace proteins that are more surface active but arrive at the interface more slowly.

4.4. Differently depleted proteins

It is interesting to examine the proteins that do not fit the relationship between adsorptivity and abundance. These are divided into three groups in Table 3. The first group is defined as containing

the most depleted proteins and the second as containing the least depleted ones, on LTIC, on silica or on both. The last group is made up of proteins showing opposite depletion propensities towards the LTIC and silica adsorbents. Only proteins whose concentrations in plasma are neither too high (under 3 mg ml^{-1}) for the least depleted nor too low (above 0.3 mg ml^{-1}) for the most depleted are listed. For example, fibrinogen, despite its relatively high abundance, is very susceptible to depletion. In less than 5 min it has virtually all disappeared from the solution.

Table 3

The most (+) and least (–) depleted plasma proteins on LTIC and silica powders from PBS diluted plasma

Plasma protein	Normalized amount	On LTIC	On silica	Adsorptivity
Fibrinogen	12	+	+	Most depleted
α_2 HS glycoprotein	8	+	+	
α_2 macroglobulin	4	+	+	
Plasminogen	6	+		
α_1 acid glycoprotein	6	–	–	Least depleted
Prealbumin	8	–	–	
Hemoglobin	1	–		
Hemopexin	22	+	–	Opposite depletion
Apo A I	21	–	+	
Apo A II	4	–	+	

However, α_1 acid glycoprotein is hard to deplete even though it belongs to the low-concentration class.

4.5. Role of solubility of protein

On comparing the solubility of the most and least depleted proteins in Table 4, one immediately spots some connections. Column 2 of Table 4 indicates the influence of ethanol on the solubility of the proteins [24,25]. The general trend is that the least depleted group can tolerate more ethanol without precipitation than the most depleted group. Column 3 shows the effects of an inorganic salt, ammonium sulfate. Again, a higher tolerance means higher stability of the protein to this substance [24,25]. The most depleted proteins apparently precipitate at lower molar concentrations. Less soluble proteins are more surface active in terms of adsorption behavior [26], although the reverse relation may not hold (hemoglobin is extremely soluble and also extremely surface active [26]). This correlation should probably be considered together with the type of solid substrate. Multilayer adsorption should also reflect the nature of the substrate. Otherwise, there would be very few proteins with low solubility in plasma.

4.6. Some individual plasma proteins

(A) Albumin

Albumin is one of the least adsorbed plasma proteins in terms of the depletion percentage. It binds only weakly to silica [27] and to some polymer surfaces [28]. It has been ranked as the protein with the lowest affinity to silica, in comparison to fibrinogen (the highest), lysozyme, IgG, ribonuclease, etc. [29]. Its low surface activity has been recognized [30] and is more noticeable in competitive adsorption processes [22,31], which is understandable. In blood, the biological functions of albumin (transport and colloid osmotic pressure) demand that it has a high concentration and thus high solubility. Hence, it should not be expected to have a high surface activity.

(B) Fibrinogen

Fibrinogen is a typical "most depleted" protein. Tables 1 and 2 show that it is almost completely depleted in the presence of small amounts of adsorbent at very short times. Near total depletion of fibrinogen has also been observed on polyurethane particles and on glass beads [32]. According to the irreversibility of its adsorption on to LTIC [27], fibrinogen cannot displace previously adsorbed albumin or other adsorbed plasma proteins from the surface. The same experiment also indicates that the surface concentration of albumin from dilute plasma on LTIC is about 50% of that from pure albumin at a similar albumin solution concentration. Hence, the albumin deposited from dilute plasma is not likely to be displaced. Fibrinogen is not preferentially adsorbed onto LTIC, compared with albumin, from their binary solutions. Therefore, owing to its small share in the total protein mass, only a small number of fibrinogen molecules can even touch the LTIC surface before the surface is rapidly covered by proteins.

These facts suggest that fibrinogen molecules may reside on the surface of adsorbed proteins, i.e., multilayer adsorption. This property of fibrinogen can be attributed to its low solubility, and its propensity to precipitate. Its low solubility can be demonstrated by the fact that fibrinogen has the lowest tolerance towards either ethanol or ammonium sulfate among the proteins in Table 4.

Table 4

Solution stability of the plasma proteins with the most or least adsorptivities towards LTIC^a

Plasma protein	Ethanol (%)	[(NH ₄) ₂ SO ₄] (M)
Fibrinogen	8 (7.2) ^b	0.6 (7.0) ^b
α_2 HS glycoprotein	20 (5.8)	1.0-1.4 (7.0)
Hemopexin	18 (5.2)	2.4-3.2 (5.0)
α_2 macroglobulin	25 (5.7)	1.2-1.8 (7.0)
α_1 acid glycoprotein	70 (6.2)	2.4-4.0 (5.0)
Albumin	40 (5.2)	2.6-8.0 (7.0)
Prealbumin	18 (5.2)	2.6 (5.0)
Haptoglobin	40 (5.8)	1.9-2.2 (7.0)

^a Adapted from Ref. [25].

^b pH values are in parentheses.

Doolittle [33] considered fibrinogen as one of the least soluble proteins in plasma, in contrast to α_1 acid glycoprotein that has an unusually high solubility [34]. We propose that this low solubility renders the fibrinogen surface active.

(C) Hemoglobin

Hemoglobin is a protein with a very high surface activity, higher than that of fibrinogen [26], but shows small depletion on LTIC. Blood carries little free hemoglobin (concentration about 0.003 mg ml^{-1} [22]). The hemoglobin detected is probably bound to haptoglobin [35]. The appearance and depletion of hemoglobin is actually due to hemoglobin from the haptoglobin complex rather than free hemoglobin. The low depletion thus represents the low surface activity of the complex.

(D) Apolipoproteins

Table 3 includes two apolipoproteins (apo A I and apo A II) that behave differently towards the two adsorbents. As Table 2 shows, silica completely adsorbs all the detectable apolipoproteins, indicating a high affinity of apolipoproteins towards silica. However, it is a little misleading to examine only the apolipoproteins; since the apolipoproteins in plasma contain lipids, their adsorption properties should be determined by the entire protein-lipid complex. As apo A I and apo A II are mostly contained in high-density lipoproteins (HDLs) [36], it is reasonable to suggest that it is the HDL that adsorbs differently onto the two substrates. HDL adsorbs onto the silica powders according to the DA data, and its high surface activity has been recognized [4]. It also adsorbs onto polyvinyl chloride and polystyrene. Preadsorption of HDL can inhibit adsorption of the three major proteins: albumin, fibrinogen, and IgG [4]. However, its surface activity does not stand out on the LTIC substrate, which further reflects the equal adsorptive tendency of the surface towards different proteins.

(E) Hemopexin

Hemopexin is an interesting protein. It is the only other major protein that has different depletion properties on LTIC and on silica, together

with the apolipoproteins. Independent work by Tingey [32] provides further evidence that hemopexin also exhibits unique adsorption behavior towards polyurethanes and glass. Table 4 reveals its apparent different stability towards the two precipitants, ethanol and ammonium sulfate. It exhibits low stability to the organic compound but high stability to the salt. Are these two kinds of chemicals in any way analogous to carbon and silica? From its different tolerances towards ethanol and ammonium sulfate, hemopexin seems to have a strong interaction with the latter. However, the complication that precipitation is sometimes accompanied by protein denaturation prevent us from carrying out further analysis at this time [37].

4.7. Is Fibrinogen Displaced?

It has been established that fibrinogen can be displaced [38] or its adsorption can be suppressed [39] by other plasma proteins [27]. Transient adsorption of fibrinogen onto hydrophilic surfaces is a definition of one of the Vroman effects. In the present work, however, neither displacement of fibrinogen nor suppression of its adsorption is observed on either carbon (Fig. 3) or silica (data not shown, but the DA of fibrinogen is almost the same for 5 min depletion and 12 h depletion). A large decrease in fibrinogen adsorption onto silica plates has been observed by the radiolabeling method with the same plasma sample [27], implying that the fibrinogen-displacing proteins (high-molecular weight kininogen and factor XII) were present and surface active. We need more experimental data to explain such a lack of displacement.

5. Conclusions

LTIC and silica substrates deplete plasma proteins similarly. However, the DA does not necessarily represent the affinity of a protein towards a solid surface in competitive adsorption, owing to the complexity of the process. In a depletion experiment, the measured competitive adsorptivity of a protein is determined more by its solubility than by the type of solid surface involved. Generally, proteins at low concentrations in plasma are more

easily adsorbed while proteins of high abundance tend to stay in solution. A related conclusion is that proteins that have low solubility or are readily precipitated are depleted more completely than those with higher solubility. Fibrinogen represents the first category; its depletion on both substrates is very significant owing to its low solubility and high surface activity. Albumin exemplifies the second group; it is the least adsorbed in terms of the depletion percentage, showing a relatively low surface activity. Although proteins are all surface active, their surface activities can be very different and are manifested mostly in competitive adsorption experiments.

Three proteins, hemopexin, apolipoprotein A I, and apolipoprotein A II, are depleted differently in the presence of LTIC and silica adsorbents. It would be informative to correlate protein molecular structure to their solution and adsorption properties [26]. This requires a close examination of protein structures, such as amino acid sequences, secondary and tertiary structures, domain structure, charge distribution, etc. Computer graphics can be very helpful [40] in this regard.

Acknowledgments

We thank Sorin Biomedica for providing the LTIC sample. This work was supported by the Center for Biopolymers at Interfaces, University of Utah.

References

- [1] D.F. Williams, Blood compatibility, Vol. 1, CRC Press, Boca Raton, FL, 1987, p. 6.
- [2] J.D. Andrade and V. Hlady, *Ann. N.Y. Acad. Sci.*, 516 (1987) 158.
- [3] S.W. Kim and R.G. Lee, in R.E. Baier (Ed.), *Applied Chemistry at protein interfaces*, ACS, Washington, DC, 1975, p. 218.
- [4] A. Bantjes, W. Breemhaar, T. Beugeling, E. Brinkman and D.J. Ellens, *Makromol. Chem., Suppl.*, 9 (1985) 99.
- [5] S.M. Slack and T.A. Horbett, *J. Colloid Interface Sci.*, 124 (1988) 535.
- [6] J.L. Brash and P. ten Hove, *Thromb. Haemostat.*, 51 (1984) 326.
- [7] G.K. Limber, C.H. Glenn and R.G. Mason, *Thromb. Res.*, 5 (1974) 735-746.
- [8] D.J. Lyman, L.C. Metcalf, D. Albo, K.F. Richards and J. Lamb, *Trans. Am. Soc. Artif. Intern. Organs*, 20 (1974) 474-479.
- [9] P.K. Weathersby, T.A. Horbett and A.S. Hoffman, *Trans. Am. Soc. Artif. Intern. Organs*, 22 (1976) 242-252.
- [10] N.P. Ziats, D.A. Pankowsky, B.P. Tierney, O.D. Ratnoff and J.M. Anderson, *J. Lab. Clin. Med.*, 116 (1990) 687.
- [11] R. Bravo, in J.E. Celis and R. Bravo (Eds.), *Two-dimensional gel electrophoresis of proteins: methods and applications*, Academic Press, Orlando, FL, 1984, p. 1.
- [12] C.-H. Ho, V. Hlady, G. Nyquist, J.D. Andrade and K.D. Caldwell, *J. Biomed. Mater. Res.*, 25 (1991) 423.
- [13] C.-H. Ho, M.S. Thesis, University of Utah, 1990.
- [14] N.L. Anderson, R.P. Tracy and N.G. Anderson, in F.W. Putman (Ed.), *The plasma proteins: structure, function, and genetic control*, Vol. 4, Academic Press, Orlando, FL, 1984, p. 221.
- [15] L. Anderson, *Two-dimensional electrophoresis: operation of the ISO-DALT system*, Large Scale Biology Press, Washington, DC, 1988.
- [16] C.R. Merrill and D. Goldman, in J.E. Celis and R. Bravo (Eds.), *Two-dimensional gel electrophoresis of proteins: methods and applications*, Academic Press, Orlando, FL, 1984, p. 93.
- [17] L. Feng, Ph.D. Dissertation, University of Utah, 1993.
- [18] A.D. Haubold, R.A. Yapp and J.C. Bokros, in M.B. Bever (Ed.), *Encyclopedia of materials science and engineering*, Vol. 1, Pergamon, Oxford, 1986, p. 514.
- [19] L. Feng and J.D. Andrade, *J. Biomed. Mater. Res.*, in press.
- [20] R.P. Tracy and D.S. Young, in J.E. Celis and R. Bravo (Eds.), *Two-dimensional gel electrophoresis of proteins: methods and applications*, Academic Press, Orlando, FL, 1984, p. 193.
- [21] T. Matsuda, *Trans. Am. Soc. Artif. Intern. Organs*, 30 (1984) 353.
- [22] J.L. Brash, in C.P. Sharma et al. (Eds.), *Blood compatible materials and devices*, Technomic, Lancaster, 1991, p. 3.
- [23] L. Vroman and A.L. Adams, in J.L. Brash and T.A. Horbett (Eds.), *Proteins at interfaces*, ACS Symp. Ser. 343, Washington, DC, 1987, p. 154.
- [24] H.E. Schultz and J.F. Heremans, *Molecular biology of human proteins: with special reference to plasma proteins*, Vol. 1, Elsevier, Amsterdam, 1966, Chapters 1 and 2.
- [25] W. Melander and C. Horvath, *Arch. Biochem. Biophys.*, 183 (1977) 200.
- [26] T.A. Horbett and J.L. Brash, in J.L. Brash and T.A. Horbett (Eds.), *Proteins at interfaces*, ACS Symp. Ser. 343, Washington, DC, 1987, p. 1.
- [27] L. Feng and J.D. Andrade, *Biomaterials*, 15 (1994) 323.
- [28] R.C. Eberhart et al., in S.L. Cooper and N.A. Peppas (Eds.), *Biomaterials: interfacial phenomena and applications*, Adv. Chem. Ser. Vol. 199, ACS, Washington, DC, 1982, p. 293.

- [29] F. Kozin, B. Millstein, G. Mandel and N. Mandel, *J. Colloid Interface Sci.*, 88 (1982) 326.
- [30] T.A. Horbett, in S.L. Cooper and N.A. Peppas (Eds.), *Biomaterials: interfacial phenomena and applications*, Adv. Chem. Ser. Vol. 199, ACS, Washington, DC, 1982, p. 233.
- [31] W. Norde, *Adv. Colloid Interface Sci.*, 25 (1986) 267.
- [32] K. Tingey, Ph.D. Dissertation, University of Utah, 1993.
- [33] R.F. Doolittle, in F.W. Putman (Ed.), *The plasma proteins: structure, function, and genetic control*, Vol. 2, Academic Press, Orlando, FL, 1984, p. 110.
- [34] H.G. Schwick and H. Haupt, in F.W. Putman (Ed.), *The plasma proteins: structure, function, and genetic control*, Vol. 4, Academic Press, Orlando, FL, 1984, p. 167.
- [35] F.W. Putman, in F.W. Putman (Ed.), *The plasma proteins: structure, function, and genetic control*, Vol. 2, Academic Press, Orlando, FL, 1975, p. 1.
- [36] G. Camejo and V. Munoz, in C.E. Day (Ed.), *High-density lipoproteins*, Marcel Dekker, New York, 1981, p. 131.
- [37] T.M. Przybycien and J.E. Bailey, *Enzyme Microb. Technol.*, 11 (1989) 264.
- [38] J. Brash, *Ann. N.Y. Acad. Sci.*, 516 (1987) 206.
- [39] P. Wojciechowski, P.T. Hove and J.L. Brash, *J. Colloid Interface Sci.*, 111 (1986) 455.
- [40] D. Horsley, J. Herron, V. Hlady and J.D. Andrade, in J.L. Brash and T.A. Horbett (Eds.), *Proteins at interfaces*, ACS Symp. Ser. 343, Washington, DC, 1987, p. 290.



ELSEVIER

Colloids and Surfaces B: Biointerfaces 6 (1996) 149

COLLOIDS
AND
SURFACES

B

Corrigendum

Corrigendum to "Protein adsorption on to low-temperature isotropic carbon

4. Competitive adsorption on carbon and silica by two-dimensional electrophoresis"

[Colloids and Surfaces B: Biointerfaces 4 (1995) 313–325]¹

L. Feng, J.D. Andrade*

Department of Bioengineering and Department of Materials Science and Engineering, 2480 MEB, University of Utah,
Salt Lake City, UT84112, USA

The authors would like to make it clear that the development of the quantitative 2-dimensional gel electrophoresis technique for the study of protein adsorption via a solute depletion approach was first carried out, and the methodology developed, by C.-H. Ho, V. Hlady, G. Nyquist, J.D. Andrade and K.D. Caldwell, *J. Biomed. Mater. Res.*, 28 (1991) 423, and discussed and described in detail in C.-H. Ho, M.S. Thesis, University of Utah, 1990. The work has been further described, presented, and expanded in the paper by Hlady et al., *Clin. Mater.*, 13 (1993) 85–93, and has since been described in other publications and presentations.

The way the references were presented and cited in our paper may have misled the reader into thinking that this methodology and technique was first developed and applied by Feng and Andrade. That is indeed not the case. We hope this note clarifies the situation.

Protein adsorption on low temperature isotropic carbon: V. How is it related to its blood compatibility?

L. FENG and J. D. ANDRADE*

*Department of Bioengineering and Department of Materials Science and Engineering,
2480 MEB, University of Utah, Salt Lake City, UT 84112, USA*

Received 14 January 1994; accepted 4 January 1995

Abstract—Based on our research on blood protein interactions with low temperature isotropic carbon (LTIC) and data from the literature, we propose that the carbon surface has strong interactions with adsorbed proteins. In this paper we focus on how a relatively blood-compatible material interacts with plasma proteins. We present our results on the structure and properties of the LTIC surface utilizing SEM, STM, XPS, and contact angle measurements. We briefly review protein adsorption on LTIC using DSC, impedance, radioisotopes, and two-dimensional gel electrophoresis. LTIC is characterized by a microporous, oxidized, hydrophobic, and domain mosaic structure. Surface polishing smoothens the roughness and removes the porosity, while largely destroying the ordered atomic texture, making the surface more random and more amorphous. The LTIC surface denatures all adsorbed proteins studied. The rate of protein adsorption is high and the surface concentration is large. The LTIC surface adsorbs all proteins without preference. The surface also tenaciously retains proteins such that they cannot be displaced by buffer or exchanged by proteins in solution. We conclude that LTIC accomplishes its blood compatibility through a passivating film of strongly adsorbed bland proteins, which do not interact with platelets nor participate in blood coagulation. We also suggest mechanisms for the production of such a film by the LTIC surface.

Key words: Blood compatibility; biomaterial; low temperature isotropic carbon; surface structure; protein adsorption.

INTRODUCTION

Significance

Blood compatibility or hemocompatibility is an essential requirement of prosthetic blood-contacting materials [1-3]. It has long been a challenge to prevent the surface of implants from forming thrombus, emboli, or other surface implicated adverse effects [2-6]. So far no man-made biomaterial is even close to endothelium in its blood compatibility [7]. It is generally agreed that the blood compatibility of a material is mainly determined by its surface properties [8], including chemical composition, morphology, microstructural heterogeneity, crystallinity, hydrophobicity, hydrophilicity, surface energy, molecular mobility, charge density, electric conductivity, and redox potential. Although many pieces of the 'jigsaw puzzle' have been identified, thanks to the work from past decades [9], we still lack a fundamental mechanism to put these pieces together to achieve a more complete understanding of blood compatibility. Therefore, we designed a series of experiments to study the surface of low temperature isotropic carbon (LTIC) and its adsorption properties towards two plasma proteins, albumin and fibrinogen, and several model proteins [10]. Some of the work has been published or is in press [11-15]. This paper briefly summarizes

* To whom correspondence should be addressed.

that extensive set of studies and integrates all the experiments, thus displaying a broad view on how and why LTIC behaves.

Rationale

There were several reasons for choosing LTIC: (1) It is one of the best long term blood-compatible implantable materials in comparison to other prosthetic biomaterials [16–19]. LTIC and its cousins, ultra-low temperature isotropic carbon (ULTIC) and glassy carbon (GC), have been widely applied in medical devices, including artificial heart valves [1, 16, 20], dental implants [16, 17], orthopedic implants [16, 18], and vascular grafts [21–23]. (2) LTIC represents a large family of carbons that generally show some degrees of biocompatibility, including diamond-like carbon [24, 25], pyrolytic graphite [26] carbon-carbon composites [27, 28] carbon fibers [29, 30], and even diamond [26], in addition to LTIC, ULTIC, and GC. So they must have something in common that grants them 'biocompatibility'. (3) LTIC is an interesting material because it possesses some properties that are not generally considered relevant to a 'good' blood compatible material [6, 31]. Table 1 summarizes how LTIC disobeys some empirical 'general rules'. Strictly speaking, these rules are controversial and certainly cannot be applicable to every case. That is why we think that studying this material may result in more insight into the nature of blood compatibility.

It has been generally agreed that the first major event when an implant contacts blood is adsorption of plasma protein [39–44]. The adsorbed protein layer then determines the routes of subsequent processes (Fig. 1) [3]. Blood contacting surfaces indirectly exert their effects through proteinaceous overlayers [38, 45]. How plasma proteins adsorb on a surface is a central issue in addressing the problem of thrombosis [31]. Table 2 documents major studies concerned with protein adsorption on carbon surfaces.

Working hypotheses

Carbon surfaces are thought to be conditioned by adsorbed proteins. The debate is focused on how the proteinaceous film passivates the surface. We consolidate the related hypotheses into two major ones.

The weak interaction hypothesis, suggested by Gott [19], Baier [47], and Nyilas [52, 53], states that the carbon surface is chemically inert and thus does not strongly interact with proteins. Microdomains of carbon may also provide a 'balanced' force to accommodate proteins [51, 59, 60]. The adsorbed proteins preserve their native conformations at the blood-solid interface and the adsorption process should be reversible; adsorbed proteins are exchangeable [61, 62].

Table 1.

LTIC does not fit the conventional 'wisdom' for blood compatible materials.

A blood compatible material is expected to be:	LTIC is:
Hydrophilic [31–33]	Hydrophobic
Soft (low modulus) [31, 32, 34]	Hard (high modulus)
Low surface energy [32, 35, 36]	Relatively high surface energy
Nonconductive [37, 38]	Electrical conductive
Negative resting potential vs NHE [37, 38]	Positive resting potential vs NHE

A good blood compatible material should have

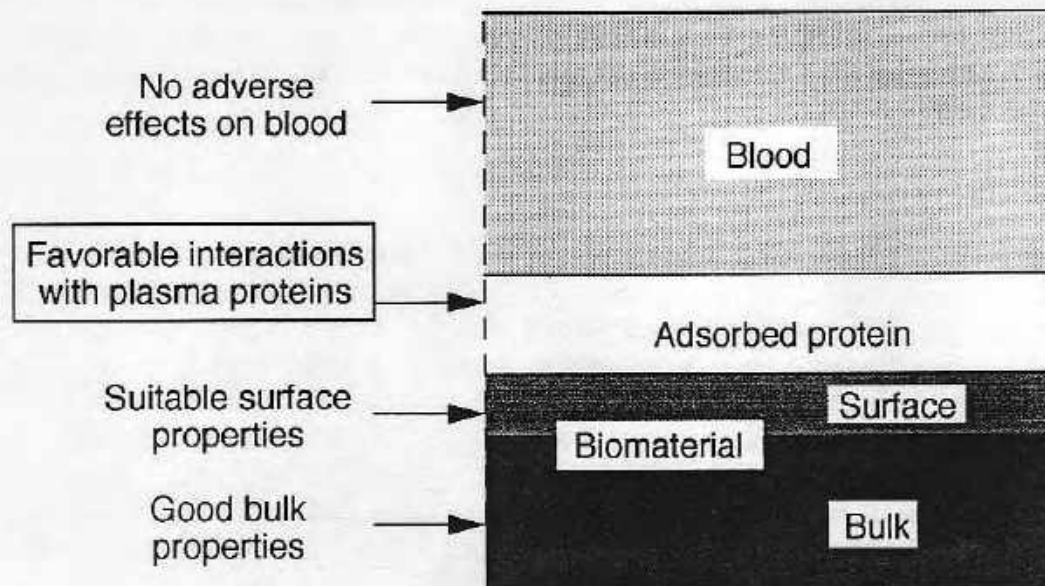


Figure 1. Mediating function of adsorbed plasma proteins and the important role of protein adsorption in blood compatibility of a biomaterial.

The strong interaction hypothesis, proposed by Sevastianov [43], Kaelble [51], Sharma [58], and others [16, 63], suggests that the LTIC surface is coated with a thick film of bland plasma proteins. The proteins are held so tenaciously that they cannot be easily removed. The surface becomes blood compatible through modification by this 'bland' proteinaceous film, most likely albumin [64]. According to this hypothesis, the conformation of the inner layer of adsorbed proteins should be changed to achieve a strong protein-surface interaction. This adsorption process should be irreversible; proteins are not exchangeable.

Techniques

LTIC was first evaluated by four surface analytical instruments: scanning electron microscopy (SEM) for surface morphology, X-ray photoelectron spectroscopy (XPS) for surface compositions, contact angle goniometry for surface hydrophobicity, and scanning tunneling microscopy (STM) for microdomains and atomic structure. Four major experimental methods, along with others, were then employed to study the adsorption process and the state of adsorbed proteins from different aspects. Figure 2 depicts the characteristics and functions of the four techniques: calorimetry, impedance, radioisotopes, and electrophoresis.

Proteins

Two proteins were selected for the study: human serum albumin and human plasma fibrinogen. Albumin is the preponderant protein in blood, its abundance outweighing all the rest of plasma proteins [69]. Adsorption of this protein has a profound influence on the succeeding events [40, 63, 70-74]. Fibrinogen plays a central role in hemostasis [65, 71].

Not only does it participate in the coagulation cascade [65], but it also promotes adhesion of platelets and activates them when adsorbed onto certain solid surfaces [75–77]. The adsorption of some small proteins was also studied to take the advantage of their simple and well known structures. Total human plasma was used when studying competitive protein adsorption from multicomponent solutions or when eluting adsorbed proteins with plasma solutions.

LTIC substrate

Three forms of LTIC substrates were utilized: plates, fragments and powders, with nearly identical bulk structures and compositions. LTIC has a quasi crystalline turbostratic structure [16, 17]. The crystalline structure is disorganized. Within a layer there are many defects: voids, dislocated atoms, and unsaturated bonds, which distort the planeness. There is no order between the layers [78, 79]. Table 3 summarizes some important surface properties of LTIC from the literature. Briefly, LTIC is hydrophobic; it has a relatively high surface energy; its dispersion to polar ratio is large; it contains a large amount of surface oxygen after being polished; and it has great tendency to accept electrons in electrolyte solutions. Carbons are chemically stable.

Table 2.

Major protein adsorption work on biomedical carbons

Author	Experiment	Main conclusions	References
Baier, R. E.	Critical surface tension of LTIC	It drops from 50 to 30 dyn cm ⁻¹ after blood exposure	[47]
Bokros, J. C.	Rest potential of LTIC before and after implantation	It drops from +400 mV to -360 mV. It suggests protein conditioning	[17]
Bruck, S. D.	Effects of electric conductivity	Higher conductivity shows better compatibility	[48]
Caprani, A.	AC impedance	Ions participate in adsorption processes	[49, 50]
Halbert, S. P.	Plasma protein activity	They are not affected by LTIC	[16]
Kaelble, D. H.	Effects of surface energy	High dispersion and low polar nature of LTIC favors retaining proteins	[51]
Nyilas, E.	Microcalorimetry and electrophoresis	Little adsorption heat of proteins on LTIC means little conformational change	[52, 53]
Riccitelli, S. P.	SEM	LTIC tenaciously binds proteins	[54]
Ruckenstein, E.	Balance of polar and dispersion surface free energy	Surface structure of LTIC may be altered under water due to interfacial reconstruction	[55]
Schaldach, M.	Effects of electronic surface before and after implantation	Matching of electronic parameters of LTIC surfaces to that of proteins results in good compatibility	[56, 57]
Sharma, C. P.	Surface energy calculation	LTIC adsorbs most plasma proteins nonselectivity	[58]
Williams, D. F.	Ellipsometry on LTIC	Adsorbed proteins form 200–400 Å films	[18]

EXPERIMENTAL OBSERVATIONS

We carried out two sets of experiments: LTIC surface analysis and protein adsorption [10]. In this section, we discuss our data from XPS and goniometry. The results from SEM and STM and the corresponding discussion can be found elsewhere [10, 11]. We briefly mention the major conclusions of the second set, as the adsorption results have been published [14] or are in press [12, 13, 15]. Refer to [10–15] for details of experiments, results, and discussion.

Surface properties

LTIC is characterized by a micro porous, oxidized, hydrophobic, and domain mosaic structure. Scanning electron microscopy (SEM) shows that LTIC has a very porous

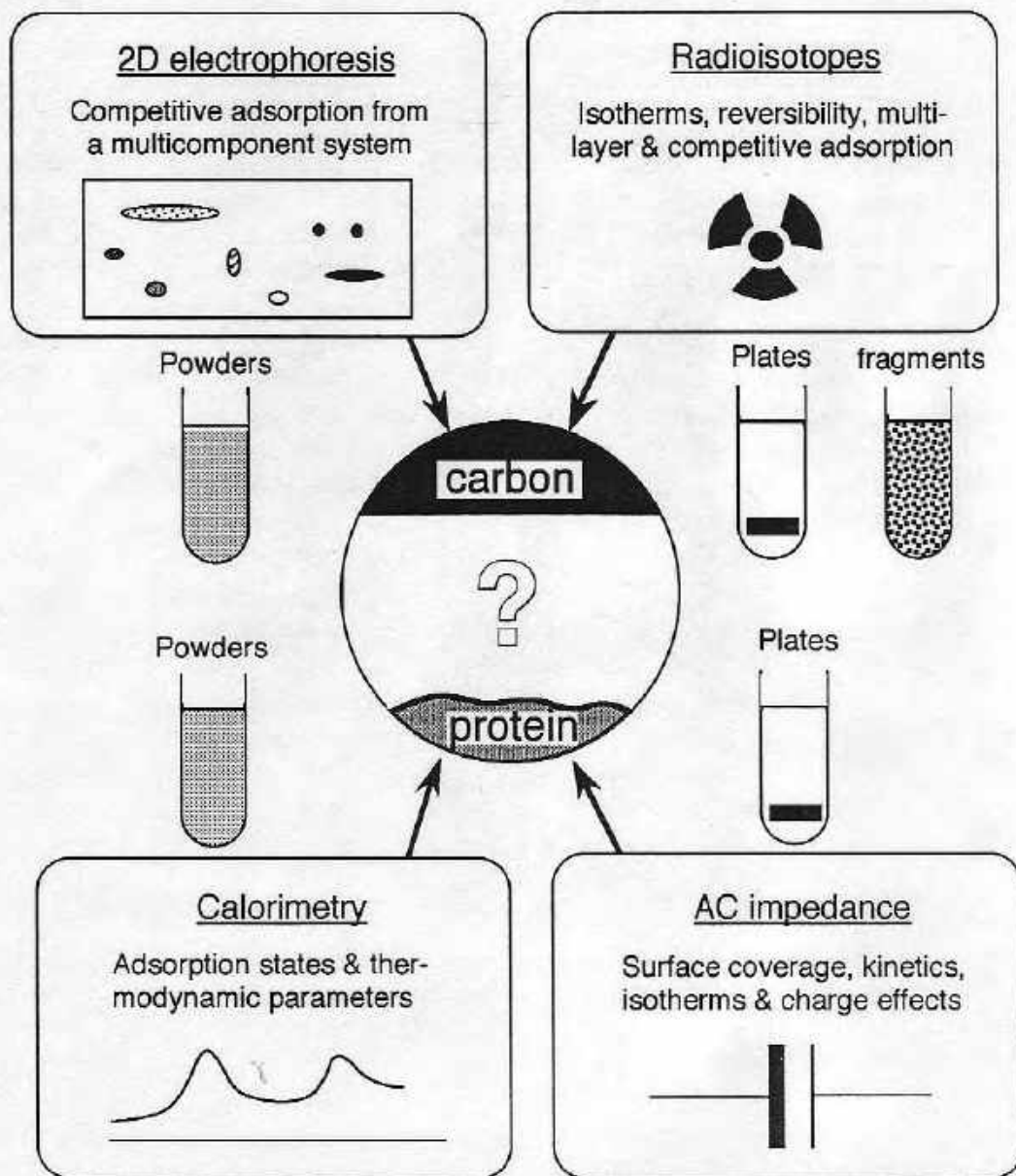


Figure 2. Characteristics and functions of four major techniques applied to protein adsorption.

Table 3.
Surface properties of LTIC

Property	Value	Treatment	Refs.
Contact angles against water	80 deg	Diamond polishing	[47]
Critical surface tension	50 dyn cm ⁻¹	Diamond polishing	[47]
	50 dyn cm ⁻¹	ULTIC	[18]
Hydrophobicity	Hydrophobic	Powders	[78]
Charge density	-1.1 mC cm ⁻²	Powders	[78]
Oxygen content (O/C)	2-3/100	Unpolished plates	[81, 82]
	10/100	Polished plates	[81, 82]
	10/100	Powders	[80]
Oxygen containing groups		Polished	[81, 82]
ether-like	60%		
quinone-like	25%		
ester- or carboxyl-like	15%		
Rest (spontaneous) potential	+400 mV	Polished	[9,16]

surface, consisting of many 'sintered' granules. Their sizes are from 1 to 10 μm with many hollows among them [10]. STM further unveils details of LTIC surfaces [11], which are formed from patched quasi crystalline domains (crystallites) with the sizes of 2-8 nm. Since individual domains are oriented randomly, different domains contribute different surface properties, giving LTIC heterogeneous characteristics. Upon polishing, the surface is converted to a much smoother one and the pores have disappeared, presumably filled by the polished carbon debris. Polishing largely destroys the ordered atomic texture, producing a more random, amorphous and homogeneous surface with smaller domain sizes.

Table 4 lists the elemental composition of LTIC surfaces from the wide and narrow scans of XPS. The oxygen contents for the polished and the powder samples are similar to the values measured by others [78, 82,83]. The oxygen content for the as deposited LTIC plates is about 12%, which is much higher than the 3% reported in the literature [82]. The powders have a slightly higher oxygen content than the fragments from which they were made, probably because they have more edges or defects. Instrumental sensitivity is inadequate to detect the trace amounts of possibly remaining polishing particles, i.e. Al_2O_3 . These impurities, if they are present, should not severely affect our general conclusions because most of the adsorption studies were carried out with unpolished fragments or

Table 4.
Elemental compositions of LTIC surfaces

Sample	Chemical composition (%) ^a				O/C ratio ^b %
	C	O	Si	N	
As deposited plates	86.6	9.6	2.3	1.5	12
0.3 mm alumina polished	90.3	8.2	1.5	0.0	11
Emery paper polished	88.8	9.1	2.1	0.0	12
Fragments	86.1	10.2	3.7	0.0	13
Powders	86.2	10.5	3.4	0.0	15

^aFrom the wide scans

^bFrom the narrow scans

Table 5.
Contact angles of water on LTIC

Polishing suspension	Contact angle (deg)	Standard deviation (deg)	Number of measurements
0.3 μm alumina	58.6	1.4	7
1.0 μm diamond	70.3	1.5	10
600 grit emery paper	61.7	1.5	3

powders except for the impedance measurements (Fig. 2), whose results are consistent with those from the radioisotope [13] studies.

Contact angles on polished LTIC range from 60 (polished by alumina or Emery paper) to 70 deg (polished by diamond) (Table 5), showing a hydrophobic nature. These contact angles are close to the ones in the literature, though a little lower. Contamination is not considered to be a factor for the lower values, because in the Emery paper polishing, what finally ground the carbon surface was the pyrolytin carbon debris on top of the grinding particles.

Denaturation of adsorbed proteins [12]

Surface induced denaturation is a process of protein unfolding in the presence of the surface, implying a strong interaction between them. Usually a hydrophobic surface tends to denature adsorbed proteins due to hydrophobic interactions [37, 85–87]. From its hydrophobic nature we expected that LTIC would denature proteins. Our DSC study shows that LTIC denatures all the proteins studied in a number of buffers of different pH [12].

Adsorption kinetics and amounts [10, 13–15]

We utilized AC impedance to investigate protein adsorption on LTIC electrodes, by measuring the change in double layer capacitance. The parameter 'normalized capacitance change' (NCC) was used as a measure of adsorbed amounts. Adsorption kinetics was analyzed by two terms: $t_{1/2}$ and $t_{80\%}$, the times for NCC to reach half and 80% of the plateau value, respectively. The data in Table 6 shows relatively high rates of protein adsorption on LTIC from moderate solution concentrations compared with those on gold. When protein concentration is above 0.10 mg ml^{-1} , $t_{1/2}$ is achieved within 20 s. When the concentration is above 1.0 mg ml^{-1} , $t_{1/2}$ for albumin is within 10 s and $t_{80\%}$ within 2 min. Albumin

Table 6.
 $t_{1/2}$ and $t_{80\%}$ for some adsorption cases

Electrode	Protein	Conc. (mg ml^{-1})	$t_{1/2}$ (s)	$t_{80\%}$ (min)
LTIC	Albumin	3.0	10	1.7
LTIC	Albumin	1.0	9	2.1
LTIC	Albumin	0.50	12 ± 0	2.6 ± 0.2
LTIC	Albumin	0.10	20	3.0
Gold	Albumin	0.50	29	7
LTIC	Fibrinogen	0.05	22 ± 3	2.0 ± 0.3
Gold	Fibrinogen	0.05	14	2.3
LTIC	Lysozyme	0.50	12 ± 5	2.0 ± 0.6

adsorbs on LTIC faster than on gold but the rate of fibrinogen adsorption is similar on both substrates. The kinetic studies show that the capacitance change at carbon-water interfaces due to protein adsorption is initially linear with the square root of adsorption time and then linear with the natural logarithm of adsorption time. This indicates that the adsorption process is initially diffusion controlled but later involves heterogeneous interactions between the surface and proteins. The AC impedance measurements further imply that the electrostatic interaction is not apparently significant in the interactions between the LTIC surface and the proteins studied. There is a strong indication that the hydrophobic interaction is the dominant force.

Both impedance and radioisotope-labeling techniques produced similar protein adsorption isotherms [13,14]. Isotherms of albumin and fibrinogen on LTIC show that the surface concentrations do not reach the plateaus until high bulk concentrations are used and that the surface concentrations are high at the plateaus for both proteins, indicating that LTIC has a strong tendency to adsorb proteins.

The high affinities of proteins for the LTIC surface can be further revealed by competitive adsorption from protein mixtures [14]. Adsorption of albumin and fibrinogen onto LTIC from diluted plasma solutions is only moderately suppressed despite the competition of other proteins. Competitive adsorption from an albumin/fibrinogen binary system confirms that there is no preferential adsorption of either albumin or fibrinogen on LTIC.

Irreversibility of adsorption [14]

Adsorbed proteins on LTIC can hardly be displaced either by buffer, by protein solution, or even by 2% SDS solution. Overnight displacement of desorbed albumin or fibrinogen from LTIC in these eluents is seldom beyond 5%. Protein exchange experiments also show that even multilayer proteins are not easily displaced. This work clearly demonstrates a very important attribute of the LTIC surface: it tenaciously and irreversibly adsorbs proteins. In fact, no effective way has been found to completely elute adsorbed proteins from LTIC. This coincides with the general observation that protein adsorption is irreversible on some hydrophobic surfaces [3, 43,88], suggesting such strong adsorption is very likely emanating from the hydrophobic interaction.

DISCUSSION

A composite process

We now hypothesize what happens when LTIC is brought into contact with blood? The protein-surface interaction is a composite process composed of about four stages: diffusion, adsorption, denaturation, and modification. Although they take place successively for individual protein molecules, these four stages can overlap with one another for the whole system. They are treated as isolated sequences only for the purpose of clarity. Although a similar process has been proposed for other materials, we utilize it for the specific case of LTIC with discussion of carbon's particular characteristics.

Diffusion. When LTIC first contacts blood, plasma proteins begin to collide with the solid surface. The collision rate is predominately determined by the protein concentration in blood (C) and to a lesser extent by the diffusion coefficient (D). The collision rate of a particular protein at the interface (n) can be estimated by [32]:

Table 7.
Proportional parameters for the 'big twelve' plasma proteins^a

Protein	Concentration (mg ml ⁻¹)	(μ mol)	Diffusion coef. (10 ⁻⁷ cm ² s ⁻¹)	CD ^{1/2} (μ mol cm s ^{1/2})
Albumin	40	600	6.1	0.469
IgG	8-17	100	4.0	0.063
LDL	4.0	2	2.0	0.001
HDL	3	18	4.6	0.012
α -Macroglobulin	2.7	3.3	2.4	0.002
Fibrinogen	2-3	7.5	2	0.003
Transferrin	2.3	30	5.0	0.021
α -antitrypsin	2	40	5.2	0.029
Haptoglobin	2.0	20	4.7	0.014
C3	1.6	9	4.5	0.006
IgA	1-4	15	4	0.009
IgM	0.05-2	1	2.6	0.001

^a Adapted from [69]

$$n = \left(\frac{2}{\pi}\right)^{1/2} \cdot C \cdot D^{1/2}. \quad (1)$$

Table 7 shows the concentrations, diffusion coefficients, and the proportional parameters, $CD^{1/2}$, of the twelve most concentrated plasma proteins (concentrations higher than 1 mg ml⁻¹) [69]. Obviously proteins with the highest abundance and the largest diffusion coefficients will collide with the surface in greatest numbers [89].

Adsorption. The protein molecules that hit the surface are promptly retained by the surface. LTIC does not discriminate or select among the plasma proteins. Thus the composition of adsorbed proteins is similar to that of proteins that collide with the bare surface. Among the initially adsorbed proteins, albumin is the most abundant one (about 70% of the total), plus a small proportion of IgG (Table 7), whereas fibrinogen contributes no more than 4%. The adsorption of proteins of the contact activation system is very low due to their low plasma concentrations. For instance, the concentration in human plasma is 30 μ g ml⁻¹ for Hageman factor, 70 μ g ml⁻¹ for high molecular weight kininogen, and 50 μ g ml⁻¹ for prekallikrein [64]. These only represent 0.04, 0.09, and 0.06% of total plasma proteins, respectively.

Denaturation. The adsorbed proteins are rapidly denatured by the LTIC surface through hydrophobic interactions. Globular plasma proteins are likely flattened on the surface, resulting in a dense and relatively impervious protein film that completely covers the LTIC surface [43]. Little or no bare LTIC surface is exposed to blood after this adsorption process. The proteins that intimately reside on the surface are tenaciously held. The association is so strong that ordinary means of elution cannot remove them. Thus the protecting film is stable and resistant to being displaced.

Modification. Since LTIC is actually covered, protected, and thus modified by the bland proteins (albumin and perhaps the albumin-IgG complex [90]), this protein covered surface becomes blood compatible. The proteinaceous film prevents the surface from

contacting potentially active plasma proteins (e.g., Factor XII) and platelets. The film does not activate them nor does it trigger the coagulation cascade.

There are several hypotheses on how albumin passivates solid surfaces: (a) albumin inhibits surface contact initiation by blocking the surface active sites [91, 92]; (b) albumin complexes surface activated materials, most likely plasma proteins [73, 91]; and (c) the inhibitory effect of albumin on platelet adhesion is due to absence of binding residues [93].

Even though adsorbed albumin in some isolated areas will occasionally detach for some reasons, the spots will be instantaneously replenished and patched by adsorption of circulating albumin so that the entire protecting film remains intact.

Uniqueness of LTIC

The hypothesis of surface conditioning by proteinaceous films is not new [94]. Using albumin to make a surface more blood compatible has been proposed and practiced for many years [40, 63, 74, 95]. In fact all the surfaces that contact blood are conditioned by plasma proteins. What is unique for LTIC and perhaps other carbons is that they possess the following characteristics.

Very stable albuminated overlay. The protein protecting film on LTIC consists of mostly bland proteins, which is the result of its nonselective adsorption and the absence of displacement of adsorbed proteins. This property gives the surface a relatively permanent blood compatibility. Albumin should be the first protein to arrive at surfaces because of its high concentration [96]. The question is if the surface can adsorb and retain the colliding albumin strongly. Even though some materials have been albuminated upon contacting blood, the albumin film may not completely cover the surface; the adsorbed albumin can be gradually displaced by other surface active proteins, or the albumin layer can be proteolytically degraded [74]. These mechanisms may be realized when the surface has a lower affinity to albumin (most surfaces do) than to other proteins, decreasing the effectiveness of the conditioning. In conclusion, the high affinity to all adsorbed proteins including albumin may be the most valuable property for LTIC and perhaps other carbons.

High surface energy and dispersion force. Strong interactions of LTIC with proteins may originate from its relatively high surface energy in addition to its hydrophobicity. Usually, surface free energy can be approximated by the critical surface tension (γ_c) for a solid surface [36]. Contrary to common hydrophobic polymers that have γ_c around 30 dyn cm⁻¹, the γ_c of LTIC is 50 dyn cm⁻¹ [47]. High surface energy can result in a high tendency for adsorption. The hydrophobic interaction may be treated as a 'passive interaction' because its driving force is from the surrounding water; not directly from the attraction of the solid surface [97]. On the other hand, high surface energy might provide a 'positive' component, which can facilitate protein adhesion. Consequently, LTIC may have a greater intrinsic capability of adsorbing and retaining plasma proteins than low surface energy polymers. High surface energy may also help adsorb more proteins. The thicker proteinaceous film may provide stronger protection. Baier has proposed a route to achieve thromboresistance: using materials with high surface energy [35]. Surfaces of high energy may also tend to denature proteins [37]. However, high surface energy alone may not be sufficient to prevent adsorbed protein from desorption. The dominant factor for the irreversibility may still be the hydrophobic interaction.

Modest hydrophobicity. Despite being hydrophobic, LTIC surfaces contain a fairly large amount of oxygen whereas common hydrophobic polymers only have hydrophobic chains, such as polyethylene and Teflon. The presence of surface oxygen produces a less hydrophobic surface for LTIC than that of polyethylene or Teflon. Optimally oxidized surfaces may actually be favored in the interaction with proteins since proteins should not be very hydrophobic because even their hydrophobic residues have polar groups and they are attached via polar peptide bonds. For example, proteins show maximum affinity to surfaces of intermediate polarity [85, 98]. For example, albumin binds more strongly to silicone rubber whose hydrophilicity has been increased [95]. The resistance of adsorbed albumin and IgG to elution by SDS increases with the oxygen content of polystyrene [99]. LTIC still has a heterogeneous surface after polishing but with smaller domains, which can have distinct hydrophobicity if the oxides cluster at the defect areas. The balance of the polar and nonpolar components and the nano separation of hydrophobicity should strengthen the protein-surface interaction by providing proper sites for different peptide segments. Hence, the surface heterogeneity of LTIC is also important. Its function is not necessarily in preserving the native conformation of adsorbed proteins but rather in enhancing the adhesion between the surface and the adsorbed denatured proteins.

Low dynamic movement. Almost all organic polymers have dynamic surfaces at room temperature. Their surface composition and structures are constantly changing to accommodate variations in the environment [100]. Such a dynamic process may weaken the association of the surface and the adsorbed protein. Sevastianov has indicated that high chain mobility induces a considerable decrease of surface blood compatibility by provoking formation of structured ion layers at the interface [43]. Chain motion in LTIC is severely restricted by the two dimensional network. Subsequently, rigid LTIC acts as a solid ground for proteins to anchor, fortifying their association with the surface.

The π - π electron interaction. Molecules can associate with each other by forming π - σ or π - π complexes, often called charge-transfer or electron donor-acceptor interactions [101]. Porath and Larsson observed that aromatic amino acids (tryptophan, tyrosine, and phenylalanine) strongly interacted with Sephadex gel coupled to aromatic groups [101, 102]. Jennissen and Demirel found that proteins had much stronger interactions with alkyl agaroses when the alkyl chain contained a sulfur atom, which has non-bonding lone electron pairs [103, 104]. They suggested that charge-transfer interactions play a unique and important role in those cases. Composed of fused imperfect aromatic rings, LTIC should be able to interact with aromatic amino acid residues of adsorbed proteins via such charge-transfer interactions. Different oxidation may produce different surface regions with different interactions, the quinone-like group can be an electron acceptor and the phenol-like one should behave as an electron donor [102]. The charge-transfer interaction cannot only partially explain why LTIC tenaciously adsorbs proteins, it also produces a hypothesis as to why LTIC strongly denatures proteins: strong interactions with aromatic groups that are often buried inside the protein help produce protein unfolding (denaturation). The hydrophobic interaction between LTIC and proteins may be partly due to this charge-transfer interaction [101].

Test results of the hypotheses

Results from the summarized research enable us to test the two hypotheses put forward in the beginning of this paper. Almost every bit of information collected indicates that there

is a very strong interaction between the LTIC surface and the adsorbed protein. Thus the second hypothesis (strong interaction) is considered more realistic and merits further investigation.

Establishment of protein passivation may also explain some of the apparently controversial behavior of LTIC, tabulated in Table 1: (1) the hydrophobic surface becomes relatively hydrophilic because the adsorbed proteins orient their hydrophobic moieties towards the solid surface and the hydrophilic ones to the aqueous environment; (2) the original high surface energy is screened; (3) the process of transferring electrons can be suppressed by blocking electron transfer pathways; and (4) the net charge of LTIC can also be masked by the proteinaceous layer.

In summary, since LTIC is covered by plasma proteins, its surface properties are the result of this proteinaceous film. The function of the carbon substrate is to dictate the composition, structure, and stability of the proteinaceous layer.

Acknowledgements

We thank Sorin Biomedica for providing LTIC samples. We acknowledge Dr. C. Bruckner-Lea, Mr. C-H. Ho, Dr. J-S. Li, Dr. I-N. Chang, and Mr. P. Dryden for help with instrumentation. We also appreciate very useful discussions with Drs. V. Hlady, J. McIntyre, K. Caldwell, and C-Z. Hu. This work was supported by the Center for Biopolymers at Interfaces, University of Utah, USA.

REFERENCES

1. K. C. Dellsperger and K. B. Chandran, in: *Blood Compatible Materials and Devices*, p. 153, C. P. Sharma *et al.* (Eds). Technomic, Lancaster, PA (1991).
2. D. F. Williams, *Blood Compatibility*, Vol. 1. CRC Press, Boca Raton, FL (1987).
3. J. L. Brash, in: *Blood Compatible Materials and Devices*, p. 3, C. P. Sharma *et al.* (Eds). Technomic, Lancaster, PA (1991).
4. E. F. Leonard, V. T. Turitto and L. Vroman, *Ann. NY Acad. Sci.* **516** (1987).
5. L. Vroman and E. F. Leonard, *Ann. NY Acad. Sci.* **283** (1977).
6. J. P. Cazenave, J. A. Davies, M. D. Kazatchkine and W. G. van Aken, *Blood-Surface Interactions*. Elsevier, Amsterdam (1986).
7. M. A. Gimbrone, *Ann. NY Acad. Sci.* **516**, 5 (1987).
8. B. D. Ratner, A. B. Johnston and T. J. Lenk, *J. Biomed. Mater. Res.* **21** (suppl. A1), 59 (1987).
9. T. H. Spaet, *Ann. NY Acad. Sci.* **516**, 1 (1987).
10. L. Feng, PhD Dissertation, University of Utah (1993).
11. L. Feng and J. D. Andrade, *J. Biomed. Mater. Res.* **27**, 177 (1993).
12. L. Feng and J. D. Andrade, *J. Biomed. Mater. Res.* in press (1995).
13. L. Feng and J. D. Andrade, *J. Colloid Interface Sci.* **166**, 419 (1994).
14. L. Feng and J. D. Andrade, *Biomaterials* **15**, 323 (1994).
15. L. Feng and J. D. Andrade, *Colloids Surfaces*, in press (1995).
16. J. C. Bokros, L. D. LaGrange and J. Schoen, *Chemistry and Physics of Carbon* **9**, 103 (1972).
17. J. C. Bokros, *Carbon*, **15**, 355 (1977).
18. A. D. Haubold, H. S. Shim and J. C. Bokros, in: *Biocompatibility of Clinical Implant Materials*, Vol. 2, p. 3, D. F. Williams (Ed.). CRC Press, Boca Raton, FL (1981).
19. V. L. Gott and A. Furuse, *Med. Instrum.* **7**, 121 (1973).
20. D. F. Williams, in: *Blood Compatibility*, Vol. 2, p. 107, D. F. Williams (Ed.). CRC Press, Boca Raton, FL (1987).
21. A. D. Haubold, R. A. Yapp and J. C. Bokros, in: *Encyclopedia of Materials Science and Engineering*, Vol. 1, p. 514, M. B. Bever (Ed.). Pergamon Press, Oxford, UK (1986).
22. P. Aebischer, M. B. Goddard, H. F. Sassen, T. J. Hunter and P. M. Galletti, *Biomaterials* **9**, 80 (1988).
23. P. Arru, M. Santi, F. Vallana, G. Majni, G. Ottaviani and A. Paccagnella, in: *High Tech Ceramics*, p. 117, P. Vincenzini (Ed.). Elsevier, Amsterdam (1987).

24. A. C. Evans, J. Franks and P. J. Revell, *Surf. Coatings Technol.* **47**, 662 (1991).
25. L. A. Thomson, F. C. Law, N. Rushton and J. Franks, *Biomaterials* **12**, 37 (1991).
26. E. L. Olcott, *J. Biomed. Mater. Res. Symp.* **5**, 209 (1974).
27. E. Chignier, J. R. Monties, B. Butazzoni, G. Dureau and R. Eloy, *Biomaterials* **8**, 18 (1987).
28. C. Baquey, L. Bordenave, N. More, J. Caix and B. Basse-Cathalinat, *Biomaterials* **10**, 435 (1987).
29. J. Bejui and G. Drouin, *CRC Crit. Rev. Biocompatibility* **4**, 79 (1988).
30. L. Claes, L. Durselen, H. Kiefer and W. Mohr, *J. Biomed. Mater. Res.* **21** (suppl. A3), 319 (1987).
31. E. W. Merrill, *Ann. NY Acad. Sci.* **516**, 196 (1987).
32. J. D. Andrade and V. Hlady, *Adv. Polym. Sci.* **79**, 3 (1986).
33. J. D. Andrade, *Med. Instrum.* **7**, 110 (1973).
34. Y. Ikada, *J. Biomed. Mater. Res.* **15**, 697 (1981).
35. R. E. Baier, *Bull. NY Acad. Med.* **48**, 257 (1972).
36. D. J. Lyman, W. M. Muir and I. J. Lee, *Trans. Am. Soc. Artif. Int. Organs* **11**, 301 (1965).
37. B. Ivarsson and I. Ljunstrom, *CRC Crit. Rev. Biocompatibility* **2**, 1 (1986).
38. N. Ramasamy, T. R. Lucas, B. Stanczewski and P. N. Sawyer, in: *Topics in Bioelectrochemistry and Bioenergetics*, Vol. 3, p. 243, G. Milazzo (Ed.), Wiley, Chichester, UK (1980).
39. R. E. Blaier and R. C. Dutton, *J. Biomed. Mater. Res.* **3**, 191 (1969).
40. D. J. Lyman, K. Knutson, B. McNeill and K. Shibatani, *Trans. Am. Soc. Artif. Intern. Organs* **21**, 49 (1975).
41. L. Vroman, A. L. Adams, M. Klings, G. C. Fisher, P. C. Munoz and R. P. Solensky, *Ann. NY Acad. Sci.* **283**, 65 (1977).
42. A. S. Hoffman, *Ann. NY Acad. Sci.* **516**, 96 (1987).
43. V. I. Sevastianov, *CRC Crit. Rev. Biocompatibility* **4**, 109 (1988).
44. T. A. Horbett and J. L. Brash, in: *Proteins at Interfaces*, p. 1, J. L. Brash and T. A. Horbett (Eds.), ACS Symp. 343, ACS, Washington, DC (1987).
45. D. Shasby, in: *Endothelial Cell*, Vol. 1, p. 39, CRC Press, Boca Raton, FL (1988). U.S. Ryan, ed.
46. J. D. Andrade (Ed.), *Surface and Interfacial Aspects of Biomedical Polymers*, Vol. 2: *Protein Adsorption*, p. 1, Plenum, New York (1985).
47. R. E. Baier, V. L. Gott and A. Feruse, *Trans. Am. Soc. Artif. Int. Organs* **16**, 50 (1970).
48. S. D. Bruck, *Polymer* **16**, 25 (1977).
49. P. Bernebeu and A. Caprani, *Biomaterials* **11**, 258 (1990).
50. A. Caprani and F. Lacour, *Bioelectrochem. Bioenerg.* **26**, 241 (1991).
51. D. H. Kaelble and J. Moacanin, *Polymer* **18**, 475 (1977).
52. T-H. Chiu, E. Nyilas and L. R. Turuse, *Trans. Am. Soc. Artif. Int. Organs* **24**, 389 (1978).
53. T-H. Chiu, E. Nyilas and D. M. Lederman, *Trans. Am. Soc. Artif. Int. Organs* **22**, 498 (1976).
54. S. D. Riccitelli, F. H. Bilge and R. C. Eberhart, *Trans. Am. Soc. Artif. Intern. Organs* **30**, 420 (1984).
55. E. Ruckenstein and S. V. Gourisankar, *J. Colloid Interface Sci.* **101**, 436 (1984).
56. A. Bolz and M. Schaldach, *Artif. Organs* **14**, 260 (1990).
57. P. Baurischmidt and M. Schaldach, *J. Bioeng.* **1**, 261 (1977).
58. C. P. Sharma, *J. Colloid Interface Sci.* **97**, 615 (1984).
59. J. D. Andrade, S. Nagaoka, S. Cooper, T. Okano and S. W. Kim, *ASAIO Trans.* **34**, 75 (1987).
60. C. Nojiri, T. Okano, N. Takemura, H. Koyanagi and T. Akutsu, in: *Abstract of 4th World Biomaterials Congress*, p. 449, Berlin (1992). The Biomaterials Society.
61. E. W. Salzman, J. Lindon, D. Brier and E. W. Merrill, *Ann. NY Acad. Sci.* **283**, 114 (1977).
62. I. Lundstrom and H. Elwing, *J. Colloid Interface Sci.* **136**, 68 (1990).
63. S. W. Kim, S. Wisniewski, E. S. Lee and M. L. Winn, *J. Biomed. Mater. Res.* **11**, 23 (1977).
64. H. Y. K. Chuang, in: *Blood Compatibility*, Vol. 1, p. 88, D. F. Williams (Ed.), CRC Press, Boca Raton, FL (1987).
65. D. F. Williams (Ed.), in: *Blood Compatibility*, Vol. 1, p. 5, CRC Press, Boca Raton, FL (1987).
66. K. S. W. Sing, in: *Characterization of Powder Surfaces*, p. 25, G. D. Parfitt and K. S. W. Sing (Eds.), Academic Press, London (1976).
67. M. Silverberg and A. P. Kaplan, in: *Inflammation Research*, Vol. 2, p. 165, G. Weissmann (Ed.), Raven Press, New York (1981).
68. F. Kozin, B. Millstein, G. Mandel and N. Mandel, *J. Colloid Interface Sci.* **88**, 326 (1982).
69. J. D. Andrade and V. Hlady, *Ann. NY Acad. Sci.* **516**, 158 (1987).
70. R. G. Lee and S. W. Kim, *J. Biomed. Mater. Res.* **8**, 393 (1974).
71. R. Sipehia and A. S. Chawla, *Biomater. Org.* **10**, 229 (1982).

72. R. C. Eberhart, *Ann. NY Acad. Sci.* **516**, 78 (1987).
73. H. Sato, T. Tomiyama, H. Morimoto and A. Nakajima, in: *Proteins at Interfaces*, p. 77, J. L. Brash and T. A. Horbett (Eds). ACS Symp. 343, ACS, Washington, DC (1987).
74. J. R. Keogh, F. F. Velander and J. W. Eaton, *J. Biomed. Mater. Res.* **26**, 471 (1992).
75. M. A. Packham, G. Evans, M. F. Glynn and J. F. Mustard, *J. Lab. Clin. Med.* **73**, 686 (1969).
76. E. Nyilas and T.-H. Chiu, *Artif. Organs* **2** (Suppl.), 56 (1978).
77. S. M. Slack and T. A. Horbett, *J. Biomater. Sci. Polym. Edn.* **2**, 227 (1991).
78. T.-H. Chiu, E. Nyilas and F. J. Micale, in: *Extended Abstract, 13th Biennial Conference on Carbon*, p. 9, Irvine, CA (1977).
79. J. L. Kaae, *Carbon* **23**, 665 (1985).
80. R. H. Dauskardt and R. O. Ritchie, in: *Abstract of 4th World Biomaterials Congress*, p. 478, Berlin (1992). The Biomaterials Society.
81. F. J. Schoen, in: *Biocompatible Polymers, Metals, and Composites*, p. 239, M. Szycher (Ed.). Technomic, Lancaster, PA (1983).
82. R. N. King, J. D. Andrade, A. D. Haubold, and H. S. Shim, in: *Photon, Electron, Ion Probes of Polymer Structure and Properties*, p. 382, D. W. Dwight et al. (Eds). ACS Symp. 162, Washington, DC (1981).
83. K. L. Smith and K. M. Black, *J. Vac. Sci. Technol.* **A2**, 744 (1984).
84. H. P. Boehm, in: *Structure and Reactivity of Surfaces*, p. 144, C. Morterra, A. Zecchina and G. Costa (Eds). Elsevier, Amsterdam (1989).
85. W. Norde, *Adv. Colloid Interface Sci.* **25**, 267 (1986).
86. A. L. Iordanski, A. J. A. Polischuk and G. E. Zaikov, *Rev. Macromol. Chem. Phys.* **C23**, 33 (1983).
87. D. R. Lu and K. Park, *J. Colloid Interface Sci.* **144**, 271 (1986).
88. B. W. Morrissey, *Ann. NY Acad. Sci.* **283**, 50 (1977).
89. H. Shirahama, J. Lyklema and W. Norde, *J. Colloids Interface Sci.* **139**, 177 (1990).
90. S. F. Mohammad and D. B. Olsen, *ASAIO Trans.* **35**, 384 (1989).
91. R. C. Eberhart, M. Munro, J. R. Frautschi, M. Lubin, F. J. Clubb and V. I. Sevastianov, *Ann. NY Acad. Sci.* **516**, 78 (1987).
92. E. A. Kulik, I. D. Kalinin and V. I. Sevastianov, *Art. Organs* **15**, 386 (1991).
93. C. D. Forbes, J. M. Courtney, G. D. O. Lowe and M. Travers, in: *Blood Flow in Artificial Organs and Cardiovascular Prostheses*, p. 89, J. C. Barbenel et al. (Eds). Clarendon Press, Oxford, UK (1989).
94. J. D. Andrade, D. L. Coleman, S. W. Kim and D. J. Lentz, in: *Artificial Liver Support*, p. 84, R. Williams and I. M. Murry-Lyon (Eds). Pitman Medical, London (1975).
95. C.-C. Tsai, J. R. Frautschi and R. C. Eberhart, *ASAIO Trans.* **34**, 559 (1988).
96. J. L. Brash, in: *Modern Aspects of Protein Adsorption on Biomaterials*, p. 39, Y. F. Missirlis and W. Lemm (Eds). Kluwer, Dordrecht, Netherlands (1991).
97. J. N. Isrealachvili, *Intermolecular and Surface Forces*, p. 102 and 207, Academic Press, London (1985).
98. W. Norde and J. Lyklema, *J. Biomater. Sci. Polym. Edn* **2**, 183 (1990).
99. S. I. Ertel, B. D. Ratner and T. A. Horbett, *J. Colloid Interface Sci.* **147**, 433 (1991).
100. K. G. Tingey, J. D. Andrade, C. W. McGary and R. J. Zdrahala, in: *Polymer Surface Dynamics*, p. 153, J. D. Andrade (Eds). Plenum Press, New York (1988).
101. J. Porath, *J. Chromatogr.* **159**, 13 (1978).
102. J. Porath and B. Larsson, *J. Chromatogr.* **155**, 47 (1978).
103. H. P. Jennissen and A. Demirelou, *J. Chromatogr.* **597**, 93 (1992).
104. A. Demirelou and H. P. Jennissen, *J. Chromatogr.* **521**, 1 (1990).

Structure and Adsorption Properties of Fibrinogen

Li Feng and Joseph D. Andrade

Department of Bioengineering, University of Utah,
Salt Lake City, UT 84112

This paper correlates molecular structure of fibrinogen to its adsorption properties at the solid-water interface. These properties play an integral role in helping fibrinogen fulfill its biological functions. We first introduce some unique surface (interfacial) attributes of fibrinogen by comparing it to other plasma proteins. We consider its concentration on solid surfaces, effects of solid substrates, adsorption kinetics and isotherms, competitive adsorption, structural adaptivity, and platelet-binding ability. We then examine its structural organization by utilizing available data from the primary structure, immunochemical properties, structural stability, solubility, microscopic images, X-ray diffraction data, and information on proteolytic fragments. By analyzing the amino acid sequences, we estimate the flexibility and hydropathy along individual polypeptide chains. We inspect the net charge and hydrophobicity of individual structural domains. We pay special attention to the less addressed A α chain, especially to its contribution to fibrinogen adsorptivity. While discussing its characteristics, we try to correlate the structure of fibrinogen to its properties.

Fibrinogen plays an indispensable role in hemostasis of vertebrate animals: blood coagulation (conversion of fibrinogen to fibrin through proteolysis of thrombin and polymerization of fibrin monomers into fibrin clots) and platelet aggregation (binding to platelets and linking them together or immobilizing them on a surface) (1-4). These two processes usually happen simultaneously, resulting in a platelet-fibrin plug (hemostatic thrombus) (5).

Besides interacting with solution proteins (thrombin, plasmin), fibrinogen has other interfacial interactions: binding to cells (platelets, endothelium (6) and leukocyte (7)) and associating with non-biological surfaces. Because of its cell adhering propensity, fibrinogen is categorized as a cell adhesive protein, together with fibronectin, vitronectin, and von Willebrand Factor (vWF) (6,8-10), all containing the Arg-Gly-Asp (RGD) sequence (11-13). Fibrinogen is a "sticky" protein, having a strong tendency to adsorb onto various surfaces. These properties earn fibrinogen the reputation of causing thrombogenesis on biomaterials.

The origin of the surface activity of fibrinogen has not been thoroughly studied. Since it is important for our understanding of blood compatibility, we wish to explore these areas: How is the surface activity of fibrinogen related to its molecular structure? How does its structure help its platelet binding function? Is fibrinogen unique or is it similar to other surface active proteins?

Recently a large volume of data concerning structure and properties of proteins have become available. We can address the molecular structure of fibrinogen and its relation to the adsorption properties although we still lack the details of its secondary and tertiary structures. In this paper we focus on its interactions with solid surfaces, antibodies and platelets and correlate its primary and domain structures to its adsorptivity at the solid-water interface and to platelet binding induced by surface adsorption. Our analysis of amino acid sequences is based on human fibrinogen.

Adsorption Properties

Although most proteins are amphipathic and surface active, the degree of their surface activity is different. Fibrinogen shows high surface activity at solid-water interfaces, manifested from its high surface concentration, high adsorption competitiveness, and persistence on most surfaces. Strong association with a solid surface seems to be a property of many of the proteins participating in blood coagulation, including Hageman factor, high molecular weight kininogen (HMWK), and plasma prekallikrein (14).

High Surface Concentration. More fibrinogen is usually adsorbed than most other proteins (15-21). Part of this is likely due to its high molecular weight. However, as will be discussed later, other contributing factors include its strong lateral interactions, producing close packing of adsorbed fibrinogen films and its surface activity, resulting in multilayer adsorption (17,22,23,24).

Low Substrate Influence. The adsorption of fibrinogen is less affected by surface nature of materials (21,25-28). Like most proteins, fibrinogen is usually adsorbed more on hydrophobic surfaces (27), but the difference is smaller than in the case of most other proteins. An increase in hydrophilicity of a surface may not substantially reduce fibrinogen adsorption (29). For example, fibrinogen can adsorb on hydrophilic as well as on hydrophobic surfaces in similar amounts (21,30). It adsorbs more on sulfonated polyurethane, which is more hydrophilic than polyurethane (16,31). Fibrinogen can bind to heparin, a negative but hydrophilic substance, as do fibronectin, vitronectin, and vWF (32). It can also adhere to some protein "repelling" surfaces (29,31,33,34).

Transient Adsorption Kinetics. The adsorption kinetics of fibrinogen from dilute plasma onto some hydrophilic surfaces often shows a maximum at some point, followed by decreasing surface concentration with time. Called the Vroman effect (20,27,35), this phenomenon is believed to reflect a process where the adsorbed fibrinogen is gradually displaced by other even more surface active proteins on these surfaces, such as HMWK, Hageman factor, or high density lipoprotein (36,37).

Maximum in Isotherms. When adsorbed from dilute plasma, the isotherm of fibrinogen sometimes has a maximum (20,35). The plasma concentration at which the maximum occurs seems to be higher on more hydrophobic surfaces (36). This pattern is also considered to be related to displacement of fibrinogen.

Competitive Adsorptivity. Perhaps the best way to describe the high surface activity of fibrinogen is to compare the ratio of its surface concentration to solution concentration to those of other proteins in a multi-protein adsorption process (38-42). Some proteins, such as albumin, can show considerable adsorption from single protein solutions, but its surface concentration may be drastically reduced in the presence of other proteins, even trace proteins (17,40). Albumin has a low affinity for many surfaces and is easily displaced by many plasma proteins, including fibrinogen (9,43-45). Acid glycoprotein is another representative protein with low surface activity (46). On the other hand, the adsorption of fibrinogen is much less affected by the presence of other proteins (17). Fibrinogen often displaces other already adsorbed proteins (45).

Structurally Labile Protein. Some parts of fibrinogen are rather compliant, as deduced from ease in surface induced denaturation (27,39,47,48) and low thermal denaturation temperature (49,50). Conformational change is more easily revealed by means of proteolysis or antigen-antibody bonding. After local cleavage by an enzyme or bonding to an antibody, fibrinogen often undergoes a global conformational change, expressing many neo-binding sites.

Platelet Binding. Fibrinogen is very active in binding to platelets or other cells. The binding not only immobilizes platelets onto a surface or brings them together to form a gel network, it can also activate the bound cells (51,52).

Structural Characteristics And Their Consequences

A Massive Molecule with Many Molecular Domains. Figure 1 presents a molecular model of human fibrinogen, adapted from several sources and based on electron microscopic images (53-56), X-ray diffraction analyses of modified fibrinogens (55,57), and calorimetric measurements (49). A dimer of molecular weight (Mw) of 340,000 daltons, fibrinogen consists of three pairs of non-identical polypeptide chains and two pairs of oligosaccharides. The Mw of the A α chain is 66,066 (610 residues), B β chain 52,779 (461 residues), γ chain 46,406 (411 residues) (4), and each oligosaccharide 2,404 (58). The negatively charged and hydrophilic carbohydrate moiety may contribute a repulsive force between fibrinogen or fibrin molecules, enhancing the solubility of fibrinogen and structurally setting fibrin to assemble into a normal clot (58,59). They do not have a large contribution to fibrinogen clottability (60). There are no x-ray diffraction data on the secondary and tertiary structures of fibrinogen. Measurements by CD, Raman spectroscopy, and FTIR indicate that the native molecule contains about 35% α -helix, 10-30% β -sheet, and 14% β -turn (61,62).

The structurally distinguishable regions of fibrinogen are: a lone central E domain, two distal D domains, two α helical coiled coils, two α C domains, and a pair of junctions between them. The E domain contains all the N terminal ends of the six polypeptide chains linked by disulfide bonds. The D domain consists of the C terminal ends of the B β and the γ chains, and a small portion of the A α chain. The coiled coil, made of three α -helices, connects the D domain to the E domain. It is interrupted in the middle by a small non-helical, plasmin sensitive region (2,63). In the context of this paper, the α C domain contains only the C terminal third of the A α chain (391-610). Although the middle third of the A α domain (200-390) has no definite domainal structure (63-66), we call it the α M domain (M for middle). The masses are 32,600 for the E domain, 67,200 for the D domain, 42,300 for the 2/3 α C chain (the α C and α M domains), and 39,100 for the coiled coil (1).

Figure 2 shows the occurrence of the three chains in the different domains and sub-domains for a half molecule (65,67), and the sites of carbohydrate attachment (2). This figure helps us deduce domain properties from analysis of the polypeptide chains. There are four proteolytically splittable sub-domains in the D domain, two of which are formed by the B β chain and two by the γ chain (50,57,61). Here the defined E or C domains are molecular domains, not equivalent to fragment E (Mw 45,000) or D (Mw 100,000), degradation products from plasmin digestion (62). Fibrinogen is susceptible to plasmin cleavage, producing different sized fragments depending upon the digestion conditions (50,68,69). The plasmin cleavage sites along individual chains have been illustrated (70).

Structure and Properties of Individual Chains and Domains. Assuming that the adsorption properties of fibrinogen are largely determined by its somewhat independently acting domains, we utilize a domain approach to facilitate our analysis of this complex protein (71).

Net charge. Figure 3 shows the net charges of individual domains at pH 7.4. The data are calculated according to the amino acid composition of each domain and the charge of the carbohydrate (72). The values shown are an approximation because of the uncertainty of the charge of His and of the exact positions of charged residues (71). The result of pH titration of fibrinogen gives a net charge of -7 at the pH 7 (22), which is close to our calculated value: -10. Figure 3 assumes that the charge of Glu and Asp is -1, Lys and Arg +1, His +0.33 (one out of three His residues bears a unit positive charge).

The E and D domains are negative while the α C domain is positive. The D sub-domains have different net charges (Figure 3). In cases where electrostatic interactions play a major role, fibrinogen may orient its appropriate domains to interact with the surface. For example, the D (or less probably E) domains may be favored to adsorb on positively charged surfaces. Likewise the positively charged α C domain may be more favorably attracted to negative surfaces. Even though the global fibrinogen molecule has a net negative charge (-10), a negative surface may adsorb via the α C domains. HMWK and Hageman factor can effectively displace adsorbed fibrinogen from negatively charged glass (73), perhaps because both have domains with much higher positive charge density. Figure 4 clearly shows the high density positively charged region along the peptide chains of HMWK and Hageman factor, compared with the A α chain of fibrinogen. Low molecular weight kininogen does not have such a sequence and does not displace fibrinogen. Considering its size, fibrinogen has a low charge density.

Structural stability. Figure 5 shows the thermal denaturation temperatures of fibrinogen at pH 8.5 (49). The E domain and coiled coils are relatively thermostable whereas the D and α C domains are thermolabile, suggesting that the D and α C domains have lower structural stability (74). They are thus "soft" domains, readily changing their conformations (75,76). Such softness may provide the domains with high adaptivity to maximize their contact area with a surface during adsorption (41). Calculated according to Ragone scale (77), Figure 6 shows that the α C domain is flexible, especially in the α M domain. The disappearance of the α C domain under electron microscopy may be due to its structural collapse in the presence of substrate. Structural adaptivity of proteins is an important parameter contributing to the adsorptivity. The D and α C domains should be more surface active than the other domains (74,78).

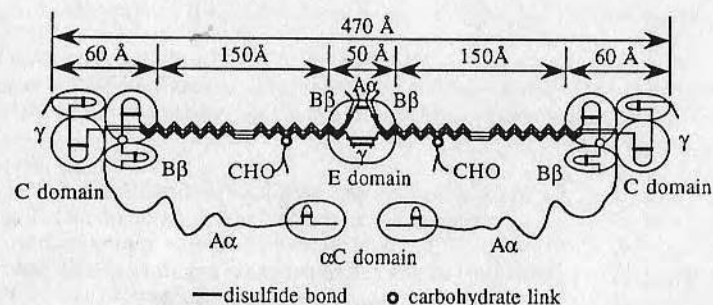


Figure 1. Molecular model of fibrinogen and its individual domains. (Fibrinogen actually exists in an antiparallel arrangement. The shown parallel structure is just for convenience).

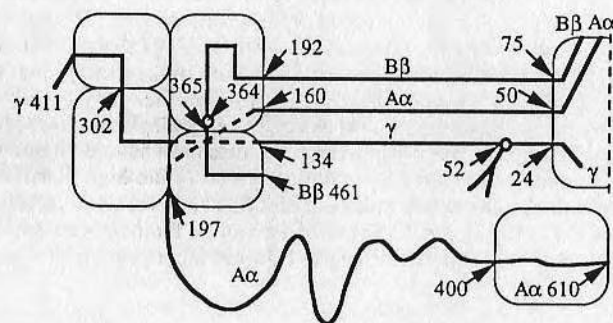


Figure 2. Polypeptide segments in individual domains of human fibrinogen.

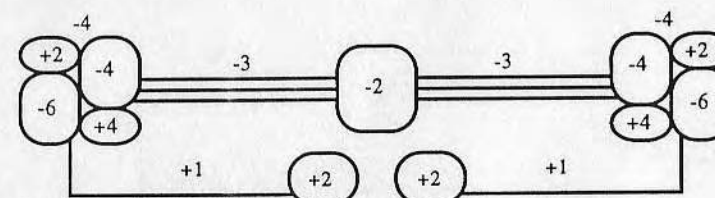


Figure 3. Net charges on individual domains and sub-domains.

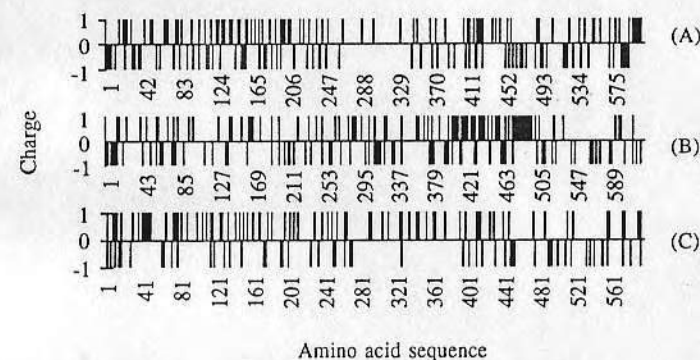


Figure 4. Charge distributions along three polypeptides of human fibrinogen Aα chain (A), human HMWK(B), and human Hageman factor (C). The charge of His is shown as +1. HMWK and Hageman factor have very dense positive charge between 400 to 510 and 290 to 400, respectively.

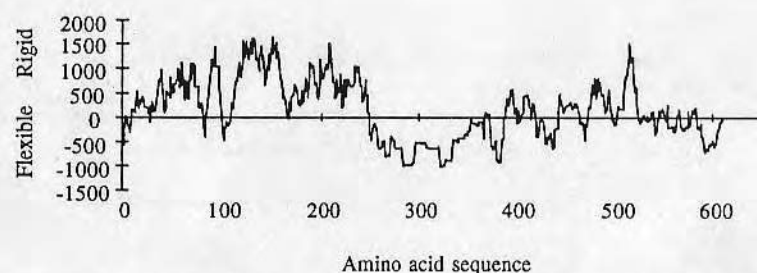


Figure 5. Thermal denaturation temperatures of fibrinogen after Privalov (49).

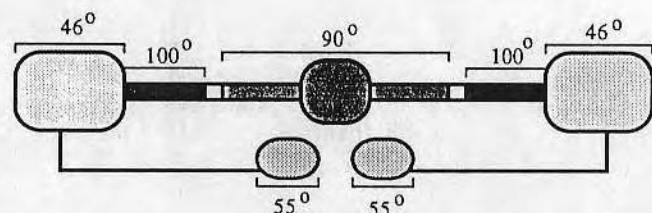


Figure 6. Flexibility of human fibrinogen A α chain, computed using Ragone(77) scale.

Hydrophobicity. Figure 7 plots the hydrophathy of the 3 polypeptide chains according to the Ponnuswamy scale (79). The hydrophobicity order is γ chain > B β chain > A α chain. The E and D domains apparently have comparable hydrophobicity, the α C domain is slightly more hydrophilic, and the α M domain has the highest hydrophilicity. The hydrophobic region of the α C domain may provide interactions between the α C domains or with the E domain (64). The hydrophobic, soft D domain should be preferentially adsorbed onto hydrophobic surfaces via hydrophobic interactions.

Immunogenicity and Surface Topography. Fibrinogen can bind to a large number of antibodies (5). It is estimated that a single fibrinogen molecule can accommodate about 35 antibodies simultaneously (80). It has two kinds of epitopes: exposed ones on the native protein and latent ones that do not bind to their antibodies unless the native molecule is conformationally changed (5,51). The A α chain is the most surface exposed and readily cleaved by a wide variety of proteases (52,65,70,81-83). The γ chain is the least exposed (65,84), hidden in the E and D domains, and in the coiled coil (85). The accessibility of the three chains in native fibrinogen can be produced by analyzing their binding activity to a variety of antibodies (5,52,81,84,85). The exposures of domains can be ranked as highest for the α M domain, followed by the α C domain, then the D domain, with the E domain last. The coiled coil native fibrinogen is inactive in binding to antibodies. Once fibrinogen is perturbed this region seems to express more neo-epitopes than any other domain whereas the α M domain has probably the fewest changes.

Immunochemical analysis is a sensitive tool to interrogate allosteric effects among the domains. Delicately balanced in structure, the global fibrinogen molecule has an amazing ability to respond to very local structural alterations. For example, when fibrinogen is converted to fibrin, some latent epitopes of the γ chain in the C domain become expressed. That suggests that information on conformational changes induced at the N termini of A α and B α chains in the E domain is transmitted to the γ chain in the C domain (82). Reversibly, removal of the C terminal end of the A α chain in the α C domain will conformationally rearrange the central domain (86). These phenomena suggest that there is good communication among the domains (65,81). They function cooperatively, and are not totally independent in action (49). The coiled coil is likely a conduit for the transmission of allosteric changes from one domain to another (65).

Platelet Binding Sites. Native fibrinogen can bind to stimulated platelets (8). Conformationally perturbed fibrinogen can also bind to unstimulated platelets and activates the bound platelets, causing them to aggregate and secrete (51,52,87). Fibrinogen possesses six platelet binding sites, three different pairs located at the D domains (γ 400-411), the α C domains (RGDS of A α 572-575), and the coiled coils (RGDF of A α 95-98), respectively (12). While the RGD sequence is a common cell recognition region (10), some cells, like endothelium, do not recognize γ 400-411 (6). Although not available to unstimulated platelets (12), the RGDF sequence of native fibrinogen can bind to ADP-stimulated platelets (11). The C terminus of γ 400-411 and the RGDS sequence of immobilized fibrinogen actively participates in binding to unstimulated platelets (12). Both regions also directly interact with ADP-stimulated platelets (11). However, the A α chain is only 20-25% as effective as the γ chain, and the RGD sequences of fibrinogen are thought not to be essential to platelet aggregation (88). In fact, the A α chain of fibrinogens of some species do not have the RGD sequence at all (14). It has been speculated that these cell-binding sequences in a fibrinogen molecule cooperatively enhance the affinity of fibrinogen for platelets (89).

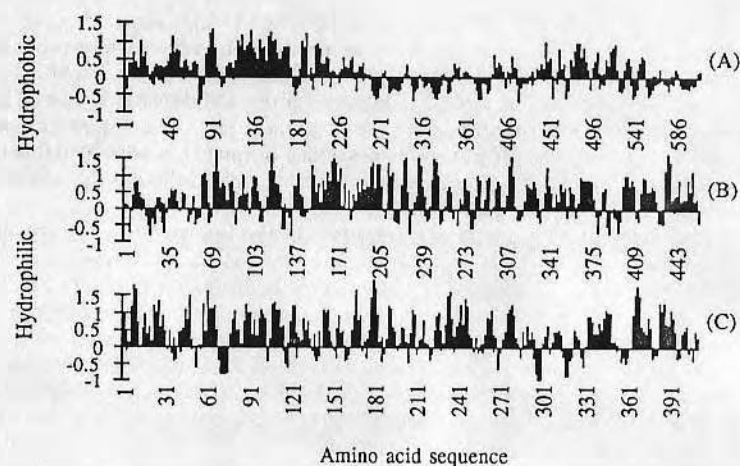


Figure 7. Hydropathy of three polypeptide chains of human fibrinogen, computed using Ponnuswamy scale (19). (A) A α , (B) B β and (C) γ .

We suggest the such broad distribution of these sites can ensure that fibrinogen maintain its cell binding ability for different situations. Evidence shows that the native or near native tertiary structure is essential for fibrinogen to bind to platelets (28,51,90,91), and to express its polymerization sites (92). The multi-binding ability allows adsorbed fibrinogen in various adsorption states to interact with platelets. Some of the platelet binding sites are likely protected from alteration by surfaces. Usually only certain domains are favored by a particular surface. Some domains are adsorbed and probably denatured, anchoring fibrinogen on the surface. Others not directly interacting with the surface have their platelets binding sites preserved so fibrinogen can interact with platelets while adhering to a surface. Depending on the type of surface, immobilization can be provided by a particular domain and binding by another. For instance, on glass it is likely that the α C domain adheres to the surface and the site on the D domain bind to platelets. On a hydrophobic surface the D domain more likely adsorbs to the surface, leaving the α C domain available to interact with platelets.

Platelet binding is likely faster than surface-induced denaturation. Immobilized fibrinogen may bind to and activate platelets prior to its full scale denaturation. Surfaces with microphase separation (87), with balanced polar and non-polar characters (73,93), or with high protein affinity (94) show better blood compatibility, presumably because they can interact with all the domains of fibrinogen, destroy the binding sites, and thus disabling its ability to bind to platelets.

Importance of the α C Chain (α C and α M domains). The α C domain is often near or on the E domain (95), forming nodules observed by electron microscopy (51,96). Studies indicate that the α C domains show a considerable homology among species (97). Although the α M domains vary, the nature of their tandem repeats are conserved (14,66). This overall similarity suggests that the α C chain plays an important role. Unfortunately, its biological function has not been clearly defined (98). The α C chain is not considered as a structural component for the formation of a fibrin clot, but it may be a factor promoting (66,99), branching (63), and stabilizing (100) the normal assembly of fibrin. Fibrinogen with the α C chain portions deleted show retarded polymerization and lower clottability (64).

The conformation of the α C chain has not been completely solved. Although the α C chain seems to have neither α -helix nor β -sheet (2), it does show a compact structure (55), with a defined thermal denaturation temperature (49,64). The α M domain has high hydrophilicity and low intra-molecular cohesion (Figs. 7 and 6), providing high solubility, flexibility and mobility. The α C domain contains a hydrophobic (A α 470-520) and hydrophilic (A α 550-610) region (Figure 7).

Although less attention has been given to it (66,72), more evidence is showing that the α C domain may be partly responsible for the surface activity of fibrinogen. The α C domain seems to have a strong tendency to interact with another α C domain (72,95), enhancing lateral interactions between fibrinogen molecules (39,40). Electron microscopy reveals that a free 40,000 α C fragment cleaved by plasmin can bind to the α C domains of fibrin (95). It is reported that the α C domains have a complementary site so that they can be strongly tied together intra-molecularly (49,66,64,101), forming a super α C domain; often seen as a fourth domain by electron microscopy (57). They also bind to the corresponding regions inter-molecularly, bringing individual fibrinogen or fibrin molecules together, guiding fibrin monomers to polymerize, and regulating the structure of fibrin clots (63). Covalent bonding between two α C chains from two fibrin molecules by Factor XIIIa further stabilizes fibrin polymers (63,102). The α C domain can attach to the E domain, producing an apparently larger central domain (56) and blocking the antibody accessibility of the γ

chain in the E domain (65). Because of its uncertain position related to the bulk molecule, the α C chain prevents fibrinogen from crystallization (55).

Inter-molecular association of the α C domains may contribute to fibrinogen's susceptibility to precipitation and thus its low solubility (103). The interaction between the α C chains can also enhance lateral interactions among adsorbed fibrinogen molecules (104). Although the α C chain is more hydrophilic than the other chains, fibrinogen actually becomes more soluble in aqueous solutions without it. The cleavage starts at the C terminus of the α C chain and gradually extends towards the N-terminus, producing modified fibrinogen with the α C chain of different lengths. The longer the α C segment chopped off, the higher the solubility of the modified fibrinogen (105,106).

We suggest that the α C chain acts as a "pioneer" for adsorption. The α M domain has high flexibility and mobility, permitting high collision frequencies of the α C chain with a surface. The α C domain easily changes its conformation and adheres to a surface by either the hydrophobic or hydrophilic regions, or is attracted to negative surfaces. The cooperation of the two domains results in a highly mobile "hand". The α M domain can also locally associate with themselves or with the α M domain of another molecule. This segment possesses an accordion structure composed of a series of tight turns, a series of imperfect 13-residue repeats. Most the β -turns contain a Trp residue at the fourth position, which acts as a "meager toe-hold" for inter-chain interaction. It is proposed that the stickiness of the α C chain is due to the exposure of the "caged" Trp residues on the α A chain (66,72). Fibrinogen is seen to attach to the solid surface by one end from a solution droplet and extend in the direction of the receding edge as the droplet continues to dry, suggesting that the α C domain is the first to adhere to the surface (96). Sometimes presumed dimers on hydrophilic silica may actually be single fibrinogen molecules with the α C chain stretched from the D domain (30). In addition to electrostatic forces, the interaction between a hydrophilic surface and the hydrophilic α C chain may be due to the formation of hydrogen bonds between their mutual hydrophilic groups.

Based on the above discussion, we are able to make a number of predictions. The interaction between the α C domain and a surface should not be strong since the chain is neither very hydrophobic nor highly positive. Fibrinogen adsorbed on a surface via its α C domain alone can be readily displaced by other surface active proteins (27), or eluted by sodium dodecyl sulfate (SDS) (90,97). Only when other domains later begin to adhere to the surface does fibrinogen adsorption become increasingly strong, reducing its displacement and elutability. The presence of albumin in solution can inhibit this process and thus slows down the decrease in SDS elutability (90,97). At low plasma concentration, fibrinogen has sufficient time to use all its domains interacting with surfaces. Thus the surface concentration increases with plasma concentration. When the plasma concentration is high enough, adsorption of other proteins prevents fibrinogen from contacting the surface through domains other than the α C domain. Such adsorbed fibrinogen can be easily displaced, resulting in a decrease in surface fibrinogen with increasing plasma concentration. This can explain the maximum in adsorption isotherms of fibrinogen vs. plasma concentration. Surfaces strongly interacting with the α C domain may improve the blood compatibility. For example, despite more fibrinogen adsorbed sulfonated polyurethane has a longer thrombin time (16,107). In addition to the suspected heparin like behavior of the sulfonated polyurethanes, the interaction may cause a change in adsorbed fibrinogen and increase its resistance to thrombin attack.

Very large proteins tend to show high surface activity. However, mass is not necessarily the major driving force. For example, adsorbed fibrinogen (Mw 340,000) can be displaced by Hageman factor (Mw 78,000) from glass (108), or by hemoglobin (Mw 64,650) from several surfaces (36). What is really important is that

high Mw proteins usually contain highly diverse structures and multi-domain organization. These characteristics usually offer them the necessary ingredients for high surface activity, such as structural flexibility, high charge density, hydrophobicity, etc. As we have seen, higher heterogeneity of structure can result in higher surface activity, as it provides the opportunity for proteins to optimize their interactions with different surfaces.

Postscript

Fibrinogen is a well built molecule. Its primary and domain structures dictate its physicochemical properties. It contains domains ensuring rapid, strong interactions with non-biological surfaces. Although fibrinogen is not very hydrophobic, it is surface active enough to accumulate at interfaces. Fibrinogen can cooperatively change its conformation, providing a sensitive structure which "senses" foreign surfaces and permits quick reactions. It has the ability to activate platelets through adsorption and is often only slowly inactivated by surfaces.

Acknowledgments

We thank the Center for Biopolymers at Interfaces, University of Utah, for supporting this work.

Literature Cited

1. Doolittle, R.F. *Ann. Rev. Biochem.* **1984**, *53*, 195.
2. Doolittle, R.F. In *The molecular basis of blood diseases*, 2nd Ed.; Stamatoyanopoulos, G., Saunders, Philadelphia, PA, 1994; pp. 701.
3. Smith, G.F. In *The thrombin*; Machovich, R., CRC-Press, Boca Raton, FL, 1984, Vol. 1., Chapter 4.
4. Shafer, J.A.; Higgins, D.L. *CRC-Crit. Rev. Clin. Lab. Sci.* **1988**, *26*, 1.
5. Plow, E.F.; Edgington, T.S. *Seminars Thromb. Hemostasis* **1982**, *8*, 36.
6. Cheresch, D.A.; Berliner, S.A.; Vicente, V.; Ruggeri, Z.M. *Cell* **1989**, *58*, 945.
7. Altieri, D.C.; Plescia, J.; Plow, E.F. *J. Biol. Chem.* **1993**, *268*, 1847.
8. Phillips, D.R.; Charo, I.F.; Parise, L.V.; Fitzgerald, L.A. *Blood* **1988**, *71*, 831.
9. Fabrizio-Homan, D.J.; Cooper, S.L. *J. Biomater. Sci., Polym. Ed.* **1991**, *3*, 27.
10. Berliner, S.A. *Pept. Res.* **1988**, *1*, 60.
11. Hawiger, J. *Biochemistry* **1989**, *28*, 2909.
12. Savage, B.; Ruggeri, Z.M. *J. Biol. Chem.* **1991**, *266*, 11227.
13. Lambrecht, L.K. *Thromb. Res.* **1986**, *41*, 99.
14. *Blood compatibility*; Williams, D.F., Ed.; CRC, Boca Raton, FL, 1987, Vol. 1., Chapter 2.
15. Absolom, D.R.; Zingg, W.; Neumann, A.W. *J. Biomed. Mater. Res.* **1987**, *21*, 161.
16. Santerre, J.P. *J. Biomed. Mater. Res.* **1992**, *26*, 39.
17. Feng, L.; Andrade, J.D. *Biomaterials* **1994**, *15*, 323.
18. Baszkin, A.; Lyman, D.J. In *Biomaterials 1980*. Winter, G.D. Eds.; Wiley, Chichester, 1982, pp. 393-397.
19. Young, B.R.; Pitt, W.G.; Cooper, S.L. *J. Colloid Interface Sci.* **1988**, *124*, 28.
20. Wojciechowsky, P.; ten Hove, P.; Brash, J.L. *J. Colloid Interface Sci.* **1986**, *111*, 455.
21. Weathersby, P.K.; Horbett, T.A.; Hoffman, A.S. *J. Bioengineering* **1977**, *1*, 393.
22. Valerio, F.; Balducci, D.; Lazzarotto, A. *Environ. Res.* **1987**, *44*, 312.

23. Lahav, J. *J. Colloid Interface Sci.* **1987**, 119, 262.
24. Pankowsky, D.A. *J. Vasc. Surg.* **1990**, 11, 599.
25. Schmitt, A. *J. Colloid Interface Sci.* **1983**, 92, 145.
26. Kibing, W.; Reiner, R.H. *Chromatographica* **1978**, 11, 83.
27. Slack, S.M.; Horbett, T.A. *J. Biomed. Mater. Res.* **1992**, 26, 1633.
28. Rapoza, R.J.; Horbett, T.A. *J. Biomed. Mater. Res.* **1990**, 24, 1263.
29. Maechling-Strasser, C. *J. Biomed. Mater. Res.* **1989**, 24, 1385.
30. Nygren, H.; Stenberg, M.; Karlsson, C. *J. Biomed. Mater. Res.* **1992**, 26, 77.
31. Okkema, A.Z.; Visser, S.A.; Cooper, S.L. *J. Biomed. Mater. Res.* **1991**, 25, 1371.
32. Mohri, H.; Ohkubo, T. *Arch. Biochem. Biophys.*, **1993**, 303, 27.
33. Bergstrom, K. *J. Biomater. Sci., Polym. Ed.* **1992**, 3, 375.
34. Amiji, M.; Park, K. *Biomaterials* **1992**, 13, 682.
35. Slack, S.M.; Horbett, T.A. *J. Colloid Interface Sci.* **1993**, 124, 535.
36. Poot, A. *J. Biomed. Mater. Res.* **1990**, 24, 1021.
37. Brash, J.L. *Blood* **1988**, 71, 932.
38. Kim, S.W.; Lee, R.G. In *Applied chemistry at protein interfaces*, Baier, R.E., Ed.; ACS, Washington, DC, 1975, pp. 218-229.
39. Bagnall, R.D. *J. Biomed. Mater. Res.* **1978**, 12, 203.
40. Lensen, H.G.W. *J. Colloid Interface Sci.* **1984**, 99, 1.
41. Norde, W. *Adv. Colloid Interface Sci.* **1986**, 25, 267.
42. Park, K.; Mao, F.W.; Park, H. *J. Biomed. Mater. Res.* **1991**, 25, 407.
43. Fabrizio-Homan, D.J.; Cooper, S.L. *J. Biomed. Mater. Res.* **1991**, 25, 953.
44. Sunny, M.C.; Sharma, C.P. *J. Biomater. Appl.* **1991**, 6, 89.
45. Voegel, J.C.; Pefferkorn, E.; Schmitt, A. *J. Chromatogr.* **1988**, 428, 17.
46. Feng, L.; Andrade, J.D. *Colloids and Surfaces*, **1994**, in press.
47. Katona, E.; Neumann, A.W.; Moscarello, M.A. *Biochim. Biophys. Acta* **1978**, 534, 275.
48. Feng, L.; Andrade, J.D. *J. Biomed. Mater. Res.*, **1994**, in press.
49. Privalov, P.L. *J. Mol. Biol.* **1982**, 159, 665.
50. Medved, L.V.; Litvinovich, S.V.; Privalov, P.L. *FEBS* **1986**, 202, 298.
51. Shiba, E. *Am J. Physiol.* **1991**, 260, C965.
52. Ugarova, T.P. *J. Biol. Chem.* **1993**, 268, 21080.
53. Mosesson, M. *J. Mol. Biol.* **1981**, 153, 695.
54. Gollwitzer, R.; Bode, W.; Karges, H.E. *Thromb. Res.* **1983**, suppl 5, 41.
55. Weisel, J.W. *Science* **1985**, 230, 1388.
56. Beijbom, L. *J. Ultrastruct. Mol. Struct. Res.* **1988**, 98, 312.
57. Rao, S.P.S. *J. Mol. Biol.* **1991**, 222, 89.
58. Langer, B.G. In *Fibrinogen 3: biochemistry, biological functions, gene regulation and expression*; Mosesson, M.W., Eds.; Excerpta Medica, Amsterdam, 1988, pp. 63-68.
59. Townsend, R.R. *J. Biol. Chem.* **1982**, 257, 9704.
60. Nishibe, H.; Takahashi, N. *Biochim. Biophys. Acta* **1981**, 661, 274.
61. Doolittle, R.F. *Protein Sic.* **1992**, 1, 1563.
62. Azpiazu, I.; Chapman, D. *Biochim. Biophys. Acta* **1992**, 1119, 268.
63. Weisel, J.W.; Papsun, D.M. *Thromb. Res.* **1987**, 47, 155.
64. Medved, L.V.; Gorkun, O.V.; Privalov, P.L. *FEBS Lett.* **1983**, 160, 291.
65. Plow, E.F.; Edgington, T.S.; Cierniewski, C.S. *Ann. N.Y. Acad. Sci.* **1983**, 408, 44.
66. Doolittle, R.F. In *Fibrinogen, thrombosis, coagulation, and fibrinolysis*; Liu, C.Y.; Chien, S., Eds.; Plenum, New York, NY, 1990, pp. 25-37.
67. Litvinovich, S.V.; Medved, L.V. *Mol. Biol.* **1988**, 22, 744.
68. Marder, V.J.; Budzynski, A.Z. *Thrombos. Diathes. Haemorrh.* **1975**, 33, 199.

69. Nieuwenhuizen, W. In *Fibrinogen and its derivatives*. Muller-Berghaus, G., Eds.; Excerpta Medica, Amsterdam, 1986, pp. 245-256.
70. Henschen, A. *Thromb. Res.* **1983**, Suppl. 5, 26.
71. Andrade, J.D. et al. *Croatia Chem. Acta* **1990**, 63, 527.
72. Doolittle, R.F. et al. *Nature* **1979**, 280, 464.
73. Tengvall, P. *Biomaterials* **1992**, 13, 367.
74. Wahlgren, M.C.; Paulsson, M.A.; Arnebrant, T. *Colloid and Surfaces A: Physicochem. Eng. Aspects* **1993**, 10, 139.
75. Arai, T.; Norde, W. *Colloids and Surfaces* **1990**, 51, 1.
76. Wei, A.P.; Herron, J.N.; Andrade, J.D. In *From Clone to Clinic*, Crommelin, D.J.A.; Schellekens, H., Eds.; Kluwer, Amsterdam, 1990, pp. 305-313.
77. Ragone, R. *Protein Engineering* **1989**, 2, 479.
78. Norde, W.; Favier, J.P. *Colloids and Surfaces* **1992**, 64, 87.
79. Ponnuswamy, P.K. *Prog. Biophys. Mol. Biol.* **1993**, 59, 57.
80. Telford, J.N. *Proc. Natl. Acad. Sci. USA* **1980**, 77, 2372.
81. Fair, D.S.; Edgington, T.S.; Plow, E.F. *J. Biol. Chem.* **1987**, 256, 8018.
82. Zamarron, C.; Ginsberg, M.H.; Plow, E.F. *Thromb. Haemostats* **1990**, 64, 41.
83. Schielen, W.J. *Blood* **1991**, 15, 2169.
84. Tanswell, P. *Thrombos. Haemostas.* **1979**, 41, 702.
85. Cierniewski, C.S.; Budzynski, A.Z. *J. Biol. Chem.*, **1987**, 262 13896.
86. Cierniewski, C.S. *Thromb. Res.* **1979**, 14, 747.
87. Elam, J.H.; Nygren, H. *Biomaterials* **1992**, 13, 3.
88. Farrell, D.H. *Proc. Natl. Acad. Sci., USA* **1992**, 89, 10792.
89. Mohri, H.; Ohkubo, T. *Peptides* **1993**, 14, 353.
90. Chinn, J.A.; Ratner, B.D.; Horbett, T.A. *Biomaterials* **1992**, 13, 322.
91. Lindon, J. *Blood* **1986**, 68, 355.
92. Cierniewski, C.S.; Kloczewiak, M.; Budzynski, A.Z. *J. Biol. Chem.* **1986**, 261, 9116.
93. Mori, A. *Biomaterials* **1986**, 7, 386.
94. Feng, L.; Andrade, J.D. *J. Biomater. Sci., Polym. Ed.*, **1994**, in press.
95. Veklich, Y.I. *J. Biol. Chem.* **1993**, 268, 13577.
96. Rudee, M.L.; Price, T.M. *Ultramicroscopy* **1981**, 7, 193.
97. Chinn, J.A. *J. Biomed. Mater. Res.* **1991**, 25, 535.
98. Hirschbaum, N.; Budzynski, A.Z. In *Fibrinogen 3: biochemistry, biological functions, gene regulation and expression*; Mosesson, M.W., Eds.; Excerpta Medica, Amsterdam, 1988, pp. 297-300.
99. Cierniewski, C.S.; Budzynski, A.Z. *Biochemistry* **1992**, 31, 4248.
100. Koopman, J. *J. Clin. Invest.* **1993**, 91, 1637.
101. Siebenlist, K.R. *Blood Coagul. Fibrinolysis* **1993**, 4, 61.
102. Sobel, J.H. *Biochemistry* **1990**, 29, 8907.
103. Young, B.R.; Pitt, W.G.; Cooper, S.L. *J. Colloid Interface Sci.* **1988**, 125, 246.
104. Murthy, K.D. *Scanning. Microsc.* **1987**, 1, 765.
105. Mosesson, M. *Biochemistry* **1966**, 5, 2829.
106. Mosesson, M. *Ann. N.Y. Acad. Sci.* **1983**, 97.
107. Silver, J.H. *Trans. Soc. Biomater.* **1990**, 13, 139.
108. Tengvall, P. *Biomaterials* **1992**, 13, 367.

RECEIVED December 22, 1994

copy

Submitted to
J. Chemical Education
1995
unpublished

AN ICON REPRESENTATION OF PROTEIN
STRUCTURE AND PROPERTIES

Feng - ~~J. D. Andrade~~
Protein Icons - 95

L. Feng and J. D. Andrade*

Dept. of Bioengineering
2480 MEB
University of Utah
Salt Lake City, UT 84112

* To whom correspondence should be addressed

ABSTRACT

We developed a set of ~~prototypes~~ ^{have} of icons (cartoons) to represent ^{particular} characteristics of protein structure and its surface and interfacial properties. The goal is to give a direct and easily understood graphical view of protein molecules or their ^{structural} molecular domains so that the readers will be ~~immediately~~ ^{immediately} impressed and able to quickly comprehend what they are seeing. An icon is intended to describe two aspects of a structure or property parameter: what it is ^{its magnitude} and how much it is. This paper tabulates sixteen icons and their physical meanings. It also shows examples of their application on ~~some~~ ^{to} typical proteins and to ~~domains~~ ^{small} proteins.

It is ^{to} ~~of~~ importance to know ^{the} structure and properties of proteins ^{to} understand their interrelationship ^{Fields which require a thorough} in order to better work with them in the areas ^{understanding of protein structure and properties include} of biology, biochemistry, genetic and protein engineering, biomaterials, ^{pharmaceuticals, and the} medicinal and food industries, etc. ^P However, representing those characteristics

can be ~~a~~ tough endeavor because of the complexity of protein structure and of the diversity of properties. Recently we proposed a multi-parameter radial plot (the Tatra plot*) for examining ~~a number of variables of~~ protein structure and surface properties. ~~As a graphical multi-axis coordinate system,~~ ^{variables} The Tatra plot ~~was aimed to provide a visual representation for searching the correlativity~~ ^{facilitating} among the parameters, especially for ~~connecting surface behavior of a protein~~ ^{relating interfacial activity} to its structure. In the present paper, we further ~~developed a total picturesque~~ ^{have we an icon} expression of protein structure and properties, ~~an icon or cartoon~~ ^{to} representation. Our initiative is to create a new way of ~~describing~~ ^{visualized} proteins or their domains. We hope that such a directly perceptible and easily understood ~~graphical view~~ ^{representation} can immediately impress the readers and enable them ^{the viewer} to quickly comprehend what they are seeing.

An icon is intended to outline two aspects of a parameter of either structure or property: what it is and how much it is. For the former, the icon ^{shows} sketches the nature of an character, which can be a "steady state" (e.g., molecular weight) or a "dynamic process" (e.g., surface tension kinetics). The challenge for the icon is how to represent the essence of the parameter in an understandable way with minimal use of text. As can be imagined, ^{usually} describing a dynamic process is more difficult than a steady state. ^{inherent} ^{constant property} Occasionally plots are borrowed to make things clear. For the latter, the icon ^{also} shows the degree of ^{property} change by the magnitude of a scale (e.g., temperature), the amount of a quantity (e.g., denaturants), the size of an object (e.g., attractive

There are over ~~50~~ literally tens of thousands of different proteins in complex

~~Stochastic~~ Unique
Properties

surface hydrophobicity), or the ^{number or concentration} population of an entity (e.g., surface charge). A quantitative approximation is expressed as ¹three levels: low, medium, ^{or} and high. Thus a set of three icons were designed to describe a parameter, but only one of them ^{is} used for a given protein.

In designing ^{an} icon we ^{must} have tried to balance two criteria: comprehensivity and simplicity. An icon should be easily understood ^{as to the} as for what structure or property it represents. It is also desirable for it to provide some semi-quantitative information. ^{However,} ^{to be readily} ~~Meanwhile,~~ An icon has to be simple enough ~~not to cause~~ ^{assimilated and understood} headache. ^{After all,} The icon is a symbolic representation: a simple but relatively complete graphic ~~is all we need~~ to achieve our goal. Usually ^a compromise ^{has} ~~to be made~~ between these two criteria for a specific icon, since enhancing the comprehensivity ^{often sacrifices} ~~could sacrifice~~ the simplicity, or vice versa. For ~~that matter~~ ^{of} picture always serves as the main body of an icon. ~~Although sometimes necessary,~~ ^{kept to} the use of text is controlled as a minimum ~~to keep the icon simple.~~

^{here} In this paper most icons were derived for the parameters ⁱⁿ the Tatra plot. ^{those parameters related to} ~~Therefore, the exemplified properties are focused on surface and interfacial ones.~~ For a better understanding of the icons ^{the} individual parameters are ~~first~~ introduced in Table 1, together with their symbols, units, and physical meanings. The parameters are roughly divided into five groups: molecular size, structural stability, hydrophobicity, hydrophilicity, and surface activity. Table 2 lists the corresponding ^{ing} icons, some of which are self-explanatory, but ~~some of which need some interpretation.~~ ^{line 3 in Table 2} The third set of icons illustrates the concentration of guanidinium chloride (GdnHCl) required for 50% protein to become denatured, i.e., the GdnHCl stability. The icons show the process of denaturation of a protein chain from a folded state to an unfolded one. The amount of added GdnHCl salt from the spoon stands for the stability of

a protein; the larger the amount, the more stable the protein. The fifth ^{line illustration} ~~are a~~ description of a ^{the} ~~process of~~ decrease in solution surface ~~intension~~ ^{the} due to adsorption of protein at the air/water interface. ~~As the protein is kept at a low~~ ^{protein} concentration (10 $\mu\text{g/ml}$), the rate is determined by how fast the protein is ^{the} ~~denatured~~ ^(native) at the interface. ^{So the icons show the time for the round} ~~the icons show the time for the round~~ ^{to be} converted to the elliptical one. ~~Just for the comparison,~~ ^(denatured) ~~for the decrease in~~ solution surface tension at high protein concentration (50 $\mu\text{g/ml}$), ~~the rate~~ ^{the} is dependent upon the hydrophobicity of native protein (the fifteenth set of icons). ~~The effective surface hydrophobicity is also a measure of hydrophobicity of native proteins.~~ The icons show the the degree of this property by the area of a hydrophobic patch, which is unwettable by a water droplet. Finally, the last set ^{of icons} depicts the adsorptivity of ~~a~~ protein in a competitive adsorption process. The degree of relative surface activity of a protein can thus be estimated. The icons portray an adsorption process in a binary protein system, indicating different adsorptivity of the protein of interest (darker ones).

Fig. 1-3 demonstrate some applications of the listed icons. Fig. 1 is the icon representations of three globular proteins - superoxide dismutase (SOD), lysozyme (LSZ) and myoglobin (MGB), whose Tatra plots have been published. Table 3 interprets the result of the individual parameters for the three proteins in Fig. 1. Fig. 2 compares some parameters of human serum albumin (HSA) and human fibrinogen (HFG), from which we immediately learn the following facts: HSA is a middle sized molecule with relatively high density of disulfide bonds; it ^{has} ~~have~~ very high solubility in buffer but relatively low adsorptivity. On the other hand, HFG is a large molecule with relatively few disulfide bonds; its solubility is low but its adsorptivity is rather high. The icons can also be utilized to show characteristics of individual domains within a molecule. ~~To distinguish individual~~

at ?

domains and their properties are important in analysis of large multi-domain proteins since many of their properties are largely determined by the domains rather than the global molecule. Fig. 3 shows three properties of three major domains of HFG₃E, D, and A α C. Evidently the A α C domain is more hydrophilic than the other two and it is slightly positively charged, in contrast to the E and D domain, which are negatively charged. Both the D and A α C domains have low thermal denaturation temperatures but the E domain denatures at very high temperature.

In summary, we showed in this paper that structure and property parameters can be illustrated by a graphic expression - the icon representation. This may be served as a simple and efficient means to convey a complex parameter. *protein structure and properties* involved in protein structure and properties.

So - go on - how can you develop diagrams to hypotheses or conclusions?

Table 1 Parameters selected for the icon representation

Group	Parameter	Symbol	Unit	Physical meaning
Size	Molecular weight	Mw	Dalton	Volume of proteins
Structural stability	Temperature of thermal denaturation ^{a)}	Td	°C	Thermal stability
	GdnHCl concentration for 50% denaturation	[GdnHCl] _{1/2}	Molar	GdnHCl stability
	Compressibility	<i>thermo parameter</i> $(\beta)^3$		A measure of protein hardness
	Rate constant of surface tension kinetics at low bulk concentration (10 μ g/ml)	k ₁ (low)	hr ⁻¹	Rate of surface-induced denaturation
	Number of disulfide bonds	S-S	Integer number	More disulfide bonds make a protein more stable
Hydrophobicity	Effective surface hydrophobicity ^{b)}	ESH	?	Hydrophobicity of proteins in their native states
	Ratio of polar-nonpolar amino acids	P-N	%	Chain hydrophobicity
	Average α -moment multiplied by fraction of α -helices	F $\mu\alpha$	<i>integrated ratio of</i> ?	A measure of quantity and amphiplicity of α -helices
	Average β -moment multiplied by fraction of β -sheets	F $\mu\beta$?	A measure of quantity and amphiplicity of β -sheets
Hydrophilicity	Percent accessible area of negatively charged oxygen atoms	O ⁻ %	%	Inversely related to protein effective hydrophobicity
	Net surface charge (positive or negative)	S σ	Integer number	Increasing surface polarity and thus hydrophilicity
	Solubility in buffer ^{c)}	<i>So?</i>	mg/ml	Higher solubility means higher hydrophilicity
Surface activity	Steady-state surface pressure at bulk concentration of 50mg/ml	Π_{ss}	dynes/cm	Air/water interfacial activity of proteins at equilibrium
	Rate constant of surface concentration (50 μ g/ml)	k ₁ (high)	hr ⁻¹	Dependent of hydrophobicity of native proteins
	Adsorptivity	Γ_m		Relative adsorbed quantity from a multi-component system

a) pH dependent

b) Measured by *cis*-PnA binding and hydrophobic interaction chromatography (?)

c) Solvent dependent

c) (solubility) (parameter) (So) ?

Table 2

		Low	Medium	High
Size	Mw	AAAAAAAAAAAAAAAAAAAA	AAAAAAAAAAAAAAAAAAAA A AAAAAAAAAAAAAAAAAAAA	AAAAAAAAAAAAAAAAAAAA A AAAAAAAAAAAAAAAAAAAA A AAAAAAAAAAAAAAAAAAAA
	Td (°C)			
Structural stability	[GdnHCl] _{1/2}			
	k ₁ (low)			
	S-S			

Hydrophobicity	ESH			
	P-N			
	Fxμ _α			
	Fxμ _β			

use α -helix
symbol
lllll

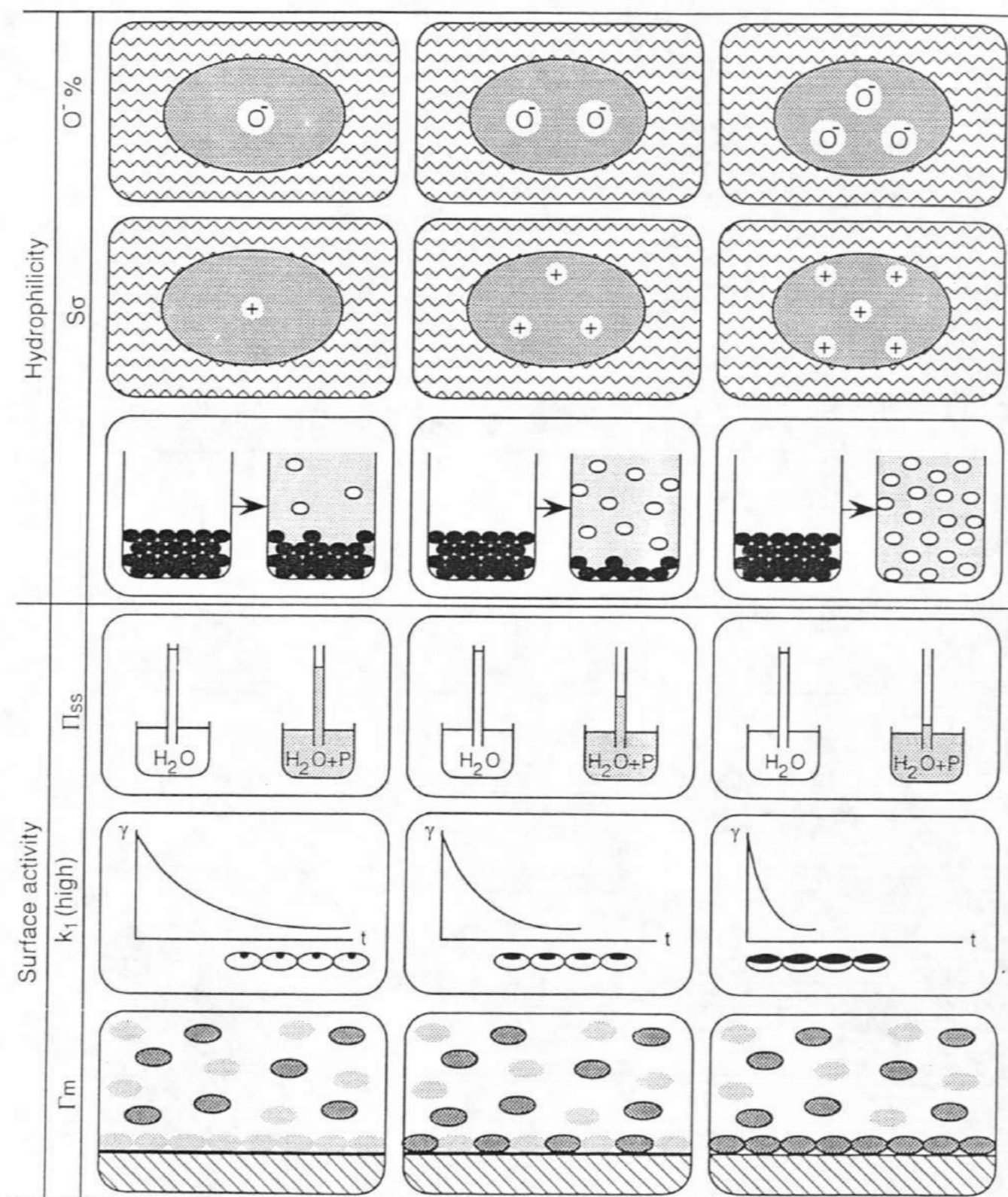
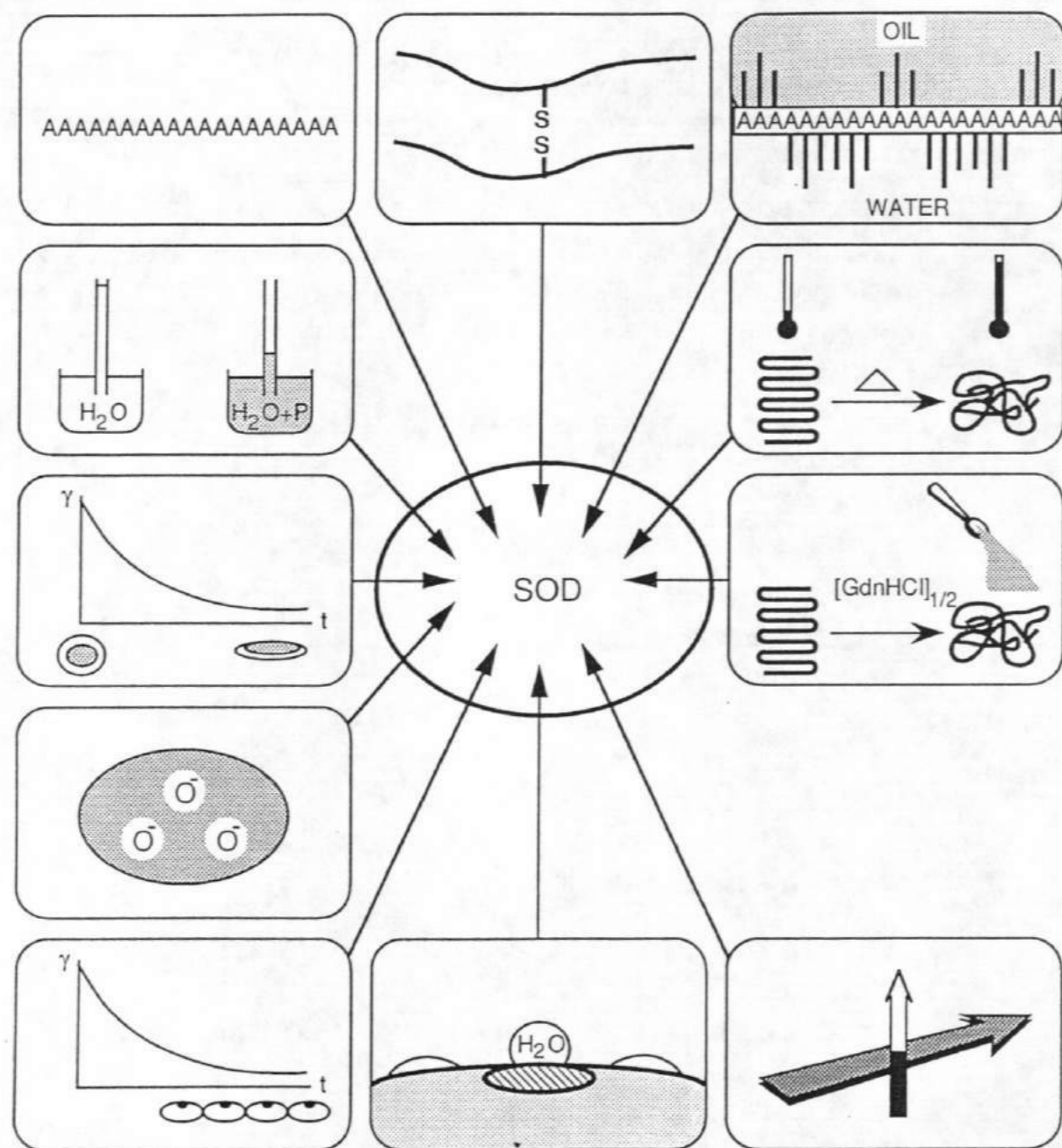


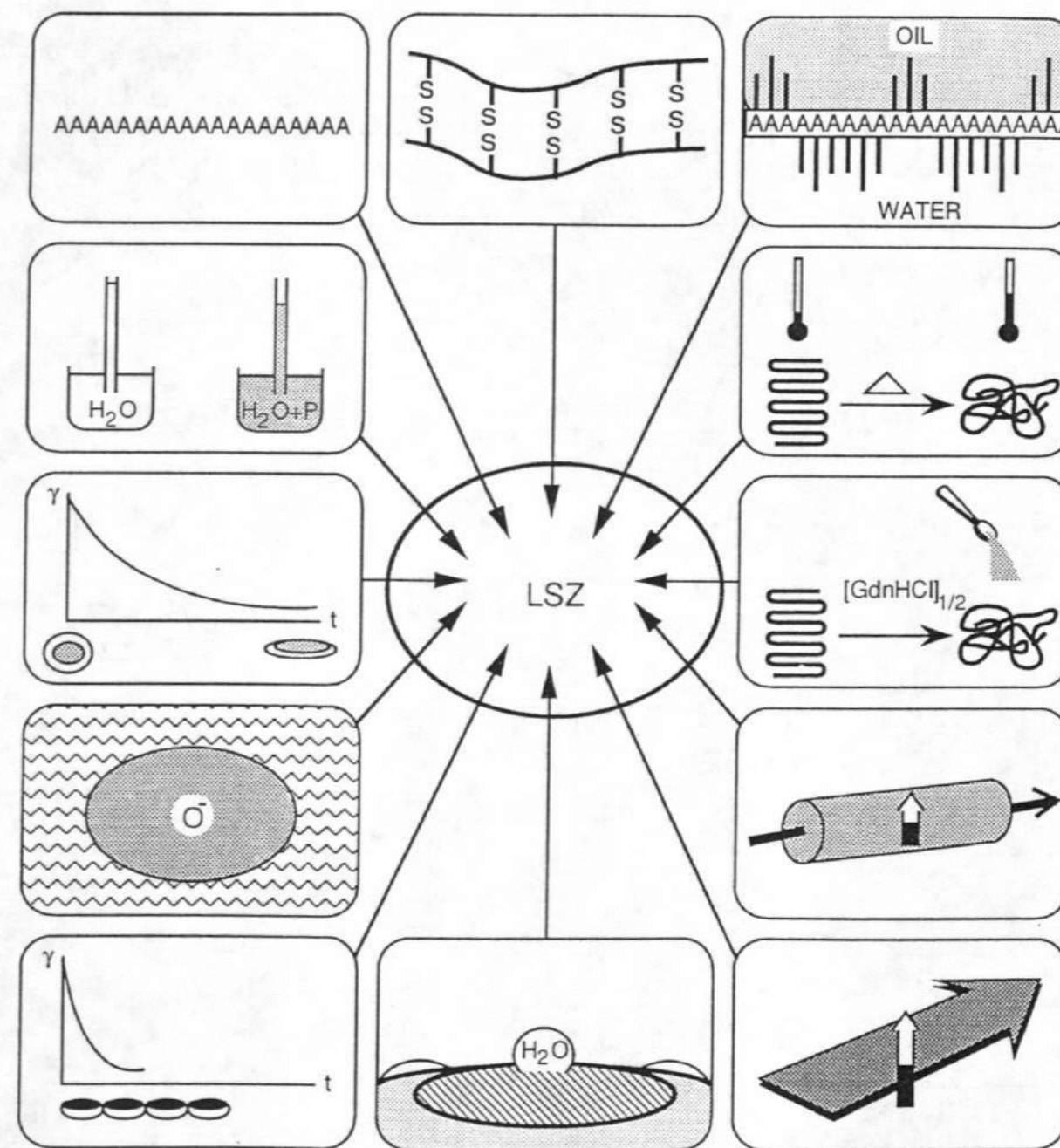
Table 3 Parameters described by icons for SOD, LSZ, and MGB (parameters are clockwise counted beginning at the left corner)

Parameter	Comparison	Remark
Mw	SOD=LSZ=MGB	All are small proteins
S-S	LSZ>SOD>MGB	MGB is a soft protein but the other two are much harder
N-P	MGB>SOD=LSZ	
Td	SOD>LSZ>MGB	
[GdnHCl] _{1/2}	SOD>LSZ>MGB	
Fμ _α	MGB>LSZ	SOD has no α-helix
Fμ _β	SOD>LSZ	MGB has no β-sheet
ESH	LSZ>MGB>SOD	
k ₁ (high)	LSZ>MGB>SOD	For native states, LSZ has the highest
O ⁻ %	SOD>MGB>LSZ	
k ₁ (low)	MGB>LSZ=SOD	



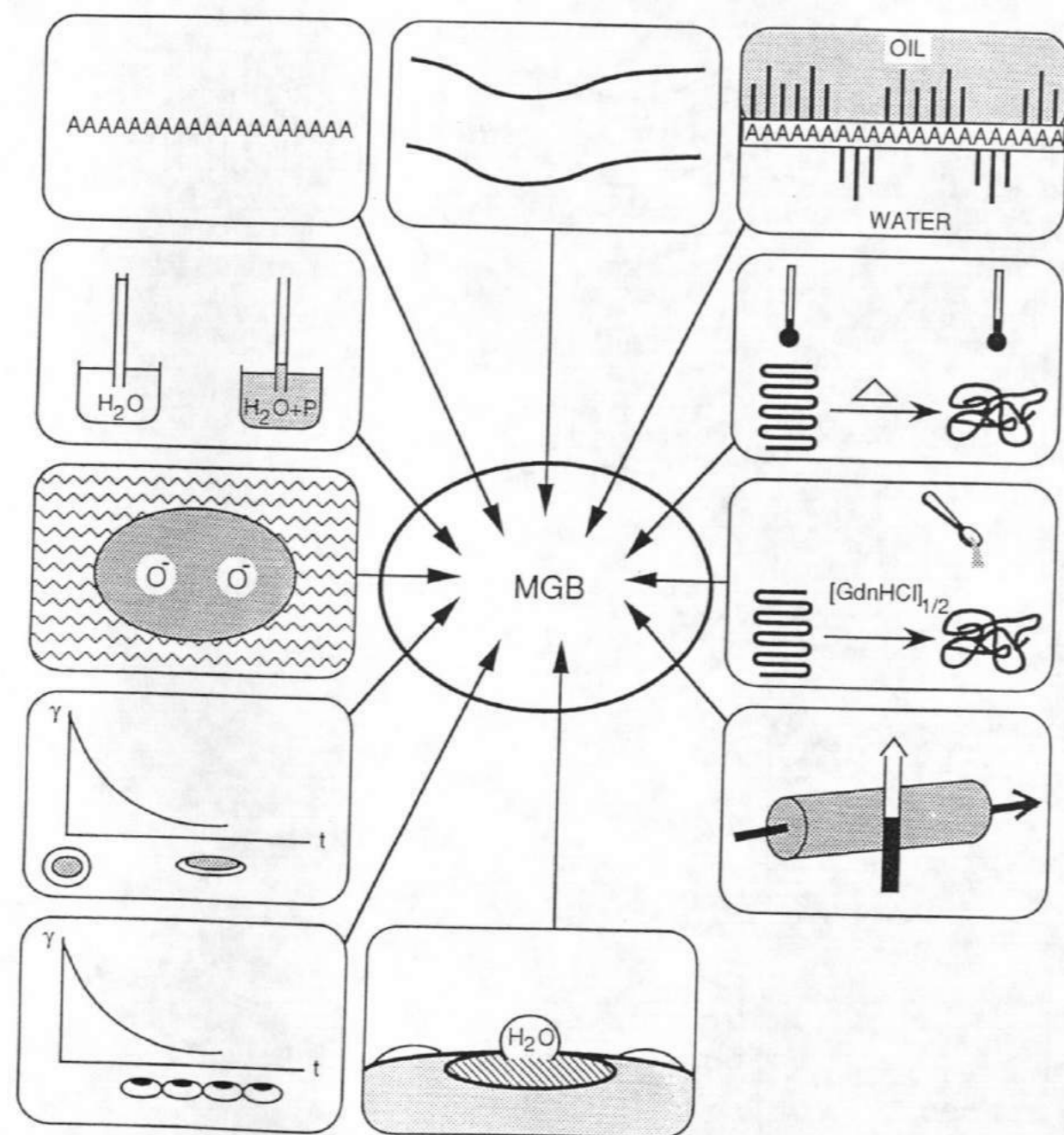
(A) SOD

Fig. 1



(B) LSZ

Fig. 1



(C) MGB

Fig. 1

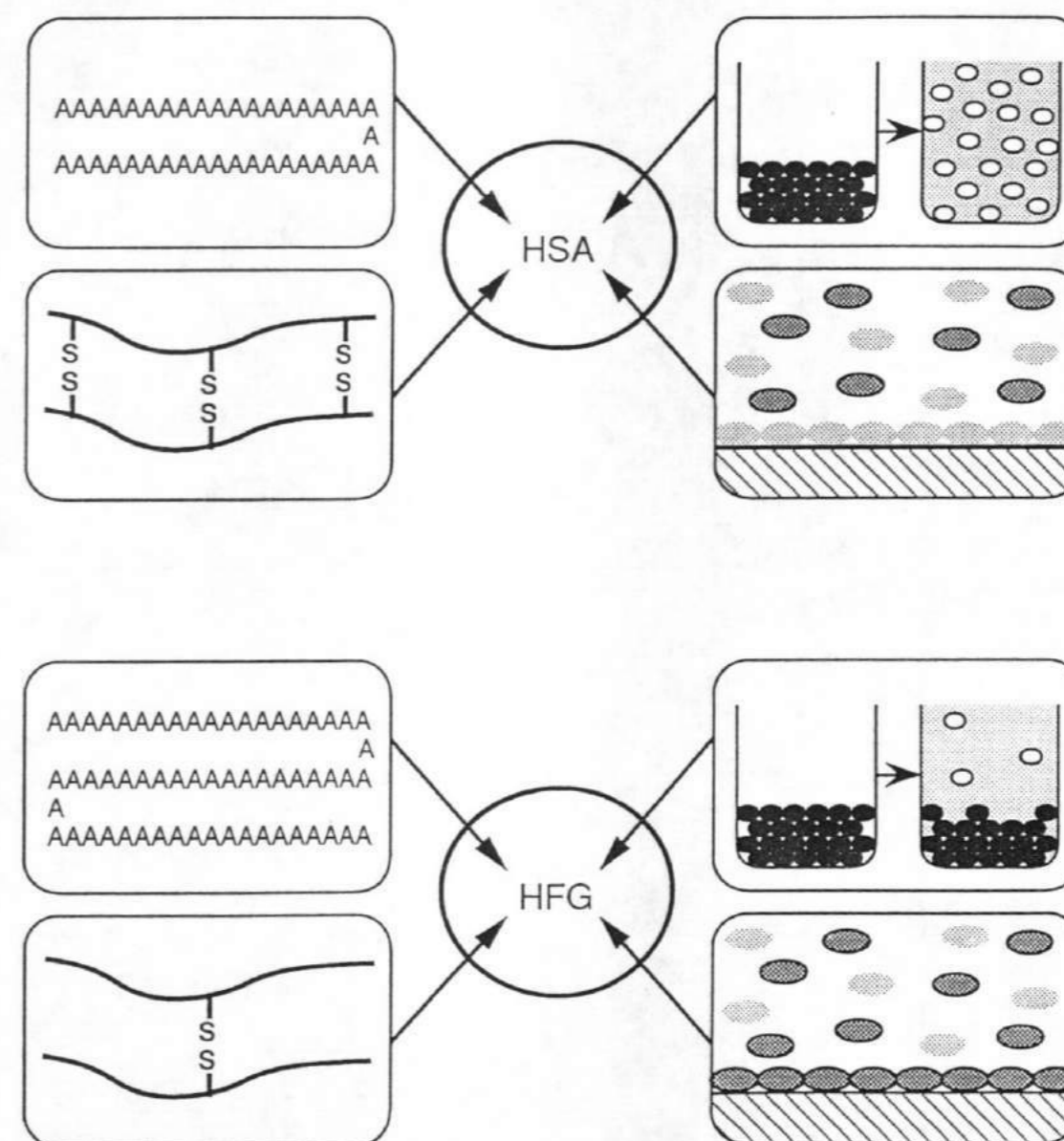
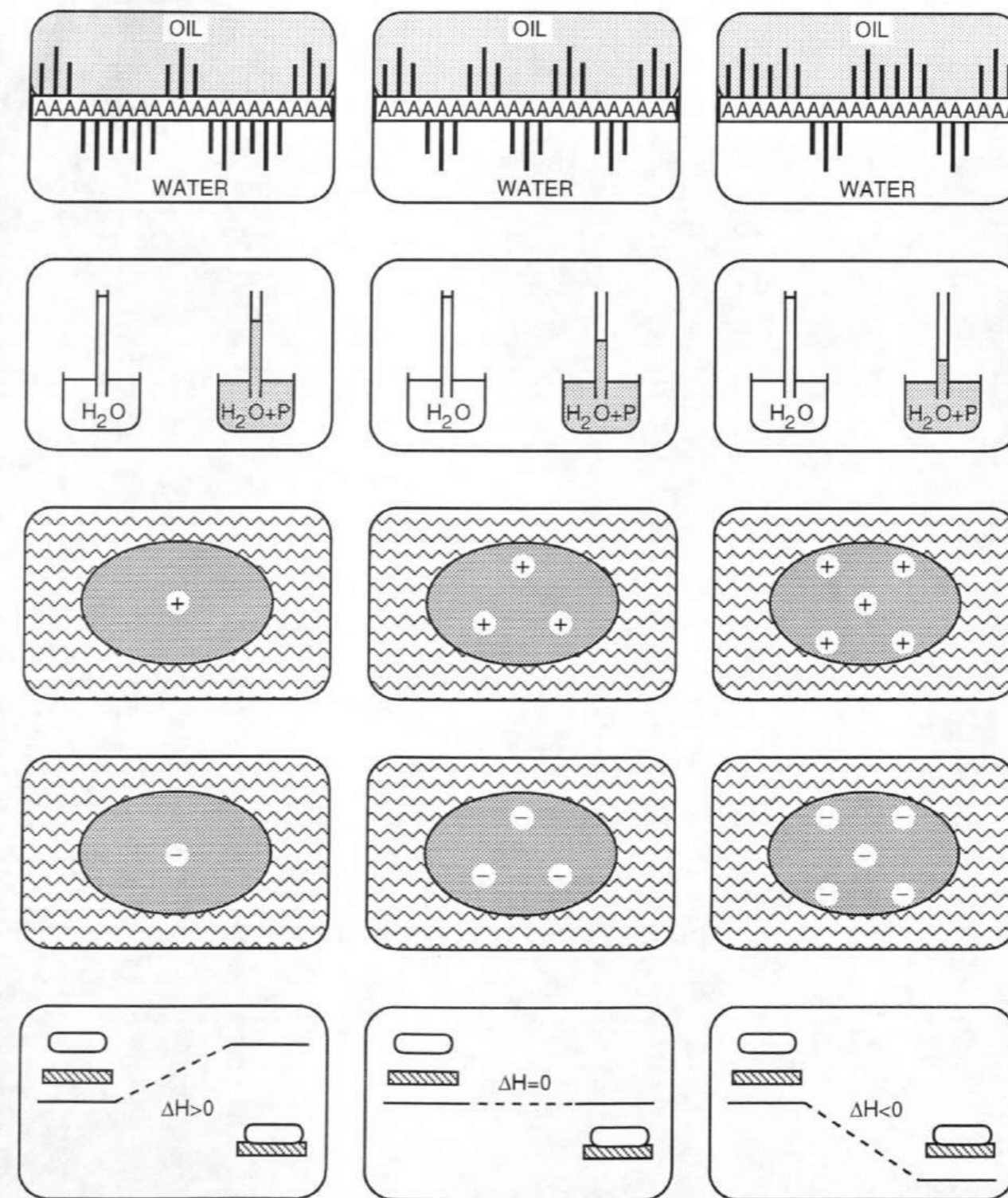
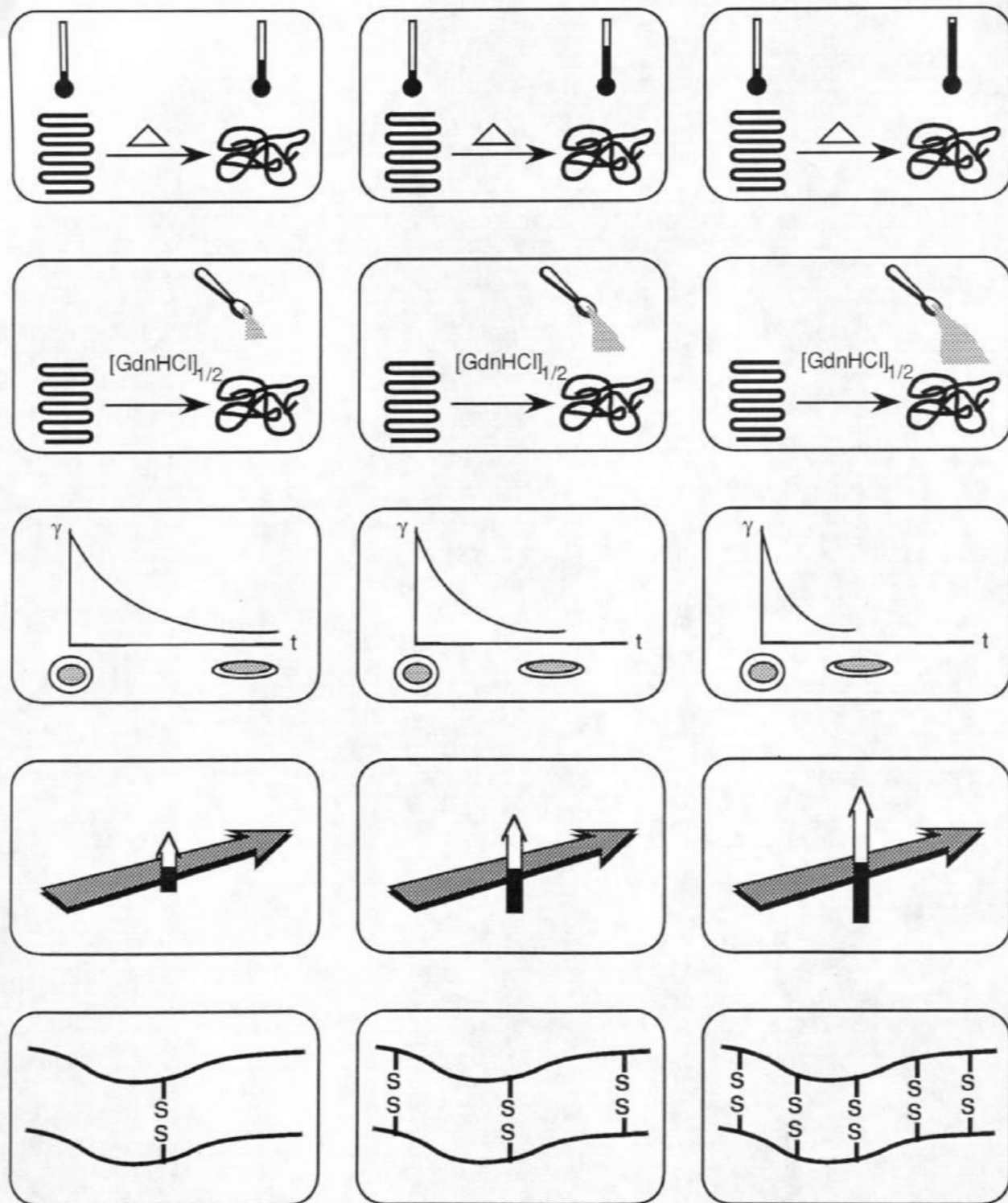
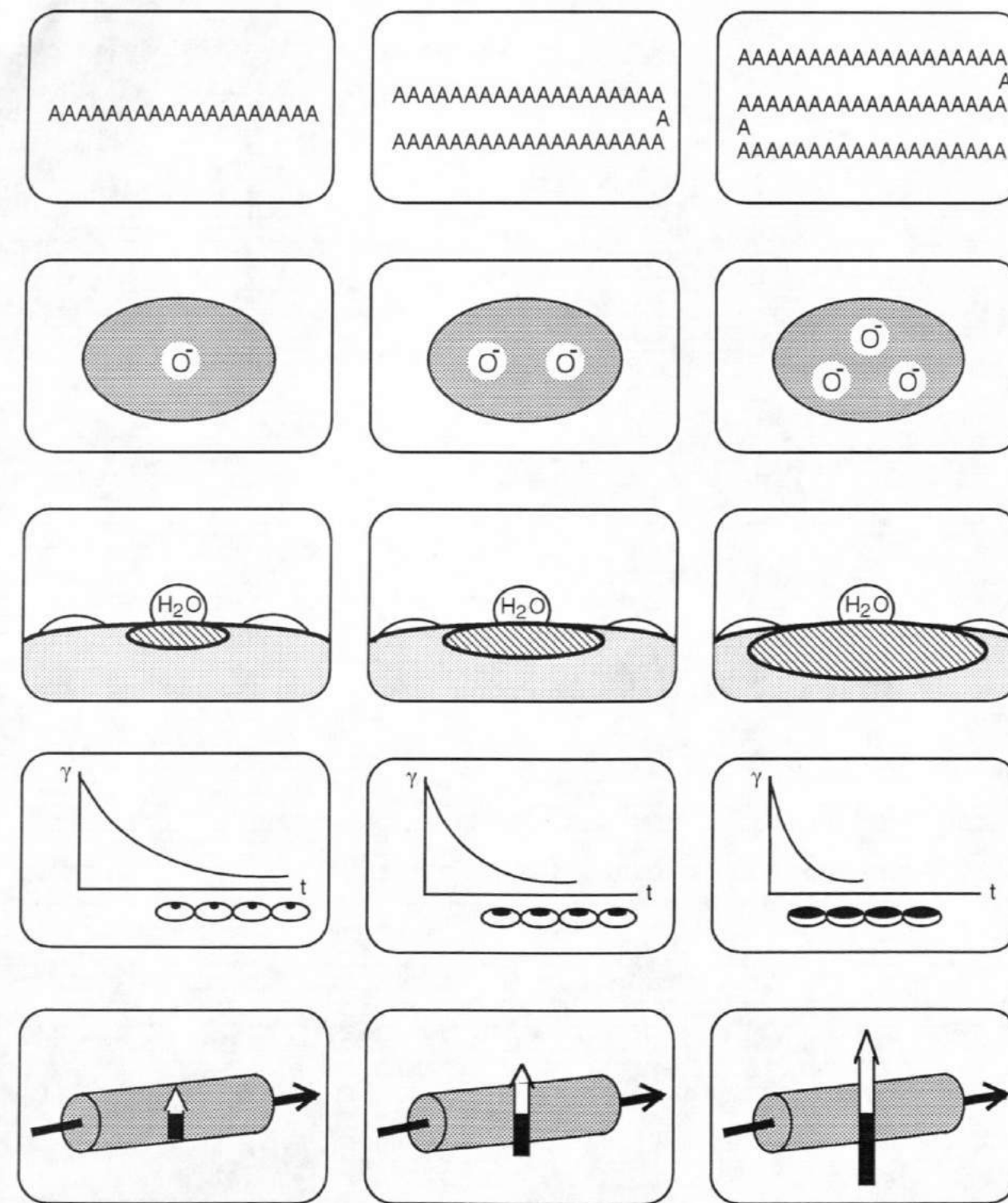
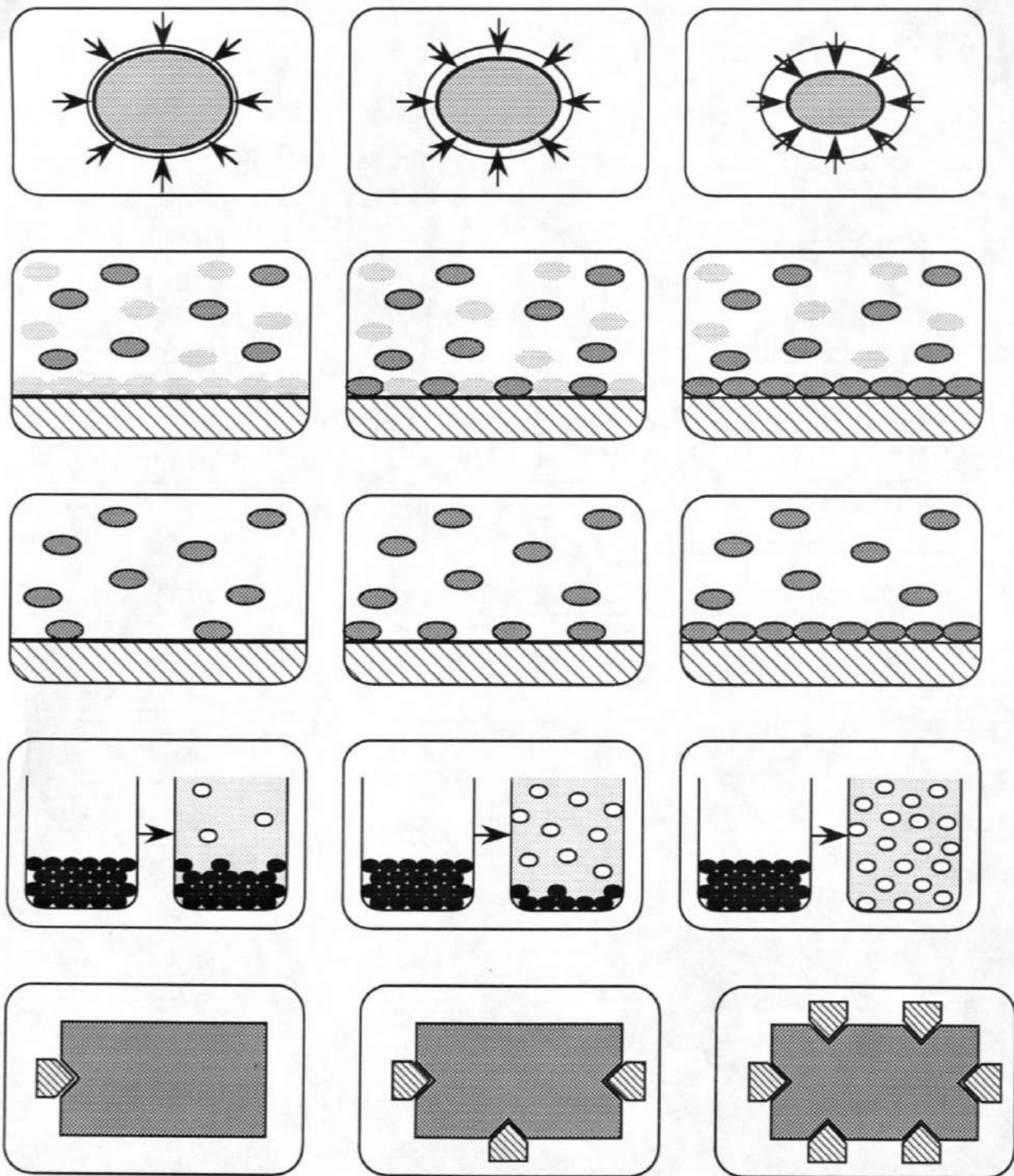
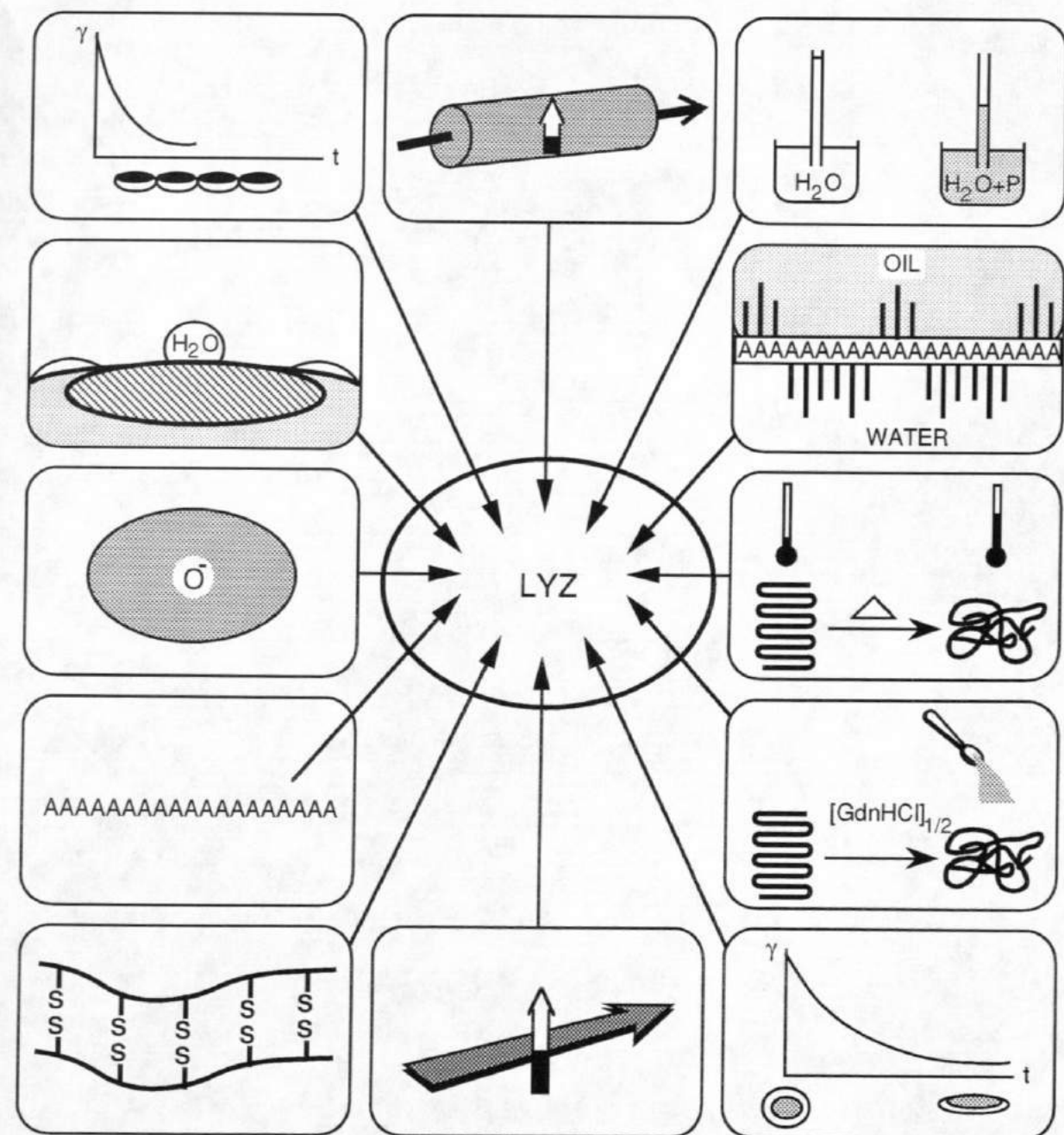
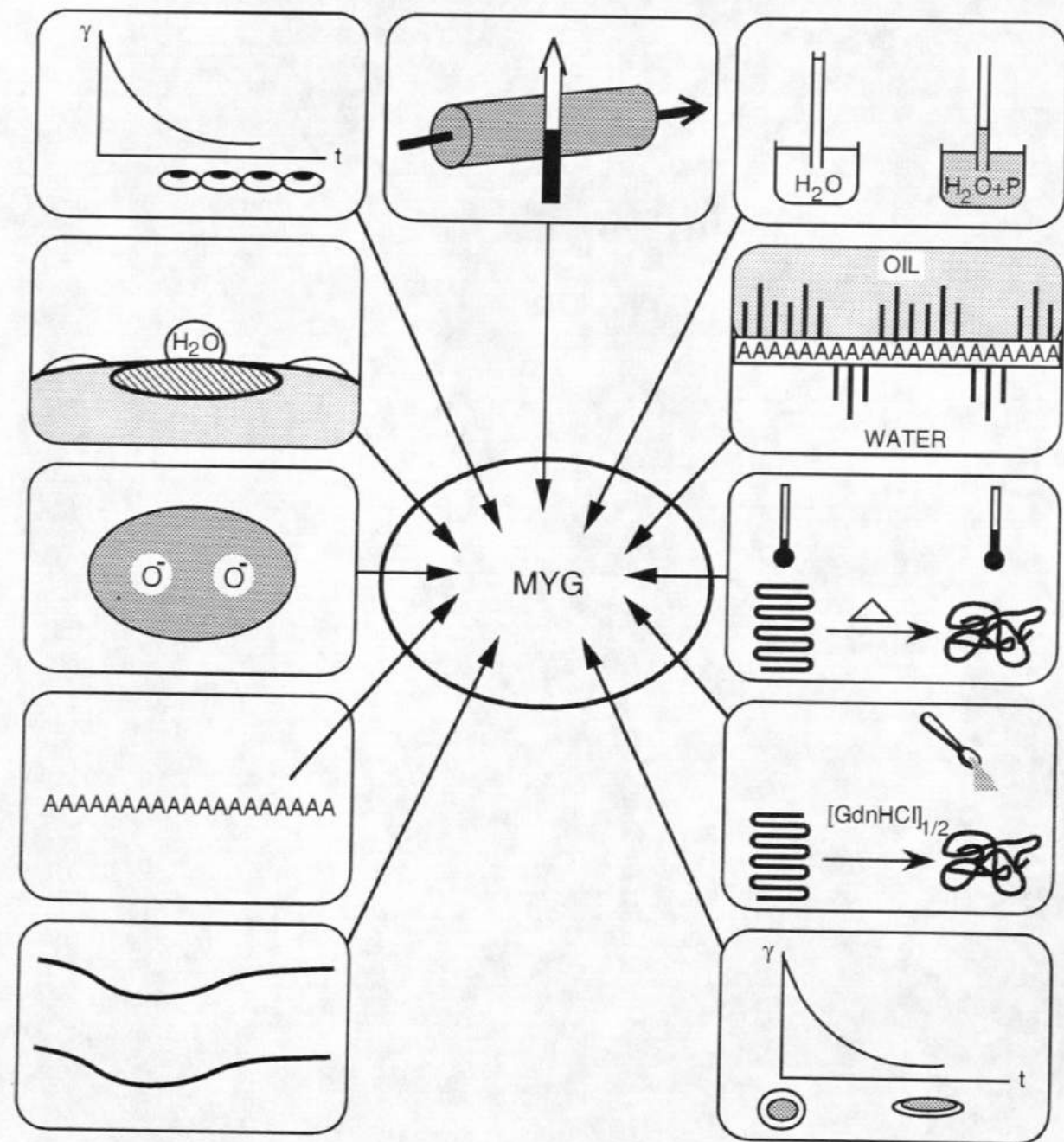
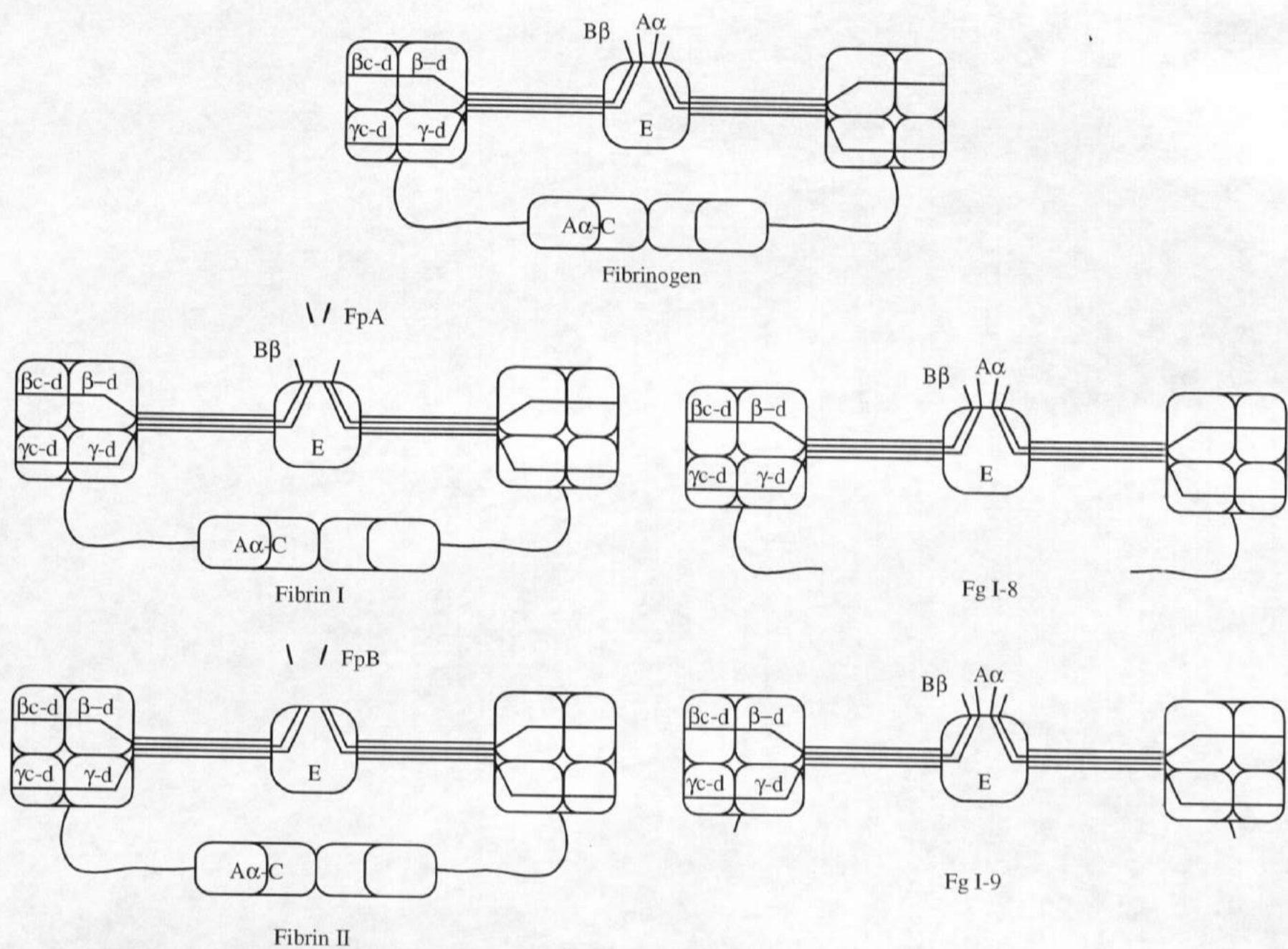


Fig. 2









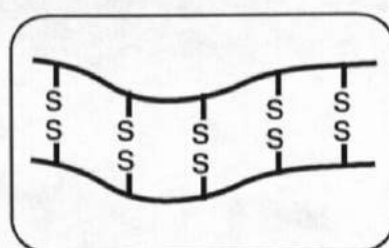
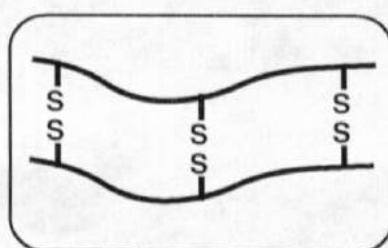
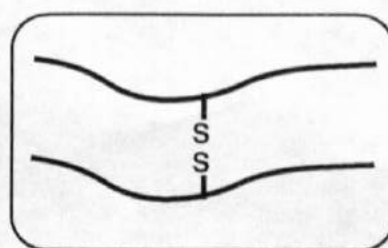
Fg I-8

Fg I-9

Parameter	Meaning	Icon representation		
		Low	Medium	High
Molecular weight	Size of protein	AAAAAAAAAAAAAAAAAAAA	AAAAAAAAAAAAAAAAAAAA AAAAAAAAAAAAAAAAAAAA AAAAAAAAAAAAAAAAAAAA	AAAAAAAAAAAAAAAAAAAA AAAAAAAAAAAAAAAAAAAA AAAAAAAAAAAAAAAAAAAA AAAAAAAAAAAAAAAAAAAA
Temperature of thermal denaturation	Thermal stability			
GdnHCl conc. of 50% denaturation	GdnHCl stability			
Hydraulic compressibility	Protein hardness			
Rate constant of γ at low bulk concentration	Process of surface denaturation			

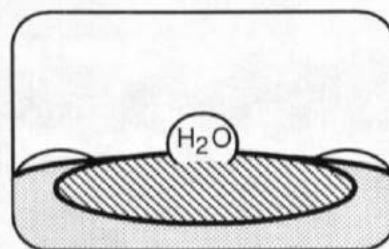
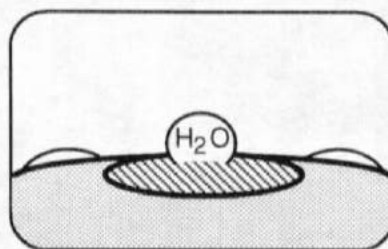
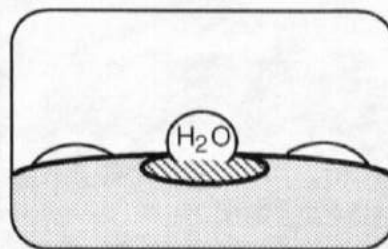
Number of
disulfide bonds

protein
structure
stability



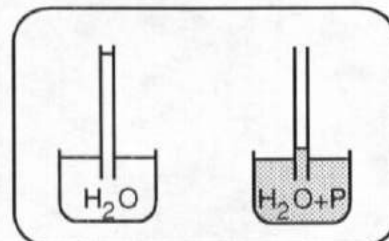
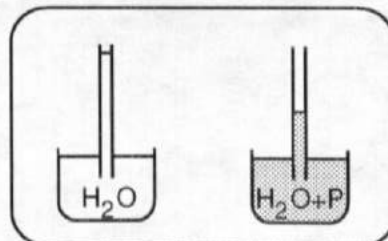
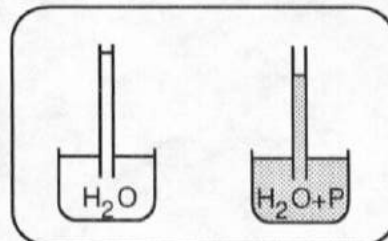
Effective
surface
hydrophobicity

Hydrophobicity
native states



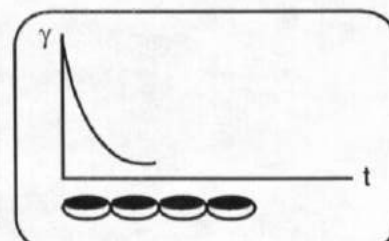
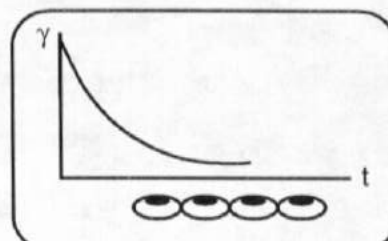
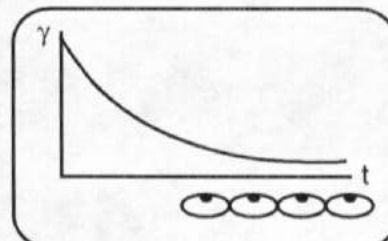
Steady-state
surface
pressure

Air/water
Surface
activity



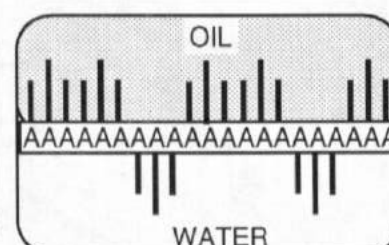
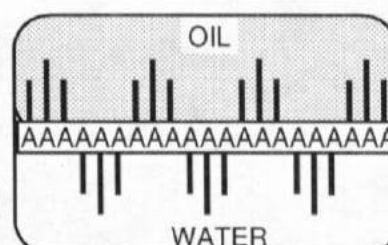
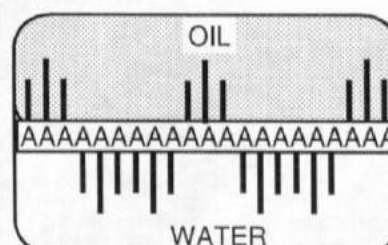
Rate constant
of γ at high bulk
concentration

Hydrophobicity
in native states



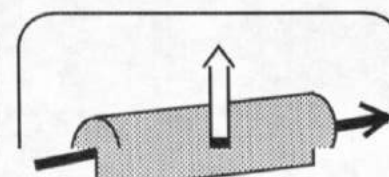
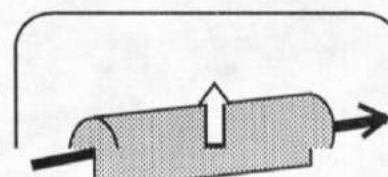
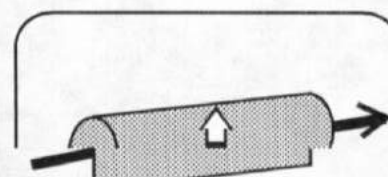
Ratio of
nonpolar
residues in
sequence

Estimated
hydrophobicity

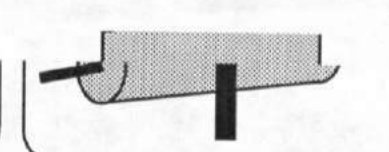
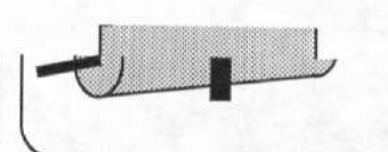
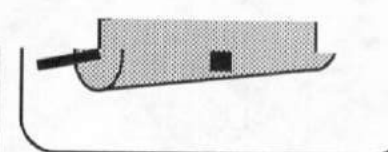


α -moment
multiplied by

Amphiphilicity
of α -helices

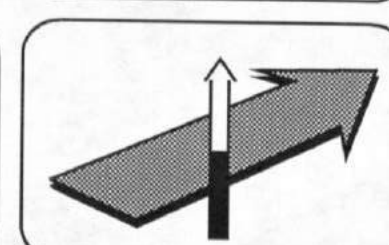
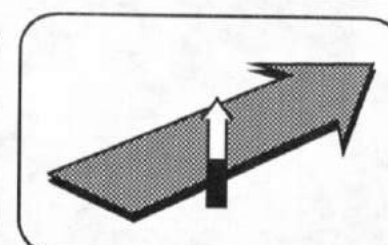
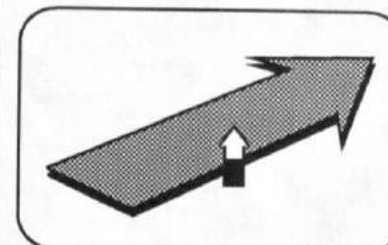


α -helix traction



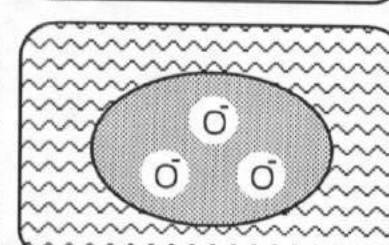
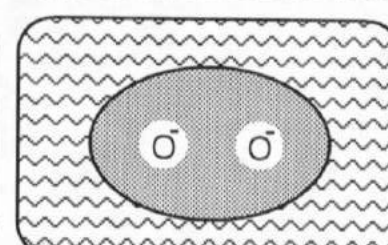
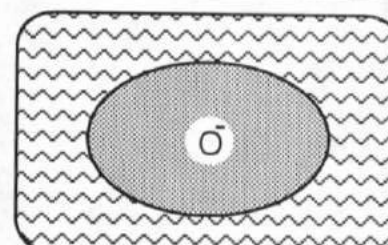
β -moment
multiplied by
 β -sheet fraction

Amphiphilicity
of β -sheets



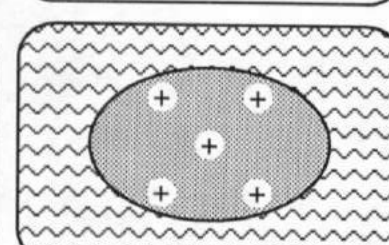
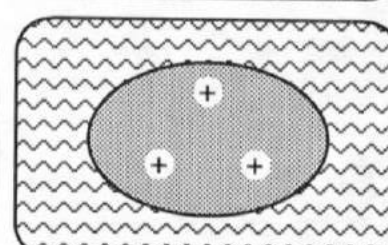
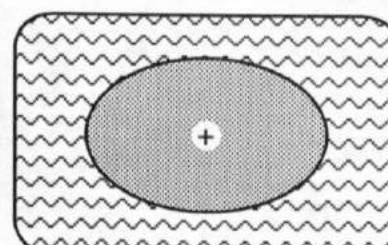
Accessible
negatively
charged
oxygen atoms

An inverse
measure of
hydrophobicity



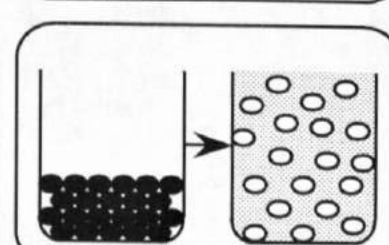
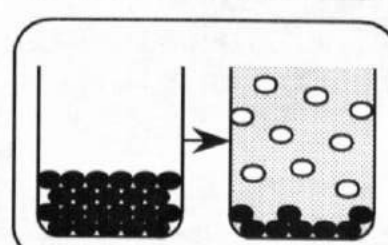
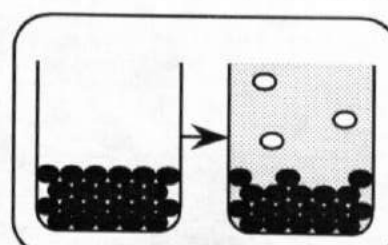
Surface
charge
density

Surface
charge and
hydrophilicity



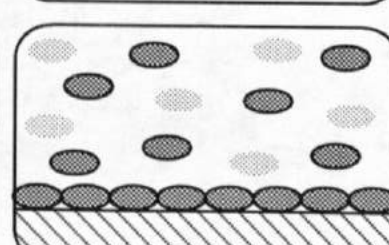
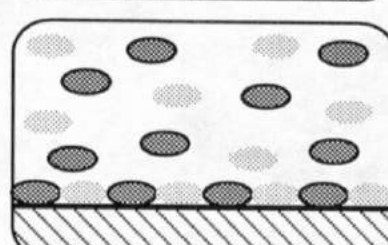
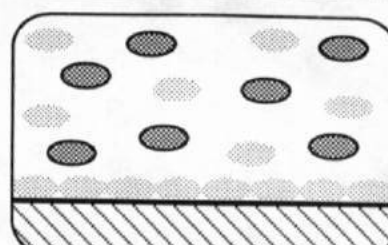
Quantities
dissolved at
physiological
conditions

Solution
solubility
and stability



Γ in competitive
protein
adsorption

Relative
surface
activity



Submitted to *Protein Engineering*

*~ 1996
unpublished*

THE STRUCTURE AND SURFACE PROPERTIES OF A MOLECULAR
MACHINE - FIBRINOGEN

L. Feng and J. D. Andrade*

Department of Bioengineering
2480 MEB
University of Utah
Salt Lake City, UT 84112

* To whom correspondence should be
addressed

ABSTRACT

This paper correlates molecular structure of fibrinogen to its properties at solid-water interfaces. These properties play an integral role in helping fibrinogen fulfill its biological function. We first introduce some unique surface (interfacial) attributes of fibrinogen by comparing it to other plasma proteins. We consider its surface concentration, effects of solid substrates, adsorption kinetics and isotherm⁵, competitive adsorption, structural adaptivity, and platelet-binding ability. We then examine its structural organization by utilizing available data from the primary structure, immunochemical properties, structural stability, solubility, microscopic images, X-ray diffraction data, and information on proteolytic fragments. By analyzing the amino acid sequences, we estimate the flexibility and hydrophobicity along individual polypeptide chains. We also inspect the net charge and hydrophobicity of individual structural domains. We pay special attention to the less addressed A α chain, especially its contribution to fibrinogen surface activity. While discussing its characteristics, we try to correlate the structure of fibrinogen to its properties. In conclusion, we claim that fibrinogen is a molecular machine designed for hemostasis. Its surface behavior is intimately related to its structure.

INTRODUCTION

Fibrinogen is an intriguing plasma protein. It plays an indispensable, two-fold role in the hemostasis of all vertebrate animals: blood coagulation and platelet aggregation (Doolittle, 1984 and 1994, Smith, 1984, Shafer and Higgins, 1988). The former process consists of the conversion of fibrinogen to fibrin through proteolysis of thrombin, and the polymerization of fibrin monomers into fibrin clots (Doolittle, 1984, Smith, 1984, Shafer and Higgins, 1988). The latter involves the binding of fibrinogen to platelets, linking them together or immobilizing them on a surface, and producing platelet aggregates. During hemostasis, these two processes usually happen simultaneously and are closely integrated with each other, resulting in a platelet-fibrin plug (hemostatic thrombus) (Plow et al., 1987).

Besides interacting with a variety of solution proteins (thrombin, plasmin, collagen), fibrinogen demonstrates two other special abilities with respect to the interfacial interaction: binding to cells, such as platelets, endothelium (Cheresh, 1989) and leukocytes (Altier et al., 1993), and associating with non-endothelial (non-biological) surfaces like those of prosthetic implants. Because of its cell adhering characteristics, fibrinogen is categorized as a cell adhesive protein, in the same family as fibronectin, vitronectin, and von Willebrand Factor (vWF) (Cheresh et al., 1989, Phillips et al., 1988, Fabrizio-Homan and Cooper, 1991, Berliner et al., 1988). All these adhesive proteins have at least one identified cell binding site, containing the Arg-Gly-Asp (RGD) sequence (Hawiger et al., 1989, Savage and Rugger, 1991). Once deposited on surfaces, these proteins often promote platelet deposition (Savage and Rugger, 1991, Lambrecht et al., 1986). It is well known that fibrinogen is a "sticky" protein, having a strong tendency to adsorb onto various surfaces from blood, plasma, or aqueous buffer solution. This property, combined with its platelet binding propensity, earns fibrinogen a notorious reputation: a protein causing thrombogenesis on biomaterials.

Unlike the relatively understood interaction between fibrinogen and platelets (Cheresh et al., 1989, Berliner et al., 1988), the origin of surface activity of fibrinogen has not been thoroughly studied. In order to obtain insight into the blood compatibility of biomaterials, we wish to know the following: How is the surface activity of fibrinogen related to its molecular structure? As a molecular machine, how does the structure of fibrinogen help its platelet binding function? Is fibrinogen unique or is it similar to other surface active proteins in terms of different levels of structure (primary, secondary, tertiary, and quaternary)?

Thanks to the rapid progress in molecular biology and protein science, a large volume of data concerning structure and properties of proteins have become available. We address ^{the} molecular structure of fibrinogen and correlate its structure to its surface properties, despite the fact that we lack many details of its secondary and tertiary structures. Here we focus on the physical interaction of fibrinogen with solid surfaces in aqueous solution, and its interactions with other proteins (antibodies) and platelets. We correlate the primary (amino acid sequences) and quaternary (domain) structures of fibrinogen to its surface and interfacial properties: adsorptivity at the solid-water interface and platelet binding induced by surface adsorption. The conversion of fibrinogen to fibrin in coagulation will not be specifically discussed, as this process has been intensively studied (Doolittle, 1984 and 1994, Smith, 1984, Shafer and Higgins, 1988) and is not directly related to the fibrinogen-surface interaction. Our analysis of amino acid sequences is based on human fibrinogen. General conclusions should be applicable to fibrinogens of other species, as their composition, polypeptide chains, and molecular configurations are very similar (Murakawa et al., 1993). Except for its antigenicity, we do not discuss ~~the~~ ^{the} fibrinogen-protein interaction ^{that is} beyond our focus here. The dependence of fibrinogen on divalent ~~cations~~ ^{cations} will not be discussed although it is very important (Phillips, et al., 1988).

INTERFACIAL PROPERTIES

Most proteins are amphipathic molecules and are therefore intrinsically surface active. However, their surface activities are different, manifested by their adsorbed amounts, the ratio of their surface concentration to their solution concentration in protein mixtures, and their resistance to being eluted or displaced from surfaces. Fibrinogen shows high surface activity at solid-water interfaces, as it typically exhibits high surface concentration, high competitiveness in adsorption from protein mixtures, and persistence on most surfaces, compared with most other proteins. Such a tendency to associate with a surface seems to be a generic property among the plasma proteins that participate in the blood coagulation process, including Hageman factor (Factor XII), high molecular weight ~~molecular~~ kininogen (HMWK), and plasma prekallikrein (Williams, 1987). This suggests that ~~the~~ high surface activity may be related to ~~their~~ biological functionality, as contact activation involves interactions between proteins and surfaces. It is thus beneficial to analyze how protein structure results in high surface activity, especially for fibrinogen. In this section, we briefly introduce some properties of fibrinogen related to its interactions with surfaces. Although these properties are well known, the interfacial behavior has not been clearly understood from a molecular structure point of view.

High adsorbed amount

Fibrinogen usually has a higher surface concentration than most other proteins adsorbed from solutions of equal bulk concentration (Absolom et al., 1987, Santerre et al., 1992, Feng and Andrade, 1994b, Baszkin and Lyman, 1982, Young et al., 1988, Wojciechowsky et al., 1986, Weathersby et al., 1977). Part of this is likely due to its high molecular weight; few fibrinogen molecules produce a large mass on a surface. However, as will be discussed later, being big is neither a necessary nor a sufficient factor for high deposition (Valerio et al., 1987). Other contributing factors include its strong lateral

interactions between individual molecules, producing close packed adsorbed fibrinogen films, and surface activity, resulting in the ability to reside on the surface of already adsorbed proteins, i.e., multilayer adsorption (Lahav, 1987, Feng and Andrade, 1994b, Pankowsky et al., 1990). ^{may} Compared with the more usually observed monolayer adsorption (Schmitt et al., 1983), ^{may} More fibrinogen ~~can~~ be accommodated because of such possible multilayer adsorption.

Low substrate influence

The adsorption of fibrinogen is less affected by variation in the nature of the surface (Kibing and Reiner, 1978, Slack and Horbett, 1992, Weathersby et al., 1977, Schmitt et al., 1983, Rapoza and Horbett, 1990), implying that fibrinogen readily interacts with different surfaces. Like other proteins, fibrinogen is usually adsorbed more on hydrophobic surfaces than on hydrophilic ones (Slack and Horbett, 1992), but the difference is smaller than ^{for other} most proteins. The main difference of surface concentration among proteins is on hydrophilic surfaces (Tengvall et al., 1992). An increase in hydrophilicity alone may not substantially reduce fibrinogen adsorption (Maechling-Strasser, 1989). For example, fibrinogen can adsorb on hydrophilic as well as on hydrophobic surfaces ⁱⁿ with similar amounts (Weathersby et al., 1977, Nygren et al., 1992). Fibrinogen even adsorbs more on a polyurethane when it is sulfonated and thus becomes more hydrophilic (Santerre et al., 1992, Okkema et al., 1991). Like other adhesive proteins, fibrinogen can bind to heparin, a negative but hydrophilic substance, presumably through electrostatic interactions with heparin-binding sites, similar to those of fibronectin, vitronectin, and vWF (Mohri and Ohkubo, 1993a).

Transient adsorption kinetics

The adsorption kinetics of fibrinogen from complex protein mixtures (e.g., plasma) on some hydrophilic surfaces like glass usually shows a maximum at a very short adsorption time, followed by decreasing surface concentration with time. Called the Vroman effect (Slack and Horbett, 1988 and 1992, Wojciechowsky et al., 1986), this phenomenon is believed to reflect a process where the adsorbed fibrinogen is gradually displaced by other even more surface active proteins, such as HMWK, factor XII, or high-density lipoprotein (HDL) (Poot et al., 1990, Brash et al., 1988). Such displacement of adsorbed proteins indicates that different proteins have different affinities for a particular surface and that protein adsorption is a dynamic process with continuous adsorption, desorption, and displacement at the interface.

Maximum in isotherms

When adsorbed from dilute plasma, the surface concentration of fibrinogen initially increases, passes a maximum, and decreases (Slack and Horbett, 1988, Wojciechowsky et al., 1986). The plasma concentration at which the maximum occurs seems to be higher on more hydrophobic surfaces (Horbett, 1984). This pattern is also considered to be related to displacement of fibrinogen. Competitivity increases as unoccupied surface adsorption sites become less frequent. In this case not only protein composition, but also its concentration and thus the protein surface occupancy play a role.

Competitive adsorptivity

Perhaps the best way to describe the high surface activity of fibrinogen is to compare the ratio of its surface concentration to solution concentration to those of other proteins in a multi-protein adsorption process (Kim and Lee, 1975, Bagnall, 1978, Lensen et al., 1984, 36, Norde, 1986, Park et al., 1991). The ratio represents the ability of a protein to occupy

surface sites and to resist being displaced, and it varies among proteins. Some proteins, such as albumin, can show considerable adsorption from single protein solutions, but its surface concentration may be drastically reduced in the presence of other proteins, even though these are trace proteins (Lensen et al., 1984, Feng and Andrade, 1994b). This more frequently occurs on a hydrophilic surface, for which the differences of the affinity are larger among different proteins (Feng and Andrade, 1994b). Albumin has a relatively low affinity for many solid surfaces, having a low inhibitory effect on adsorption of other proteins, or being easily displaced by many plasma proteins, including fibrinogen (Fabrizius-Homan and Cooper, 1991 and 1991a, Sunny and Sharma, 1991, Voegel et al., 1988). Acid glycoprotein is another representative protein with low surface activity (Feng and Andrade, 1994a). On the other hand, the adsorption of fibrinogen is much less affected by the presence of other proteins; on hydrophobic surfaces the adsorbed amount of fibrinogen from dilute plasma is comparable to that from the single protein solution (Feng and Andrade, 1994b). Instead of being displaced, fibrinogen often displaces other already adsorbed proteins (Voegel et al., 1988). The high surface affinity of fibrinogen can be further demonstrated by its ability to adhere on so called protein "repelling" surfaces, such as highly hydrophilic, polyethylene oxide and on protein-coated surfaces (Bergstrom et al., 1992, Amiji and Park, 1992, Okkema et al., 1991, Maechling-Strasser, 1989). Fibrinogen and other surface active proteins can adsorb on such surfaces in fairly large quantities (Lahav, 1987, Feng and Andrade, 1994b, Young et al., 1988, Fabrizio-Homan and Cooper, 1991).

Structurally labile protein

Some parts (or domains) of fibrinogen show a rather compliant organization, manifested by ease in surface induced denaturation (Bagnall, 1978, Katona et al., 1978, Feng and Andrade, 1994, Slack and Horbett, 1992) and low thermal denaturation

temperature (Privalov, 1982, Medved, et al., 1986), demonstrating that small external perturbations can cause a significant changes in its secondary and tertiary structures and thus properties. The conformational change is more easily revealed by means of proteolysis or antigen-antibody binding. After local cleavage by an enzyme or bonding to an antibody, fibrinogen often undergoes a global conformational change, expressing many neo-binding sites (see later discussion).

Platelet binding

Fibrinogen is very active in binding to platelets or other cells through the interaction of its particular residues with cellular receptors, membrane proteins (integrins). The binding not only immobilizes platelets onto a surface or brings them together to form a gel network, it can also activate the bound cells (Shiba et al., 1991, Ugarova et al., 1993).

STRUCTURAL CHARACTERISTICS AND THEIR CONSEQUENCES

A massive molecule with many molecular domains

Fig. 1 present a molecular model of human fibrinogen, adapted from several sources based on electron microscopic images (Mosesson et al., 1981, Gollwitzer et al., 1983, Weisel, et al., 1985, Beijbom et al., 1988), X-ray diffraction analyses of modified fibrinogens (Weisel, et al., 1985, Rao et al., 1991), and calorimetric measurements (Privalov, 1982). A dimer of molecular weight (Mw) of 340,000 daltons, fibrinogen consists of three pairs of nonidentical polypeptide chains and two pairs of oligosaccharides. The Mw of the A α chain is 66,066 (610 residues), B β chain 52,779 (461 residues), γ chain 46,406 (411 residues) (Shafer and Higgins, 1988), and each oligosaccharide 2,404 (Langer, 1988). There are a total of 29 interensemble, interchain, and intrachain disulfide bonds, three of them joining the two half molecules into a whole (Doolittle, 1994, Smith, 1984). Fibrinogen is converted to fibrin by thrombin which cleaves fibrinopeptide A 1-15

from the A α chain and fibrinopeptide B 1-14 from the B β chain. The three non-identical chains are descendents from a common ancestor (Doolittle, 1994); there is some homology among the amino-terminal (N-terminal) thirds of all three chains (15% between any two) (Watt et al., 1979). For the carboxyl terminal (C teminal) 2/3 ends, while there is little homology between the A α chain to any other two, the sequences of the B β chain and γ chain are about 40% identical (Doolittle, 1992). The negatively charged and hydrophilic carbohydrate moiety may contribute a repulsive force between fibringen or fibrin molecules, enhancing the solubility of fibringen and inducing fibrin to assemble into a normal clot (Townsend et al., 1982, Langer, 1988). They do not, however, have a large contribution to clottability (Nishibe and Takahashi, 1981).

There is no detailed experimental data on the secondary and tertiary structures of fibrinogen, as native fibrinogen has not been crystallized in a form suitable for X-ray diffraction. Measurements by CD, Raman spectroscopy, and FTIR indicate that the native molecule contains about 35% α -helix, 10-30% β -sheet, and 14% β -turn (Doolittle, 1992, Azpiazu and Chapman, 1992). The secondary structures of the γ chain has been predicted by Doolittle (1992) using homology methods.

The major structurally distinguishable regions of fibrinogen are (Fig. 1): a lone central E domain, two distal D domains, two α helical coiled coils, two α C domains, and a pair of junctions between the coiled coil and the α C domain. In the literature, the α C domain and the junction are considered as the α C domain (Medved et al., 1985). The E domain contains all the N terminal ends of the six polypeptide chains linked by disulfide bonds. This domain is also called N disulfide knot (N-DSK). The D domain consists of the C terminal ends of the B β and the γ chains, and a small portion of the A α chain. The coiled coil, made of three α -helices, connects the C domain to the E domain. It is interrupted in the middle by a small non-helical, plasmin sensitive region (Doolittle et al., 1994, Weisel and Papsun 1987). In the context of this paper, the α C domain contains only the C terminal

third of A α chain (391-610). The middle third of A α domain (200-390) connects the C terminus of the coiled coil (Medved et al., 1983) and the α C domain. Although this region has no definite domain structure (Weisel and Papsun 1987, Plow et al., 1983, Doolittle, 1990, Medved et al., 1983), we call it the α M domain (M standing for middle), in comparison with the α C domain, for convenience. As will see later, the striking difference between these two domains is their hydrophobicity. The masses are 32,600 for the E domain, 67,200 for the D domain, 42,300 for the 2/3 α C chain, and 39,100 for the coiled coil (Doolittle, 1984).

Fig. 2 shows the occurrence of the three chains in the different domains and subdomains for a half molecule (Litvinovich and Medved, 1988, Plow et al., 1983); and the sites of carbohydrates attachment (Doolittle, 1994) are also shown. There are four proteolytically splittable subdomains in the D domain, two of which are formed by the B β chain and two by the γ chain (Medved et al., 1986, Rao et al., 1991, Doolittle, 1992). The defined E or C domains are molecular domains in a fibrinogen molecule. They are not equivalent to fragment E (Mw 45,000) or D (Mw 100,000), degradation products from plasmin digestion, as the latter contain part of the coiled coil residues in addition to the corresponding domains (Azpiazu and Chapman, 1992). For example, fragment D contains the D domain plus part of the coiled coil residues (A α 105-197, β 134-461 and γ 63-411) (Litvinovich and Medved, 1988, Cierniewski, 1986a). Fibrinogen is susceptible to plasmin cleavage, producing different sized fragments depending upon the digestion conditions (Medved et al., 1986, Marder and Budzynski, 1975, Nieuwenhuizen, 1986). The plasmin cleavage sites along individual chains have been illustrated (Henschen, 1983).

Structure and properties of individual chains and domains

We propose that the surface properties of a global fibrinogen molecule are largely determined by its individual domains since they are separated and presumably behave more

or less independently during adsorption (Andrade et al., 1990). This domain approach is, of course, oversimplified, as the individual domains actually do not act alone. Nevertheless, our analysis will provide some important insight into this fascinating protein.

Net charge. Fig. 3 shows the net charges of individual domains of fibrinogen at pH 7.4. The data are calculated according to the amino acid composition of each domain, assuming that the charge of Glu and Asp is -1, Lys and Arg +1, His +0.33 (an average value for His), and the charge of carbohydrate. Since the ionization of His at pH 7.4 depends on the local environment (Stryer, 1981), we assume that one out of three His residues bears a unit positive charge (Doolittle, 1979). The values are an approximation because of the uncertainty of the charge of His and of the exact positions of chargeable residues (Andrade et al., 1990). According to the results of pH titration, fibrinogen bears a net charge of -7 at pH 7 (Valerio et al., 1987), which is close to our calculated value: -10.

As can be seen from Fig. 3, the E and D domains are negatively charged while the α C domain is positive. Neither the D nor α C domains have high net charge, though. The D subdomains have different net charges: both the B β and γ chains have net negative charges in the subdomains of their N terminal ends, but net positive charges in those of their C terminal ends. In cases where electrostatic interactions play a major role (usually on hydrophilic surfaces), fibrinogen may orient its appropriate domains to interact with the surface, depending on the charge of the substrate. For example, the D (or less probably E) domains, due to their negative net charges, may be favored to adsorb on positively charged hydrophilic surfaces. The slightly positively charged α C domain should be favorably attracted to negative surfaces. Even though the global fibrinogen molecule has a net negative charge (-10), a negative surface may be able to electrostatically adsorb it via the α C domains. This may be the mechanism for fibrinogen adsorbed from plasma onto negative surfaces like glass. For the same reason HMWK and Hageman factor can effectively displace already adsorbed fibrinogen from glass (Tengvall et al., 1992), because

both have domains with much higher positive charges, so both have much stronger interactions with glass. Fig. 4 clearly show a high density of positive charge region along the peptide chains of HMWK and Hageman factor, compared with the chains of fibrinogen. Low molecular weight kininogen (LMWK) does not have this region and, as expected, can not displace fibrinogen from glass.

Structural stability. Fig. 5 shows the thermal denaturation temperatures of fibrinogen at pH 8.5 (Privalov, 1982). The E domain and coiled coils are thermostable whereas the D and α C domains are thermolabile, suggesting that the D and α C domains have lower structural stability (Wahlgren et al., 1993). The D and α C domains are thus "soft" domains (Arai and Norde, 1992; Wei, et al.), readily changing their conformations due to mechanical shear or the presence of surface. Such potential for structural rearrangement may provide the domains with the ability to maximize their contact area and to optimize interaction with the surface during adsorption (Norde, 1986). As Fig. 6 illustrated, the A α chain in the α C domain is very flexible, especially in the α M domain, thanks to the predominant hydrophilic Ser and Gly residues (Doolittle, 1979). The softness of the α C domain may explain its disappearance from electron microscopical images; the microscopic substrate may have severely denatured the α C domain. Structural adaptivity of proteins is a very important parameter contributing to the adsorptivity. Both the D and α C domains should be more surface active than the other domains due to their tendency to conformationally alter (Norde and Favier, 1992, Wahlgren et al., 1993).

Hydrophobicity. Fig. 7 plots the hydrophathy of three polypeptide chains according to the Ponnuswamy scale (Ponnuswamy, 1993). The hydrophobicity order is γ chain > B β chain > A α chain. There are of course differences in the hydrophobicity among the three domains, due to the local hydrophobicity of the chains in different domains. The E and D domains apparently have comparable hydrophobicity, the α C domain is slightly more hydrophilic, and the α M domain has the highest hydrophilicity, which perhaps gives the C

terminal third of A α chain the ability to freely "swim" and move around in an aqueous environment. Yet the α C domain does have hydrophobic components which may result in associations between these domains or with the E domain (Medved et al., 1983). The hydrophobicity differences among the domains may also determine which domain is more favorable for adsorbing on a particular surface. The hydrophobic, soft D domain should be preferentially adsorbed onto hydrophobic surfaces via hydrophobic interactions, resulting in stronger adsorption. Both the D domain and α C domain may be involved due to their structural flexibility, in addition to their hydrophobicity.

The diversity of the hydrophobicity among the fibrinogen domains may be responsible for some confusion in the literature. There are very different results on the hydrophobicity of global fibrinogen, depending on the measuring techniques and thus what was measured. Absolom et al. (1987) claims that fibrinogen is more hydrophobic than IgG and albumin. The chromatographic data of Kibing and Reiner (1978) agree. The polar/nonpolar ratio of amino acid residues calculated by Paul et al. indicates that fibrinogen is more hydrophilic (Paul and Sharma, 1981). Through contact angle measurements, van Oss shows that fibrinogen is very hydrophilic (van Oss, 1990).

Immunogenicity and surface topography

Fibrinogen is a very active antigen and can elicit and bind to a large number of antibodies (Plow and Edgington, 1982). It is estimated that a single fibrinogen molecule can accommodate about 35 antibodies simultaneously at binding saturation (Telford et al., 1980). The exposure of individual chains to the solution can be detected by their ability to bind antibodies, for either native or conformationally altered fibrinogen. Fibrinogen has two kinds of epitopes: exposed epitopes on the surface of the native protein and "buried" (latent) epitopes that do not bind to their antibodies unless the native molecule is conformationally changed as a result of proteolysis, adsorption, or other perturbation

(Shiba et al., 1991, Plow and Edgington, 1982). Here, the term "buried" does not necessarily mean not in contact with solution; rather it means not accessible to antibodies, due to a variety of factors, including steric hindrance. As Fig. 8 indicated, the A α chain is the most surface exposed and readily cleaved by a wide variety of proteases (Plow et al., 1983, Henschen, 1983, Fair et al., 1987, Ugarova et al., 1993, Zamarron et al., 1990, Schielen et al., 1991). The γ chain is the least exposed (Plow et al., 1983, Tanswell et al., 1979), hidden in the E and D domains, and in the coiled coil (Cierniewski and Budzynski, 1987). Only 10% of antibodies raised to fibrinogen are against the γ chain (Plow and Edgington, 1982). A picture (Fig. 9(A)) of the accessibility of the three chains in native fibrinogen can be produced by analyzing their binding activity to a variety of antibodies (Tanswell et al., 1979, Plow and Edgington, 1982, Cierniewski and Budzynski, 1987, Fair et al., 1987, Ugarova et al., 1993). The exposures of domains can be ranked as highest for the α M domain, followed by the α C domain, then the D domain, with the E domain last. The coiled coil is very inactive in binding to antibodies in native fibrinogen. Interestingly, once fibrinogen is perturbed, this region seems to express more neo-epitopes than any other domain, whereas the α M domain has probably the fewest changes (Fig. 9(B)).

Immunochemical analysis is a sensitive tool to interrogate allosteric effects among the domains. Delicately balanced in structure, the global fibrinogen molecule has an amazing ability to respond by local structural alterations. For example, when fibrinogen is converted to fibrin, some latent epitopes of the γ chain of the C domain become expressed. That suggests that the information of the conformational changes induced at the N termini of α and β chains in the E domain is transmitted to the γ chain of the C domain (Zamarron et al., 1990). Reversibly, removal of the C terminal end of the A α chain in the α C domain will bring about conformational rearrangement of the central domain (Cierniewski et al., 1979). These phenomena suggest a model that in different environments domains have frequent

conformational interactions and communication (Plow et al., 1983, Fair et al., 1987). They function cooperatively and are not totally independent in action (Privalov, 1982). The coiled coil is likely a conduit for the transmission of allosteric changes from one domain to another (Plow et al., 1983).

Platelet binding sites

Native fibrinogen can bind to stimulated platelets, e.g., by thrombin, collagen, or adenosine diphosphate (ADP) (Phillips et al., 1988). Conformationally perturbed fibrinogen, e.g., through enzymatic cleavage or surface immobilization, can also bind to unstimulated fibrinogen. The binding often activates the bound platelets (Elam and Nygren, 1992). The fibrinogen molecule possesses six platelet binding sites (Fig. 9); all likely share common or mutually exclusive sites on the membrane glycoprotein IIb-IIIa (Plow et al., 1987, Phillips et al., 1988, Lam, 1986, Mohri and Ohkubo, 1993b, Andrieux et al., 1989). Three different pairs are located at the D domains (C terminal of γ 400-411), the two α C domains (RGDS of A α 572-575), and the two coiled coils (RGDF of A α 95-98), respectively (Savage and Rugger, 1991).

While the RGD sequence is a ubiquitous cell recognition region (Berliner et al., 1988), some cells like endothelium do not recognize γ 400-411 (Cheresh et al., 1989). The RGDF A α 95-98 region in native fibrinogen is not available to unstimulated platelets (Savage and Rugger, 1991). Even on adsorbed fibrinogen, this site may still not be accessible or not active enough, as unstimulated platelets do not attach to immobilized fragment E on some surfaces (Savage and Rugger, 1991), probably because the RGDF sequence is constrained by flanking residues and thus not accessible to the cell receptor (Cheresh et al., 1989, Hawiger et al., 1989). The RGDF sequence can be implicated in binding ADP-stimulated platelets (Andrieux et al., 1989). The RGDS sequence A α 572-575 of immobilized fibrinogen actively participates in binding to unstimulated platelets,

together with C terminus γ 400-411 (Savage and Rugger, 1991). The binding can lead to platelet activation, including aggregation and secretion (Shiba et al., 1991, Ugarova et al., 1993). Both regions also directly interact with ADP-activated platelets (Hawiger et al., 1989). Although both the $A\alpha$ and γ chains support platelet aggregation, the $A\alpha$ chain is only 20-25% as effective as the γ chain, and the RGD sequences of fibrinogen are thought to be not essential to this process (Farrel, 1992). In fact, the $A\alpha$ chain of fibrinogens of some species do not have the RGD sequence at all (Murakawa et al., 1993). This does not mean that these $A\alpha$ chains do not bind to platelets, however. They may bind to platelets via different sequences, like the C end of the γ chain. It has been speculated that all these cell sequences in a fibrinogen molecule cooperatively enhance the affinity of fibrinogen for platelets (Mohri and Ohkubo, 1993b).

Such a broad distribution of many cell binding sites may have more than a cooperative ^{significance} meaning (Fig. 9). Their presence is perhaps to ensure that fibrinogen preserves its cell binding ability under different circumstances. Evidence shows that the native, or near native, tertiary structure is essential for fibrinogen to bind to platelets (Shiba et al., 1991, Chinn et al., 1992, Rapoza and Horbett, 1990, Lindon et al., 1986), or for expression of its polymerization sites (Cierniewski et al., 1986). Severely denatured fibrinogen no longer binds to platelets. Since the platelet binding regions are spread throughout the molecule on different domains, fibrinogen is able to bind to platelets via different domains whenever they are available and intact. This multi-binding ability allows adsorbed fibrinogen of various adsorption states to interact with platelets in various adsorption states. Located on different domains with different surface properties, some of the platelet binding sites are likely protected from alteration by surface induced denaturation. Only certain domains are favored by a particular surface because their surface characteristics complement those of the surface (hydrophobicity, charge, hydrogen bonding, etc.). These domains are adsorbed and probably denatured, anchoring fibrinogen

on the surface. Other domains not directly interacting with the surface have their platelet binding sites intact. The cooperative functioning among the domains enables fibrinogen to interact with platelets while adhering to a surface. Depending on the type of surface, immobilization can be provided by a particular domain and platelet binding by another one. For instance, on glass it is likely that the αC domain adheres to the surface and the site on the D domain binds to platelets. On a hydrophobic or positively charged surface the D domain more likely adsorbs to the surface, leaving the αC domain free to interact with platelets. Again, the information of an adsorbed domain can be transmitted to a remote non-adsorbed domain activates its cell binding activity.

The platelets' binding process can be fast, while surface-induced denaturation can be slow. Immobilized fibrinogen may have bound to platelets and activated them prior to full scale denaturation of the adsorbed protein. That is probably why adsorbed fibrinogen can bind to platelets, before it is severely denatured. Some surfaces with microphase separation (Elam and Nygren, 1992), with balanced polar and non-polar character (Tengvall et al., 1992, Mori et al., 1986), or with high protein affinity (~~Feng and Andrade, in preparation~~) have better blood compatibility, as they can interact with different domains of fibrinogen, destroy the binding sites, and thus neutralize fibrinogen's ability to bind to platelets.

Importance of the C terminal 2/3 $A\alpha$ chain (αC chain)

Fibrinogen is usually considered to have a trinodular shape, the two distal D domains connected to the central E domain by the coiled coils, probably because only three nodules are readily seen by electron microscopy (Mosesson et al., 1981, Gollwitzer et al., 1983, Weisel, et al., 1985, Beijbom et al., 1988), although the αC domains are often near or on the E domain (Veklich et al., 1993). Nodules produced by the αC domains can occasionally be observed (Weisel, et al., 1985, Rudee and Price, 1981), however. As Rudee and Pric (1981) indicated, visibility of the αC domain strongly depended on the

sample substrates used. In contrast to the β and γ chains, the α C domain, and certainly the α M domain, are given less attention (Doolittle et al., 1979, Medved et al., 1985).

The α chains vary considerably among species, but their overall structures are similar (Doolittle, 1990, Murakawa et al., 1993), indicating they may play important roles. However, the biological function the α C chain, often called the protuberance or free swimming appendage, has not been clearly defined (Hirschbaum and Budzynski, 1988). The α C chain is not considered as a structural component for the formation of a fibrin clot, but it may be a factor promoting (Medved et al., 1985, Cierniewski and Budzynski, 1992), branching (Weisel and Papsun 1987), and stabilization (Koopman et al., 1993) of the normal assembly of fibrin structure. The fibrinogen with the α C chain portions deleted by plasmin digestion, called fragment X, shows retarded polymerization and lower clottability (Medved et al., 1983). From consideration of the adsorption of fibrinogen at solid-water interfaces, we discovered that the α C domain has ~~few~~ ^{several} very interesting properties that may be at least partly responsible for the surface activity of fibrinogen.

The conformation of the α C chain protuberance has not been completely solved. Although the α C chain seems to have neither α -helix nor β -sheet (Doolittle, R.F., 1994), the α C domain shows a compact structure (Weisel, et al., 1985), with a defined thermal denaturation temperature (Privalov, 1982, Medved et al., 1983). Due to its high hydrophilicity and low intramolecular cohesion, the α M domain provides high solubility, flexibility and mobility in solution. The α C domain is relatively hydrophobic. Analysis of its residues indicates that the α C domain contains a contrast feature: a hydrophobic (A α 470-520) region and a hydrophilic (A α 550-610) region (Fig. 7).

The α C domain is seemingly "eager" to interact with another α C domain and with other surfaces (Doolittle, 1979, Veklich et al., 1993), increasing the lateral interactions between fibrinogen molecules (Bagnall, 1978, Lensen et al., 1984). Electron microscopy reveals that a free 40,000 α C fragment cleaved by plasmin can bind to the α C domains of

fibrin (Veklich et al., 1993). It is reported that the α C domains have a complementary site so that they can be strongly tied together intra-molecularly (Privalov, 1982, Medved et al., 1983 and 1985, Siebenlist et al., 1993), forming a super α C domain (often seen as a fourth domain in electron microscopy (Weisel, et al., 1985). They also bind to the corresponding regions inter-molecularly, bringing individual fibrinogen or fibrin molecules together, guiding fibrin monomers to polymerize, and perhaps regulating the structure of fibrin clots (Medved et al., 1985, Weisel and Papsun, 1987). Covalent bonding between two α C chains from two fibrin molecules through Factor XIIIa further stabilizes fibrin polymers (Weisel and Papsun, 1987, Sobel, 1990). The α C domain can attach to the E domain, producing an apparently larger central domain (Gollwitzer et al., 1983) and blocking the antibody accessibility of the γ chain in the E domain (Plow et al., 1983) (Fig. 1). Because of its protruberant, uncertain position related to the bulk molecule, the α C chain prevents fibrinogen from crystallization. Only after the α C chain is deleted can the modified fibrinogen crystallize (Weisel, et al., 1985).

Association of the α C domains between fibrinogen molecules may be responsible for its susceptibility to precipitation and thus its low solubility (Young et al., 1988a). The interaction between α C chains can also enhance lateral interactions among adsorbed fibrinogen molecules, as adsorbed fibrinogen tends to show a uniform film (Murthy et al., 1987). Although the α C chain is more hydrophilic, fibrinogen actually becomes more soluble in an aqueous solution with part of the α C chain cut off by plasmin. The cleavage starts at the C terminus of the α C chain and gradually extends towards the N-terminus, producing modified fibrinogen with the α C chain of different lengths, including zero. The longer the α C segment chopped off, the higher the solubility of the modified fibrinogen (Mosesson, 1966 and 1983).

We think that the α C chain behaves as "pioneer" or "scout" for adsorption of fibrinogen. The α M domain has high flexibility and mobility, permitting high collision

frequencies of the α C chain with a surface. The α C domain readily alters its conformation due to the high structural adaptivity (softness); it has a tendency to adhere to a surface due to the hydrophobic and hydrophilic regions and can interact with negatively charged surfaces due to the net positive charge. The two domains are both indispensable to the stickiness of fibrinogen: the α C domain perhaps serving as the anchoring group and the α M domain providing the α C domain with a high collision rate. Studies indicate that the α C portions show a considerable homology among species (Murakawa et al., 1993). Although the α M portions show variability in sequences among species, the nature of their tandem repeats are conserved, differing only in their repeat lengths (Doolittle, 1990, Murakawa et al., 1993). The α M domain can also locally associate with itself or with the α M domain of another molecule. This segment possesses an accordion structure composed of a series of tight turns, a series of imperfect 13-residue repeats. Most of the β -turns contain a Trp residue at the fourth position, which acts as a "meager toe-hold" for inter-chain interaction. It is proposed that the stickiness of the α C chain is due to the exposure of "caged" Trp residues on the A α chain (Doolittle, 1979 and 1990). Fibrinogen is seen to attach to the solid surface by one end in a solution droplet, extending in the direction of the receding edge as the droplet continues to dry, suggesting that the α C domain is the first to adhere to the surface (Rudee and Price, 1981). Sometimes presumed dimers on hydrophilic silica may actually be single fibrinogen molecules with the α C chains stretched from the D domain (Nygren et al., 1992). In addition to electrostatic forces, the interaction between a hydrophilic surface and the hydrophilic α C chain may be due to the formation of hydrogen bonds between their mutual hydrophilic groups.

According to the above discussion, a number of predictions can be made. The interaction between the α C domain and a surface may not be strong as the chain is neither very hydrophobic nor very positively charged. Fibrinogen adsorbed on a surface via its α C domain alone can be readily displaced by other surface active proteins (Slack and Horbett,

1992), or eluted by sodium dodecyl sulphate (SDS) (Chinn et al., 1991 and 1992). This is perhaps related to the Vroman effect, because initially only the α C domain contacts the surface. Hydrophobic surfaces have a stronger retaining power through hydrophobic interactions with the α C domain, showing a less clear Vroman effect (Tengvall et al., 1992). Only when other domains later begin to adhere to the surface does fibrinogen adsorption become increasingly strong, reducing its displacement and elutability. Coexistence of albumin in solution can inhibit this process and thus slow down the decrease in SDS elutability (Chinn et al., 1991 and 1992). At low plasma concentration, fibrinogen has sufficient time to interact with the surfaces through all of its domains except for the α C domain, due to the small rate of collision. Thus the surface concentration increases with the plasma concentration. When the plasma concentration is high enough, the high collision rate of the many plasma proteins prevent fibrinogen from contacting the surface through domains other than the α C domain. Such adsorbed fibrinogen can of course be easily displaced, resulting in a decrease in surface fibrinogen with increasing plasma concentration. This is likely what happens in adsorption isotherms of fibrinogen as a function of plasma concentration. Strong interactions of the α C domain with a surface may be responsible for enhanced blood compatibility. Despite more fibrinogen adsorbed, sulfonated polyurethane has a longer thrombin time (Santerre et al., 1992, Silver et al., 1990). In addition to the suspected heparin like behavior of the sulfonated polyurethanes, the interaction may cause a change in adsorbed fibrinogen and increase its resistance to thrombin attack. *It was recently reported (Gato, 1994)*

We further suggest an important inference from the above discussion. Very large proteins often possess high surface activity compared with small proteins. However, mass is not necessarily the major driving force. For example, adsorbed fibrinogen (Mw 340,000) can be displaced by Hageman factor (Mw 78,000) ^{on} glass (Tengvall et al., 1992), or by hemoglobin (Mw 64,650) ^{on} several surfaces (Horbett, 1984). What really

that the α C domain ~~is~~ has a higher affinity for polyether urethane nylon 22 polymers than for glass or hydrophobic surfaces.

happens is that high Mw proteins usually contain highly diverse structures and ^a multidomain organization. These characteristics offer them the necessary ingredients for high surface activity, such as structural flexibility, high charge density, hydrophobicity, etc. As we have seen, the higher heterogeneity of structure can result in higher surface activity, as it provides the opportunity for proteins to optimize their interactions with surfaces.

CONCLUSIONS

Fibrinogen is a ^{well} ~~very smartly~~ built molecular machine. Its primary and domain structures dictate its physicochemical (including interfacial) properties, which are important in fulfilling its physiological and biochemical functions in hemostasis. It contains domains which ensure rapid, strong interactions with non-biological surfaces. Fibrinogen is not very hydrophobic (Jensen, personal communication) so it has a relatively high concentration in blood, but it is surface active enough to accumulate at an interface. Another characteristic is its ability to cooperatively change conformation, providing a sensitive structure to "sense" the presence of foreign surfaces and to react to such surfaces. Still another property is its ability to activate platelets through adsorption, while being only slowly inactivated by the presence of surfaces. By considering fibrinogen's "intelligence" and "stubbornness", we should be able to fool or disable fibrinogen, or other proteins by designing biomaterials with appropriate surfaces for better blood compatibility.

CONCLUSIONS

We thank the Center for Biopolymers at Interfaces, University of Utah, for supporting this work.

REFERENCES

- Absolom, D.R., Zingg, W. and Neumann, A.W. (1987) *J. Biomed. Mater. Res.*, **21**, 161-171.
- Altier, D.C., Plescia, J. and Plow, E.F. (1993) *J. Biol. Chem.*, **268**, 1847-1853.
- Amiji, M. and Park, K. (1992) *Biomaterials*, **13**, 682-692.
- Andrade, J.D., Hlady, V., Wei, A-P. and Golander, C-G. (1990) *Croatica Chem. Acta*, **63**, 527-538.
- Andrieux, A., Hudry-Clergeon, G., Ryckewaert, J.J., Chapel, A., Ginsberg, M.H., Plow, E.F. and Marguerie, G. (1989) *J. Biol. Chem.*, **264**, 9258-9265.
- Arai, T. and Norde, W., *Colloids and Surfaces*, **51**, 1-15 (1990).
- Azpiazu, I. and Chapman, D. (1992) *Biochim. Biophys. Acta*, **1119**, 268-274.
- Bagnall, R.D. (1978) *J. Biomed. Mater. Res.*, **12**, 203-217.
- Beijbom, L., Larsson, U., Kaveus, U. and Hebert, H. (1988) *J. Ultrastruct. Mol. Struct. Res.*, **98**, 312-319.
- Baszkin, A. and Lyman, D.J. (1982) In Winter, G.D., Gibbons, D.F. and Plenk, H. (eds.), *Biomaterials 1980*. Wiley, Chichester, pp. 393-397.
- Bergstrom, K., Holmberg, K., Safran, J., Hoffman, A.S., Edgell, M.J., Kozlowski, A., Hovanes, B.A. and Harris, J.M. (1992) *J. Biomater. Sci., Polym. Ed.*, **3**, 375-388.
- Berliner, S.A., Roberts, J.R., Thorn, M.L. and Ruggeri, Z.M. (1988) *Pept. Res.*, **1**, 60-64.
- Brash, J.L., Scott, C.F., ten Hove, P., Wojciechowski, P. and Colman, R.W. (1988) *Blood*, **71**, 932-939.
- Cheresh, D.A., Berliner, S.A., Vicente, V. and Ruger, Z.M. (1989) *Cell*, **58**, 945-953.
- Chinn, J.A., Posso, S.E., Horbett, T.A. and Ratner, B.D. (1991) *J. Biomed. Mater. Res.*, **25**, 535-555.
- Chinn, J.A., Ratner, B.D. and Horbett, T.A. (1992) *Biomaterials*, **13**, 322-332.
- Cierniewski, C.S. (1979) *Thromb. Res.*, **14**, 747-764.

- Cierniewski, C.S., Kloczewiak, M. and Budzynski, A.Z. (1986) *J. Biol. Chem.*, **261**, 9116-9121.
- Cierniewski, C.S. (1986a) *Biochim. Biophys. Acta*, **261**, 9116-9121.
- Cierniewski, C.S. and Budzynski, A.Z. (1987) *J. Biol. Chem.*, **262**, 13896-13900.
- Cierniewski, C.S. and Budzynski, A.Z. (1992) *Biochemistry*, **31**, 4248-4253.
- Doolittle, R.F., Watt, K.W.K., Cottrell, B.A., Strong, D.D. and Riley, M. (1979) *Nature*, **280**, 464-468.
- Doolittle, R.F. (1984) *Ann. Rev. Biochem.*, **53**, 195-229.
- Doolittle, R.F. (1990) In Liu, C.Y. and Chien, S. (eds.), *Fibrinogen, thrombosis, coagulation, and fibrinolysis*. Plenum, New York, pp. 25-37.
- Doolittle, R.F. (1992) *Protein Sci.*, **1**, 1563-1577.
- Doolittle, R.F. (1994) In Stamatoyannopoulos, G. et al. (eds.), *The molecular basis of blood diseases, 2nd Ed.* Saunders, Philadelphia, pp. 701-723.
- Elam, J.H. and Nygren, H. (1992) *Biomaterials*, **13**, 3-8.
- Fabrizius-Homan, D.J. and Cooper, S.L. (1991) *J. Biomater. Sci., Polym. Ed.*, **3**, 27-47.
- Fabrizius-Homan, D.J. and Cooper, S.L. (1991a) *J. Biomed. Mater. Res.*, **25**, 953-971.
- Fair, D.S., Edgington, T.S. and Plow, E.F. (1987) *J. Biol. Chem.*, **256**, 8018-8023.
- Farrel, D.H., Thiagarajan, P., Chung, D.W. and Davie, E.W. (1992) *Proc. Natl. Acad. Sci., USA*, **89**, 10792.
- Feng, L. and Andrade, J.D. (1994), *J. Biomed. Mater. Res.*, in press.
- Feng, L. and Andrade, J.D. (1994a) *Colloids and Surfaces*, in press.
- Feng, L. and Andrade, J.D. (1994b) *Biomaterials*, in press.
- Gollwitzer, R., Bode, W. and Karges, H.E. (1983) *Thromb. Res.*, **suppl 5**, 41-53.
- Hawiger, J., Kloczewiak, M., Bednarek, M.A. and Timmons, S. (1989) *Biochemistry*, **28**, 2909-2914.
- Henschen, A. (1983) *Thromb. Res., Suppl. 5*, 26-39.

- Hirschbaum, N. and Budzynski, A.Z. (1988) In Mosesson, M.W., Amrani, D.L., Siebenlist, K.R. and DiOrio, J.P. (eds.), *Fibrinogen 3: biochemistry, biological functions, gene regulation and expression*. Excerpta Medica, Amsterdam, pp. 297-300.
- Horbett, T.A. (1984) *Thromb. Haemostas.*, **51**, 174-181.
- Katona, E., Neumann, A.W. and Moscarello, M.A. (1978) *Biochim. Biophys. Acta*, **534**, 275-285.
- Kibing, W. and Reiner, R.H. (1978) *Chromatographica*, **11**, 83-88.
- Kim, S.W. and Lee, R.G. (1975) In Baier, R.E. (ed.) *Applied chemistry at protein interfaces*, ACS, Washington, DC, pp. 218-229.
- Koopman, J., Haverkate, F., Grimbergen, J., Lord, S.T., Mosesson, M.W., DiOrio, J.P., Siebenlist, K.S., Legrand, C., Soria, J. and Soria, C. (1993) *J. Clin. Invest.*, **91**, 1637-1643.
- Lahav, J. (1987) *J. Colloid Interface Sci.*, **119**, 262-274.
- Lam, S.C.-T., Plow, E.F., Smith, M.A., Andrieux, A., Ryckweert, J.-J., Margueie, G. and Ginsberg, M.H. (1986) *J. Biol. Chem.*, **262**, 947-950.
- Lambrecht, L.K., Young, B.R., Stafford, R.E., Park, K., Albrecht, R.M., Mosher, D.F. and Cooper, S.L. (1986) *Thromb. Res.*, **41**, 99-117.
- Langer, B.G. (1988) In Mosesson, M.W., Amrani, D.L., Siebenlist, K.R. and DiOrio, J.P. (eds.), *Fibrinogen 3: biochemistry, biological functions, gene regulation and expression*. Excerpta Medica, Amsterdam, pp. 63-68.
- Lensen, H.G.W., Bargeman, D., Bergveld, P., Smolders, C.A. and Feijen, J. (1984) *J. Colloid Interface Sci.*, **99**, 1-8.
- Lindon, J., Kushner, L., Merrill, E.W. and Salzman, E.W. (1986) *Blood*, **68**, 355-362.
- Litvinovich, S.V. and Medved, L.V. (1988) *Mol. Biol.*, **22**, 744-752.

- Maechling-Strasser, C., De Jardin, P., Galin, J.C. and Schmitt, A. (1989) *J. Biomed. Mater. Res.*, **24**, 1385-1393.
- Marder, V.J. and Budzynski, A.Z. (1975) *Thrombos. Diathes. Haemorrh.*, **33**, 199-207.
- Medved, L.V., Gorkun, O.V. and Privalov, P.L. (1983) *FEBS Lett.*, **160**, 291-295.
- Medved, L.V., Gorkun, O.V., Manyakov, V.F. and Belitser, V.A. (1985) *FEBS Lett.*, **181**, 109-112.
- Medved, L.V., Litvinovich, S.V. and Privalov, P.L. (1986) *FEBS*, **202**, 298-302.
- Mohri, H. and Ohkubo, T. (1993a) *Arch. Biochem. Biophys.*, **303**, 27-31.
- Mohri, H. and Ohkubo, T. (1993b) *Peptides*, **14**, 353-357.
- Mori, A., Ito, Y., Sisido, M. and Imanishi, Y. (1986) *Biomaterials*, **7**, 386-392.
- Mosesson, M.W. (1966) *Biochemistry*, **5**, 2829-2835.
- Mosesson, M.W., Hainfeld, J., Wall, L. and Haschemeyer, R.H. (1981) *J. Mol. Biol.*, **153**, 695-718.
- Mosesson, M. (1983) *Ann. N.Y. Acad. Sci.*, 97-113.
- Murakawa, M., Okamura, T., Kamura, T., Shibuya, T., Harada, M. and Niho, Y. (1993) *Thromb. Haemost.*, **69**, 351-360.
- Murthy, K.D., Diwan, A.R., Simmons, S.R., Albrecht, R.M. and Cooper, S.L. (1987) *Scanning. Microsc.*, **1**, 765-73.
- Nieuwenhuizen, W. (1986) In Muller-Berghaus, G. Scheefers-Borchel, U., Selmaye, E. and Henschen, A. (eds.), *Fibrinogen and its derivatives*. Excerpta Medica, Amsterdam, pp. 245-256.
- Nishibe, H. and Takahashi, N. (1981) *Biochim. Biophys. Acta*, **661**, 274-279.
- Norde, W. (1986) *Adv. Colloid Interface Sci.*, **25**, 267-340.
- Norde, W. and Favier, J.P. (1992) *Colloids and Surfaces*, **64**, 87-93.
- Nygren, H., Stenberg, M. and Karlsson, C. (1992) *J. Biomed. Mater. Res.*, **26**, 77-91.

- Okkema, A.Z., Visser, S.A. and Cooper, S.L. (1991) *J. Biomed. Mater. Res.*, **25**, 1371-1395.
- Pankowsky, D.A., Ziats, N.P., Topham, N.S., Ratnoff, O.D. and Anderson, J.M. (1990) *J. Vasc. Surg.*, **11**, 599-606.
- Park, K., Mao, F.W. and Park, H. (1991) *J. Biomed. Mater. Res.*, **25**, 407-411.
- Paul, L. and Sharma, C.P. (1981) *J. Colloid Interface Sci.*, **84**, 546-549.
- Phillips, D.R., Charo, I.F., Parise, L.V. and Fitzgerald, L.A. (1988) *Blood*, **71**, 831-843.
- Plow, E.F. and Edgington, T.S. (1982) *Semin. Thromb. Hemostasis*, **8**, 36-56.
- Plow, E.F., Edgington, T.S. and Cierniewski, C.S. (1983) *Ann. N.Y. Acad. Sci.*, **408**, 44-59.
- Plow, E.F., Marard, G. and Ginsberg, M. (1987) *Biochem. Pharmacology*, **36**, 4035-4040.
- Ponnuswamy, P.K. (1993) *Prog. Biophys. Mol. Biol.*, **59**, 57-103.
- Poot, A., Beugeling, T., van Aken, W.G. and Bantjes, A. (1990) *J. Biomed. Mater. Res.*, **24**, 1021-1036.
- Privalov, P.L. (1982) *J. Mol. Biol.*, **159**, 665-683.
- Ragone, R., Facchiano, F., Facchiano, A., Facchiano, A.M. and Colonna, G. (1989) *Protein Engineering*, **2**, 479-504.
- Rao, S.P.S., Poojary, M.D., Elliott, B.W., Melanson, L.A., Oriel, B. and Cohen, C. (1991) *J. Mol. Biol.*, **222**, 89-98.
- Rapoza, R.J. and Horbett, T.A. (1990) *J. Biomed. Mater. Res.*, **24**, 1263-1287.
- Rudee, M.L. and Price, T.M. (1981) *Ultramicroscopy*, **7**, 193-195.
- Santerre, J.P., ten Hove, P., VanderKamp, N.H. and Brash, J.L. (1992) *J. Biomed. Mater. Res.*, **26**, 39-57.
- Savage, B. and Rugger, Z.M. (1991) *J. Biol. Chem.*, **266**, 11227-11233.
- Sato, H. (1994) *Abst. Amer. Chem. Soc.*, **207**, COL-92.

- Schielen, W.J., Adam, H.P., van Leuven, K., Voskuilen, M., Tesser, G.I. and Nieuwenhuizen, W. (1991) *Blood*, **15**, 2169-2173.
- Schmitt, A., Varoqui, R., Uniyal, S., Brash, J.L. and Pusiner, C. (1983) *J. Colloid Interface Sci.*, **92**, 145-156.
- Shafer, J.A. and Higgins, D.L. (1988) *CRC-Crit. Rev. Clin. Lab. Sci.*, **26**, 1-41.
- Shiba, E., Lindon, J.N., Kushner, L., Matsueda, G.R., Hawiger, J., Kloczewiak, M., Kudryk, B. and Salzman, E.W. (1991) *Am J. Physiol.*, **260**, C965-C974.
- Siebenlist, K.R., Mosesson, M.W., DiOrto, J.P., Soria, J., Soria, C. and Caen, J.P. (1993) *Blood Coagul. Fibrinolysis*, **4**, 61-65.
- Silver, J.H., Hart, A.P., Jozefowicz, M. and Cooper, S.L. (1990) *Trans. Soc. Biomat.*, **13**, 139.
- Slack, S.M. and Horbett, T.A. (1988) *J. Colloid Interface Sci.*, **124**, 535-551.
- Slack, S.M. and Horbett, T.A. (1992) *J. Biomed. Mater. Res.*, **26**, 1633-1649.
- Smith, G.F. (1984) In Machovich, R. (ed.), *The thrombin Vol.1*. CRC-Press, Boca Raton, FL, Chapter 4.
- Sobel, J.H., Thibodeau, C.A., Kolks, M.A. G. and Canfield, R.E. (1990) *Biochemistry*, **29**, 8907-8916.
- Stryer, L. (1981) *Biochemistry*, 2nd ed. Freeman, New York, Chapter 1.
- Sunny, M.C. and Sharma, C.P. (1991) *J. Biomater. Appl.*, **6**, 89-98.
- Tanswell, P., Gollwitzer, R., Stan-Lotter, H. and Timpl, R. (1979) *Thrombos. Haemostas.*, **41**, 702-708.
- Telford, J.N., Nagy, J.A., Hatcher, P.A. and Scheraga, H.A. (1980) *Proc. Natl. Acad. Sci. USA*, **77**, 2372-2376.
- Tengvall, P., Askendal, A., Lundstrom, I. and Elwing, H. (1992) *Biomaterials*, **13**, 367-374.

- Townsend, R.R., Hilliker, E., Li, Y-T., Laine, R.A., Bell, W.R. and Lee, Y.C. (1982) *J. Biol. Chem.*, **257**, 9704-9710.
- Ugarova, T.P., Budzynski, A.Z., Shattil, S.J., Ruggeri, Z.M., Ginsberg, M.H. and Plow, E.F. (1993) *J. Biol. Chem.* 268, 21080-21087
- Valerio, F., Balducci, D. and Lazzarotto, A. (1987) *Environ. Res.*, **44**, 312-320.
- van Oss, C.J. (1990) *J. Protein Chem.*, **9**, 487-491.
- Veklich, Y.I., Gorkun, O.V., Medved, L.V., Nieuwenhuizen, W. and Weisel, J.W. (1993) *J. Biol. Chem.*, **268**, 13577-85.
- Voegel, J.C., Pefferkorn, E. and Schmitt, A. (1988) *J. Chromatogr.*, **428**, 17-24.
- Watt, K.W.K., Takagi, T. and Doolittle, R.F. (1979) *Biochemistry*, **18**, 68-76.
- Wahlgren, M.C., Paulsson, M.A. and Arnebrant, T. (1993) *Colloid and Surfaces A: Physicochem. Eng. Aspects*, **10**, 139-149.
- Wei, A-P, Herron, J.N., and Andrade, J-D. (1990) *From Clone to Clinic*. Kluwer Pub. and Schellekens, H (eds). Amsterdam pp-305-313.
- Weisel, J.W., Stauffacher, C.V., Bullitt, E. and Cohen, C. (1985) *Science*, **230**, 1388-1391.
- Weisel, J.W. and Papsun, D.M. (1987) *Thromb. Res.*, **47**, 155-163.
- Weathersby, P.K., Horbett, T.A. and Hoffman, A.S. (1977) *J. Bioengineering*, **1**, 393-410.
- Williams, D.F. (ed.), (1987) *Blood compatibility Vol.1*. CRC-Press, Boca Raton, FL, Chapter 2.
- Wojciechowsky, P., ten Hove, P. and Brash, J.L. (1986) *J. Colloid Interface Sci.*, **111**, 455-465.
- Young, B.R., Pitt, W.G. and Cooper, S.L. (1988) *J. Colloid Interface Sci.*, **124**, 28-43.
- Young, B.R., Pitt, W.G. and Cooper, S.L. (1988a) *J. Colloid Interface Sci.*, **125**, 246-260.
- Zamarron, C., Ginsberg, M.H. and Plow, E.F. (1990) *Thromb. Haemostats*, **64**, 41-46.

FIGURE CAPTIONS

- Fig. 1 Molecular model of fibrinogen and its individual domains.
- Fig. 2 Peptide segments that are included in individual domains of human fibrinogen.
- Fig. 3 Net charges on individual domains and subdomains.
- Fig. 4 Charge distributions along three polypeptides of human fibrinogen A α chain, human HMWK, and human Hagemen factor (Factor XII). The charge of His is shown as +1. HMWK and Hagemen factor have very dense positive charge between 400 to 510 and 290 to 400, respectively.
- Fig. 5 Thermal denaturation temperatures of fibrinogen.
- Fig. 6 Flexibility of human fibrinogen A α chain, computed using Ragone et al. (1989) scale.
- Fig. 7 Hydropathy of three polypeptide chains of human fibrinogen, computed using Ponnuswamy (1993) scale.
- Fig. 8 Antibody exposures of three polypeptide chains of human fibrinogen.
- Fig. 9 Epitopes of fibrinogen on both native (A) and conformationally altered molecules.

The calibration curve (Fig. 4) obtained by the NPM agrees with Min's data¹ and predicts a linear range from 1 nM up to about 100 μ M. Higher [NADH] results in enzyme saturation for [BL] used. The lower limit of the NADH linear range from Min's data is related to detector sensitivity and background signal. We scanned different [RCHO] from 0.06 mM to 600 mM to simulate the RCHO inhibition using the NPM with the same reaction conditions in Fig. 4 except the initial [NADH] at 10 μ M. We obtained a light intensity maximum at [RCHO] 6 mM, which agrees with the experiment. This shows that the Baldwin *et al.* model rate constants 1 are appropriate for our conditions.¹ Other conditions such as the ratio of OR/BL are also very important.¹

Other than peak height, there are initial rate and integration over a certain time period as parameters to analyse the calibration. We also evaluated the effect of [BL] on the light output profile. [BL] was scanned from 1 pM to 100 pM. The light intensity peak height is proportional to the [BL] in this NADH concentration range. But the shape and the decay of the emission kinetics are the same.

In conclusion the NPM simulates the NADH \rightarrow FMNH₂ \rightarrow light reaction kinetics and it fits with certain experimental data and provides a meaningful calibration curve. The NPM provides a basis for the modelling and simulation of analyte-specific bacterial bioluminescence-based biosensors. We are continuing to revise and optimise the NPM for different analytical conditions.

ACKNOWLEDGEMENTS

We thank Dr. DJ Min and DA Bartholomeusz for helping us with the bioluminescence system and the instrument.

REFERENCES

1. Min DJ. Toward specific biosensors based on bacterial bioluminescence. Ph.D. Thesis, University of Utah, 1999.
2. Francisco WA, Abu-Soud HM, Raushel FM, Baldwin TO. Studies on the kinetic mechanism of the bacterial luciferase-catalyzed reaction. In: Hastings JW, Kricka LJ, Stanley PE. editors. Bioluminescence and Chemiluminescence. Chichester: Wiley, 1993:113-7.
3. Lei B, Tu S-C. Mechanism of reduced flavin transfer from *Vibrio harveyi* NADPH-FMN oxidoreductase to luciferase. Biochemistry 1998; 37: 14623-9.
4. <http://www.gepasi.org>

ENZYME KINETICS MODEL OF THE BACTERIAL LUCIFERASE REACTIONS FOR BIOSENSOR APPLICATIONS

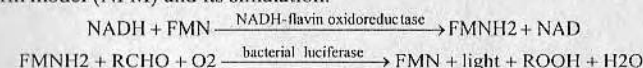
Y FENG¹, RH DAVIES², JD ANDRADE^{1,2}

¹ Dept of Materials Science and ² Bioengineering, University of Utah, 2480 Merrill Engineering Building, Salt Lake City, UT 84112-9202, USA

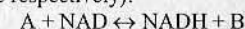
E-mail: yf3@utah.edu

INTRODUCTION

We are developing devices using bioluminescence-based reactions to measure metabolites in bio fluids. Our NADH sensing platform involves NADH, FMN, RCHO, NADH-flavin mononucleotide (FMN) oxidoreductase (OR, *Vibrio fischeri*), and bacterial luciferase (BL, *Vibrio harveyi*). Here we present a practical NADH platform model (NPM) and its simulation:



The reaction coupling analyte to NADH is (where A and B are the reduced and oxidized form of the analyte respectively):



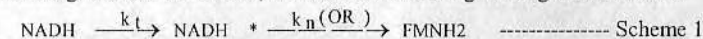
Min used a common first order reaction to model FMNH₂ production.¹ Baldwin *et al.* showed a detailed model of the BL-catalyzed light emitting reaction.² Tu *et al.* presented a scheme for the OR catalysed reaction producing the needed FMNH₂ to "feed" the light emitting reaction.³ Based on Baldwin *et al.* and Min's model and rate constants, a simplified NPM was constructed using Gepasi.⁴

METHODS

Gepasi simulates the kinetics of systems of biochemical reactions. Given the individual reactions, rate constants and initial condition, concentrations are calculated as a function of reaction time. The light output is proportional to the instantaneous light emitter species E'-FMNHOOR.

RESULTS AND DISCUSSION

We begin the simulation by analysing the FMNH₂ production. Although there is a detailed model from Tu *et al.*,³ we chose Min's method¹ because it is simple and accurate enough for our simulation, whose focus is the engineering of biosensors:



NADH* is the concentration of NADH after mixing, k_t in the first step represents the time delay (0.018 s⁻¹) obtained from fitting our whole NPM. The second step is catalysed by OR and $k_n = A^* [\text{OR}] / K_m$ where A is the specific activity of the OR (U/mg, 1U = 1.67 * 10⁻⁸ mol*s⁻¹, 18 U for OR), [OR] (brackets

represent concentrations) (10 pM) and K_m (Michaelis constant for NADH) 50 μM .¹ So the rate constant k_n is 1.5 s^{-1} . The $[\text{FMNH}_2]$ varying with time is shown in Fig. 1.

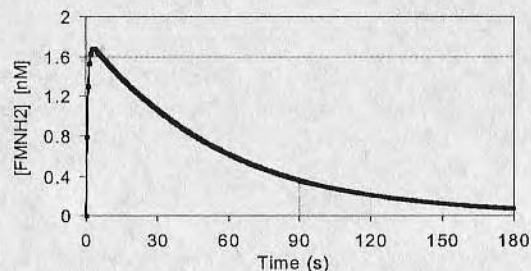


Figure 1. $[\text{FMNH}_2]$ varies with reaction time (including $\text{FMNH}_2 \rightarrow \text{FMN}$ auto oxidation) and rate constant is 4.7 s^{-1} . Initial condition: $[\text{OR}] 10 \text{ pM}$, $[\text{NADH}] 1 \mu\text{M}$.

To couple the FMNH_2 to light emission, there are different hypotheses about how FMNH_2 is utilized by BL.^{2,3} Here we focus only on a quantitative simplified estimate of light emission where the detailed steps are included in combined rate constants. We begin the simulation by building the Baldwin *et al.* BL light-emitting model (Fig. 2).² The RCHO inhibition of the model agrees with Baldwin *et al.* data.² The error is less than 5% (not shown here), which means our simulation is reasonably correct.

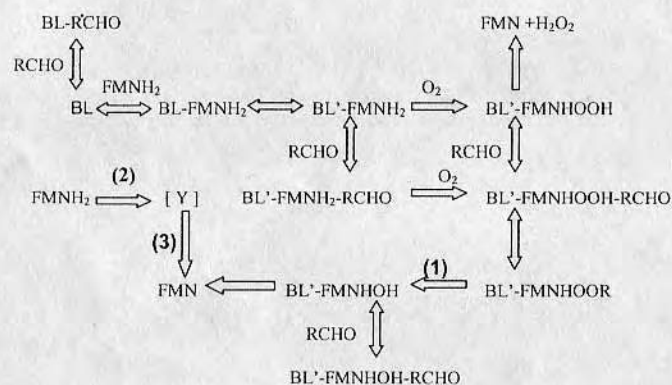


Figure 2. Bioluminescence reaction scheme.²

Then we directly coupled FMNH_2 production (scheme 1) to Baldwin's model (Fig. 2), whose experimental conditions are given and compared to Min's value in parenthesis: $[\text{O}_2]$ 120 μM (300 μM , estimated), $[\text{BL}] 75 \mu\text{M}$ (10 pM), $[\text{FMNH}_2] 15 \mu\text{M}$ (less than 1.6 nM), $[\text{RCHO}] 100 \text{ mM}$ (6 mM). The NPM was finalized by the following 2 adjustments. The rate constant of reaction (1) (Fig. 1) was modified from 1.1 s^{-1} to 0.018 s^{-1} . Reactions (2) and (3) (Fig. 2) were combined to give $\text{FMNH}_2 \rightarrow \text{FMN}$ and the rate constant is estimated as 10 s^{-1} . The light profile produced by the NPM and Min's data¹ are compared in Fig. 3.

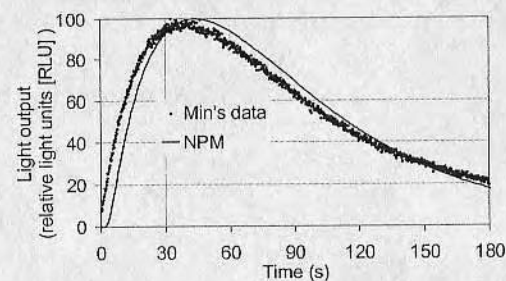


Figure 3. Comparison of light output profiles. Conditions for both: $[\text{OR}] 10 \text{ pM}$, $[\text{BL}] 10 \text{ pM}$, $[\text{NADH}] 1 \mu\text{M}$, $[\text{O}_2]$ 300 μM (estimated) and total assay volumes 250 μL . Note: These experimental conditions are constant for all of our simulations in order to compare with Min's data.¹

From Fig. 3 the simulated kinetics are about 2s slower. The reason is in our model we have to compromise between treatment of the delay time and decay kinetics. The NPM was used to obtain the simulated NADH calibration curve, Fig. 4. The conditions are the same as Fig. 3 except for $[\text{NADH}]$. The validity of the NPM under other experimental conditions is being evaluated.

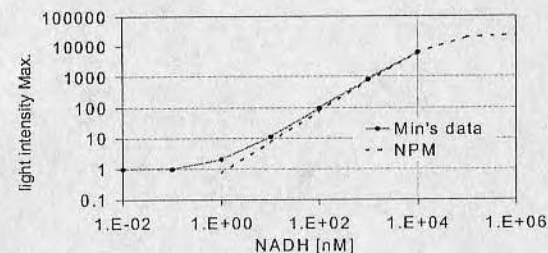
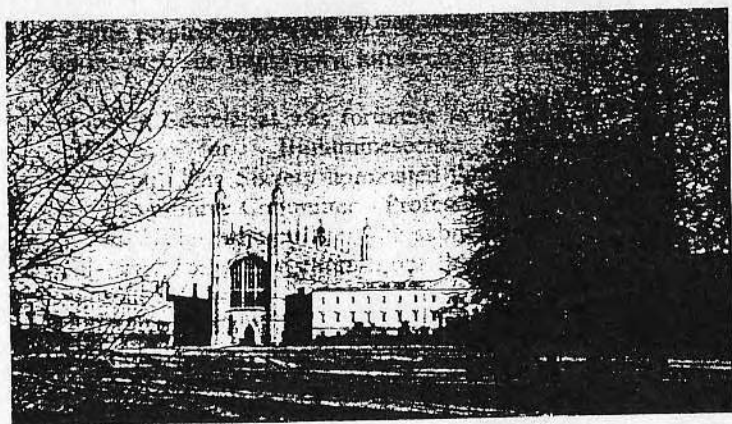


Figure 4. NADH calibration curve predicted by the NPM.

BIOLUMINESCENCE & CHEMILUMINESCENCE

Progress & Current Applications



editors

Philip E. Stanley

Cambridge Research & Technology Transfer Ltd., England

Larry J. Kricka

*Department of Pathology & Laboratory Medicine
University of Pennsylvania School of Medicine, USA*

 **World Scientific**
New Jersey • London • Singapore • Hong Kong

Published by

World Scientific Publishing Co. Pte. Ltd.

P O Box 128, Farrer Road, Singapore 912805

USA office: Suite 1B, 1060 Main Street, River Edge, NJ 07661

UK office: 57 Shelton Street, Covent Garden, London WC2H 9HE

British Library Cataloguing-in-Publication Data

A catalogue record for this book is available from the British Library.

BIOLUMINESCENCE & CHEMILUMINESCENCE: PROGRESS & CURRENT APPLICATIONS

Copyright © 2002 by World Scientific Publishing Co. Pte. Ltd.

All rights reserved. This book, or parts thereof, may not be reproduced in any form or by any means, electronic or mechanical, including photocopying, recording or any information storage and retrieval system now known or to be invented, without written permission from the Publisher.

For photocopying of material in this volume, please pay a copying fee through the Copyright Clearance Center, Inc., 222 Rosewood Drive, Danvers, MA 01923, USA. In this case permission to photocopy is not required from the publisher.

ISBN 981-238-156-2

This book is printed on acid-free paper.

Printed in Singapore by Uto-Print